University of Glasgow

Palmer, Elizabeth Ann (2010) *Studies on the herpes simplex virus type 1 UL32 DNA packaging protein.* PhD thesis.

http://theses.gla.ac.uk/1987/

Copyright and moral rights for this thesis are retained by the author

A copy can be downloaded for personal non-commercial research or study, without prior permission or charge

This thesis cannot be reproduced or quoted extensively from without first obtaining permission in writing from the Author

The content must not be changed in any way or sold commercially in any format or medium without the formal permission of the Author

When referring to this work, full bibliographic details including the author, title, awarding institution and date of the thesis must be given

Glasgow Theses Service
http://theses.gla.ac.uk/
theses@gla.ac.uk

Studies on the herpes simplex virus type 1 UL32 DNA packaging protein

By

Elizabeth Ann Palmer

A thesis presented for the degree of Doctor of Philosophy in the Faculty of Biomedical and Life Sciences at the University of Glasgow

MRC Virology Unit
Church Street
Glasgow
G11 5JR

April 2010

Abstract

The work presented in this thesis is concerned with the characterisation of the UL32 gene of herpes simplex virus type 1 (HSV-1). UL32 encodes an essential 596 amino acid cysteine-rich, zinc-binding protein that is highly conserved throughout the herpesviruses. The UL32 protein is essential for the cleavage of concatemeric viral DNA into monomeric genomes and their packaging into preformed capsids. Conservation is highest at the C-terminus and three CxxC motifs are present in almost all known herpesvirus UL32 sequences

The UL32 antibodies available in the laboratory at the beginning of the project were incapable of detecting small amounts of UL32 protein and so new rabbit antisera were created. Soluble extracts from insect cells infected with a UL32-expressing baculovirus (AcUL32) were fractionated by anion exchange chromatography and the UL32-containing fractions used to immunise rabbits. The resultant antisera successfully recognised UL32 from transfected, HSV-1 infected and baculovirus infected cells on western blots, and UL32 in transfected cells by immunofluorescence.

I performed random mutagenesis of the UL32 gene in an effort to examine structure-function relationships within this protein, and generated a panel of 37 mutants containing 5 amino acid insertions at distinct positions. The abilities of these mutants to complement the DNA packaging and growth defects of a virus lacking a functional copy of UL32 (the null mutant *hr*64) were examined and 15 of the mutants retained functionality in both assays. A complete correlation was found between the ability of mutants to support growth and DNA packaging, suggesting that the key functions of UL32 are confined to the DNA packaging pathway. There was also good correlation with the degree of amino acid conservation within UL32, with most of the mutants which abolished functionality being located in the highly conserved regions, and the functional mutants in less conserved regions. A number of site-specific mutants were also created, in which the paired cysteine residues were replaced with serines (i.e. CxxC to SxxS). Mutation of the first and third cysteine pairs (from the N-terminus) completely abrogated growth and packaging, whereas significant functionality was maintained following mutagenesis of the central pair. Finally, removal of the C-terminal 4 amino acids also resulted in generation of a non-functional protein.

Generation of an HA-tagged UL32 construct and the introduction of this into HSV-1 allowed the localisation of UL32 in infected cells to be studied. In contrast to previous

reports, I detected UL32 predominantly in the nuclei of infected cells, co-localising with ICP8 in replication compartments. DNA packaging has previously been shown to occur within the replication compartments and a number of the other packaging proteins also localise to these sites. It was previously reported that UL32 played a role in the localisation of capsids to the replication compartments. However, work presented in this thesis shows this not to be the case, and that capsid proteins VP5 and VP19C were correctly localised in replication compartments during infections with the UL32 mutant *hr*64. I found no evidence of UL32 interaction with the UL6, UL25 or UL17 DNA packaging proteins in HSV-1 infected or transfected cells, or using immunoprecipitation from baculovirus-expressed cells.

Immunofluorescence studies of co-transfected cells showed that UL15 could direct the partial re-localisation of UL32 from the cytoplasm to the nucleus. The addition of the other terminase subunits UL28 and UL33 caused the complete re-localisation of UL32 to the nucleus, suggesting that UL32 might interact with the terminase complex. Fifteen of the insertional mutants were completely re-localised to the nucleus in the presence of UL15, UL33 and UL28, with eleven further mutants showing an intermediate phenotype of partial nuclear localisation. The ability to at least partially co-localise with the terminase complex appeared necessary for the ability of the mutants to support virus growth and DNA packaging, suggesting that this interaction may be essential for the function of UL32. However, no interaction could be demonstrated between UL32 and any of the individual terminase subunits using immunoprecipitation from insect cells.

A series of experiments was undertaken to further characterise the UL32 protein. A new UL32 mutant virus (Δ32EP) was generated by insertion of a kanamycin resistance cassette in place of a large portion of the UL32 gene. This mutant had an indistinguishable phenotype from *hr*64, confirming that the main function of UL32 is within DNA packaging. The functional conservation between HSV-1 UL32 and the homologues from HCMV and VZV was examined, but neither protein could support the growth of Δ32EP. DNA fragments from replicated concatemeric DNA from Δ32EP infected cells behaved similarly to wt HSV-1 fragments in PFGE, suggesting that UL32 is not involved in the resolution of branched structures within the genome prior to packaging.

UL32 had previously been reported to bind zinc, and this was confirmed using a zinc-release colourimetric assay. The amount of zinc bound to soluble baculovirus-expressed UL32 was quantified, showing that UL32 bound zinc in a 1:1 molar ratio. UL32 does not

share all of the characteristics of a zinc finger motif, but the results of the mutagenesis experiments suggest that the outer CxxC/CxxxC motifs may be important for zinc binding.

Because of its zinc-binding properties and potential interaction with the terminase complex, the DNA binding properties of UL32 were also investigated. It was found that UL32 did not bind to dsDNA containing either the minimal packaging sequence (Uc-DR1-Ub) or an unrelated non-HSV-1 sequence using an electrophoretic mobility shift assay (EMSA).

Contents

List of tables and figures

Acknowledgements

Firstly, I would like to thank the MRC and Duncan McGeoch, for allowing me to undertake my PhD in the Virology Unit. It has been an enjoyable three years and I have made many good friends.

I am hugely grateful to Nigel Stow for his enthusiastic supervision and guidance, giving me plenty of technical and practical advice and reassuring me when needed. Thanks must also go to the other members of lab 201, especially Lily and Mary for technical support and Val for interesting discussions and advice in the mornings, and thanks to all for the lovely cakes.

I must also mention my fellow PhD students, especially Chris and Beka, for fun lunchtime chat and cake and milkshake when needed. Thanks to all my friends at Northside netball club for really tough competition to take my mind off work, great friendship and a lot of good laughs on our weekends away! An extra big thank you to my brilliant friends Joanna and Teresa, for being there for me, good advice and counselling, and lots of good gossip over a cup of tea or glass of wine.

I would like to thank my family for their support – David, well done for getting the PhD before me! A huge and heartfelt thank you to my mum and dad (how are the mutants?!) for all their much-needed support and throughout my life always believing I could do it - even if they didn't always understand what "it" was. Finally, to Ian, there is not enough space to express my love and gratitude, you have helped me in every way possible – thanks for practical advice, encouragement, looking after me and always being there. I really could not have done this without you.

Authors Declaration

The author was a recipient of a Medical Research Council studentship. Unless otherwise stated, all work presented in this thesis was carried out by the author.

Abbreviations

µCi	- microcurie
µg	- microgram
µl	- microlitre
µM	- micromolar
µm	- micrometre
aa	- amino acid
AcMNPV	- *Autographa californica* nucleopolyhedrovirus
ADP	- adenosine diphosphate
Amp	- ampicillin
ATP	- adenosine triphosphate
ATPase	- adenosine triphosphatase
bp	- base pair
BHK (cells)	- baby hamster kidney (cells)
cam	- chloramphenicol
CAV	- cell associated virus
CCSC	- C capsid-specific component
CIP	- calf intestinal phosphatase
CLB	- cell lysis buffer
coIP	- co-immunoprecipitation
CPE	- cytopathic effect
CRV	- cell released virus
Cy5	- cyanine-5
dATP	- 2’ –deoxyadenosine-5’-triphosphate
dCTP	- 2’ –deoxycytidine-5’-triphosphate
dGTP	- 2’ –deoxyguanosine-5’-triphosphate
DMEM	- Dulbecco’s modified Eagle’s medium
DMSO	- dimethylsulphoxide
DNA	- deoxyribonucleic acid
DNase	- deoxyribonuclease
d.p.i.	- days post infection
ds	- double stranded
dTTP	- 2’ –deoxythymidine-5’-triphosphate
E	- early

E. coli	- Escherichia coli
EBV	- Epstein-Barr virus
EDTA	- ethylenediaminetetra-acetic acid
EM	- electron microscopy
EMSA	- electrophoresis mobility shift assay
EtBr	- ethidium bromide
FCA	- Freund's complete adjuvant
FCS	- foetal calf serum
FIA	- Freund's incomplete adjuvant
FITC	- fluorescein isothiocyanate
GMEM	- Glasgow’s modified Eagle’s medium
GPCMV	- guinea pig cytomegalovirus
GST	- glutathione-S-transferase
HCF	- host cell factor
HCMV	- human cytomegalovirus
HeBS	- hepes buffered saline
hepes	- N-[2,-hydroxyethyl]piperazine-H’-[2-ethane sulphonic acid]
HHV	- human herpesvirus
HS	- heparin sulphate
HSV-1	- herpes simplex virus type 1
HSV-2	- herpes simplex virus type 2
h	- hours
h.p.i.	- hours post infection
HRP	- horseradish peroxidase
IE	- immediate early
IHF	- integration host factor
IP	- immunoprecipitation
kan	- kanamycin
kbp	- kilobase pairs
kDa	- kilo daltons
KSHV	- Kaposi’s sarcoma-associated herpesvirus (HHV-8)
L	- late
LB	- L-broth
M	- molar
MBP	- maltose binding protein
MCS	- multiple cloning site

mg	- milligram
MGS	- Mutation Generation System
MIEP	- major immediate early promoter
min	- minutes
ml	- millilitre
mM	- millimolar
mm	- millimetre
NBCS	- newborn calf serum
nm	- nanometre
NPT	- non-permissive temperature
NP40	- nonidet NP40 detergent
NTB	- nick-translation buffer
$^{\circ}$C	- degrees Celsius
ORF	- open reading frame
OsHSV-1	- Ostreid herpesvirus 1
PAR	- 4-(2-pyridylazo) resorcinol
PBS	- phosphate buffered saline
PCMB	- p-chloromercuribenzoic acid
PCR	- polymerase chain reaction
p.f.u.	- plaque forming unit
PFGE	- pulsed-field gel electrophoresis
PMSF	- phenylmethylsulphonyl fluoride
PrV	- pseudorabies virus
PT	- permissive temperature
PVDF	- polyvinylidene fluoride
RCs	- replication compartments
RNA	- ribonucleic acid
RNAi	- RNA interference
RNase	- ribonuclease
rpm	- revolutions per minute
RSB	- reticulocyte standard buffer
RSC	- rabbit skin cell
SDS	- sodium dodecyl sulphate
SDS-PAGE	- SDS- polyacrylamide gel electrophoresis
sec	- second
*Sf*21 (cells)	- *Spodoptera frugiperda* strain 21 (cells)

ss	- single stranded
SSC	- standard saline citrate
strep	- streptomycin
TEMED	- N,N,N’,N’-tetra-methyl-ethylene diamine
tet	- tetracycline
TGN	- trans-Golgi network
Tris	- 2-amino-2(hydroxymethyl)-1,3-propandiol
Triton X-100	- octyl phenoxy polyethoxy ethanol
ts	- temperature sensitive
TBS	- Tris buffered saline
U	- units
UV	- ultra violet
V	- volts
v/v	- volume ÷ volume
VZV	- varicella-zoster virus
w/v	- weight ÷ volume
wt	- wild type
X-Gal	- 5-bromo-4-chloro-3-indolyl-(-D-galacto pyranoside)

Amino acids

Alanine	Ala	A	Leucine	Leu	L
Arginine	Arg	R	Lysine	Lys	K
Asparagine	Asn	N	Methionine	Met	M
Aspartate	Asp	D	Phenylalanine	Phe	F
Cysteine	Cys	C	Proline	Pro	P
Glutamate	Glu	E	Serine	Ser	S
Glutamine	Gln	Q	Threonine	Thr	T
Glycine	Gly	G	Tryptophan	Trp	W
Histidine	His	H	Tyrosine	Tyr	Y
Isoleucine	Ile	I	Valine	Val	V

1 Introduction

The work presented in this thesis is concerned with the characterisation of the herpes simplex virus type 1 (HSV-1) UL32 protein and its role within the viral DNA cleavage and packaging process. This introduction discusses the general properties of herpesviruses and gives an outline of the viral life cycle. The process of DNA packaging in herpesviruses and related bacteriophage is also described in detail, including an outline of our current knowledge of the UL32 protein. Finally the aims of this project are introduced.

1.1 Herpesviruses

The herpesviruses comprise an abundant group of large double-stranded DNA (dsDNA) viruses infecting a wide range of hosts. Morphologically, herpesviruses have a unique virion architecture and historically the definition of a herpesvirus was based upon this. A large linear dsDNA genome of between 124 kbp (simian varicella virus) and 295 kbp (cyprinid herpesvirus 1) is tightly packed within an icosahedral capsid, which is encased in an amorphous protein layer known as the tegument. This is surrounded by the host-derived lipid envelope containing virus encoded membrane-associated glycoproteins.

Over 100 herpesviruses have been identified, infecting a wide range of vertebrate hosts including mammals, birds, amphibians and fish. More recently a single herpesvirus has been described that infects a number of marine bivalve species (Arzul *et al.*, 2001; Davison *et al.*, 2005). Despite the varied host range within the family, each individual herpesvirus appears to infect very few host species (often only one natural host). Herpesviruses are very well adapted to their natural hosts, and severe infection is usually observed only in the very young, the foetus or the immuno-compromised. Viruses can, however, occasionally cross species and here more severe disease may be seen. An example of this is B virus (Macacine herpesvirus 1, previously Cercopithecine herpesvirus 1) which is endemic in macaques and causes no disease, although zoonotic infection of humans can result in encephalitis with a fatality rate of over 70% if not treated (Huff & Barry, 2003).

Many herpesviruses have the ability to establish a persistent infection (latency) in the host. During latency, the genome exists in a 'dormant' state as a circular episome within cells and can persist for the lifetime of the infected individual, evading detection by the immune system. Reactivation from latency leads to productive infection and recurrence of disease.

1.1.1 Classification of herpesviruses

Recently the International Committee on Taxonomy of Viruses (ICTV) has accepted a new taxonomy of herpesviruses, whereby the former family *Herpesviridae* has been split into three families (*Herpesviridae, Alloherpesviridae* and *Malacoherpesviridae*), which are now incorporated into the new order of *Herpesvirales*. This new classification was proposed by the *Herpesviridae* study group (Davison *et al.*, 2009) and is based on phylogenetic data. New genera have also been formed within families by the transfer of species from previously established genera and identification of new species, along with the renaming of some herpesviruses infecting non-human primates to reflect the host genus rather than the host sub-family.

The first group within the *Herpesvirales*, the family *Herpesviridae*, encompasses viruses infecting birds, mammals and reptiles. This is split into three subfamilies of *Alphaherpesvirinae, Betaherpesvirinae* and *Gammaherpesvirinae*.

The *Alphaherpesvirinae* sub-family includes, among others, herpes simplex viruses 1 and 2 (genus: *Simplexvirus*) and varicella-zoster virus and pseudorabies virus (genus: *Varicellovirus*). The *Alphaherpesvirinae* are neurotropic and establish latency in neuronal ganglia innervating the site of initial infection. They replicate relatively rapidly and efficiently in a number of cell lines in tissue culture.

The *Betaherpesvirinae* includes human cytomegalovirus (genus: *Cytomegalovirus*) and human herpesviruses 6 and 7 (genus: *Roseolovirus*). This sub-family also now includes a newly created genus, the *Proboscivirus* - the only representative of which is a herpesvirus infecting elephants (Richman *et al.*, 1999). The *Betaherpesvirinae* are characterised by a slower replication and more restricted host range in culture and the establishment of latency in cells of the monocyte lineage.

The *Gammaherpesvirinae* sub-family includes Epstein-Barr virus (genus: *lymphocryptovirus*) and Kaposi's sarcoma-associated herpesvirus (genus: *Rhadinovirus*). Two new genera, the *Macavirus* and *Percavirus* have been created within the *Gammaherpesvirinae*. This sub-family of viruses are lymphotrophic, with a variation in replication cycle length. They have a more restricted host range *in vitro* than either of the other sub-families and establish latency in T or B lymphocytes.

The estimated number of protein-coding genes in the *Herpesviridae* varies from 70 in VZV to 165 in HCMV. 43 genes, which are denoted 'core' genes, are present in each of the sub-families, providing evidence of a common evolutionary ancestor (McGeoch & Davison, 1999). Many of these core genes are involved in the replication or packaging of the viral DNA, or encode proteins that are present in the virion.

The newly-formed *Alloherpesviridae* family consists of herpesviruses infecting amphibians and bony fish. These form a group that are essentially unrelated to the *Herpesviridae* by analysis of amino acid conservation and as such they have been classified as a separate family in the new taxonomy (Davison *et al.*, 2009). However, their identification as a family of the *Herpesvirales* can be demonstrated by similarity in virion morphology and maturation (Booy *et al.*, 1996; Davison & Davison, 1995).

The third family is the *Malacoherpesviridae*, whose only member is a herpesvirus infecting invertebrates, named Ostreid herpesvirus 1 (OsHV-1) (Davison *et al.*, 2005). Again, the *Malacoherpesviridae* are very distantly related to the *Herpesviridae* and sequence analysis did not demonstrate any similarity between the structural proteins of OsHV-1 and other herpesviruses. Despite these differences in amino acid sequence, the virions of OsHV show the characteristic herpes virus morphology and OsHV-1 was first identified as a herpesvirus by the presence of these virions in lesions of infected oysters (Farley *et al.*, 1972). Studies of the virion by cryo-electron microscopy (cryo-EM) confirmed the structural similarity between OsHV-1 capsids and other herpesviruses (Davison *et al.*, 2005).

As mentioned, there is very little sequence similarity between the three families of herpesviruses and genetically they are only tenuously related to each other. Although many core genes can be identified as conserved within families, only one protein has an amino acid sequence that is conserved among the three families in a way to suggest a common ancestor. This gene, which encodes the ATPase of the DNA packaging complex, also has relatives in T4-like bacteriophage (Davison, 1992; Davison, 2002; Rao & Black, 1988). It is therefore not completely *Herpesvirales*-specific, although similarities in capsid assembly and the DNA packaging process between herpesviruses and dsDNA bacteriophage suggest that they too have a common evolutionary ancestor.

Phylogenetic trees of herpesviruses show similarity with the phylogeny of the corresponding host organisms, which is taken as evidence for co-evolutionary development

of virus and host lineages (McGeoch *et al.*, 1995). This co-evolution may also explain the restricted host-range of many herpesviruses.

1.1.2 Human *Herpesviridae*

Eight herpesviruses have been identified that infect human hosts (Human herpesviruses [HHV] 1-8), encompassing all three subfamilies of the *Herpesviridae*. In general, these viruses do not cause serious illness upon primary infection of immuno-competent hosts, and infections can often be asymptomatic.

Herpes simplex virus type 1 (HSV-1, HHV-1) is the prototype in the *Alphaherpesvirinae*, and as such has been extensively studied. Primary infection occurs in the epithelial cells of the skin and mucosa near the mouth, and life-long latency is established in ganglia innervating the site of primary infection (Stevens & Cook, 1971). HSV-2 (HHV-2) is very similar to HSV-1 in its pattern of infection, but is primarily associated with infections of the genitalia. The third human alphaherpesvirus is varicella-zoster virus (VZV, HHV-3). This is the causative agent of chickenpox in children (varicella), which is characterised by a vesicular skin rash. Later reactivation of the virus from the neurons in which VZV establishes latent infection results in the adult disease shingles (zoster).

Three members of the *Betaherpesvirinae* also have human hosts. Human cytomegalovirus (HCMV, HHV-5) is most widely studied of this family. Infection is asymptomatic in most individuals and acute disease is mainly seen in those who are immuno-compromised or immuno-suppressed. HCMV can establish latent infection in blood monocytes (Sinclair & Sissons, 2006). HCMV is also a major cause of neonatal disease through congential infection, often resulting in damage to the brain and nervous system. Human herpesviruses 6 and 7 (HHV-6 and HHV-7) are lesser-studied viruses that are the causative agents of exanthema subitum (Roseola), a near-universal childhood disease associated with the appearance of a rash.

Two viruses within the *Gammaherpesvirinae* are known to infect humans, and these have both been associated with various tumours. The first is Epstein Barr virus (EBV, HHV-4). EBV is one of the most prevalent herpesviruses and many individuals become infected in childhood, showing no symptoms. When primary infection with EBV occurs during adolescence or young adulthood, it can cause infectious mononucleosis (glandular fever), characterized by fever, sore throat and fatigue. EBV establishes latency in B-lymphocytes

and can transform B-lymphocytes *in vitro*. It has been implicated in nasopharyngeal carcinoma, Hodgkin's disease and Burkitt's lymphoma, although establishment of these cancers is also dependent on many other factors (Joseph, 1999). Human herpesvirus 8, otherwise known as Kaposi's sarcoma-associated herpesvirus (KSHV), again causes very few symptoms in healthy individuals. In AIDS patients, however, KSHV is the causative agent of Kaposi's sarcoma, a tumour characterised by lesions on the skin, respiratory tract or intestinal tract.

1.2 Herpes simplex virus type 1

HSV-1 is the prototype member of the *Alphaherpesvirinae*, and has been one of the most intensely studied herpesviruses. Primary infection with HSV-1 of healthy individuals is not a serious global health issue, as it is normally asymptomatic. It is estimated, however, that between 60 and 95% of adults are latently infected with either HSV-1 or 2 (although HSV-1 is predominant) (Brady & Bernstein, 2004). The virus can then lie dormant for the individual's lifetime, periodically reactivating to disseminate viral particles. Symptoms occur when the virus is reactivated, caused normally by physical trauma, stress or nerve damage. A variety of symptomatic diseases are associated with primary HSV-1 infection or reactivation (Dwyer & Cunningham, 2002), including most commonly orolabial lesions (coldsores) and genital ulcers (although HSV-2 is still the main cause of genital herpes). More serious manifestations can include herpetic keratitis (leading to keratoconjuctivitis and corneal scarring), herpes encephalitis caused by replication of HSV-1 in the brain, and neonatal infection. Some correlational evidence has also implicated HSV-1 infection with Alzheimer's disease, when combined with a particular allele of the gene encoding apolipoprotein E. However, the full importance of the virus in the disease and the mechanisms by which it contributes to Alzheimer's are still unclear (Itzhaki, 2004).

1.3 HSV-1 virion

As with all herpesviruses, the mature infectious HSV-1 virion is composed of four distinct structural components. The dsDNA genome is enclosed within an icosahedral capsid, which is surrounded by a proteinaceous tegument and host-derived lipid envelope. An electron micrograph along with diagrammatic representation of the HSV-1 virion is shown in figure 1.1

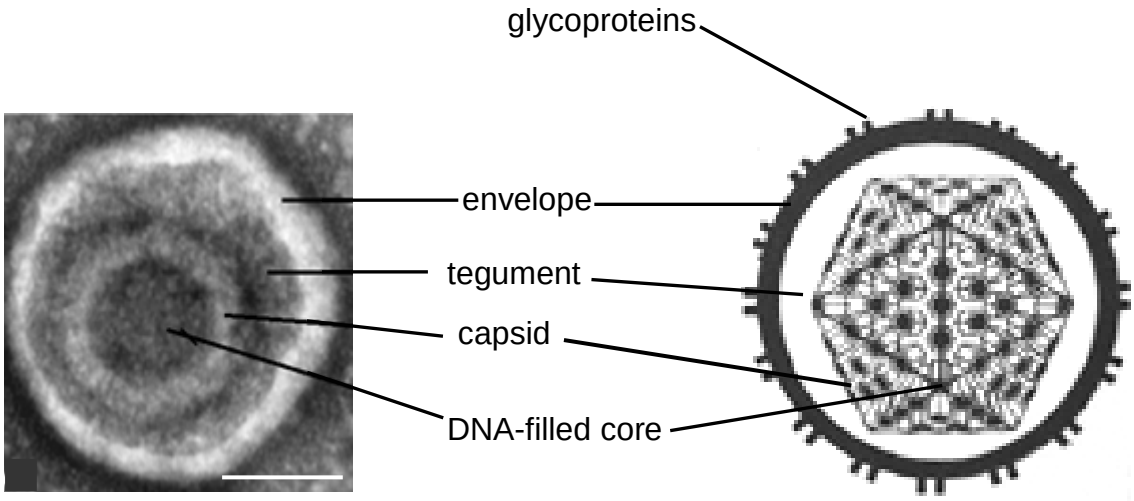

Figure 1.1: The HSV-1 virion.
Electron micrograph of a negatively stained HSV-1 virion and cartoon representation, showing the components comprising the virion. A DNA-filled icosahedral capsid is surrounded by a proteinaceous tegument and a host-derived lipid envelope studded with glycoproteins. Scale bar is 100 nm. (Adapted from Roizman and Knipe, 2001)

1.3.1 Genome

The HSV-1 genome is a linear double-stranded DNA molecule, approximately 152 kbp in length. The genome comprises two covalently linked components, designated as L (long) and S (short), each containing a unique sequence (U_L and U_S respectively). Inverted repeats flank the unique sequences, with U_L flanked by TR_L (terminal repeat long) and IR_L (internal repeat short), and U_S flanked by TR_S (terminal repeat long) and IR_S (internal repeat short). The U_L region is 107.9 kbp and U_S is 12 kbp and together these encode about 72 proteins. The long and short repeat sequences are 9.2 kb and 6.6 kb respectively and encode a further three proteins, RL1 (ICP34.5) and RL2 (ICP0) within R_L and RS1 (ICP4) within R_S. The gene organisation and nomenclature of HSV-1 is shown in figure 1.2. Historically, the proteins of HSV-1 were assigned virion protein (VP) or infected cell protein (ICP) numbers, but sequencing of the genome has allowed identification of the corresponding genes for these proteins. The gene and protein nomenclature for proteins discussed in this thesis is shown in table 1.1

A direct repeat of 250-500 bp (the *a* sequence) lies at the genomic termini and also in an inverted orientation at the junction between L and S segments. There can be multiple copies of the *a* sequence at the L terminus and junction, with only a single copy at the S terminus. The remainder of TR_L/IR_L and TR_S/IR_S excluding the *a* sequence are referred to as the *b* and *c* sequences respectively. Therefore the full structure of the genome can be represented as a_m-b-U_L-*b*'-a'_n-c'-U_S-*c*-*a*, where ' indicates inverted orientation and *n* and *m* are the number of *a* sequence repeats (see figure 1.3A). It is within the *a* sequence that the *cis*-acting sequences required for packaging of the genome lie (see section 1.5.3).

The repeat sequences allow inversion of the two unique regions relative to one another, generating four isomers of the genome, as shown in figure 1.3B. The significance of these inversion events in the replication of herpesviruses is unknown, but populations of virions have equimolar ratios of these isomers (Hayward *et al.*, 1975)

The HSV-1 genome also includes three *cis*-acting sequences that act as origins of replication for the genomic DNA. One copy of ori_L is present in the U_L region, lying between ORFs UL29 and UL30 (Spaete & Frenkel, 1985). Two identical copies of ori_S are found in the repeat regions flanking U_S between genes RS1 and either US1 or US12 (Stow,

1982). The two types of origin share considerable homology and many features, including binding sites for the viral UL9 protein on either side of a central A/T rich region. It is unclear why the HSV-1 genomes contain multiple origins. There is some redundancy as a virus deleted in both copies of ori_S could replicate DNA in a tissue culture system, although the rate of DNA synthesis was slower than that of wt HSV-1 (Igarashi *et al.*, 1993). Furthermore, the single ori_L has also shown to be dispensible in tissue culture (Polvino-Bodnar *et al.*, 1987).

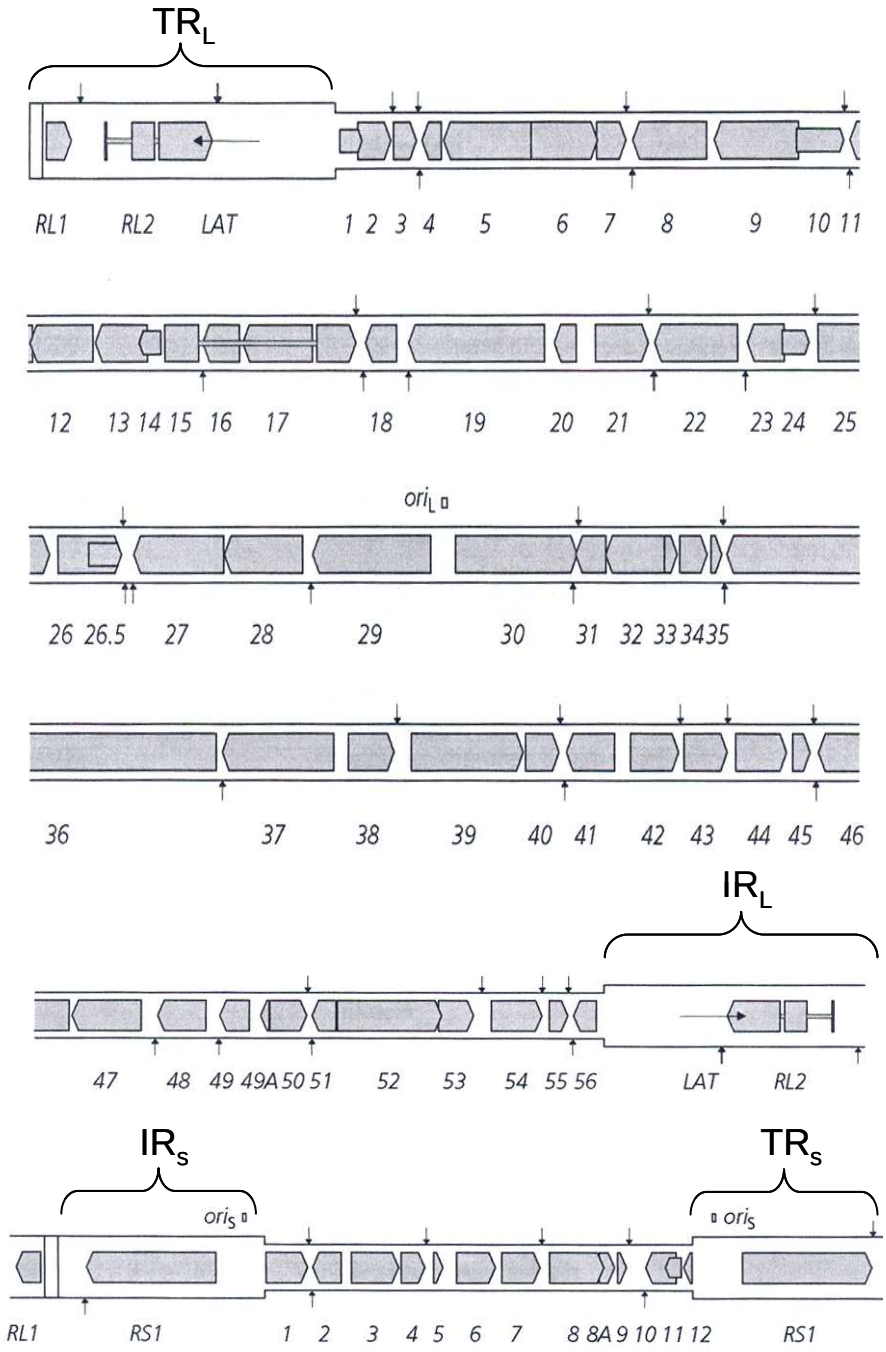

Figure 1.2: Gene organisation within HSV-1.
The organisation and nomenclature of genes within the HSV-1 genome is shown, with the shaded arrows indicating protein coding regions (showing the direction of transcription). The genes encoded within the U_L region have the prefix UL (UL1-UL56), and those encoded within U_S are denoted US1-US12. The thicker sections show the repeat regions (TR_L, IR_L, IR_S and TR_S), which encode a further three genes, RL1, RL2 and RS1. The position of the LAT transcript within R_L is marked, as are the locations of the origins of replication (*ori*$_L$ and *ori*$_S$). The vertical arrows indicate possible polyadenylation site for mRNAs. (Adapted from Davison & Clements, 1997)

Gene	Protein name (if applicable)	Function
Glycoproteins		
UL1	gL	Membrane fusion and entry – interacts with gH
UL10	gM	Secondary envelopment
UL22	gH	Membrane fusion and entry – interacts with gL
UL27	gB	Initial attachment to cells and membrane fusion
US6	gD	Receptor binding, membrane fusion and entry
UL44	gC	Initial attachment to cells
US8	gE	Acquisition of viral envelope during secondary envelopment
Capsid and tegument proteins		
UL19	VP5	Major capsid protein
UL18	VP23	Triplex protein
UL38	VP19C	Triplex protein
UL35	VP26	Minor capisd protein bound to hexons
UL26.5	VP22a	Major scaffolding protein
UL26	VP21*	Minor scaffolding protein
UL26	VP24*	Maturational protease
	VP16	Tegument protein – transactivator of IE gene expression
UL41	vhs	Tegument protein – virion host shut-off protein
UL36	VP1/2	Tegument protein –involved in nuclear entry and egress
Infected cell proteins		
RL2	ICP0	Transcriptional activation and de-repression of genome
RS1	ICP4	Transcriptional regulator
US1	ICP22	Trasncriptional activator
UL54	ICP27	Transcriptional activator and inhibition of mRNA splicing
RL1	ICP34.5	Neurovirulence factor
US12	ICP47	TAP transporter inhibitor
DNA replication proteins		
UL30		DNA polymerase catalytic subunit
UL42		DNA polymerase processivity subunit
UL5		Helicase subunit of helicase-primase complex
UL52		Primase subunit of helicase-primase
UL8		Helicase-primase subunit (processivity factor)
UL29	ICP8	Single stranded DNA binding protein
UL9		Origin binding protein

Table 1.1: Nomenclature of genes and proteins described within this thesis.
* VP21 and VP24 are derived from the N and C terminal portions of the full-length UL26-encoded precursor.

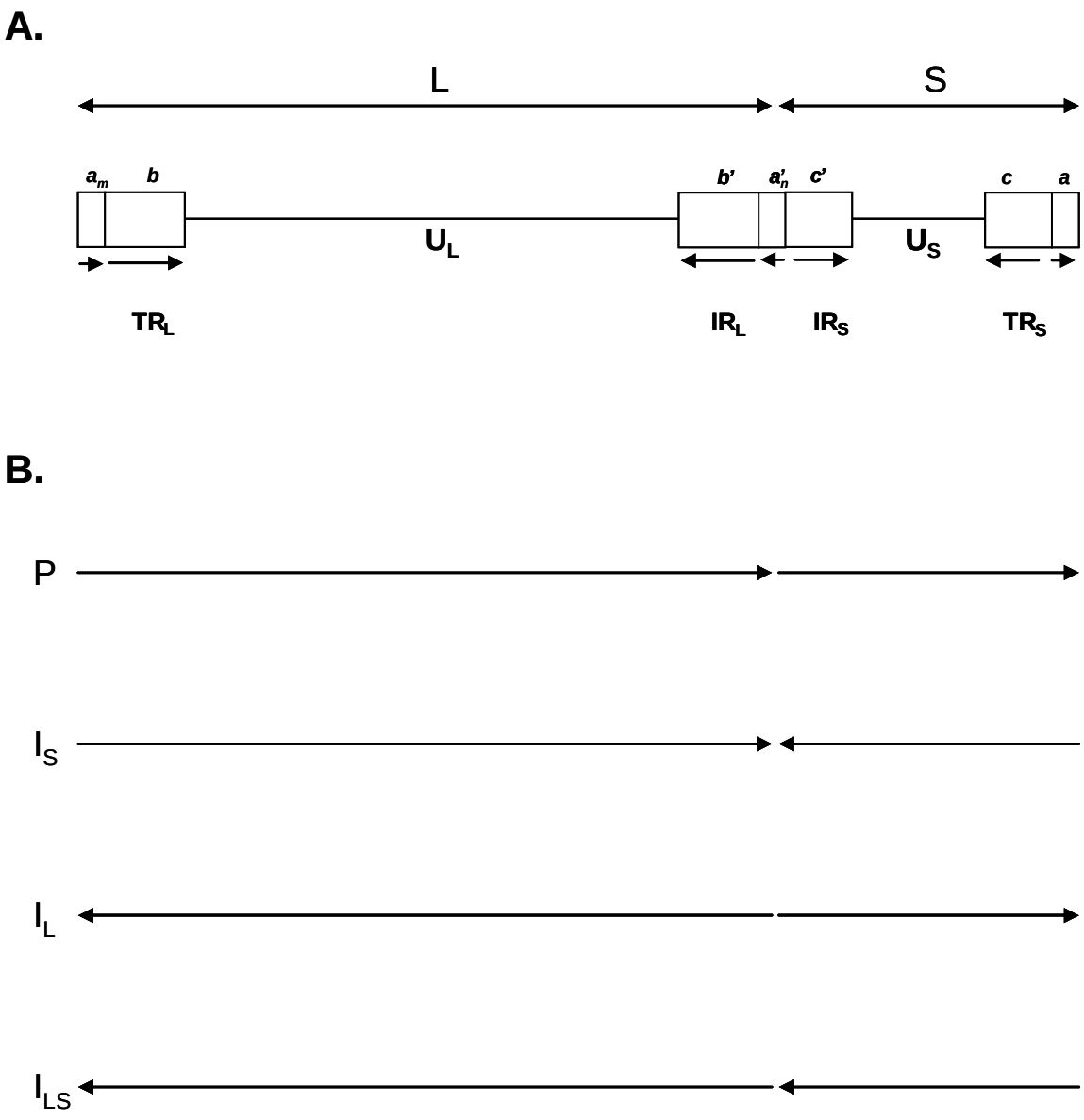

Figure 1.3: HSV-1 genome structure and isomers.

A. The structure of the HSV-1 genome is represented above (not to scale). The unique regions U_L and U_S are shown as single horizontal lines with the flanking repeats, R_L and R_S, shown as rectangles. The regions of R_L and R_S lacking the *a* sequence are denoted *b* and *c*, respectively. Terminal (TR_L and TR_S) and internal (IR_L and IR_S) repeats are inverted with respect to each with their relative orientations indicated by arrows. The *a* sequence, required for DNA cleavage and packaging, is present at each terminus and in an inverted orientation (*a'*) separating IR_L and IR_S. *m* and *n* indicate that there can be multiple copies of the a sequence at the L terminus and the L-S junction.

B. The unique regions of the genome can invert relative to each other, giving rise to four isomers of the genome. P = prototype; I_S = inverted U_S; I_L = inverted U_L; I_{LS} = inverted U_L and U_S.

1.3.2 Capsid

As with all herpesviruses, the HSV-1 capsid is a T=16 icosahedral shell, with the genomic DNA packed tightly into the capsid in a liquid-crystalline array (Booy *et al.*, 1991). The capsid structures of widely diverged members of the herpesviruses are similar, even when there is no sequence similarity between the proteins making up the capsid (for example HSV-1 and CCV) and despite a wide variation of genome lengths, all *Herpesviridae* have a capsid diameter between 125 nm (HSV-1) and 130 nm (HCMV) (Butcher *et al.*, 1998). In agreement with this, electron microscopy has shown that HCMV (the largest genome in the *Herpesviridae*) is more densely packed than the HSV-1 genome (Bhella *et al.*, 2000).

The HSV-1 capsid is 125 nm in diameter and approximately 15 nm thick (Booy *et al.*, 1991). A reconstruction of the HSV-1 capsid has been determined to 8.5 Å and is shown in figure 1.4. It consists of 162 capsomers made up of the major capsid protein VP5, comprising 150 hexons and 11 pentons. The hexons are the faces of the icosahedron, showing 6-fold rotational symmetry, with the penton vertices showing the 5-fold symmetry. The final vertex is the portal for DNA entry (discussed further in section 1.6.1). Hexons and pentons are connected in groups of three by complexes known as triplexes (320 in total). In HSV-1 the triplexes are heterodimers comprising two copies of VP19C and one copy of VP23. The final protein making up the capsid shell is VP26, with one molecule of this bound to each hexon-associated VP5. VP26 is believed to play a role tegument attachment, however it is not required for capsid assembly. The capsomers are assembled around a proteinaceous scaffold made up of the viral protease (encoded by the UL26 gene) and pre-VP22a (encoded by the UL26.5 gene). The structure of the HSV-1 capsid is reviewed by Homa and Brown (1997).

Four species of capsid have been identified by electron microscopy within HSV-1 infected cells, as shown in figure 1.5. The first species to form are the procapsids, which are spherical in shape and contain the internal scaffold. During infection, the maturation of procapsids due to cleavage of the internal scaffold can give rise to A-, B- and C- capsids, distinguishable by electron microscopy and sucrose gradient centrifugation (Gibson & Roizman, 1972). A-capsids are empty structures with no DNA or scaffold inside. B-capsids have a proteinaceous core which is the cleaved form of the protein scaffold, but no

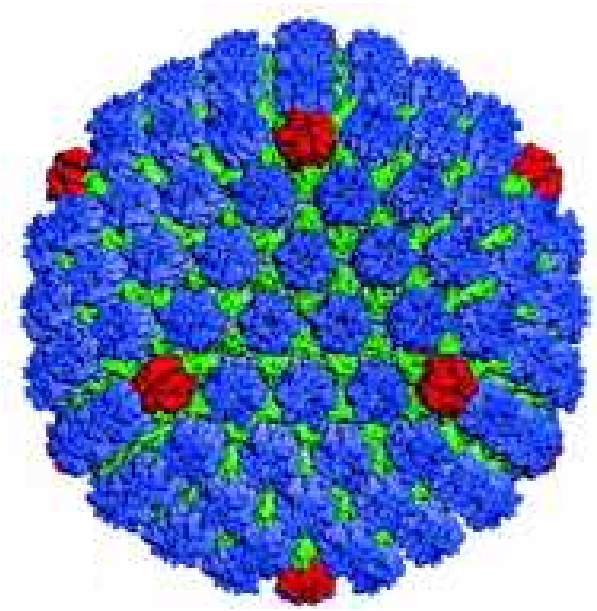

Figure 1.4: 3D reconstruction of HSV-1 capsid.
Cryo-electron microscopy and 3D reconstruction of HSV-1 B capsid at 8.5 Å resolution. A shaded surface view showing the capsid consisting of 160 capsomers, showing the 150 hexons in blue. The 12 vertices (red) are 11 pentons and the portal. However, because of symmetry imposed during image reconstruction, the portal cannot be distinguished. The triplexes are shown in green. (adapted from Zhou *et al*., 1999)

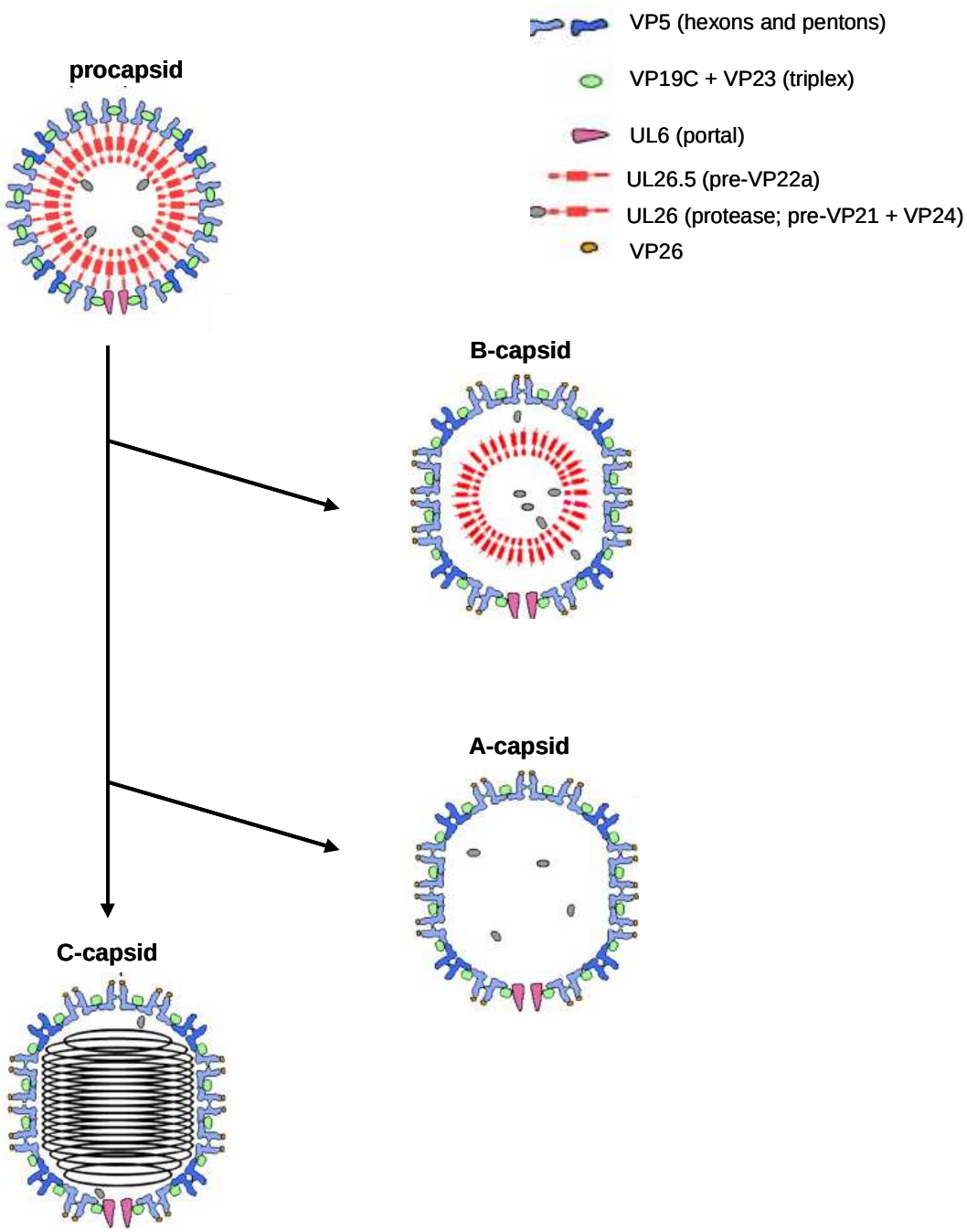

Figure 1.5: Capsid types found in HSV-1 infected cells.
Four capsid species have been identified in HSV-1 infected cells. The first of these is the spherical procapsid, comprised of major capsid protein VP5 arranged in hexons and pentons, coordinated by triplex proteins VP19C and VP23. Procapsids also contain one unique vertex made up of a dodecamer of the portal protein UL6. The procapsid contains an internal scaffold made up of proteins encoded by genes UL26 and UL26.5. Successful maturation of the procapsid results in the formation of angularised C-capsids which lack the internal scaffold, but instead contain the genomic DNA. A- and B- capsids are formed as dead-end products of the maturation process, with B-capsids containing cleaved scaffold protein and A- capsids containing neither scaffold nor DNA. (Adapted from Trus *et al.*, 2007)

DNA. Both of these capsid types are dead-end products of the DNA packaging pathway. C-capsids, however, contain viral DNA and can mature into infectious virions.

The processes of capsid assembly and maturation are believed to resemble that in bacteriophages, and are discussed further in section 1.4.6.

1.3.3 Tegument

All herpesviruses have a layer of protein called the tegument that lies between the virion envelope and the capsid. The tegument consists of multiple, virus-encoded proteins that can account for nearly half the total virion protein. A recent proteomics analysis suggested 23 potential tegument proteins in HSV-1 (Loret *et al.*, 2008) . Historically, the tegument has been described as amorphous, but there is growing evidence for an ordered addition of tegument during assembly, with multiple interactions driving tegumentation and virion formation (Mettenleiter, 2006). Although the tegument is not highly structured, the inner tegument does show a small degree of icosahedral symmetry where it interacts with the pentons of the capsid (Zhou *et al.*, 1999). The highly conserved inner tegument protein UL36 has been shown to interact with VP5 and this interaction may act as the link that binds the capsid to the tegument in the infectious virion. The use of cryo-electron tomography has suggested that the tegument may be asymmetrically distributed around the capsid (Grunewald *et al.*, 2003), and yeast-two-hybrid screens have been used to determine interactions between tegument proteins (Vittone *et al.*, 2005). Tegument proteins enter the cell as part of the incoming virion and are involved in many processes both before and after viral protein synthesis, for example targeting of virus components to the nucleus, transactivation of viral gene expression, regulation of host cell gene expression. Other tegument proteins are involved in DNA packaging and assembly of virions at a later stage of infection (Kelly *et al.*, 2009).

1.3.4 Envelope

The outer layer of the HSV-1 virion is a host-cell derived envelope. This envelope is a lipid-bilayer studded with virally-encoded glycoproteins, visible in negatively-stained electron microscope preparations as short spikes that are non-randomly distributed. The precise number of envelope glycoproteins varies among herpesviruses, with 13 described in HSV-1 (Loret *et al.*, 2008). The glycoproteins have roles in attachment and entry into the cell (discussed in section 1.4.1).

The viral envelope is acquired through a two-step budding process, whereby the virus acquires a primary envelope whilst budding through the inner nuclear membrane, is de-enveloped when budding from the lumen of the nuclear membrane into the cytoplasm, and is re-enveloped (secondary envelopment) at the trans-golgi network (TGN) before exit from the cell (discussed in section 1.4.7).

1.4 HSV-1 replication cycle

The lytic replication cycle has been studied most comprehensively in HSV-1, and appears to be similar in all herpesviruses. It is summarised in figure 1.6 and each stage is described in more detail in the following sections.

1.4.1 Attachment and entry

Alphaherpesviruses most commonly infect epithelial cells of mucosal membranes and the sensory neurons that innervate those epithelia. Entry involves attachment to specific and non-specific receptors on the surface of cells using the glycoproteins in the viral membrane. Of the 13 or more HSV-1 viral glycoproteins, infection in cell culture requires the co-ordinated action of at least four of these – gB, gD, and a heterodimer of gH/gL.

The initial attachment to cells involves binding of the virion to the heparin sulphate (HS) moieties of the cell-surface proteoglycans, an interaction that can be mediated independently by either glycoprotein gC or gB. However, this binding has been shown to be reversible, and although it significantly enhances the efficiency of HSV-1 infection, it is not essential in cell culture. Viruses either lacking gC, or with a mutation in gB which abolishes its interaction with HS are still infectious, albeit at a much reduced level. However, deletion of both gB and gC together completely abrogates infectivity (Herold *et al.*, 1994; Laquerre *et al.*, 1998). Recently it has been suggested that another host receptor may also mediate interaction with gB, since a soluble form of gB was shown to interact with different cell types independent of HS (Bender *et al.*, 2005).

The next stage of entry involves the interaction of gD with one of several potential entry receptors. Three classes of receptors have been identified on mammalian cells by virtue of the fact that addition of these proteins allows virus entry into infection-resistant CHO cells.

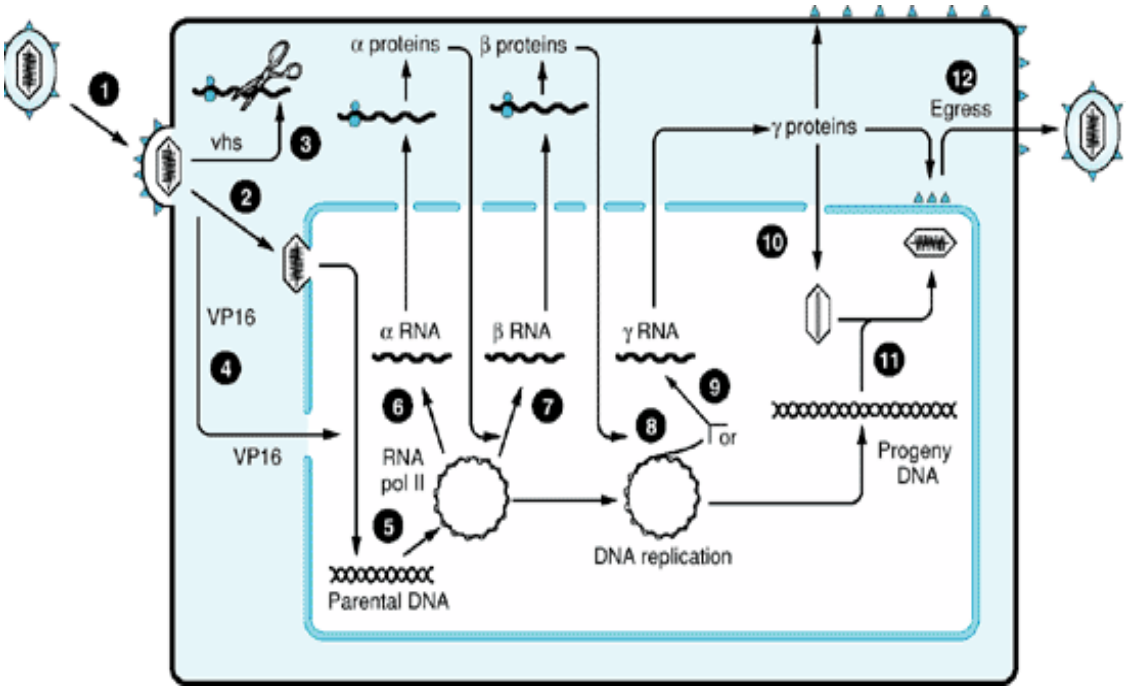

Figure 1.6: The lytic replication cycle of HSV-1.

(1) The virion attaches to the cell plasma membrane via specific interactions between the viral glycoproteins and cellular receptors. The virion envelope then fuses with the plasma membrane, releasing the capsid and tegument proteins into the cytoplasm. (2) The capsid is translocated to the nuclear pore via microtubules, where the viral genome is released into the nucleus via the nuclear pore. (3) The virion host shut-off (vhs) protein causes degradation of host messenger RNA (mRNA). (4) The tegument protein VP16 localizes into the nucleus where it can act to transactivate the cascade of viral gene expression. (5) The viral DNA circularizes prior to DNA transcription and replication. (6) There is temporal expression of the three classes of viral genes, transcribed by host RNA polymerase II. Firstly the immediate early (α) genes are transcribed and five of the six α proteins act to regulate subsequent viral gene expression in the nucleus. (7) The IE proteins transactivate early (β) gene transcription. (8) The β genes encode proteins required for replication of the viral genome. (9) Viral DNA synthesis stimulates L (γ) gene expression. (10) The γ proteins are mainly structural proteins involved in assembly of the procapsid in the nucleus. (11) The concatemeric replicated DNA is cleaved into unit length genomes and packaged into the preformed procapsid, generating C-capsids. (12) The filled capsid acquires a primary envelope when budding through the inner nuclear membrane and is de-enveloped as it buds from the lumen of the nucelar membrane into the cytoplasm. This capsid acquires tegument proteins in the cytoplasm. The tegumented capsid then forms a final enveloped virion by budding into the trans-golgi network and the virion exits from the cell through the secretary pathway (Adapted from Roizman & Knipe, 2001)

These are the TNF family member Herpes Virus Entry Mediator (HVEM) (Montgomery *et al.*, 1996), Ig superfamily members nectin-1 and -2 (Geraghty *et al.*, 1998), and a 3-*O*-modified form of heparin sulphate (Shukla *et al.*, 1999).

Following initial attachment and binding to the cell, the process of fusion occurs. Three different pathways for entry of HSV-1 into cells have been proposed, depending on the type of host cell. The first route identified was via fusion at the plasma membrane and this route can be visualised by electron microscopy in neurons and is well documented in Vero and Hep2 cells. Although this was long considered the only route of entry, in many other cell types, HSV-1 virions are endocytosed. Fusion with the endosomal membrane has been shown to occur via two possible entry mechanisms, both pH-dependent and pH-independent (Nicola *et al.*, 2003; Wittels & Spear, 1991).

In all three routes of entry, binding of gD to one of its receptors is thought to cause a conformational change in gD and trigger fusion of the viral envelope with the appropriate cellular membrane, as reviewed by Garner (2003). Fusion requires gB and a heterodimer of glycoproteins, gH/gL, as deletion of these proteins produces mutant viruses that can bind to cells but not internalise. The key role in fusion is thought to be played by glycoproteins gB and gH, which are both conserved in the *Herpesviridae*, whereas gL is required for correct trafficking of gH to the viral envelope (Hutchinson *et al.*, 1992).

Fusion of the viral envelope with a cellular membrane releases the capsid and tegument into the cytoplasm. Some tegument proteins remain in the cytoplasm but the capsid and other associated inner tegument proteins are transported to the nucleus via microtubules. It has been shown that agents that de-stabilise microtubules block this transport of capsids in different cell types (Topp *et al.*, 1996; Topp *et al.*, 1994). This microtubule transport is mediated by the retrograde motor dynein, which is known to transport organelles towards the nucleus (Dohner *et al.*, 2002). The viral proteins mediating this interaction with dynein have not been identified, but VP26 is thought to be involved, and it has been shown that some inner tegument proteins are needed for capsid transport along microtubules in vitro (André *et al.*, 2006).

Once the capsids have reached the nucleus, they dock at the nuclear pore and release the genome into the nucleus. This process of uncoating the genome is thought to involve cellular factors Ran-GTP and importin β (Ojala *et al.*, 2000). Viral proteins including UL36 and UL25 are also essential for these early events following infection, as certain

virus mutants with lesions affecting these proteins fail to release viral DNA into the cell nucleus (Preston *et al.*, 2008; Roberts *et al.*, 2009). An interaction has been described between UL25 and a component of the nuclear pore complex, CAN/Nup214, and furthermore, depletion of CAN/Nup214 delayed the release of viral DNA into the nucleus (Pasdeloup *et al.*, 2009). The portal protein UL6 is cleaved upon viral DNA exit from the capsid (Newcomb *et al.*, 2007).

1.4.2 Localisation of HSV-1 DNA in infection

Upon entry into nucleus, incoming viral genomes can be seen as discrete spots surrounded by small nuclear substructures known as ND10 domains. ND10 domains comprise the major organising protein, PML, and several other cellular components including Daxx and Sp100, and their SUMO-modified isoforms (Negorev & Maul, 2001). These domains are also found in uninfected nuclei, and have a variety of functions including regulation of gene expression, chromatin dynamics, DNA repair and the interferon repsonse. It has been shown that ND10 are dynamic structures that move to accumulate around incoming genomes, rather than genomes localising to existing ND10 sites (Everett & Murray, 2005). ND10 are thought to make up part of an intrinsic cellular defence against viral infection formed around the viral DNA that act to repress the viral genome and restrict transcription.

Very soon after infection with wt HSV-1, these ND10 domains are disrupted in a process that requires the viral immediate early protein ICP0 (Maul *et al.*, 1993). ICP0 is an E3 ubiquitin ligase which induces the proteosome-dependent degradation of PML and subsequent breakup of the ND10 domains (Everett *et al.*, 1998). This disruption of ND10 and associated de-repression of the genome allows the recruitment of cellular and viral factors needed for transcription of viral proteins, resulting in the formation of small pre-replicative sites. Initial transcription and replication of HSV-1 DNA occurs in these small pre-replicative sites adjacent to the original ND10 site.

After repeated rounds of transcription and DNA replication, the pre-replicative sites form into larger replication compartments (RCs). It is here in the replication compartments that DNA replication, late gene expression, capsid assembly and DNA packaging take place. Proteins involved in DNA replication and packaging, as well as virus capsids, have been shown to localise to RCs, (de Bruyn Kops *et al.*, 1998; Lamberti & Weller, 1998; Phelan *et al.*, 1997; Yu & Weller, 1998a). These replication compartments are often defined by the presence of the HSV-1 single stranded DNA binding protein ICP8 (Quinlan *et al.*, 1984).

Many different cellular proteins have also been identified within or close to RCs, including those involved in DNA damage repair and chromatin remodelling (which interact with ICP8), and chaperones involved in the heat shock response and protein folding (Burch & Weller, 2004; Taylor & Knipe, 2004).

1.4.3 Circularisation of DNA

Soon after entry into the nucleus, the linear double stranded DNA viral genome circularises and it is this circular DNA which is thought to be the template for DNA replication (Garber *et al.*, 1993; Poffenberger & Roizman, 1985). Endless molecules can be detected as early as one hour post infection and these endless molecules have been shown to be circularised genomes rather than simply genomes that are joined end to end. (Strang & Stow, 2005). It is thought that circularisation may occur via direct ligation of the termini, although this has not been demonstrated *in vitro*, and so it is possible that homologous recombination between terminal repeats is involved. This circularisation of the genome does not require viral DNA replication or protein synthesis, indicating that the process is mediated by cellular factors (Strang & Stow, 2005). The regulator of chromatin condensation 1 (RCC1) has been implicated in genome circularisation, and infection of cells lacking RCC1 led to a block in virus replication, due to a reduction in both genome circularisation and DNA synthesis (Strang & Stow, 2007; Umene & Nishimoto, 1996). RNAi-mediated knock down of DNA ligase IV and its cofactor XRCC4 also reduces the formation of endless genomes (Muylaert & Elias, 2007). It has been suggested that one of the viral immediate early proteins, ICP4 is essential for genome circularisation (Su *et al.*, 2006), although this conflicts with the earlier data showing that no *de novo* protein synthesis is required for genome circularisation.

1.4.4 HSV-1 gene expression

All herpesviruses have a controlled temporal cascade of gene expression, with three classes of genes, designated immediate early (IE, α), early (E, β), and late (L, γ) (Honess & Roizman, 1974). Neither IE nor E genes are reliant on DNA replication for their expression, and all three classes of genes are transcribed by the host RNA polymerase II utilising viral and host transcription factors.

The IE genes begin to be expressed very soon after infection. Many of these genes encode regulatory proteins needed for early gene expression and are activated by viral and cellular

transcription factors. The viral transactivator VP16 is brought into the cell as a component of the tegument and associates with the host protein HCF. This interaction of VP16 with HCF is required for the entry of VP16 into the nucleus (La Boissiere *et al.*, 1999). This is followed by association of these two proteins with the host protein Oct-1 to form the immediate early transcription initiation complex. This complex can then bind to conserved TAATGARAT motif (where R = purine) in the IE gene promoters to stimulate transcription of the IE genes, encoding proteins ICP0, ICP4, ICP22, ICP27, ICP47 and US1.5.

The IE protein ICP0 acts as a promiscuous transactivator which can induce expression from all classes of herpesvirus genes. In transient expression assays, ICP0 was shown to act co-operatively with another IE protein, ICP4, to activate many cellular and viral genes (reviewed by Hagguland (2004).

ICP4 is involved in both positive and negative regulation of viral gene expression, and is required for efficient expression of all post-IE genes at the transcriptional level (Watson & Clements, 1980). In the absence of ICP4, all post-IE gene expression is blocked. It has been shown to bind to DNA (both consensus and non-consensus sequences) (Kristie & Roizman, 1986; Michael *et al.*, 1988). ICP4 also interacts with multiple transcription factors (TFs) and is thought to increase gene expression by facilitating the binding of TFs to the TATA box on viral β and γ promoters and enhancing formation of the pre-initiation complex (Grondin & DeLuca, 2000).

As well as stimulating viral gene expression and protein production, a number of the IE genes act to decrease host protein expression and to improve the cellular environment for the viral life cycle. ICP27 is required for post-IE viral gene expression, but also inhibits transcription of many host genes, reviewed by Smith (2005). It can also act at a later stage, post-transcriptionally, to inhibit RNA splicing and promote the export of unspliced mRNAs (Hardwicke & Sandri-Goldin, 1994). This results in decreased host protein synthesis as the host intron-containing mRNAs are not exported into the nucleus for translation. As only four lytic HSV-1 genes are spliced, this has a minimal effect on viral gene expression. Three of the four spliced HSV-1 genes are expressed from IE promoters before maximal splicing inhibition, and the fourth, UL15, is expressed as a late (γ_2) transcript. It is not yet certain how UL15 escapes this splicing inhibition, although it may be spliced using a different mechanism.

The ICP47 protein has no known role in regulating viral gene expression but is also involved in subversion of cellular processes. ICP47 acts to downregulate the host immune response by inhibiting the processing of viral peptides through the TAP pathway. This blocks the presentation of the viral peptides on MHC class I molecules to T cells and the establishment of an anti-viral T cell response (Fruh *et al.*, 1995).

Production of IE genes stimulates the next class of genes in the cascade – the early (β) genes. The E genes reach peak expression at 5-7 hours post infection. These encode the proteins responsible for viral DNA replication, and the appearance of these early gene products signals the onset of viral DNA synthesis. This stimulation of E gene expression is accompanied by a decrease in the transcription of IE genes, through a number of mechanisms. ICP4 negatively regulates its own expression by binding to DNA near the promoter. Some E genes (for example ICP8) also down regulate IE gene expression (Honess & Roizman, 1974).

The late, or γ, genes are divided into two classes depending on their expression kinetics. Leaky late (γ1) genes are expressed at low levels prior to DNA synthesis, but true late (γ2) genes have an absolute requirement for DNA synthesis. The late genes encode components of the viral particle and proteins involved in capsid assembly, encapsidation and virion maturation. As with the early genes, their expression is dependent on the presence of earlier viral proteins, for example ICP4.

1.4.5 DNA replication

DNA replication takes place in replication compartments after the expression of immediate early and early genes, using the circularised DNA as a template. As described earlier, the genome contains two related *cis*-acting sequences, ori_L and ori_S, that act as origins of replication.

The DNA is replicated using a virally-encoded replication complex comprising the proteins UL9, UL29 (ICP8), UL42, UL30, UL5, UL8 and UL52. These proteins were identified by studies which found that plasmids containing the viral origins of replication could be efficiently replicated upon co-transfection with cloned HSV-1 fragments encoding these genes (Wu *et al.*, 1988). Studies using both temperature sensitive and viral null mutants targeted to each of these genes confirmed their essential role in the replication

of DNA. The function of each of these genes is discussed below and reviewed by Lehman (1999).

UL9 encodes the origin binding protein (OBP) which exists as a homodimer and can bind to two inverted repeats within *ori*$_S$ in a co-operative fashion (Elias & Lehman, 1998). This DNA-binding activity resides in the C-terminal portion of the protein (Arbuckle & Stow, 1993). The N-terminus of UL9 possesses ATP-dependent helicase activity, which enables the protein to unwind up to 1 kbp of DNA from the origin for replication.

The UL29 gene encodes ICP8, the single-stranded DNA binding protein that is used as a marker for replication compartments. ICP8 binds single stranded DNA very effectively and cooperatively, with no sequence specificity. ICP8 interacts with the extreme C-terminus of UL9, greatly stimulating its ATPase and DNA helicase activities (Boehmer *et al.*, 1993). In conjuction with UL9, ICP8 can open up the DNA around the viral origin of replication, allowing access to the remaining replication enzymes prior to the creation of a replication fork. ICP8 has been shown to stimulate the activity of both the DNA polymerase and the helicase-primase complexes (Hamatake *et al.*, 1997; Ruyechan & Weir, 1984). The effect on the helicase-primase is mediated through an interaction between ICP8 and UL8.

The viral DNA polymerase exists as a heterodimer within cells, made up of subunits UL30 and UL42. The interaction of these two proteins is essential for viral replication (Digard *et al.*, 1993; Stow, 1993). The polymerase activity is associated with the UL30 subunit and this protein shares extensive homology with other cellular and viral DNA polymerases (Blanco *et al.*, 1991). UL30 also shows 3'-5' exonuclease activity, meaning that is has an intrinsic proof-reading ability (Knopf, 1979). The UL42 subunit binds to DNA and increases the processivity of the catalytic subunit. UL42 binds to the polymerase through multiple interactions.

The HSV-1 helicase-primase (primosome) consists of a 1:1:1 association of the UL5, UL8 and UL52 gene products. A sub-assembly of UL5 and UL52 was shown to possess ATPase, primase and helicase activity and so constitutes the core enzyme (Calder & Stow, 1990; Dodson & Lehman, 1991). UL5 specifies the helicase activity which uses either ATP or GTP to unwind DNA in the 5'-3' direction, whereas UL52 confers the primase activity of the complex. The UL8 subunit has no detectable enzymatic activities but has been shown to enhance both the helicase and primase activity of the UL5-UL52 complex.

DNA synthesis is proposed to be initiated by the interaction of UL9 and ICP8 and unwinding of the DNA at the origin of replication. ICP8 then coats the single stranded DNA and this allows the polymerase and helicase-primase complex to access the DNA and establish a replication fork. DNA replication proceeds via leading and lagging-strand synthesis.

The current widely held model for the mechanism of HSV-1 DNA replication is that it initially progresses by a UL9- and origin-dependent theta mechanism to amplify the circularised viral genome and produce multiple circular templates. This is then followed by a switch to a rolling circle mode of replication. This model and the structure of the replication forks are shown in figure 1.7. Attempts to reconstitute the origin-dependent HSV-1 theta DNA replication in a cell-free system have not been successful; however a number of factors are consistent with replication occurring via this mechanism. Genome circularisation is a pre-requisite for DNA replication, and UL9 is required at an early stage of DNA synthesis in HSV-1 infected cells (Blumel & Matz, 1995). Viral DNA also accumulates with non-linear kinetics at early stages, which cannot be accounted for by rolling circle replication alone. Furthermore, studies show that addition of a topoisomerase inhibitor can terminate DNA replication, presumably because the topoisomerase is needed for decatenation of circular molecules (Hammarsten *et al.*, 1996). The rolling circle method of replication has been demonstrated using extracts from insect cells infected with recombinant baculoviruses expressing the seven HSV-1 DNA replication genes (Skaliter & Lehman, 1994). This study also confirmed that neither UL9 nor the origin of replication is required for this later stage of DNA replication, and demonstrated that addition of UL9 can inhibit rolling circle replication in the presence of ori_S. Rolling circle replication generates long concatemers of the genome in head-to-tail fashion, and these are the substrates for DNA packaging.

It is not yet clear what the mechanism is by which the replication switches from theta to rolling circle replication. This may require a recombinational event such is seen in the switch from theta to rolling circle replication in bacteriophage λ.

Recombination during DNA replication leads to the creation of highly branched structures which need to be resolved before packaging. This function is carried out by the alkaline nuclease, UL12, discussed further in section 1.6.4.

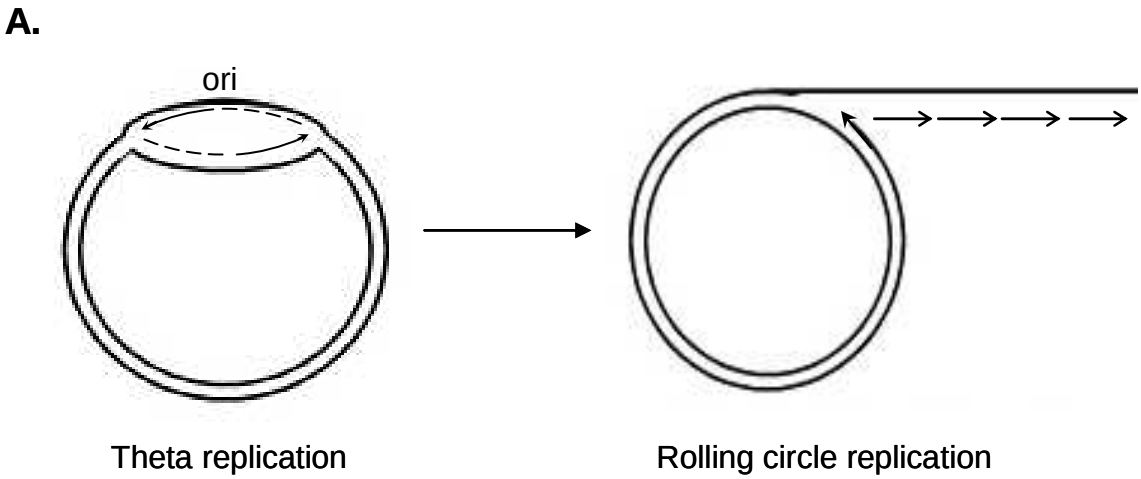

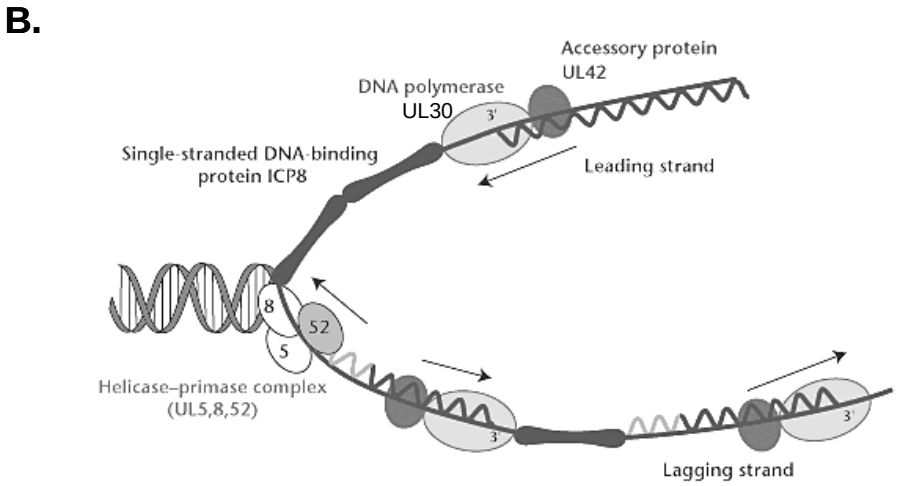

Figure 1.7: Model of HSV-1 DNA replication:

A. HSV-1 DNA synthesis is thought to originate *via* bi-directional theta replication, before switching to rolling circle replication to generate concatemeric genomes.

B. Model of a replication fork. The helicase−primase complex, consisting of viral proteins UL5, UL8 and UL52, unwinds HSV DNA at the replication fork and primes both lagging-strand and leading-strand DNA synthesis (wavy grey lines). The single-stranded DNA binding protein, ICP8, binds to single-stranded template DNA. HSV DNA polymerase (UL30) and its accessory protein, UL42, promote leading- and lagging-strand DNA synthesis (wavy black lines). The arrows indicate the direction of movement of the DNA replication proteins. Adapted from Crumpacker and Schaffer (2002)

1.4.6 Capsid assembly and DNA packaging

Following repeated rounds of DNA synthesis, concatemeric genomes accumulate within the replication compartments. After the onset of DNA synthesis, the synthesis of γ genes encoding the proteins making up the capsid increases. As these capsid proteins accumulate, they also localise to replication compartments within the nucleus, where DNA packaging occurs. A complicated network of interactions controls the nuclear localisation of these proteins, with both preVP22a and VP19C containing nuclear localisation signals and between them recruiting the other capsid proteins into the nucleus (Rixon *et al.*, 1996). Within the replication compartments, the capsid proteins are assembled into spherical procapsids with an internal scaffold (see section 1.3.2).

Recombinant baculoviruses have been a very useful tool to study the process by which procapsids are assembled and allow identification of the proteins that are absolutely essential for this. Infection of insect cells with baculoviruses encoding the six capsid proteins (VP5, VP19C, VP23, VP26, preVP22a and the UL26-encoded protease) results in formation of capsids that are morphologically indistinguishable from B capsids. However, it has also been found that the minimal number of proteins needed for assembly of capsids is four – VP5, VP19C, VP23 and one of either preVP22a (UL26.5) or the protease (UL26) (Tatman *et al.*, 1994). Omission of the UL26 protease resulted in the formation of large-cored B capsids, containing the uncleaved form of preVP22a. In cells expressing preVP22a alone, a large number of core-like structures were found, indicating that the scaffold protein can self-assemble, and this property might be essential for the process of capsid assembly.

Capsids have also been assembled in a cell-free system using extracts from cells infected with five recombinant baculoviruses expressing VP5, VP19C, VP23, preVP22a and the protease (Newcomb *et al.*, 1996). Different stages of capsid assembly were seen by electron microscopy including partial capsids (thin angular wedges), procapsids and angularised capsids, as illustrated in figure 1.8. This provided the first evidence that the spherical procapsids were the progenitors to the angularised icosahedral capsids. This confirmed that assembly begins with a small partial capsid containing these five proteins, which grows by progressive addition of small amounts of shell and core to form a larger partial capsid and then a full procapsid. Further studies with purified components

confirmed that no cell proteins were required for assembly of capsids (Newcomb *et al.*, 1999).

The portal, made up of UL6, is the only unique vertex within the capsid, and it appears to be the point at which assembly is initiated. The interaction between UL6 and the scaffold protein is essential for its incorporation (Singer *et al.*, 2005). Although capsids can be assembled in the absence of portals, these are not competent for DNA packaging and the addition of the portal at a later stage did not allow its incorporation into the partially-assembled capsids (Newcomb *et al.*, 2005).

The packaging of herpesvirus DNA into the preformed procapsid is accompanied by maturation of the capsid and the cleavage of the scaffolding proteins encoded by genes UL26 and UL26.5. These two proteins are encoded by overlapping transcripts and share identical C-termini which are where they both interact with the capsid floor (Hong *et al.*, 1996). Both proteins are cleaved within the C-terminal portion by the UL26 protease upon maturation of the capsid, releasing them from the capsid floor. Auto-cleavage of UL26 generates the protease VP24 and scaffold protein VP21, whilst cleavage of preVP22a releases the major scaffolding protein VP22a. VP24 remains within the capsid whereas VP22a and VP21 are expelled. The cleavage of the internal scaffold is essential for DNA packaging and production of infectious virus. This was shown by studies using the temperature sensitive HSV-1 mutant *ts*1201 which has a lesion in the UL26 gene, resulting in an inactive protease. At the non-permissive temperature this mutant fails to cleave the scaffold and results in the accumulation of large-cored B capsids in the nucleus, with no production of C capsids (Preston *et al.*, 1983). It has also recently been shown that the processes of scaffold cleavage and expulsion and DNA packaging stabilise the capsid (Roos *et al.*, 2009).

Capsid maturation overlaps with viral DNA packaging and the successful end product is the mature angularised C-capsid containing the full length viral genome. These are the only capsid type able to undergo nuclear egress and further maturation. As previously discussed, A and B capsids are both formed by abortive attempts at packaging and as such are dead end products. B-capsids are thought to be angularised shells containing cleaved scaffold that have not undergone a DNA packaging event, whereas empty A-capsids are found in cells infected with viruses able to initiate DNA packaging (e.g. wt HSV-1 and mutants in the UL12 and UL25 genes), but not in cells infected with other DNA packaging mutants. The process of DNA packaging is discussed in detail in section 1.5.2.

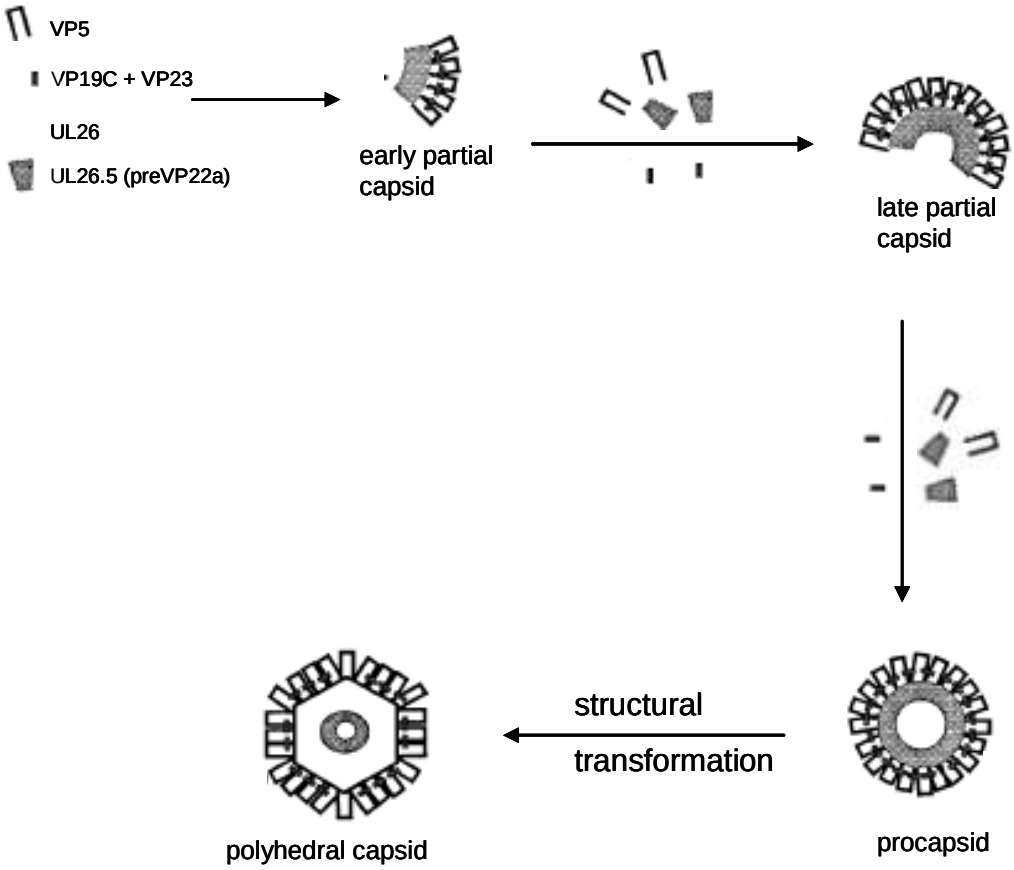

Figure 1.8: In vitro assembly of the HSV-1 capsid.

Assembly begins with an early partial capsid comprising proteins VP5, VP23, VP19C and the scaffolding proteins encoded by UL26 and UL26.5. Subsequent addition of VP5-preVP22a wedges forms a late partial capsid which finally closes, forming the spherical procapsid. This procapsid can then mature to form a angularised polyhedral capsid. No further proteins are required for the structural transformation. (adapted from Newcomb et al., 1996)

1.4.7 Maturation and egress

The current widely-accepted model for the maturation and egress of capsids is that of envelopment, followed by de-envelopment and a second re-envelopment step. In this model, DNA-filled C capsids undergo a process of primary envelopment at the inner nuclear membrane and translocate across the lumen of the nuclear membrane. This is followed by deenvelopment at the outer nuclear membrane and release of the capsids into the cytoplasm where they obtain inner tegument proteins. The capsids then acquire secondary tegument and envelope in a secondary envelopment process before exiting the cell by exocytosis (reviewed by Mettenleiter (2002; 2009).

In support of this model, stages of the envelopment and de-envelopment pathway have been visualised by electron microscopy of infected cells (Granzow *et al.*, 2001) and nuclear egress has been reconstituted *in vitro* (Remillard-Labrosse *et al.*, 2006). Furthermore, structural examination of the primary tegument of capsids within the lumen of the nuclear membrane has revealed it to be quite different to that of mature virions. The same is true of the primary envelope obtained from the INM, which has a different composition to the final envelope, containing among other proteins, UL34, but not any of the spike glycoproteins seen in the mature virion (Baines *et al.*, 2007; Fuchs *et al.*, 2002).

In order to exit the nucleus DNA-filled capsids first have to reach the nuclear membrane, which may be done by utilising actin filaments. It has been shown that nuclear actin is induced in PrV-infected cells at late times post infection, and that capsids associate with these actin filaments (Feierbach *et al.*, 2006). The first budding/envelopment step occurs at the inner nuclear membrane and requires both the UL31 and UL34 proteins. Homologues of these proteins are well conserved throughout the *Herpesviridae*, and HSV-1 or PrV mutants deleted in UL31 or UL34 do not undergo primary envelopment (Fuchs *et al.*, 2002; Klupp *et al.*, 2000; Roller *et al.*, 2000). These two proteins interact to form a complex which can break down the nuclear lamina and the layer of host chromatin at the periphery of the nucleus, possibly by interacting directly with nuclear lamins and recruiting cellular protein kinases as well as the viral protein kinase US3 (Mou *et al.*, 2008; Park & Baines, 2006; Simpson-Holley *et al.*, 2004). This disruption of the lamina allows the capsids to bud into the perinuclear space gaining a primary tegument and envelope. The capsid then translocates across the lumen of the nuclear membrane and the primary

envelope is lost by fusion with the outer nuclear membrane (ONM), releasing the capsid into the cytoplasm. Little is known about the molecular mechanisms of this fusion, but it appears to have a mechanism distinct from that of fusion during entry. A number of reports have suggested differing requirements for the gB and gH glycoproteins in the nuclear exit fusion of HSV-1 and PrV (Farnsworth *et al.*, 2007; Granzow *et al.*, 2001). US3 is also important for efficient nuclear exit.

An alternative pathway has been suggested for nuclear exit whereby nucleocapsids can also gain access to the cytoplasm through nuclear pores which are grossly enlarged during HSV-1 infection (Leuzinger *et al.*, 2005). However, other groups have demonstrated that the morphology of nuclear pores is not affected until very late in infection, and no electron microscopy images of capsids in transit through nuclear pores have been published. Overall, the great majority of the biochemical and morphological evidence supports the envelopment and de-envelopment pathway, as described above.

After nuclear egress, the capsids have to acquire the full complement of tegument proteins in order to exit the cell. The acquisition of tegument is controlled by a complex network of protein-protein interactions. Numerous physical interactions have been identified which appear to have significant redundancy, as reviewed by Mettenleiter (2006), but only a few have been demonstrated during infection using mutant viruses. The highly conserved inner tegument protein, UL36, is essential for egress and has been shown to interact with both the major capsid protein, VP5, and another component of the inner tegument, UL37. UL36 is a multifunctional protein involved in intracellular transport and vesicular transport of enveloped virions. Both UL36 and UL37 are essential for formation of virions, as deletion mutants of either of these proteins results in an accumulation of unenveloped C capsids within the cytoplasm (Desai *et al.*, 2001; Desai, 2000; Roberts *et al.*, 2009). Addition of UL36 to capsids may also be dependent on the capsid protein UL25 as these have been shown to interact following transient expression and co-immunoprecipitation (Coller *et al.*, 2007). UL36 and UL37, along with US3, constitute an inner tegument layer which coats the nucleocapsid first during tegumentation in the cytoplasm.

Secondary envelopment is driven by proteins linking the inner tegument to the outer tegument/glycoprotein complexes. One of these proteins is VP16 (UL48), which is essential for outer tegument addition (Mossman *et al.*, 2000). Yeast-two-hybrid studies have identified interactions between VP16 and a number of inner tegument and capsid proteins, including UL36, VP26 and VP19C. VP16 has also been shown to interact with

outer tegument proteins and the cytoplasmic tails of a number of glycoproteins. A complicated network of interactions has been described between the outer tegument and glycoproteins which may be responsible for secondary envelopment. However, many of these interactions show considerable redundancy and it is not yet clear which are of functional significance in viral assembly.

As discussed earlier, herpesvirus entry requires dynein-mediated microtubule transport, and conversely, virus egress requires kinesin-mediated plus-end transport (Lyman & Enquist, 2009). It is still unclear as to whether herpesviruses use the cellular ESCRT pathway and how exactly intracytoplasmic capsids are directed to sites of secondary envelopment. The viral envelope is thought to be derived from the trans-Golgi network (TGN). HSV-1- glycoproteins are synthesised in the endoplasmic reticulum and then travel to the TGN for the final envelopment. The conserved gM glycoprotein may play a role in accumulation of viral glycoproteins at the TGN by collecting viral glycoproteins at the budding site or preventing their transport to the plasma membrane (Crump *et al.*, 2004). However, gM is not required for virion formation. Several herpesvirus glycoproteins also contain endocytosis motifs in their cytoplasmic tails. This allows them to be endocytosed and so may play a role in their incorporation into the virus envelope (reviewed by Brideau (2000)). Up to 49 distinct host proteins have also been identified within HSV-1 extracellular virions, which are presumably incorporated during the packaging, tegumentation and envelopment processes (Loret *et al.*, 2008).

Once tegumentation and secondary envelopment have occurred, the vesicles containing enveloped virions are transported to the plasma membrane and infectious virus released by exocytosis. Evidence suggests that cell-to-cell spread is also important in virus dissemination. This process requires gE/gI glycoproteins in addition to those needed for extracellular spread (reviewed by Johnson (2002)).

1.4.8 Latent infection

As well as the lytic replication cycle described above, herpesviruses also have the ability to establish latency, which in HSV-1 is in the ganglia innervating the site of primary infection(Stevens & Cook, 1971). The key factors in the establishment of latency are the repression of the HSV-1 genome and the failure to initiate productive immediate early gene expression.

This absence of IE gene expression is due to a lack of transcriptional activation, as evidenced by the fact that 'quiescent' infections are established by viruses defective in the major IE transactivators (Preston & Nicholl, 1997). This may be due to the activation complex of VP16, Oct1 and HCF not forming in the neuronal cell bodies. It has been shown that HCF is located in the cytoplasm in neurons and can sequester VP16, thereby preventing it from entering the nucleus of the neuron and activating gene expression (Kristie *et al.*, 1999).

The latent genomic DNA is present as circular episome, and there is variation in latent DNA copy number in neurons (Rock & Fraser, 1983; Sawtell, 1997). Chromatin structure and modifying enzymes appear to play a role in the transcriptional activation and repression of regions of herpesvirus DNA. During productive infection, VP16 is thought to recruit activating histone acetylases and chromatin remodelling enzymes to IE promoters to allow gene expression. However in latency, the genome is maintained in a repressed state and the lytic gene promoters show a decreased association with acetylated histones (Kubat *et al.*, 2004).

During latency, only one set of viral gene products is expressed. These are the latency associated transcripts (LATs), a series of spliced RNAs expressed from the LAT gene transcription unit, which maps to the repeat sequences flanking the U_L region. The LATs are stable non-polyadenylated RNAs and no proteins are translated from these transcripts. Despite much research, the precise role of the LATs during latency is still unclear. It has been suggested that LAT null viruses have reduced reactivation from latency, although this may also be due to decreased establishment of latency in these situations (Jones, 2003). A number of studies have also implicated LATs in protecting infected neurons from death. This may be by reducing lytic viral gene expression, as expression of LATs can reduce viral gene expression and replication in cultured cells. LATs have also been found to have an anti-apoptotic function in tissue culture cells and promote the survival of infected neurons *in vivo* (Ahmed *et al.*, 2002).

The control of the lytic-latent switch and the reactivation of latency is very complex, and not yet fully understood. As the establishment of latency is due to repression of the genome and the lack of immediate early gene expression, then conversely, reactivation from latency requires de-repression of the genome, followed by IE gene expression. In both tissue culture systems and infected individuals, the virus is reactivated after an external

stimulus; for example physical trauma to tissues, UV light, or physical or emotional stress to the infected individual.

Cellular mechanisms must be involved for the initial de-repression of the genome, and HCF has been implicated in initiation of transcription after latency, as it is recruited to the IE promoters during reactivation (Whitlow & Kristie, 2009). After de-repression of the genome, IE gene expression needs to be activated and ICP0 may be involved through its transactivating ability and degradation of cellular components. This has been supported by studies confirming that ICP0 null mutant viruses show greatly reduced reactivation from latency (Halford & Schaffer, 2001). LATs have also been widely accepted to play a role in this process as LAT negative viruses reactivate less efficiently than wt HSV-1. It has recently been suggested that after the initial reactivation, *de novo* expression of VP16 also regulates entry into the lytic cycle (Thompson *et al.*, 2009).

1.5 DNA cleavage and packaging

DNA packaging represents the convergence of two independent pathways taking place in the infected cell, those of DNA replication and capsid assembly. The replicated concatemeric DNA and preformed procapsids are brought together at RCs within the cell. Packaging signals in the DNA are recognised and cleaved by a protein complex known as a terminase and a unit genome is actively inserted into the capsid through a channel at one of the capsid vertices. The processes of DNA cleavage and packaging are very tightly coupled. As described previously, DNA packaging is accompanied by cleavage of the internal scaffold of the procapsid, and associated angularisation of the capsid.

1.5.1 Bacteriophage DNA packaging

Many parallels have been drawn between HSV-1 and dsDNA bacteriophage, and similarities between capsid architecture and the packaging process have led to suggestions of a possible common ancestry between them (Baker *et al.*, 2005; Booy *et al.*, 1991; Davison, 1992; Trus *et al.*, 2004). Bacteriophage therefore represent a useful model for the study of DNA packaging within the herpesviruses.

The dsDNA phage can be split into three groups, according to differences in their genomes; 1.) Linear genomes with unique nucleotide sequence at the termini (for example λ, T7 and T3); 2.) Linear genomes with a non-unique nucleotide sequence at the ends (for example T4 and SPP1); 3.) Genomes with a covalently-attached terminal protein which primes DNA replication (for example Φ29).

Despite these differences in genome organisation, many central features of DNA packaging and the proteins involved are conserved amongst most dsDNA phage. These are discussed in more detail below and have also been reviewed (Fujisawa & Morita, 1997; Rao & Feiss, 2008).

The prohead in phage is the equivalent structure to the procapsid in herpesviruses and is assembled separately prior to DNA packaging. The prohead has one unique vertex, the portal, made up of a connector protein. To date, all connectors have been identified as a ring of 12 subunits surrounding a central channel through which the DNA is inserted. This similar structure is conserved despite very little similarity between the amino acid sequences of the different connector proteins. A narrow 'stalk' domain protrudes outside the prohead, which provides the surface for docking and assembly of the packaging motor. The prohead of Φ29 is unusual in that it also contains a small packaging RNA (pRNA). This pRNA has short complementary sequences that enable the formation of an oligomeric ring on the portal (Guo *et al.*, 1987). This pRNA is required for the docking of the packaging complex onto the portal. As with herpesviruses, assembly of the prohead is initiated around the portal structure. In some phage, the proheads can assemble in the absence of the portal protein, but these prohead shells are not competent for DNA uptake.

A packaging enzyme, known as the terminase, is essential for the encapsidation of DNA by all phage (and herpesviruses). This terminase is involved in the recognition and cleavage of viral DNA and the active translocation of the genomic DNA into the prohead. Terminases exhibit a DNA-dependent ATPase activity that is thought to provide the energy necessary to drive the thermodynamically unfavourable packaging process. In all bacteriophage studied so far, the terminase consists of a heterodimer comprising a large and small subunit. The two subunits of the terminase have been identified as encoding the different activities needed to cleave and package the DNA. The small subunit is needed for recognition of the packaging signal on the DNA concatemer, wherease the large subunit is required to bind to the connector protein on the prohead, and is responsible for cleavage and translocation of the DNA.

Several conserved motifs have been identified in the large subunits of all bacteriophage studied thus far. This includes a consensus sequence known as a Walker motif (amino acids GXXXXGKT/S), which can be found in many enzymes capable of ATP binding and hydrolysis (Walker *et al.*, 1982). Mutational analysis in bacteriophage T4 has demonstrated the importance of these motifs for functional packaging (Kondabagil *et al.*, 2006). The terminase complex also binds to the phage prohead, and by doing so, brings together the replicated DNA and the prohead shell for the packaging process. A recent paper has described the crystal structure of the small (DNA recognition) terminase subunit of phage SP6, gp1. The gp1 protein exists as an octamer in a ring-like structure with a channel through which the DNA is presumably translocated (Zhao *et al.*, 2010). These authors suggest that the terminase may stack directly on top of the portal vertex to allow DNA packaging to occur.

The different classes of dsDNA phage, based on the genome structures described above, employ slightly different methods of initiation and termination of DNA packaging. The group one phage use a sequence specific method of initiation and termination, whereby packaging is initiated by the recognition of a specific packaging signal (*pac* or *cos*) on the DNA. This is followed by an initial cleavage event to generate the genomic termini and unidirectional packaging of the genome. Packaging is terminated by a second site-specific cleavage at the packaging signal and one exact genome length of DNA is packaged. The situation in phage with group 2 genomes with non-unique terminal sequences (for example P1, P22 and T4) is slightly different. Initial cleavage occurs near to packaging signals (*pac* sites) in the genome and the DNA is packaged using the same mechanism as above. However, the termination event is not sequence dependent, and instead occurs only when the prohead is full and approximately 102% to 110% of the genome has been packaged (dependent on the phage). This results in genome ends in virions being non-identical and terminal redundancy of packaged DNA. Group 3 genomes replicate their DNA as monomers and in this case, there is no need for a DNA cleavage reaction. The protein covalently attached to the genomiC-terminus functions like the small terminase subunit, and this, the pRNA sequences and a large terminase subunit are essential for packaging (Bjornsti *et al.*, 1982; Guo *et al.*, 1987).

In all phage that replicate their DNA as concatemers, the termination of packaging is closely linked to the capsid filling. Even those phage which make precise sequence-specific cleavage events (for example λ) will ignore the termination sequences if significantly less than one genome length has been packaged (Catalano *et al.*, 1995). It has

been proposed that DNA packaging causes a conformational change in the portal, and the portal acts as a "sensor" to detect the filling of the phage head and activate cleavage by the terminase. Specific mutation of the portal in SPP1 leads to packaging of less than unit-length DNA (Tavares *et al.*, 1995).

Packaging is accompanied by an expansion in the prohead and rearrangement of the major capsid protein to generate the mature shell. The DNA is proposed to be cylindrically spooled around the axis of the portal channel. Cryo-electron microscopy has been used to examine the structural organisation of the encapsidated DNA and the DNA was found to form layers around the inside of the icosahedral shell (Cerritelli *et al.*, 1997). The DNA is under very high pressure within the phage head and is present in a liquid-crystalline state.

The phage that generate concatemers package their DNA genomes in a processive manner. After the termination cleavage, a second packaging event can be initiated from the cleaved genomic end. The terminase therefore disassociates from the DNA-filled head but remains associated with the DNA concatemer. This DNA/terminase complex is now free to bind to the next empty prohead and repeat the packaging process.

Many phage also encode proteins not directly involved in the translocation of DNA but with other roles in the packaging process. These include proteins required at a later stage of encapsidation, which are involved in retention of the packaged DNA within the phage capsid. Some phage (for example P22 and SPP1) encode head completion proteins that act to plug the portal after the full genome has been packaged. The addition of the head completion proteins may also cause release of the terminase from the phage head and form a binding site for the tail. Other phage have stabilisation proteins which bind to various sites on the external surface of the phage head, for example Soc of phage T4 (Qin *et al.*). DNA packaging is accompanied by an expansion in the prohead, revealing binding sites for these proteins.

Some phage depend on other accessory proteins for correct assembly of the prohead prior to DNA packaging. The *E. coli* host GroES-GroEL chaperone complex is required by many phage for growth and folding of their structural proteins (Tilly *et al.*, 1981; Zeilstra-Ryalls *et al.*, 1991). However, phage T4 encodes its own chaperonin, gp31, homologous to the GroES protein, which is required for correct folding the T4 major capsid protein (van der Vies *et al.*, 1994).

As in HSV-1, phage DNA replication can generate long head-to-tail concatemers which can undergo recombination, creating complex branched structures. These branches need to be resolved before the genome can be packaged. Nucleases have been identified in a number of bacteriophage, including endonuclease VII of phage T4 and endonuclease I of phage T7, where they are involved in the resolution of branches and junctions in double stranded DNA genomes (de Massy *et al.*, 1987; Kemper & Janz, 1976). These nucleases are not absolutely essential for the process of DNA packaging, but can greatly increase the generation of viable virus.

1.5.1.1 Bacteriophage lambda DNA packaging

The packaging process in bacteriophage lambda is one of the most extensively studied and is reviewed by Feiss & Catalano (2005). Since the genomic termini are generated from concatemers by signal-specific cleavage, as occurs in herpesviruses, it represents a good model for DNA packaging in HSV-1. The incoming phage genome is circularised by ligation of its cohesive ends. The λ DNA is replicated by a bi-partite mode of DNA synthesis, as in HSV-1, initially via the theta mode and then proceeding to rolling circle replication. The packaging signal is the 200 bp *cos* site found at the junction between genomes in viral concatemers. Within this is the *cos*N site, where cleavage occurs. Other sequences within this site have also been shown to be important, with *cos*B required for initiation and termination cleavage events. *cos*B contains a series of repeat elements and a binding site for the host protein IHF (integration host factor). A further site, *cos*Q, is located upstream from cosN and is needed for the termination cleavage.

The terminase is made up of the large subunit, gpA, and small subunit, gpNu1. A recombinant terminase has been purified, showing the holoenzyme has the stoichiometry of one gpA to two gpNu1 (Maluf *et al.*, 2005). gpNu1 is essential for the recognition of concatemeric DNA and assembly of the terminase complex at the portal. The N-terminal portion of gpNu1 can recognise and bind to the *cos*B site, whereas the C-terminal section is involved in binding to gpA. gpA encodes the enzymatic activities and has been shown to have endonuclease, ATPase and helicase properties (Hwang & Feiss, 1996). As with all other identified terminase large subunits, gpA contains a conserved Walker motif.

Lambda packaging is initiated by the binding of a host protein, integration host factor (IHF), to the phage DNA, which induces a bend in the duplex, allowing recruitment of gpNu1 to *cos*B. gpA, through its interaction with gpNu1 and the repeat elements of *cos*B,

then binds to the *cos*N site. This complex nicks the two DNA strands within *cos*N to produce cohesive termini. The viral gpFI protein is an accessory protein that is directly required for the packaging process and is thought to increase the transition of the terminase from a complex that is stably bound to the *cos* sequence to a DNA packaging machine (Catalano & Tomka, 1995). ATP-dependent translocation of the DNA through the portal can then occur. Packaging occurs in a unidirectional manner with concurrent hydrolysis of ATP. Packaging is terminated when the terminase reaches the next *cos* site. The genome must again be nicked, the cohesive strands separated and the terminase dissociates from the phage shell. It is thought that *cos*Q promotes a rearrangement of the terminase to allow cleavage of the DNA and termination of packaging (Feiss & Catalano, 2005).

1.5.2 HSV-1 DNA packaging

Although far less is known about HSV-1 packaging, there are many clear similarities between the processes in dsDNA phage and HSV-1. The HSV-1 procapsid and phage prohead share many structural similarities and maturation is thought to proceed via similar pathways. HSV-1 DNA packaging is reviewed by Homa and Brown (1997).

All herpesviruses encode packaging signals at their genomic termini, in a similar manner to bacteriophage λ *cos*, and the initiation and termination cleavage events are performed in a sequence-specific manner. Several of the proteins required for HSV-1 packaging perform similar roles to those in phage packaging, for example the portal and terminase enzyme. HSV-1 also encodes a protein thought to be involved in stabilisation of filled capsid (UL25) and a nuclease, analogous to those in bacteriophage, that acts to resolve branched structures following DNA replication (UL12).

A model for herpesvirus DNA packaging, consistent with the current literature, is presented in figure 1.9. Concatemeric DNA is generated by repeated rounds of DNA synthesis and preformed procapsids localise to the replication compartments by an as-yet unknown mechanism. Packaging is thought to initiate when a packaging signal on the concatemeric DNA is recognised by the viral terminase, leading to the assembly of a functional packaging complex of terminase, DNA and procapsid. The duplex is cleaved and DNA translocated through the unique portal vertex into the preformed procapsid. A second cleavage event to terminate packaging occurs when a unit length genome has been translocated. As previously mentioned, DNA packaging is accompanied by cleavage and expulsion of the scaffold protein, and angularisation of the capsid. As with bacteriophage,

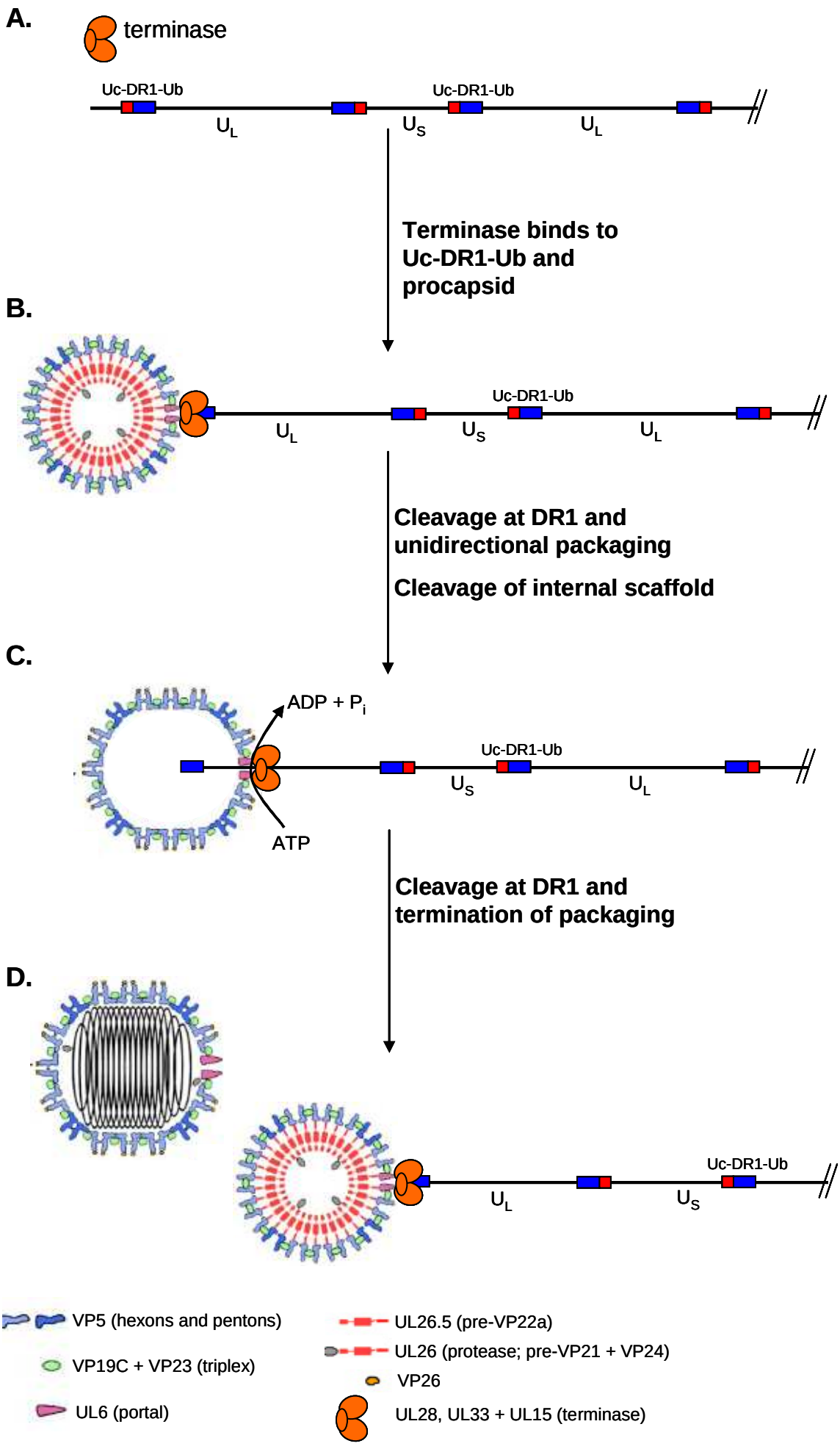
A.
terminase
Uc-DR1-Ub
Uc-DR1-Ub
U_L
U_S
U_L
Terminase binds to Uc-DR1-Ub and procapsid
B.
Uc-DR1-Ub
U_L
U_S
U_L
Cleavage at DR1 and unidirectional packaging
Cleavage of internal scaffold
C.
ADP + P_i
Uc-DR1-Ub
U_S
U_L
ATP
Cleavage at DR1 and termination of packaging
D.
Uc-DR1-Ub
U_L
U_S
VP5 (hexons and pentons)
VP19C + VP23 (triplex)
UL6 (portal)
UL26.5 (pre-VP22a)
UL26 (protease; pre-VP21 + VP24)
VP26
UL28, UL33 + UL15 (terminase)

Figure 1.9: DNA packaging by HSV-1.

A. DNA packaging is initiated when the terminase complex (UL15, UL28 and UL33) recognises the minimal packaging sequence, Uc-DR1-Ub (blue) on the replicated concatemeric DNA.

B. The terminase in turn can interact with the portal vertex (UL6) of a nascent procapsid. The terminase cleaves the DNA within DR1 and releases the S terminus (which is thought to be degraded). This results in a complex of the terminase with the L terminus of the genome, which is inserted into the procapsid.

C. Unidirectional packaging occurs, with the concurrent hydrolysis of ATP. This is accompanied by cleavage and loss of the procapsid scaffold and angularisation of the capsid.

D. When the terminase reaches the next Uc-DR1-Ub sequence, the termination cleavage releases the packaged genome inside the C capsid. Packaging is thought to be processive and the terminase remains associated with the L-terminus of the concatemer, where is can initiate another round of packaging by interacting with another procapsid.

herpesvirus packaging is thought to be processive, with multiple packaging events along a concatemer being initiated by a single terminase. The packaged DNA within the HSV-1 C-capsids also adopts a liquid-crystalline conformation resembling that of packaged DNA within bacteriophage heads.

The concatemeric DNA may also be undergoing active recombination and transcription and so is likely to be associated with numerous viral and cellular protein complexes. HSV-1 DNA in infected cells is also associated with host nucleosomes, and these protein complexes all need to be removed from the DNA prior to, or concurrent with, the packaging process, as no protein is associated with the DNA inside the capsid. The packaged DNA within the capsid is coated with spermine, which has been proposed to partially neutralise the negatively charged DNA (Gibson & Roizman, 1971). It is unclear how protein complexes are removed from the DNA, but it may be that the spermine is involved in this "stripping" of DNA prior to packaging.

The following sections discuss in greater detail the current knowledge of the processes involved in herpesvirus DNA packaging and characterisation of the proteins involved. This information has mainly come from studies using HSV-1, but work on homologous proteins in other herpesviruses, for example HCMV and PrV, has also been invaluable in furthering the understanding of herpesvirus cleavage/packaging.

1.5.3 Encapsidation signal

The *cis*-acting DNA sequences required for packaging of the HSV-1 genome are located within the *a* sequences, which are present as direct repeats at the genomic termini and in inverted orientation at the junction of the L and S sequences (Stow *et al.*, 1983). In HSV-1, the *a* sequence is 200-500 bp, depending on the virus strain (Davison & Wilkie, 1981)

The structure of the *a* sequence is shown in 1.10B. Each *a* sequence is flanked by direct repeats known as DR1 and tandem *a* sequences are separated by a single DR1. The central region of the *a* sequence comprises multiple repeats of one or two other short repeat sequences, DR2 and/or DR4. The *a* sequence also contains quasi-unique sequences of approximately 80 bp termed Ub and Uc. In virion DNA, the Uc element is adjacent to the L terminus and Ub adjacent to the S terminus.

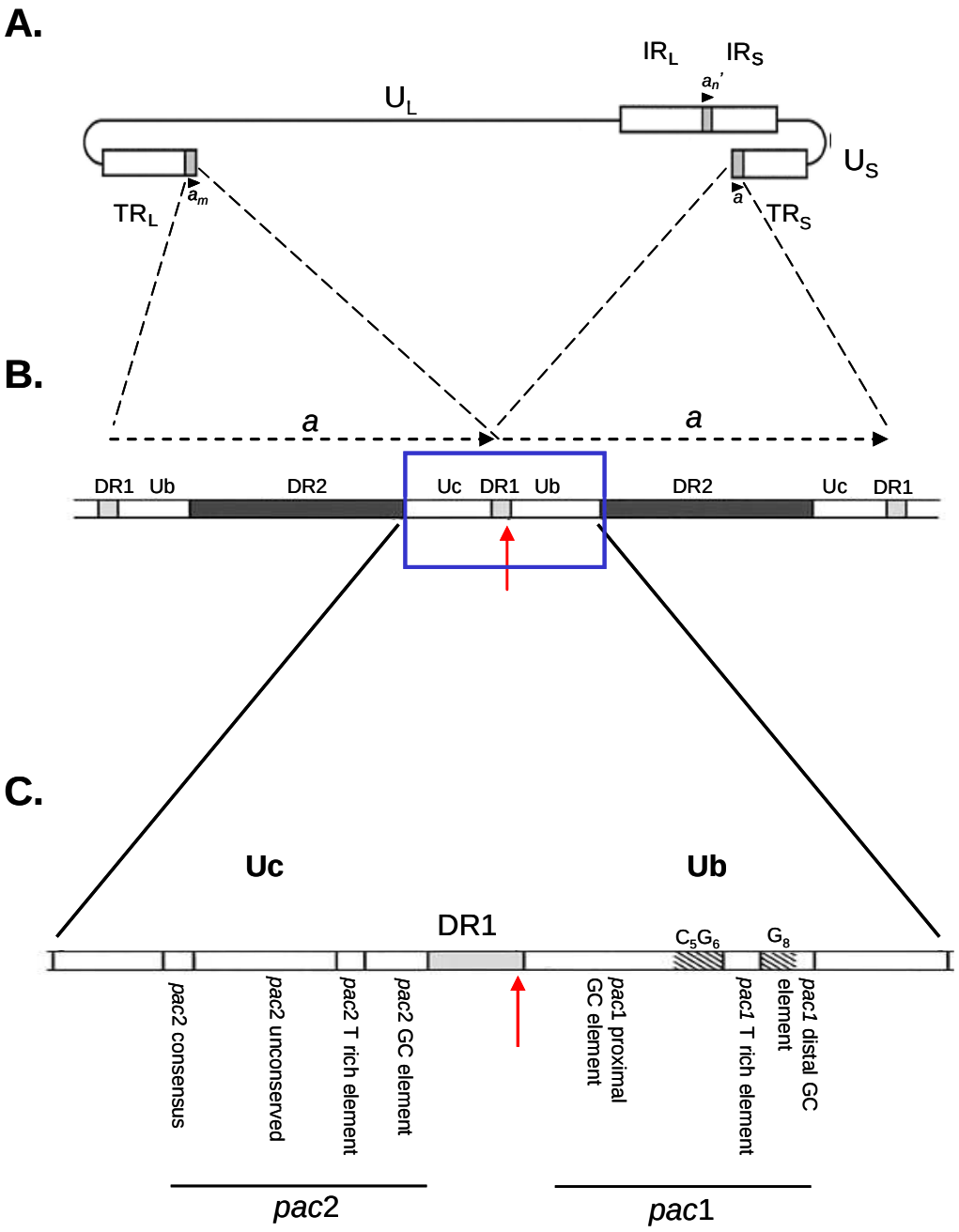

Figure 1.10: Structure of the HSV-1 packaging sequence.

A. Structure of the HSV-1 genome showing the composition and position of the repeat sequences. The orientations of the *a* sequences are indicated by arrows.

B. Circularisation of the genome by ligation of the termini brings together the two *a* sequences (indicated by the dashed arrows), separated by a DR1 repeat. This gives rise to the novel minimal packaging signal Uc-DR1-Ub (highlighted in the blue box). The site of genome cleavage is indicated by the red arrow.

C. Motifs within the Uc-DR1-Ub minimal packaging signal, indicating the *pac*1 and *pac*2 regions. The site of cleavage is indicated by the red arrow. Adapted from Hodge and Stow (2001).

Within the Ub and Uc regions are two regions, *pac*1 and *pac*2 respectively, which comprise sequences necessary for cleavage of the viral genome (Deiss *et al.*, 1986). These regions contain sequences that are highly conserved throughout the herpesviruses and it has been demonstrated that the HSV-1 *a* sequence can be functionally replaced by sequences encompassing the L-S junction of HCMV (Spaete & Mocarski, 1985). The compositions of *pac*1 and *pac*2 are shown in figure 1.10C. *Pac*1 comprises a highly conserved T rich element flanked by proximal and distal CG elements whereas *pac*2 has a consensus CGCCGCG motif with T-rich and GC-rich elements and an unconserved region.

The cleavage event occurs towards one end of the DR1 repeat, creating genomic termini containing incomplete DR1s with a single nucleotide overhang at the 3' end (Mocarski & Roizman, 1982). The majority of the DR1 sequence is associated with the L terminus. It has been suggested that the position of this cleavage is solely governed by the distance from the fixed *pac*1 and *pac*2 sequences (possibly the T elements) and that DR1 itself is not essential (Smiley *et al.*, 1990; Varmuza & Smiley, 1985). However, it has recently been shown that the sequence of DR1 is also important for initiation of cleavage, but possibly dispensable for termination (Tong & Stow, 2010). Circularisation of the genome upon entry to the cell by direct ligation of the cohesive DR1 ends fuses the *a* sequences at each terminus and therefore recreates a complete DR1 and generates a novel fragment, Uc-DR1-Ub, spanning the two end of the genome. This approximately 200 bp sequence has been identified as the minimal packaging signal (Hodge & Stow, 2001; Nasseri & Mocarski, 1988). It has been shown that a single Uc-DR1-Ub is sufficient for the packaging of viable HSV-1 genomes (Strang & Stow, 2005).

A number of different approaches have been taken to allow detailed mutational analysis of the packaging signal and identification of those sequences within Ub and Uc that are essential for genome encapsidation. The first of these involves the transfection of amplicons (bacterial plasmids encoding an origin of replication and minimal packaging signal) into mammalian cells. The provision of virus helper functions, either through superinfection with virus particles or co-transfection of viral DNA, allows amplicon DNA to be replicated and packaged so long as a functional packaging signal is present (Stow *et al.*, 1983). A second assay introduces an additional copy of the packaging signal at an ectopic site within the viral genome. The replicated DNA can then be examined to determine whether novel termini have been created due to cleavage and packaging at the ectopic site. A more recent approach involved mutating the packaging signal in the context of the viral genome, cloned as a recombinant bacterial artificial chromosome (BAC). A

cloned HSV-1 BAC from which all copies of the *a* sequence had been previously deleted (Saeki *et al.*, 1998) was used for this. Single copies of wt or specifically mutated Uc-DR1-Ub fragments were introduced into an ectopic site (the TK locus) by recombination in bacteria. The resulting recombinant BACs were transfected into mammalian cells and analysed for their ability to be cleaved at the Uc-DR1-Ub fragment and generate infectious progeny. This avoided the potential problem of recombination between ectopic and existing *a* sequences, and unlike the amplicon assays, the replicated DNA is viral and so will have a more typical frequency of packaging signals with concatemers (Tong & Stow, 2010). The most comprehensively studied packaging signals are those of HSV-1 and the murine cytomegalovirus MCMV, which have been analysed by the introduction of deletions and substitutions throughout the *pac*1 and *pac*2 regions (Hodge & Stow, 2001; McVoy *et al.*, 1998; McVoy *et al.*, 2000; Tong & Stow, 2010; Varmuza & Smiley, 1985). These studies have suggested the following general mechanism by which concatemers are cleaved and packaged.

The pac2 region is critical for DNA cleavage to initiate packaging in both HSV-1 and MCMV. Within pac2 the sequence of the T element is essential. Other important signals involved in initiation are located within the DR1 element and at or near the consensus region. The sequences of the elements flanking the pac2 T element are not important since extensive substitution mutations are tolerated. Deletion of these regions, however, severely impaired packaging, suggesting that the position of the T element relative to the DR1 and consensus signals is important in initiation of packaging and that all these motifs may function together. Following cleavage the pac2 end is inserted into the procapsid which means that in the case of HSV-1 the directionality of packaging is from the L to S end. In contrast, the pac1 region is important for the events involved in the termination of DNA packaging. All HSV-1 pac1 mutants package DNA but those affecting the proximal and distal pac1 elements, or deleting the pac1 T element are impaired in the termination of packaging, and fail to generate an S terminus. Experiments with MCMV suggest that the important sequences within the two GC-rich regions are the conserved G and C tracts that immediately flank the T element. The behaviour of the T element deletion suggests that the relative positioning of these tracts may also be crucial. More recent work has also indicated a crucial role for the DR1 element in the initiation cleavage (Tong & Stow, 2010).

1.6 HSV-1 packaging proteins

In addition to the *cis*-acting DNA sequences and those proteins making up the procapsid, six additional viral proteins are absolutely essential for DNA packaging. These are UL15, UL17, UL25, UL28, UL32 and UL33. All of these proteins are expressed from late genes and none are required for viral DNA replication or capsid assembly. UL15, UL17, UL28, UL32 and UL33, as well as the portal protein, UL6, are essential for the initiation of DNA packaging. The UL25 protein, however is not required for initiation, but appears to play a role later in the packaging process. One further protein, UL12, is indirectly involved in packaging and increases its efficiency but is not absolutely essential. The roles of these proteins in DNA packaging have been elucidated by the creation of mutant viruses using complementing cell lines, and their subsequent characterisation in non-complementing cells. The packaging-negative viruses are characterised by an accumulation of endless DNase sensitive concatemers and B capsids within the nucleus.

1.6.1 UL6

The UL6 protein is now known to form the portal that occupies the space of a penton at a single unique vertex of the capsid. Although it is not essential for the formation of capsids, it is found on all three mature capsid types and the procapsid, suggesting it is an integral part of the capsid shell (Patel & Maclean, 1995; Sheaffer *et al.*, 2001). In the absence of UL6, no viral DNA is cleaved or packaged, resulting in accumulation of endless concatemers of viral DNA, with no production of DNA-filled C capsids (Patel *et al.*, 1996a). UL6 is able to localise to the nucleus of the cell in the absence of any other viral proteins. Knock-down of the expression of the UL6 homologue in HCMV (UL104) also led to a decrease in virus growth and C capsid formation, confirming the importance of UL6 in the packaging process (Dittmer & Bogner, 2006).

Many lines of evidence indicate that UL6 forms the portal for entry of DNA in a very similar fashion to those portals identified in bacteriophage. Immunogold labelling of HSV-1 B capsids showed UL6 present at only one vertex of the capsid (Newcomb *et al.*, 2001). This study also demonstrated by electron microscopy that UL6 purified from insect cells infected with a recombinant baculovirus could form rings *in vitro*. The majority of these structures comprised of 12 copies of UL6. The structure of the rings was found to resemble those of the portals from bacteriophages P22, T4 and Φ29, and had a central channel of approximately 5 nm diameter through which the DNA is proposed to enter the capsid.

Further examination of UL6 expressed from baculovirus-infected insect cells revealed that these rings are polymorphic, exhibiting 11-, 12-, 13- and 14-fold rotational symmetry and it was suggested that it is the dodecameric form of the complex that is incorporated into procapsids (Trus *et al.*, 2004). This correlates with the situation in bacteriophage where portal variants with different numbers of subunits can be found but the only form competent to be inserted into capsids consist of a 12-membered ring. A leucine zipper motif within UL6 is essential for its self-association into stable ring structures and therefore successful DNA packaging (Nellissery *et al.*, 2007).

Much work has been carried out using cryo-electron microscopy and tomographic reconstructions to visualise the portal within the capsid shell, but there have been conflicting results. One study of A capsids identified the portal as projecting outwards from the shell (Cardone *et al.*, 2007). However, another study analysing urea-extracted capsids (to remove the pentons) identified most of the density inside the capsid shell in a similar configuration to that seen in bacteriophage P22 and ε15 (Chang *et al.*, 2007). Figure 1.11 shows a tomographic reconstruction from electron cryo-microscopy of the HSV-1 capsid and the 2 nm resolution cryo-electron microscopy of P22 bacteriophage, indicating the positions of the portals within each capsid shell. This inward-protruding model is also in agreement with the position of the portal as identified in KSHV (Deng *et al.*, 2007).

By analogy with dsDNA bacteriophage, the portal is assumed to form the docking site for the viral DNA and terminase on the capsid. Indeed immunofluorescence and immunoprecipitation studies have revealed that UL6 and the terminase subunits UL15 and UL28 interact (White *et al.*, 2003). UL6 is also required for correct association of UL15 with B capsids (Yu & Weller, 1998b).

1.6.2 UL17

The UL17 protein is dispensable for capsid assembly and viral DNA replication but required for DNA cleavage and packaging. Infection of cells with a UL17-null mutant results in an accumulation of B capsids (Salmon *et al.*, 1998).

UL17 was first identified as a component of the tegument, being the only packaging protein that is present in L particles (aberrant particles containing tegument and envelope with no capsid). It was subsequently found to also be present in the procapsid and all types

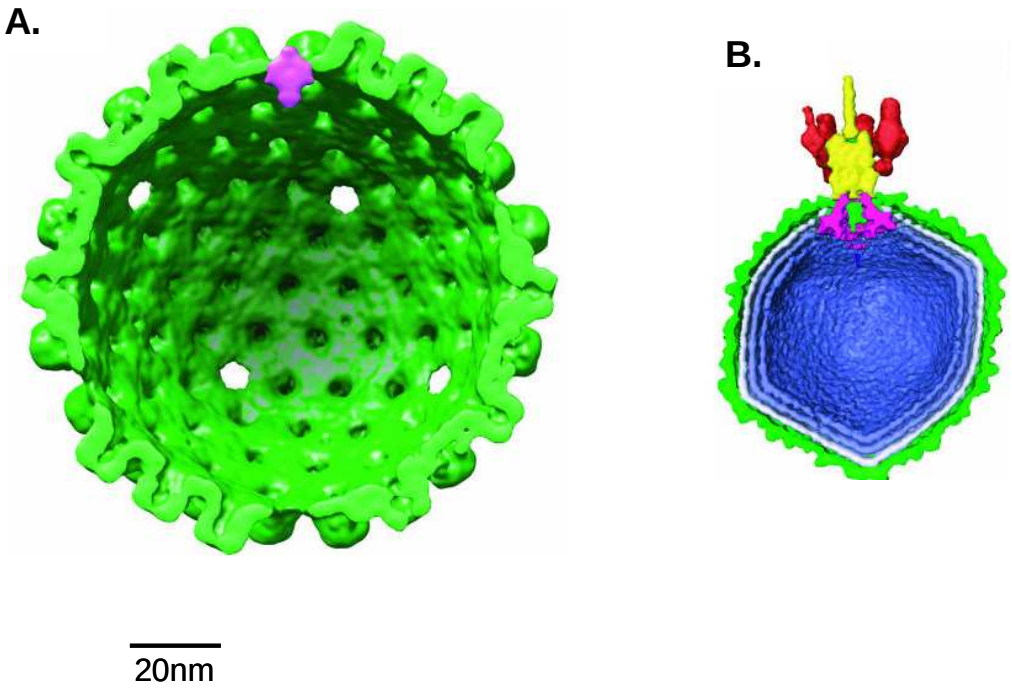

Figure 1.11: Comparison of herpesvirus and bacteriophage portal locations.

Tomographic reconstruction of the HSV-1 capsid (A). For comparison, the 2 nm resolution electron microscopy map of bacteriophage P22 is shown (B). The protal structures are indicated in pink. These figures are to scale. (Chang *et al.*, 2007)

of angularised capsid as well as the mature virion. The presence of UL17 in the procapsid suggests an early role in packaging, but it is also found in much greater amounts in virions, and so also may be important at a later stage of virion maturation (Thurlow *et al.*, 2005)

It has been suggested that UL17 may play a role in the intracellular localisation of capsid components. As previously discussed, DNA packaging occurs in replication compartments (RCs) and in wt HSV-1 infected cells the major capsid proteins are found in these RCs. However, in cells infected with a UL17-null mutant, capsid proteins VP5 and preVP22a no longer co-localised with ICP8 in RCs, but instead formed dense aggregates at the edges of infected cell nuclei (Taus *et al.*, 1998).

Immunogold staining found UL17 at multiple points on wildtype B and C capsids, and it has been shown that UL17 is required for the association of another packaging protein, UL25, with capsids. In B capsids of viruses lacking a functional UL17, the levels of UL25 were greatly decreased. This relationship appears to be reciprocal, because capsids lacking UL25 also had reduced amounts of UL17 (Thurlow *et al.*, 2006). The localisation of both of these proteins at multiple points on the capsid led to the hypothesis that they may play an indirect role within the packaging process.

1.6.3 UL25

The UL25 gene encodes a protein with roles encompassing different stages of life cycle. In contrast to the other proteins essential for DNA packaging, disruption of the UL25 gene results in an accumulation of both A and B capsids, indicating a role at a distinct stage of the packaging process (McNab *et al.*, 1998; Stow, 2001). Original studies found that during infection with a UL25 null virus, KUL25NS, the viral genome was cleaved into unit lengths with the same efficiency as wt HSV-1, but remained DNase sensitive, indicating that it was not packaged, and there was no production of C capsids. This led to the suggestion that UL25 may act to aid retention of the DNA in the capsid (McNab *et al.*, 1998).

Stow (2001) furthered these studies and found, in contrast to the results from McNab, that KUL25NS could package DNA, albeit with reduced efficiency. Furthermore, there was no evidence for genomes that had been cleaved but not packaged. Analysis of total viral DNA in cells revealed that the S terminus was significantly under-represented and the L terminus over-represented in packaged KUL25NS DNA compared to the ratios seen in wt HSV-1

DNA. This provides support for the model of HSV-1 DNA packaging occurring in an L to S direction, and implicates UL25 at a late stage in this packaging process. Pulsed-field gel analysis of packaging of both KUL25NS and amplicon DNA revealed that the packaging of full-length genomes was impaired to a larger degree than the packaging of shorter DNA molecules (Stow, 2001).

UL25 is a minor component of all capsid types and is found in greatest amounts in capsids containing DNA, with the most found in virions and C capsids, and decreasing amounts in A, B and then procapsids (Newcomb *et al.*, 2006; Sheaffer *et al.*, 2001). This, together with the phenotype of UL25 null viruses, has led to suggestions that UL25 acts to aid retention of the packaged genome in the same way as many bacteriophage proteins, either by acting as a 'plug' or to stabilise the DNA-filled capsid. One study reported that UL25 has the potential to bind double stranded DNA, supporting the theory that UL25 may act as a 'plug' at the portal (Ogasawara *et al.*, 2001). However this DNA-binding activity of UL25 has not been replicated by other laboratories and UL25 is not thought to be a portal plug. Interestingly, similar to UL25, protein gpD of phage λ is required for correct packaging of full-length genomes, but gpD deletion mutants with genomes less than 80% of wt length are viable. gpD is known to act as a head stabilisation protein, and, like UL25, is required at the late stages of packaging as the internal pressure increases as packaging nears completion.

As previously mentioned, the binding of UL25 to capsids is reliant on the presence of UL17, and this is a reciprocal interaction (Thurlow *et al.*, 2006). The association of UL25 with capsids is also mediated through interactions with other capsid proteins, VP5 and VP19C (Ogasawara *et al.*, 2001). The N-terminal 50 amino acids have been shown to be essential for the binding of UL25 to capsids (Cockrell *et al.*, 2009). Cryo-electromicroscopy has identified an extra mass on C capsids but not B capsids which is also absent from the A capsids of a UL25 null virus, which has been termed the C-capsid specific component (CCSC). This is proposed to be a heterodimer of UL17 and UL25 and is present around the vertices of the capsid (Trus *et al.*, 2007). It was suggested that as with bacteriophage, as the capsid becomes filled with DNA, conformational changes occur. This may expose sites on the capsid surface that allow binding of the CCSC. More recent work has shown UL25 to be positioned distal to the penton vertex, contacting two triplex complexes and one adjacent hexon (Conway *et al.*, 2010). A recent mutational analysis study identified some UL25 mutant proteins which could package full-length DNA but the resultant C capsids failed to be transported into the cytoplasm (O'Hara *et al.*, 2010). This

suggests that UL25 has a role in nuclear egress, perhaps through interactions with the UL31/UL34 components during primary envelopment.

UL25 is the only packaging protein that has had its crystal structure determined (Bowman *et al.*, 2006). A truncated version lacking the N-terminal region was crystallised and showed a stable core with numerous flexible loops, which may be involved in the binding of different partners during the virus life cycle. As well as its interactions with proteins on the capsid, UL25 has also been reported to bind to the tegument protein UL36. It was suggested that UL25 may therefore have a role in tegumentation as it is essential for the recruitment of UL36 to the capsid (Coller *et al.*, 2007). A recent study has also identified a role for UL25 that is very distinct from that of DNA cleavage and packaging. A temperature sensitive UL25 mutant (ts1249) shows an early block in infection, which was found to be due to a defect in uncoating of the viral genome at the NPT (Preston *et al.*, 2008).

1.6.4 UL12

Unlike the other proteins discussed here, UL12 is not absolutely essential for DNA cleavage and packaging, but it does greatly increase the efficiency of this process. The UL12 protein functions as a deoxyribonuclease with 5'-3' exonuclease and endonuclease activities, and is referred to as the viral alkaline nuclease (AN) as it is optimally effective under high pH conditions. A number of different HSV-1 mutants have been characterised with a disruption of the UL12 gene, and they all show a significant reduction in virus yield of 100-1000 fold (Patel *et al.*, 1996a; Weller *et al.*, 1990). However, no large decreases were seen in any one part of the virus life cycle – rather small reductions were observed in DNA replication, DNA packaging and egress of capsids from the nucleus (Martinez *et al.*, 1996b; Shao *et al.*, 1993; Weller *et al.*, 1990). Pulsed-field gel analysis of concatemeric DNA sythesised in the absence of UL12 showed that the DNA replication intermediates had a more complex structure than that found in wt HSV-1 infection, with an increased frequency of branches (Martinez *et al.*, 1996a).

As discussed earlier, during HSV-1 DNA replication the concatemeric DNA generated can undergo recombination events, creating complex branched structures. By analogy with dsDNA bacteriophage, which encode nucleases to resolve these branches before DNA packaging, it would be expected that HSV-1 would require a mechanism to remove the branches and junctions in the replicated DNA.

This function appears to be provided by the UL12 alkaline nuclease of HSV-1, and work on a further UL12 mutant supports this. The efficiency of both DNA replication and packaging was decreased in cells infected with an UL12 mutant compared to wt HSV-1, and the released virus had a far greater particle to p.f.u. ratio. Furthermore, gel analysis revealed abnormalities in the packaged DNA and this DNA was of reduced infectivity in transfection assays (Porter & Stow, 2004b). UL12 has also been shown to interact with the single stranded binding protein, ICP8, and this interaction mediates strand exchange *in vitro* and enhances the nuclease activity of UL12 (Reuven *et al.*, 2003; Reuven & Weller, 2005). However, no difference in intermolecular recombination was observed in cells infected with the UL12 mutant suggesting that UL12 is not required for recombination to occur during infection (Porter & Stow, 2004a)

Together, this data has led to the proposals that in the absence of UL12, the branched structures in replicated DNA are not correctly resolved and that this results in a reduction in DNA replication and packaging. However, some resolution of branches presumably occurs by an aberrant, possibly cellular process and this results in the generation of DNA containing virions which exhibit reduced infectivity.

1.6.5 Terminase – UL28, UL15, UL33

As in bacteriophage, HSV-1 has a multi-subunit terminase directly involved in the translocation of DNA into the capsid. Three proteins, UL15, UL33 and UL28 make up the putative terminase and much work has been done on clarifying the roles of each of these proteins in the packaging process. There are many lines of evidence now supporting the hypothesis of a three-subunit terminase in HSV-1, as discussed below.

The importance of each of these proteins in DNA encapsidation has been examined in null mutant viruses, isolated on complementing cell lines. Viruses disrupted in any one of these putative subunits fail to cleave or package concatemeric DNA and result in an accumulation of B capsids (Baines *et al.*, 1997; Patel *et al.*, 1996a; Tengelsen *et al.*, 1993; Yu *et al.*, 1997).

The first indication that UL15 was involved in DNA packaging came from limited sequence similarity to the gp17 large subunit of the bacteriophage T4 terminase (Davison, 1992). It has since been shown that mutations in this conserved ATP binding site of UL15 render it unable to support DNA cleavage and packaging (Yu & Weller, 1998a).

Furthermore, mutation of residues conserved between UL15 and the large subunits of phage terminases also destroyed the function of UL15 (Przech *et al.*, 2003). A direct requirement for ATP in packaging has also been shown, as depletion of ATP in infected cells prevented the encapsidation of DNA (Dasgupta & Wilson, 1999). These findings led to the proposal that UL15 is analogous to the large subunit of the terminase and provides the ATPase activity required for translocation of the DNA into the capsid. These results have been further substantiated by studies of the UL15 homologue in HCMV, UL89. Electron microscopy of UL89 has shown it to have a toroidal structure in common with a number of DNA-metabolising proteins, and it has been found to possess nuclease activity (Scheffczik *et al.*, 2002).

The UL28 protein is also thought to be a member of the terminase complex, possibly involved in the recognition and binding of viral DNA. Koslowski and colleagues first demonstrated by immunofluorescence that UL15 and UL28 interact in the absence of other proteins and that UL15 could direct the localisation of UL28 from the cytoplasm to the nucleus in co-transfected cells (Koslowski *et al.*, 1999). Furthermore, UL15 and UL28 could be co-purified as a 1:1 heterodimer from HSV-1 infected cells, suggesting that these two proteins functionally interact and that UL28 might form part of a terminase complex. Mutational analysis of UL28 indicated that at least two separate regions are involved in its interaction with UL15 (Abbotts *et al.*, 2000).

UL28 has been demonstrated to bind to novel single stranded DNA structures formed by the *pac*1 region within the *a* sequence (Adelman *et al.*, 2001). This, however, has not been confirmed, and appears to conflict with the findings that *pac*1 is required for termination but not initiation of packaging. Mutants lacking UL28 are defective in the initiation of packaging and as such it might be expected that UL28 would bind to the *pac*2 sequence. Recently, it was found that the regions of *pac*1 to which UL28 was reported to bind are defective in termination of packaging and so it is possible that UL28 is additionally involved in this process (Tong & Stow, 2010).

Studies on the UL28 homologue in HCMV, UL56, support the hypothesis that this subunit is involved in the recognition and binding of viral DNA. UL56 has been shown to bind both *pac*1and *pac*2 within the HCMV packaging signal, an interaction that is dependent on the AT rich core regions of these DNA sequences. UL56 was also able to convert a supercoiled DNA molecule containing the *a* sequence into a linear form, indicating that it encodes a nuclease activity, although the exact site of cleavage was not mapped in this

study (Bogner *et al.*, 1998). UL56 has also been demonstrated to have ATPase activity, a function that is enhanced by UL89 (Hwang & Bogner, 2002).

In contrast to the heterodimeric terminase complexes identified in bacteriophage, the HSV-1 terminase is proposed to have a third subunit, encoded by the UL33 gene. The first indication that UL33 was also a member of the terminase came from data showing that a complex of the three proteins (UL33, UL28 and UL15) could be precipitated from HSV-1 infected cells or cells infected with recombinant baculoviruses expressing these proteins (Beard *et al.*, 2002). However, it has also been reported that UL33 and UL15 interact only indirectly, and require UL28 to mediate this interaction (Yang & Baines, 2006). An analysis of the UL33 protein showed that mutations that destroyed binding to UL28 also abrogated cleavage and packaging, indicating that the UL33-UL28 interaction is essential but not sufficient for a functional terminase (Beilstein *et al.*, 2009). Far less is known about the role of UL33 in the packaging process than either of the other two terminase subunits.

All three terminase proteins show the same localisation in wt HSV-1 infected cells, colocalising with the single stranded binding protein, ICP8, in replication compartments (RCs). As previously discussed, DNA packaging takes place in these RCs, and it has been shown that UL15 is essential for localisation of UL33 and UL28 to the RCs (Higgs *et al.*, 2008). Yang and colleagues (2006) also demonstrated that the tripartate terminase complex forms in the cytoplasm and is then transported into the nucleus using the nuclear localisation signal (NLS) of UL15. Once in the nucleus, the terminase can interact with the viral DNA and procapsids, bringing these together for the DNA packaging process. UL28 and UL15 have both been demonstrated to interact with the portal, UL6, in immunofluorescence and immunoprecipitation assays (White *et al.*, 2003).

By analogy to bacteriophage terminases, it would be expected that the terminase complex would have a transitory association with capsids during the packaging process. In agreement with this, none of the terminase subunits have been detected within the mature virion. UL28 and UL15 have both been identified as a component of procapsids and A, B and C capsids (Sheaffer *et al.*, 2001). The association of UL15 with B capsids is dependent on UL6 and UL28, while, UL28 is able to associate with capsids independently of UL15. UL33 has also been shown to associate with all forms of angularised capsids and this was not dependent on UL15 or UL28 (Beard & Baines, 2004). Studies quantifying the amounts of these proteins on the different capsid types have shown that as the capsid matures, decreasing amounts of UL28, UL15 and UL33 can be detected, with each protein present

at only low levels on C capsids (Beard & Baines, 2004; Salmon & Baines, 1998; Sheaffer *et al.*, 2001; Taus & Baines, 1998; Yu & Weller, 1998b). This is consistent with the transient nature of the interaction between the terminase and the capsid, and packaging being a highly processive event. Further analysis of different types of capsid suggested that UL15 is present on A capsids, whereas UL28 is not (Beard *et al.*, 2004). This suggests that UL15 remains associated with the capsid after an abortive packaging event, whereas UL28 dissociates along with the viral DNA.

In summary, although no biochemical activities (ATPase, nuclease) have been demonstrated for the HSV-1 terminase proteins and no *in vitro* packaging system yet exists, a significant body of evidence supports the hypothesis that UL28, UL15 and UL33 do form the terminase for packaging of HSV-1 DNA.

1.7 Role of UL32 in HSV-1 DNA packaging

1.7.1 Properties of UL32

The UL32 open reading frame encompasses nucleotides 69162 to 67372 of HSV-1 and encodes a 596 amino acid protein expressed with late kinetics (McGeoch *et al.*, 1988).

The first indication that UL32 was involved in the DNA packaging process was from the studies of temperature sensitive viruses. Virus *ts*N20 (which has a lesion in the UL32 gene) was generated by UV irradiation of HSV-1 strain KOS and found to have a yield of over 1000 fold lower than wt virus at the NPT and also to be defective in nucleocapsid assembly, although the levels of DNA replication were not affected (Schaeffer *et al.*, 1973; Schaeffer *et al.*, 1974). This virus was further characterised by Sherman and Bachenheimer. They found that upon infection with *ts*N20 at the NPT the accumulated viral DNA was "endless", indicating it had not been cleaved (Sherman & Bachenheimer, 1987). Furthermore, characterisation of the capsids produced in *ts*N20 infected cells showed that only B capsids were produced at the NPT (Sherman & Bachenheimer, 1988).

The requirement for UL32 in the cleavage and packaging of HSV-1 DNA was further confirmed by the generation of a UL32 null mutant, *hr*64. *hr*64 was isolated on complementing cell lines expressing UL32, and contains a lacZ cassette inserted in an

inverted orientation into the UL32 gene at codon 274, thereby disrupting this gene (Lamberti & Weller, 1998). The characterisation of this virus confirmed that in the absence of UL32, viral DNA is still synthesised at near wt levels but the genome is not cleaved or encapsidated. This phenotype is the same as seen in with null mutants of the packaging proteins UL6, UL15, UL17, UL28 and UL33. UL32 could not be detected as a component of B capsids or virions. Furthermore, UL32 was not required for the expression or capsid association of the other DNA packaging proteins UL6, UL15, UL25 and UL28, or the protease and scaffold proteins.

An initial characterisation of the UL32 protein was carried out by Chang and colleagues. Sequence analysis identified a number of interesting motifs, including hydrophobic domains and a short sequence similar to that of aspartyl proteases. It was postulated that UL32 may be a membrane protein due to these hydrophobic stretches; however, it did not fractionate with known membrane proteins. Furthermore, UL32 does not show any protease activity, despite its similarity to some retroviral aspartyl proteases (Chang *et al.*, 1996).

The sequence of UL32 is very cysteine rich with 22 cysteines, 7 of which are conserved throughout all *Herpesviridae*, and a further 4 conserved within the *Alphaherpesvirinae* (figure 1.12). These include three CxxC/CxxxC motifs (where x represents any amino acid other than cysteine) that are completely conserved (within the exception of two betaherpesvirus sequences) and are reminiscent of motifs found in many zinc finger domains. Chang *et al.* therefore investigated the zinc binding activity of UL32 using an indirect zinc blot assay. UL32 protein expressed both in HSV-1 infected cells and from a recombinant baculovirus was blotted onto membranes which were then incubated with $^{65}ZnCl_2$. The radioactive zinc bound specifically to regions on the blot where UL32 was present, indicating that UL32 does indeed bind zinc.

There have been differing accounts of the localisation of UL32 within HSV-1 infected cells. Chang and colleagues produced antisera raised against UL32 and in immunofluorescence studies found that UL32 localised mainly to cytoplasm of infected cells, possibly indicating a function separate to that of other cleavage/packing proteins, which are all found in replication compartments (Chang *et al.*, 1996). Lamberti and Weller (1998) examined the localisation of UL32 by transfection of cells with a plasmid encoding an EE epitope-tagged UL32 construct, followed by superinfection with *hr*64. They found, in contrast to Chang *et al.*, that although UL32 localised predominantly in the cytoplasm of

MATSPPGVLASVAVCEESPGSSWKAGAFERAYVAFDPSLLALNEALCAELLTASHVIGVPPVGTLDEDVAADVVTAPSRARGGA

GDGGGSGGRGGPRNPPPDPCGEGLLDTGPFSAAAIDTFALDRPCLVCRTIELYKQTYRLSPQWVADYAFLCAKCLGAPHCAASI

FVAAFEFVYVMDRHFLRTKKATLVGSFARFALTINDIHRHFFLHCCFRTDGGVPGRHAQKQPKPSPSPGAAKVQYSNYSFLAQS

ATRALIGTLASGGEEGAGSAAGSGTQPSLTTALMNWKDCARLLDCTEGRRGGGDSCCTRAAARNGEFETVAGDREPEESPDTWA

YADLVLLLLAGTPAVWESGPQLRAAAEARRATVRQSWEAHRGARTRDVAPRFAQFTEPDAQPDLDLGPLMATVLKHGRGRGRTG

GECLLCNLLLVRAYWLALRRLRASVVRYSENNTSLFDCIVPVVDQLEADPETQPGDGGRFVSLLRAAGPEAIFKHMFCDPMCAI

TEMEVDPWVLFGHPPATHPDELLLHKAKLACGNEFEGRVCIALRALIYTFKTYQVFVPKPTALATFVREAGALLRRHSISLLSL

EHTLCTYV

Figure 1.12: Sequence of the HSV-1 UL32 protein.

The 596 amino acid sequence of the HSV-1 UL32 protein, showing the cysteine residues conserved throughout the *Herpesviridae* in red, and those conserved only within the alphaherpesviruses in green. The CxxC/CxxxC motifs described by Chang et al., (1990) are underlined.

infected cells, a portion was also present in the nucleus, co-localising with ICP8 at replication compartments.

As discussed earlier, Lamberti and Weller also reported that cleavage and packaging of the genome occurs in replication compartments. They noted that in *hr*64 infected cells, the capsids were instead localised throughout the nucleus, especially at the periphery, leading them to speculate that UL32 was essential for correct localisation of capsids for DNA packaging. However, these results have not been subsequently confirmed, and an interaction between UL32 and capsids or virions has not yet been demonstrated.

The CxxC/CxxxC motifs have also led to proposals that UL32 may act as a redox chaperone to aid the folding or localisation of other proteins. The CxxC motif is one of the most common redox motifs and is involved in the formation, isomerisation and reduction of disulphide bonds in target proteins (Fomenko & Gladyshev, 2003). This can promote correct folding of target proteins and prevent the formation of aggregates of mis-folded proteins. Disulphide bonds have been shown to be important for stability of a number of virus capsids, and disulphide bonds have also been reported in HSV-2 capsids, which have very similar morphology to HSV-1 capsids (Zweig *et al.*, 1979). Other viruses have been found to encode viral chaperones required for correct folding and localisation of capsid and/or envelope proteins, for example gp31 of bacteriophage T4, as previously discussed. Some of these proteins also contain conserved cysteine residues, used in the folding of their target proteins, for example E3 of Sindbis virus which is required for correct folding of the virus glycoprotein spike (Parrott *et al.*, 2009). A number of chaperones have also been identified within African Swine Fever Virus which are required for folding of the major capsid protein and other structural proteins (Cobbold *et al.*, 2001; Rodriguez *et al.*, 2006). All of these proteins use formation and isomerisation of disulphide bonds to direct the correct folding of proteins needed for assembly of their respective virions. It has been suggested that UL32 may be involved in the localisation and folding of the triplex protein VP19C as it was found that a portion of VP19C was mislocalised in cytoplasmic aggregates in cells infected with *hr*64 (S. Weller, personal communication). However, these observations have not been subsequently repeated and no disulphide bonds have been reported in HSV-1 capsids.

Recently, it has been reported that UL32 has a role in correct localisation of UL25 to the nucleus of infected cells (Scholtes & Baines, 2009). These authors found that in cells infected with *hr*64, significant amounts of UL25 were present in the cytoplasm. They also

found that in the absence of UL32, the ratio of soluble UL25 to UL17 was increased. No interaction between UL32 and UL25 has yet been identified.

Homologues of UL32 in other herpesviruses have also been studied in an effort to elucidate its function in the viral life cycle. The UL32 homologue in HCMV, UL52, is also essential for cleavage and packaging, as in its absence no cleaved genomes or DNA-filled C capsids could be seen (Borst *et al.*, 2008). In contrast to HSV-1 UL32, the majority of UL52 was found to localise in the nucleus, surrounding the nuclear replication compartments but not co-localising with them, perhaps indicating a slightly different role in the packaging process. It was also suggested that this localisation was dependent on the integrity of the C-terminus of UL52, as insertion of an HA tag between the final and stop codons resulted in the protein being detected throughout the cytoplasm of the cell.

The UL32 homologue of the alphaherpesvirus pseudorabies virus (PrV) is also essential for cleavage and packaging of viral DNA (Fuchs *et al.*, 2009). UL32 was found to localise in the nucleus of transfected cells, but could not be detected in large enough amounts in PrV infected cells to analyse its localisation. Interestingly, HSV-1 UL32 was able to complement the growth of a UL32 null PrV mutant virus, but the reciprocal complementation was not seen. This suggests similar functions of the UL32 protein in both viruses, but that UL32 of HSV-1 may execute additional functions that cannot be fulfilled by PrV UL32. Alternatively, the incomplete complementation could simply be due to the PrV UL32 being unable to interact with viral protein partners that are essential for the correct function of UL32 (Fuchs *et al.*, 2009).

In summary, the requirement for UL32 for HSV-1 DNA packaging is now well established, but the exact role it plays in this process is still very poorly understood. Studies have shown that it is not required for correct expression of the packaging proteins UL6, UL15, UL17, UL28, UL33 or the scaffold or protease. Unlike the other packaging proteins it cannot be detected as a component of B capsids. However, the different localisation of UL32 in infected cells compared to the other cleavage/packaging proteins has led to suggestions that it has a function distinct from those proteins already characterised. More work is required to fully understand the role of UL32 within the viral life cycle and to resolve some of the conflicting observations seen to date.

1.8 Aims of my project

The major aims of my project were to further characterise HSV-1 UL32 and investigate its role in DNA packaging.

The following four main approaches were used, and the data obtained are discussed in separate chapters of the results section.

(i) Expression and purification of the UL32 protein and the generation of new rabbit antisera.

(ii) Generation and characterisation of a panel of UL32 mutants to identify regions of the protein important for function. This included random insertional mutagenesis and also site-directed mutagenesis targeted at the conserved CxxC/CxxxC motifs and the extreme C-terminus.

(iii) Examination of the localisation of UL32 in HSV-1 infected cells, and investigation of the possible interaction of UL32 with other packaging and capsid proteins, including the terminase complex.

(iv) Characterisation of the UL32 protein, including direct measurement of bound zinc, analysis of potential DNA binding properties and the ability of herpesvirus UL32 homologues to functionally substitute for HSV-1 UL32.

2 Materials and methods

2.1 Materials

2.1.1 Chemicals and reagents

All chemicals and reagents were purchased from Sigma-Aldrich Co Ltd., except where listed below:

BDH Laboratory supplies	- Dimethyl sulphoxide (DMSO)
	- Dimethyl formamide (DMF)
Bio-Rad Laboratories	- 40% Acrylamide solution
	- 40% Acrylamide solution: N, N'-methylene-bis acrylamide 19:1
	- Ammonium persulphate
	- TEMED
	- Coomassie brilliant blue
	- PFGE certified agarose
	- LGT agarose
	- CleanCut Agarose
Citiflour	- AF1 mounting agent
GE Healthcare	- High-range rainbow molecular weight markers
	- Hybond-P membrane
	- Hybond-XL membrane
	- G-50 Microspin columns
	- Ribonuclease A (Gel filtration calibration kit)
Invitrogen Ltd.	- Lipofectamine 2000 reagent
	- Optimem
Kodak	- X-omat film
Fujifilm	- Phosphorimager screens
Finnzymes	- Mutation Generation System^{TM} Kit
Promega	- pGEM T vector
Roche	- Complete mini EDTA-free protease inhibitor cocktail tablets
	- Random primed DNA labelling kit

	- dNTPs
	- Proteinase K
MWG	- Oligonucleotides
Pierce	- Surfact-Amps^{TM} NP40

2.1.2 Buffer solutions

Buffer A	20 mM Tris-HCl, 50 mM NaCl, 10% (v/v) glycerol, 0.05% NP40, pH 7.5
Acid glycine wash	0.14 M NaCl, 0.1 M glycine, pH 3.0
Alkaline transfer buffer	0.4 M NaOH, 0.6 M NaCl
β-galactosidase fix	PBS containing 2% (w/v) formaldehyde and 0.2% (w/v) gluteraldehyde
β-galactosidase stain	PBS containing 5 mM potassium ferricyanide, 5 mM potassium ferrocyanide, 2 mM $MgCl_2$, 0.5 mg/ml X-gal.
Buffer B	20 mM Tris-HCl, 1 M NaCl, 10% (v/v) glycerol, 0.05% NP40, pH 7.5
Blocking solution	TBST containing 5% (w/v) Marvel, 10% (v/v) glycerol and 10% (v/v) FCS
STET buffer	8% (w/v) sucrose, 0.1% (v/v) Triton X-100, 50 mM EDTA, 10 mM Tris-HCl, pH 8
Chloroform:Isoamyl alcohol	24 parts chloroform:1 part isoamyl alcohol (v/v)
Cell lysis buffer (CLB) (2X)	20 mM Tris-HCl, 2 mM EDTA, 1.2% (w/v) SDS, pH 7.5
Destain	10% (v/v) methanol, 5% (v/v) glacial acetic acid
DNA loading buffer (4X)	0.1 M EDTA, 0.25% (w/v) bromophenol blue, 50% (w/v) sucrose
ECL I	0.4 mM coumaric acid, 2.5 mM luminol, 100 mM Tris-HCl, pH 8.5
ECL II	0.02% H_20_2,100 mM Tris-HCl, pH 8.5
EZ buffer	100 mM KCl, 10% (v/v) glycerol, 1% (v/v) NP40, 100 mM Tris-HCl, pH 8.0,. 1 mini protease inhibitor

	cocktail tablet per 10 ml buffer
Formaldehyde fix	5% (w/v) formaldehyde, 2% (w/v) sucrose in PBS
HEPES-buffered saline (HeBS)	137 mM NaCl, 5 mM KCl, 0.7 mM NaH_2PO_4, 55 mM D-glucose, 21 mM HEPES, pH 6.95-7.15
L-Broth (LB) Medium	170 mM NaCl, 1% (w/v) Bactopeptone, 0.5% (w/v) yeast extract
LB-agar	L-broth plus 1.5% (w/v) agar
Loening's buffer (1 X)	40 mM NaH_2PO_4, 36 mM Tris, 1mM EDTA
Membrane wash buffer	0.2 X SSC, 0.1% (w/v) SDS
Buffer M	20 mM HEPES, 5mM $MgCl_2$, 1 mM DTT, 10% (v/v) glycerol, 100 mM NaCl, 0.5 mM EDTA
Neutralising solution	0.5 M Tris-HCl, pH 7.0
Polyacrylamide gel electrophoresis (PAGE) buffer	52 mM Tris-HCl, 53 mM glycine, 0.1% (w/v) SDS
Phosphate-buffered saline (PBS)	170 mM NaCl, 3.4 mM KCl, 10 mM Na_2HPO_4, 1.8 mM KH_2PO_4, pH 7.2
PBS/1% FCS	PBS containing 1% (v/v) foetal calf serum
Permeabilisation solution	0.5% (v/v) NP40, 10% (w/v) sucrose in PBS
PFGE cell suspension buffer	20 mM NaCl, 50 mM EDTA, 10 mM Tris-HCl, pH 7.2
PFGE WASH	50 mM EDTA, 20 mM Tris-HCl, pH 8.0
Phosphate buffer (10 X)	58 mM Na_2HPO_4, 17 mM NaH_2PO_4, 68 mM NaCl, pH 7.5
Protease	20 mg/ml grade XIV protease
Proteinase K reaction buffer	100 mM EDTA, 0.2% (w/v) sodium deoxycholate, 1% (w/v) sodium lauryl sarcosine
Resolving gel buffer (RGB) (4 X)	0.4% (w/v) SDS, 1.5 M Tris-HCl, pH 8.8
RNase mix (200 X)	1 mg/ml RNaseA, 100,000 units/ml RNase T_1 in TE
SDS PAGE sample buffer (3X)	6% (w/v) SDS, 30% (v/v) glycerol, 0.3% (w/v) bromophenol blue, 210 mM β-mercaptoethanol
Stacking gel buffer (SGB) (4 X)	0.4% (w/v) SDS, 488 mM Tris-HCl pH 6.8,

Southern hybridisation buffer	7% (w/v) SDS, 0.5 M sodium phosphate buffer, 0.01 mg/ml denatured sheared calf thymus DNA, pH 7.4
Southern prehybridisation buffer	7 (w/v)% SDS, 0.5 M sodium phosphate buffer, pH 7.4
Tris-borate-EDTA (TBE)	90 mM Tris base, 89 mM boric acid, 1 mM EDTA
Tris-buffered saline (PBS)	137 mM NaCl, 5 mM KCl, 0.7 mM NaH_2PO_4, 5.5 mM glucose, 25 mM Tris-HCl, pH 7.4
TBS-Tween (TBST)	TBS with 0.25% (v/v) Tween-20
Tris-EDTA (TE)	10 mM Tris-HCl, 1mM EDTA pH 8.0
Towbin buffer	25 mM Tris, 192 mM glycine, 20% (v/v) methanol
Versene	0.6 mM EDTA, 0.002% phenol red in PBS
X-gal stock solution	20 mg/ml X-gal in dimethyl formamide

2.1.3 Cells and culture media

Baby hamster kidney 21 clone-13 (BHK) cells (MacPherson & Stoker, 1962) were obtained from the Unit's cytology department. The rabbit skin cell-derived complementing cell line UL32-5 was created by J. Thurlow (unpublished) and contains the HSV-1 UL32 gene under the control of the HSV-1 ribonucleotide reductase large subunit promoter. *Spodoptera frugiperda* (*Sf*21) cells were obtained from the Unit's cytology department.

The following tissue culture media were used in cultivation of these cells:

Invitrogen Ltd.
- Glasgow modified Essential Medium (GMEM)
- Dulbecco's modified Eagle's medium (DMEM)
- TC100
- Foetal calf serum (FCS)
- Newborn Calf Serum (NBCS)
- Penicillin/Streptomycin (P/S)

MP Biomedicals LLC
- Human Serum (HS)

Sigma-Aldrich Co. Ltd.
- Trypsin

The compositions of the tissue culture media used are listed below:

ETC10	- GMEM plus 10% NBCS, 7% tryptose phosphate broth and 1% P/S
EC5	- GMEM plus 5% NBCS and 1% P/S
EPS	- GMEM plus 1% P/S
EC2Hu3	- GMEM plus 3% HS, 2% NBCS and 1% P/S
EFC10	- DMEM plus 10% FCS and 1% P/S
EFPS	- DMEM plus 1% P/S
EFC2Hu3	- DMEM plus 3% HS, 2% FCS and 1% PS
*Sf*21 growth medium	- TC100 plus 5% FCS and 1% P/S
*Sf*21 overlay	- *Sf*21 growth medium with a 1:50 dilution of neutral red

2.1.4 Viruses

Viruses used in this work are listed below:

HSV-1 strain 17 syn+	(McGeoch *et al.*, 1988)
*hr*64 (HSV-1 UL32 null mutant)	(Lamberti & Weller, 1998)
*amb*UL12 (HSV-1 UL12 null mutant)	(Patel *et al.*, 1996b)

2.1.5 BAC genomes

Three bacterial artificial chromosomes containing HSV-1 genomes were used in the course of this work:

fHSV-1Δpac	- BAC of HSV-1 genome with *a* sequences deleted (Saeki *et al.*, 1998)
fHSV-1pac+	- fHSV-1Δpac with *a* sequence re-inserted in *Pac*I restriction site (Saeki *et al.*, 1998)
BAC O	- fHSV-1Δpac containing the rpsL-neo cassette (Tong & Stow, 2010)

2.1.6 Baculoviruses

The following baculoviruses were used in the course of this work.

AcUL6	Expressing the wt HSV-1 UL6 protein (Patel *et al.*, 1996a)
AcUL15	Expressing the wt HSV-1 UL15 protein (Abbotts *et al.*, 2000)
AcUL17	Expressing the wt HSV-1 UL17 protein (Dr V. Preston, unpublished)
AcUL25	Exopressing the wt HSV-1 UL25 protein (Thurlow *et al.*, 2005)
AcUL28	Expressing the wt HSV-1 UL28 protein (Abbotts *et al.*, 2000)
AcUL32	Expressing the wt HSV-1 UL32 protein (Dr A. Patel, unpublished)
AcUL33	Expressing the wt HSV-1 UL33 protein (Beilstein *et al.*, 2009)
AcUL12	Expressing the wt HSV-1 UL12 protein (Dr N. Stow, unpublished)
pac6	Parental baculovirus encoding the β-galactosidase gene (Bishop, 1992)

2.1.7 Bacterial strains

Transformations were performed using XL-1 Blue supercompetent cells, (Stratagene: catalogue number 200236) or electrocompetent DH10 cells (One Shot Electrocomp GeneHogs, Invitrogen Ltd.).

2.1.8 Antibiotics

The antibiotics used in this study are listed below, together with their suppliers.

SmithKline Beecham Research	- Ampicillin (Penbritin)
Sigma-Aldrich Co. Ltd.	- Chloramphenicol
	- Kanamycin
	- Tetracyclin
Invitrogen Ltd.	- Penicillin/Streptomycin (P/S)

2.1.9 Enzymes

All restriction enzymes and their appropriate buffers were supplied by Roche Diagnostics Ltd. or New England Biolabs. Other enzymes are listed below.

Sigma-Aldrich Co. Ltd.:	- RNase T_1
	- RNase A
	- DNase I
	- Lysozyme
	- Protease XVI
New England Biolabs:	- DNA polymerase I
	- DNA polymerase I Large (Klenow) fragment
	- T4 DNA ligase
Promega:	- GoTaq DNA polymerase (PCR)

2.1.10 Plasmids

Plasmids used in this work are listed below. Plasmids were supplied by Dr N. Stow unless otherwise stated. Nucleotide co-ordinates for inserted HSV-1 fragments are taken from McGeoch *et al.*, (1988).

pAT153	Vector derived from pBR322 containing ampicillin and tetracycline resistance loci (Twigg & Sherratt, 1980).
pCMV10	Mammalian expression vector specifying ampicillin resistance, and containing a MCS flanked by the HCMV major IE promoter and splicing/polyadenylation signals from SV40 (Arbuckle & Stow, 1993)
pAS30	The HSV-1 UL6 gene (nucleotides 15120 to 17323) inserted into the MCS of pCMV10 (Patel *et al.*, 1996a)
pE12	The HSV-1 UL12 gene (nucleotides 24755 to 27012) inserted into the MCS of pCMV10 (Porter & Stow, 2004a)
pE*lac*Z	pCMV10 containing the *E. coli lac*Z gene
pIM96	The HSV-1 UL25 gene cloned into the *Bam*HI site of pCMV10 (Dr V. Preston, MRC Virology Unit)
pJM9	A cDNA fragment equivalent to the spliced mRNA of UL15 in

	pCMV10 (Abbotts *et al.*, 2000).
pJM19	pJM9 with the pp65 epitope (ERKTPRVTGG) added to the C-terminus of the UL15 ORF (Abbotts *et al.*, 2000).
pMH19	The HSV-1 UL17 gene inserted into pCMV10 (Thurlow *et al.*, 2005).
pSA1	pAT153 with an HSV-1 ori_S fragment cloned into the *BamH*I site, and the HSV-1 minimum packaging signal Uc-DR1-Ub fragment cloned between the *Eco*RI and *Hind*III sites (Abbotts *et al.*, 2000).
pUL28	The HSV-1 UL28 gene (nucleotides 58182 to 55761) cloned into the *Sma*I site of pCMV10 (Abbotts *et al.*, 2000).
pUL28-GFP	pUL28 with a GFP tag inserted at the N-terminus of the UL28 ORF (Beilstein *et al.*, 2009).
pUL32	The HSV-1 UL32 gene (nucleotides 69159-67201) inserted into the MCS of pCMV10 (Dr A. Patel, MRC Virology Unit).
pUL33	The HSV-1 UL33 gene (nucleotides 69110 to 69576) cloned into the *Bam*HI site of pCMV10 (Beilstein *et al.*, 2009).
pUL33-His_6	pUL33 with a His_6 tag inserted at the C-terminus of the UL33 ORF (Dr G. Reid, MRC Virology Unit).
pGX2	The HSV-1 *Bam*HI K fragment spanning L-S junction inserted into the *Bam*HI site of pAT153 (Stow, 2001)
pVZV-*Kpn*I f	*Kpn*I f fragment of VZV, spanning nucleotides 43943 to 49984 of the VZV genome inserted into the *Pst*I site of pAT153 (Davison & Scott, 1983).
pHCMV-*Hind*III f	*Hind*III f fragment of HCMV, spanning nucleotides 65813 to 86163, inserted into pAT153.

2.1.11 Radiochemicals

α-^{32}P dCTP and α-^{32}P dGTP used were purchased from GE Healthcare, UK, at 10 μCi/μl (3000 Ci/mMole).

2.1.12 Antibodies

The following antibodies were used in this work.

Antibody:	Immunogen:	Source/reference:
Rabbit polyclonal antibodies:		
RC12	UL32 – peptide corresponding to amino acids 580-594	Dr A. Patel, MRC Virology Unit
R605	UL15 - amino acids 551-917*	Dr V. Preston, MRC Virology Unit
R148	UL33-His_6 purified from inclusion bodies*	Dr V. Preston, MRC Virology Unit
R123	UL28 – amino acids 138-785*	(Abbotts *et al.*, 2000)
R1218	UL17 - amino acids 154-703*	(Thurlow *et al.*, 2006)
R335	UL25 - amino acids 342-580 *	(Thurlow *et al.*, 2006)
R992	UL6 - amino acids 379-676 *	(Thurlow *et al.*, 2006)
Anti-capsid	HSV-1 C capsids	Gift from Dr D. Pasdeloup, MRC Virology Unit
Mouse Monoclonal antibodies:		
M7381	HSV-1 ICP8 (UL29)	(Everett *et al.*, 2004)
M2040	HSV-1 VP19C	(Adamson *et al.*, 2006)
DM165	HSV-1 VP5 (UL19)	(McClelland *et al.*, 2002)
Q1	HSV-1 UL12	(Banks *et al.*, 1983)

*these immunogens were bacterially expressed fragments.

Epitope-specific mouse monoclonal antibodies:

Mouse anti-pp65	HCMV pp65 epitope (ERKTPRVTGG)	Capricorn Products
Mouse anti-HA (F-7)	Eleven amino acid peptide derived from influenza protein haemagglutinin (YPYDVPDYA)	Santa Cruz Biotechnology Ltd
Mouse anti-actin (AC-40)	Synthetic actin C-terminal epitope (SGPSIVHRKCF)	Sigma-Aldrich Co. Ltd

Secondary antibodies:

Protein A-horseradish peroxidase conjugate	Sigma-Aldrich Co. Ltd
Goat anti-mouse IgG-horseradish peroxidase conjugate	Sigma-Aldrich Co. Ltd
Goat anti-mouse IgG-Cy5 conjugate (m-Cy5)	GE Healthcare
Goat anti-rabbit IgG-FITC conjugate (r-FITC)	Sigma-Aldrich Co. Ltd
Goat anti-mouse IgG-FITC conjugate (m-FITC)	Sigma-Aldrich Co. Ltd
Goat anti-rabbit IgG Cy5 conjugate (r-Cy5)	GE Healthcare
AlexaFluor goat anti-rabbit IgG-555 (A21428)	Invitrogen Ltd
AlexaFluor goat anti-mouse IgG-633 (A21050)	Invitrogen Ltd

2.2 Methods

2.2.1 Cell culture

2.2.1.1 Mammalian cell culture

BHK cells were grown and passaged in 175 cm^2 tissue culture flasks containing ETC10 (section 2.1.3). Confluent monolayers were washed in versene, trypsinised with 1 x trypsin in versene and resuspended in 10 ml fresh ETC10. 175 cm^2 flasks containing 50 ml fresh growth medium were seeded with $5x10^6$ cells and incubated at 37°C in an atmosphere containing 5% CO_2 until confluent.

RSC-derived cell lines were grown and passaged in 175 cm^2 tissue culture flasks as above, but the growth medium used was EFC10.

2.2.1.2 Insect cell culture

*Sf*21 cells were grown and passaged in 175 cm^2 flasks containing *Sf*21 growth medium. Confluent monolayers were washed in TC100 and the cells suspended by gentle agitation into 10 ml medium. Approximately $2x10^7$ cells were seeded into new flasks containing 50 ml fresh *Sf*21 growth medium and incubated at 28°C without CO_2.

2.2.1.3 Transient transfection of BHK cells by the calcium phosphate procedure

Monolayers of $1x10^6$ BHK cells in 35 mm dishes were set up the day before transfection. Transfection mixtures were made up of 0.5 ml Hepes-buffered saline (HeBS), 10 µg carrier calf thymus DNA (3 mg/ml) and 1 µg plasmid. 35 µl 2 M $CaCl_2$ was added, the mixture vortexed and left for 5 minutes for the calcium phosphate precipitate to form, and added to the cell monolayers from which the medium was removed. The cells were incubated at 37ºC for 45 minutes and 2 ml EC5 added. After 4 hours at 37ºC, the cells were washed and 22.5% DMSO in HeBS added to boost the transfections for 4 minutes (Stow & Wilkie, 1976). The cells were washed once again in EPS and 2 ml EC5 added. Incubation was continued overnight at 37°C.

2.2.1.4 Transfection of BHK cells using Lipofectamine 2000

Glass coverslips in 24 well plates were seeded with $1x10^5$ BHK cells per well the day before transfection. Transfections were carried out using Lipofectamine 2000 according to the manufacturer's instructions. The indicated amount of plasmid was mixed with 25 µl optimem for 5 minutes at room temperature. A mixture of 21 µl optimem and 4 µl Lipofectamine 2000 was added and incubated for a further 20 minutes at room temperature. Cells were washed twice with GMEM and overlaid with 200 µl GMEM, before addition of 50 µl of the transfection mixture. After 3 hours at 37°C, 1 ml ETC10 was added and the cells incubated for 18 hours at 37ºC.

2.2.1.5 Staining for β-gal expression

To determine the efficiency of transfection by the above methods, monolayers of BHK cells were also transfected in parallel with pE*lac*Z. 18 hours post transfection, cells were washed in PBS and 1 ml β-galactosidase fix added for 5 min. Cells were then washed twice with PBS before addition of 1 ml β-galactosidase stain. The plates were incubated at 37°C for 4-12 hours until blue-stained cells were evident. Relative transfection efficiency was calculated by determining the average number of positive (blue) cells from 5 fields of view (each field was 1 mm^2).

2.2.2 Maintenance and manipulation of *E. coli*

2.2.2.1 Transformation

For transformation of supercompetent XL1 Blue *E. coli* (Stratagene), 2 µl ligation mixture was mixed with 20 µl bacterial cells (as supplied) and incubated for 30 minutes on ice, followed by a brief heat shock (42ºC for 45 seconds, on ice for 2 minutes), and the addition of 200 µl LB without antibiotics. Bacteria were shaken at 37ºC, 225 rpm for one hour. The reaction was diluted 10 fold in LB and 100 µl plated onto LB-agar plates containing the appropriate antibiotics and incubated overnight at 37ºC. A selection of colonies was picked, inoculated into 5 ml LB (with appropriate antibiotics) and incubated at 37°C, 225 rpm, overnight. DNA was purified and analysed as described in section 2.2.3.

For transformation of electrocompetent DH10 *E. coli* (OneShot Electrocomp GeneHogs, Invitrogen Ltd.), 10 µl of a 1:10 dilution of ligation was added to 50 µl bacterial cells (as supplied) and transferred to a chilled electroporation cuvette. The cells were electroporated using a Hybaid CellShock CS-100 at 1.8 kV. 250 µl of room temperature LB without antibiotics was added and the cells incubated at 37°C, 225 rpm for one hour. The transformation was then diluted 100 fold in LB, plated onto LB-agar plates with the appropriate antibiotics and incubated at 37°C overnight. A selection of colonies was picked, cultured and DNA purified as described.

2.2.2.2 Storage of *E. coli*

5 ml LB containing the appropriate antibiotics was inoculated with *E. coli* and incubated at 37°C overnight, 225 rpm. 900 µl of the culture was added to 100 µl sterile glycerol and stored at -70°C.

2.2.3 DNA manipulation

2.2.3.1 Small scale DNA preparation (Qiagen)

DNA was purified from overnight 5 ml cultures using the Qiagen QIAprep Spin Miniprep kit according to the manufacturer's instructions. Briefly, cells were harvested by centrifugation and resuspended in buffer P1 (resuspension buffer), before alkaline lysis and neutralisation and incubation on ice. The debris was removed by centrifugation and the supernatant adsorbed to a silica membrane, washed, and plasmid DNA was eluted using 30-50 µl H_20.

2.2.3.2 Boiling lysis DNA preparation

Cells from 5 ml overnight bacterial cultures were harvested by centrifugation and DNA prepared by boiling lysis preparation (Holmes & Quigley, 1981). The cells were resuspended in 350 µl STET buffer. 25 µl 10 mg/ml lysosyme was added and the sample vortexed for 20 sec, boiled for 45 sec and the debris removed by centrifugation for 10 min at 14,100 x g. The supernatant was transferred to a sterile eppendorf tube, NaOAc added and nucleic acids precipitated by isopropanol and the sample centrifuged for a further 10 min. The pellet was washed in 70% ethanol and resuspended in 100 µl TE + RNase. DNA samples were stored at -20°C.

2.2.3.3 Large scale DNA preparation

Large scale DNA preparations were carried out from 25 ml bacterial cultures using the Qiagen Midi Kit (Tip 100) according to the manufacturer's instructions. Briefly, cells were harvested by centrifugation and resuspended in buffer P1 (resuspension buffer) before addition of P2 (an NaOH/SDS buffer) and precipitation on ice with buffer P3 (a high salt buffer with acidic pH). Precipitated material was removed by two centrifugation steps and the supernatant applied to a Tip 100 column and allowed to enter the resin by gravity flow.

The column was washed and DNA was eluted, precipitated with isopropanol and pelleted by centrifugation. The DNA pellet was then washed in 70% ethanol and resuspended in 300-500 µl H_2O.

2.2.3.4 Restriction enzyme digests

Typically, restriction enzyme digests were set up using 10 units of the specified enzyme, 1 x enzyme buffer and where appropriate, 100 µg/ml BSA, with the indicated amount of DNA in a total volume of 20 µl (unless otherwise indicated) and incubated at 37ºC for 2 hours.

If further modification of the digested DNA was required, the DNA was purified using the Qiagen QIAquick PCR Purification Kit according to the manufacturer's instructions. Five volumes buffer PB was added to the DNA and mixed. The DNA was adsorbed onto the silca membrane, washed and eluted in 50 µl 10mM Tris-HCl, pH 8.5.

2.2.3.5 Agarose gel electrophoresis

Loening's Buffer (0.5 x) or TBE buffer (1 x) containing the desired percentage of agarose was boiled and allowed to cool. Ethidium bromide was added to a concentration of 0.5 µg/ml and the agarose poured into a mould containing a well-forming comb and allowed to set. Once set, the gel was placed in a tank containing the appropriate buffer. DNA samples containing 1 x loading dye were added to individual wells and separated by electrophoresis at a constant voltage of 100 V for one hour or 20 V overnight. The DNA bands were visualised using UV light.

2.2.3.6 Purification of DNA fragments

Plasmid DNA was digested with the appropriate restriction enzymes to release the desired fragment of DNA (section 2.2.3.4). The fragments were separated by agarose gel electrophoresis and viewed using long wave UV light, and the desired fragment excised from the gel. The DNA was purified using the Qiagen QIAquick Gel Extraction Kit according to the manufacturer's instructions. Briefly, the gel slice was weighed, 3 gel volumes buffer QG added, and incubated at 50°C for 10 min with occasional vortexing. When the agarose had completely dissolved, 1 gel volume isopropanol was added and the

DNA adsorbed to the silca membrane. The membrane was washed, and the DNA eluted using 50 µl 10 mM Tris-HCl pH 8.5.

2.2.3.7 Ligation

Gel purified DNA fragments were ligated using T4 DNA ligase, using a molar ratio of 1:3 vector:insert. Ligations were set up in a final reaction volume of 10 µl including 1 µl T4 DNA ligase and 1x ligase buffer, at 16ºC overnight.

2.2.3.8 Polymerase Chain Reaction (PCR)

PCR reactions were carried out in a volume of 50 µl, containing final concentrations of approx 1 ng DNA, 0.2 mM each dNTP, forward and reverse primers at 0.2 µM, and 1 U Taq polymerase in 1 x buffer (supplemented with $MgCl_2$). 0.5 M betaine was included where specified. PCR reactions were as follows:

95ºC for 5 minutes ⟶ 25 cycles of (95ºC for 30 seconds ⟶ XºC for 60 seconds

⟶ 72ºC forY seconds) ⟶ 72ºC for 7 minutes

X (re-annealing temperature) was calculated as 5ºC below the melting temperature (Tm) of the primers. Tm for each primer = 2°C x (A+T) + 4°C x (G+C).

Y (extension time) was calculated at the rate of 60 seconds per 1000 bp.

Small aliquots of PCR products were run on 0.8% agarose gels to check that theDNA had been amplified. PCR fragments were then purified using the Qiagen QIAquick PCR purification kit.

2.2.3.9 Sub-cloning of DNA fragments

Purified PCR products were inserted into the sub-cloning vector pGEM T (Promega) to facilitate further cloning steps. Ligation reactions were set up with 1 µl T vector, 1 µl PCR fragment, 2 µl T4 DNA ligase and 5 µl 2 x rapid ligation buffer in a total volume of 10 µl and left at room temperature for one hour. 2 µl ligation reaction was used to transform 20 µl XL1-blue *E. coli* as described in section 2.2.2.1. After incubation for one hour, IPTG was added to the cultures (at 1% w/v) which were plated onto LB-agar plates containing

amp (100 µg/ml) and 2% (w/v) X-gal and incubated overnight at 37°C. White colonies were picked and used to inoculate 5 ml cultures of LB + amp. The bacteria were cultured overnight at 37°C, 225 rpm. DNA was prepared from these overnight cultures by Qiagen Spin MiniPrep (section 2.2.3.1). An aliquot of DNA was screened by restriction enzyme digestion or sequencing for presence of the PCR fragment. The PCR fragment was then excised from the T vector by cleavage with suitable restriction enzymes on either side of the insertion site and gel purified (section 2.2.3.6) prior to further cloning steps.

2.2.3.10 Insertional mutagenesis

Transposon mutagenesis was carried out using the Finnzymes Mutation Generation System according to the manufacturer's instructions. 270 ng pUL32 plasmid was incubated with the MuA transposase and the M1-Kan^R *Entransposon* in 1 x reaction buffer at 30°C for one hour. The reaction was stopped by heat inactivation of the transposase at 75°C for 10 min. The reaction was diluted 1:10 in H_20 and four aliquots (of 10 µl each) were transformed into DH10 *E.coli* by electroporation as described in section 2.2.2.1. Bacteria were plated onto four LB plates containing amp (100 µg/ml) and kan (50 µg/ml) and incubated overnight at 37°C.

Colonies were picked and inoculated into 5 ml LB cultures overnight, and DNA isolated by small scale boiling lysis (section 2.2.3.2). Clones containing the *Entransposon* within the UL32 gene were identified by restriction digestion with *Xba*I and *Kpn*I. An aliquot of each such clone was digested with *Not*I to remove the transposon. This DNA was then self-ligated and retransformed into DH10 cells (sections 2.2.3.7 and 2.2.2.1). Colonies were picked, inoculated into 25 ml LB containing the appropriate antibiotics and plasmid DNA isolated by large scale DNA preparation (section 2.2.3.3).

2.2.4 Virus techniques

2.2.4.1 Growth of HSV-1 virus stocks

Typically, 5 x 175 cm^2 flasks of BHK cells at a confluency of approximately 80% were infected with wt HSV-1 at a multiplicity of 0.01 p.f.u./cell in 40 ml EC5. Cells were incubated at 31ºC for 4-7 days until they showed cytopathic effect. The infected cells were tapped into the media, pooled and centrifuged at 835 x g for 10 min. The pellets were

resuspended in 5 ml EC5 and repeatedly freeze-thawed and sonicated to prepare the cell-associated virus stock (CAV). The supernatant was centrifuged again at 21,860 x g for 3 hours and the resulting pellet resuspended in 5 ml EC5 and sonicated extensively to prepare the cell-released virus stock (CRV). Both stocks of virus were tested for sterility on blood agar plates and titrated as described (section 2.2.4.2). Stocks of HSV-1 were stored at -70°C in aliquots, to avoid repeated freeze-thawing. Stocks of the UL32 null mutants (32ΔEP and *hr*64) were similarly prepared following infection of UL32-5 cells except that EFC5 medium was used.

2.2.4.2 Titration of HSV-1

To determine the titre of virus preparations, 10-fold serial dilutions were made in EC5. Duplicate 35 mm dishes of BHK cells were inoculated with 100 µl diluted virus for 1 hour with gentle rocking of dishes every 15 min. 2 ml of EC2Hu3 was added and the monolayers incubated at 37ºC for 3 days. The overlay was removed and 1 ml Geimsa stain added for 30 min. The Geimsa stain was washed off and the number of plaques in each dilution counted. The titre was determined as the average of the duplicate plates using the calculation:

Titre = number of plaques on 10^{-n} dilution x 10^{n} x 10 p.f.u./ml

The UL32 null mutant virus stocks were titrated onto UL32-5 cells in the same way, except that the serial dilutions were made in EFC5 and the cells overlaid with EFC2Hu3.

2.2.4.3 Infection of BHK cells

BHK cells were seeded at $1x10^{6}$ cells per 35 mm plate or $1x10^{5}$ cells per linbro well (on glass coverslips) the day before infection. Virus was diluted to achieve a multiplicity of 5 p.f.u./cell in an inoculum of 100µl (unless otherwise stated) and adsorbed for one hour at 37ºC. During adsorption, plates were gently rocked every 15 min. 2 ml EC5 was then added and the cells incubated at 37ºC for 6 or 18 hours (as specified).

2.2.4.4 Growth of baculovirus stocks

Typically, 175 cm^2 flasks of *Sf*21 cells at approximately 50% confluency were infected at a multiplicity of 1 p.f.u./cell in 20 ml *Sf*21 growth medium. Cells were incubated at 28ºC for four days and harvested by shaking into the medium. Cells were pelleted at 835 x g for 5

min. To obtain concentrated virus stock, the supernatant from this spin was centrifuged at 38,725 x g for 90 min and the resultant pellet resuspended in 4 ml *Sf*21 growth medium. Baculovirus stocks were sonicated extensively, checked for sterility on blood agar plates and stored at -70ºC.

2.2.4.5 Determination of baculovirus stock titres

To determine the titre of baculovirus stocks, 10-fold serial dilutions were made in *Sf*21 growth medium. Duplicate 35 mm dishes of *Sf*21 cells were inoculated with 100 µl diluted virus for 1 hour. 1.5% LGT agarose in *Sf*21 growth medium was melted and 2 ml of this overlaid onto the monolayers. After the agarose had set, 1.5 ml *Sf*21 growth medium was added to each dish and the cells incubated at 28°C for four days. To visualise plaques, the medium was removed from the plates and 0.5 ml of *Sf*21 overlay containing 1:50 dilution of neutral red was added to the plates for 24 hours. Plaques could then be counted and titres determined as above.

2.2.5 Complementation yield assay

BHK cells were transfected using the calcium phosphate method (as described in section 2.2.1.3) with 1 µg each test plasmid. Six hours post transfection, the cells were infected with the appropriate virus at a multiplicity of 5 p.f.u./cell (section 2.2.4.3) and returned to 37ºC. One hour after infection the cells were washed once with 0.14 M NaCl, exposed to acid glycine wash for one minute, then washed with EC5 (Rosenthal *et al.*, 1984). The cells were then incubated in 2 ml fresh EC5 at 37ºC overnight. 18 hours post infection, the cells were scraped into the medium, sonicated and viral progeny titrated on the complementing cell line, UL32-5, for 4 days at 37ºC (section 2.2.4.2).

2.2.6 Amplicon packaging assay

2.2.6.1 Transfection and superinfection of BHK cells

Monolayers of BHK cells were transfected using the calcium phosphate method (section 2.2.1.3), with 1 µg test plasmid and 0.5 µg pSA1 plasmid. 6 hours post transfection, the cells were infected with the appropriate virus at 5 p.f.u./cell (section 2.2.4.3) and returned to 37ºC for 18 hours.

2.2.6.2 Preparation of total and DNase resistant DNA

The cells were scraped into 2 ml TBS and each sample split into two equal portions for the preparation of total DNA (sample A) and DNase resistant DNA (sample B). The cells were pelleted and each A sample resuspended in 184 µl RSB containing 0.5% NP40, followed by addition of 184 µl of 2 x CLB containing 1 mg/ml protease, and incubated at 37°C for one hour. Each B sample was resuspended in 184 µl RSB containing 0.5% NP40 and 200 µg/ml DNase and incubated at 37°C for 20 minutes with occasional vortexing. This was followed by addition of 184 µl of 2 x CLB with 1 mg/ml protease for one hour at 37°C. 32 µl 4 M NaCl/0.5 M EDTA was added to all samples (A and B) which were sequentially extracted with phenol and chloroform:isoamyl-alcohol and precipitated in 1 ml EtOH for 1 hour at -80ºC or overnight at -20ºC. The DNA was pelleted by centrifugation and the pellets resuspended in 120 µl (A samples) or 60 µl(B samples) TE+RNase. One sixth of the A samples and one third of B samples (20 µl each) were digested with 5 U *Eco*RI and 5 U *Dpn*I in a total reaction volume of 40 µl for 4 hours at 37ºC. The reaction was stopped by addition of 5 x loading dye and the samples separated by electrophoresis on a large 0.8% agarose gel containing 0.5 µg/ml ethidium bromide in 0.5 x Loening's buffer at 20 V overnight.

2.2.6.3 Southern Blotting

Agarose gels were examined by UV light to confirm digestion had occurred and DNA had been efficiently recovered, and photographed. The gel was shaken in alkaline transfer buffer for 30 minutes, and blotted onto a nitrocellulose membrane (Hybond-XL) by capillary transfer in alkaline transfer buffer for 12-20 hours at room temperature (Sambrook & Russell, 2001b). The membrane was washed in 0.5 M Tris pH8 for 15 minutes and the DNA crosslinked by exposure to 120 mJ/cm of 254 nm UV light.

The membrane was incubated in a Hybaid rotating oven at 68ºC in Southern pre-hybridisation buffer for 1-3 hours, followed by blocking of non-specific binding by incubation in 20 ml Southern hybridisation buffer for 2-5 hours. Specific fragments were detected by addition of ^{32}P labelled probe (section 2.2.6.4) to the hybridisation buffer and overnight incubation at 68ºC. The blot was washed once in Southern prehybridisation buffer (45 minutes) and twice in membrane wash buffer (one hour each) before being rinsed in water and exposed to a phosphorimage screen. The screen was processed using a Personal Molecular Imager (BioRad) and analysed using Quantity One software.

2.2.6.4 ^{32}P labelling of probe by random priming

The probe for Southern blot hybridisation was labelled using the Roche Random Primed DNA Labelling Kit, following the manufacturer's instructions. The appropriate plasmid to be used as a probe was linearised by restriction enzyme digestion and purified using the Qiagen QIAquick PCR Purification Kit. Reactions were set up containing approximately 500 ng denatured linearised DNA (boiled 10 minutes, then incubated on ice 10 minutes), 2 µl each of dTTP and dATP (0.5 mM), 2 µl hexanucleotide mix, 5 U Klenow enzyme, and 2 µl each of α-^{32}P dCTP and α-^{32}P dGTP (20 µCi each) in a final volume of 20 µl. The reaction was incubated at 37ºC for one hour, and stopped by addition of 5 µl 0.2 M EDTA, followed by 25 µl 10 mM Tris-HCl, pH 8.0. The unincorporated nucleotides were removed by purification through a G-50 Microspin column and the probe denatured by addition of 40 µl 10 mM Tris-HCl, pH 8 and 20 µl 1 M NaOH. After 5 minutes, the solution was neutralised with 20 µl 1M HCl and the entire probe (110 µl) added to the tube containing the hybridisation buffer and membrane (section 2.2.6.3).

2.2.7 Analysis of proteins

2.2.7.1 SDS-PAGE

BHK cells were transfected or infected as previously described (sections 2.2.1.3 and 2.2.4.3) or *Sf*21 cells infected with recombinant baculoviruses at the indicated m.o.i.s. Cells were harvested by scraping into 1 ml PBS and pelleted. The pellets were washed 3 times in PBS and 60 µl 1 x SDS PAGE sample buffer added. The samples were boiled for 10 minutes in a water bath prior to loading on the gel.

Gels used were minigels consisting of an 8% running gel (unless otherwise specified) made with 39:1 acrylamide:bisacrylamide, and 5% stacking gel with 19:1 acrylamide:bisacrylamide. 20 µl protein samples were resolved by electrophoresis at 200 V for 45 min using a BioRad Mini-protean III kit in 1 x PAGE buffer. 10 µl high-range rainbow molecular weight markers were run on the gel as a molecular size marker.

2.2.7.2 Coomassie staining of proteins

Proteins were separated by SDS-PAGE as described above and the gel incubated in 0.2% Coomassie in destain for 30 min with gentle agitation. The gel was then washed

extensively in H_20 and boiled in a microwave oven in H_20 for 10 min to remove a large proportion of the stain. The gel was washed in destain until the protein bands were readily visible, and photographed.

2.2.7.3 Western blotting

Protein samples were separated by SDS-PAGE as described above and gels blotted onto a Hybond-P PVDF membrane using a BioRad transfer kit for 2 hours at 250 mA in Towbin buffer. The membrane was blocked by shaking in 10 ml blocking solution for 2 hours at room temperature. The primary antibody was diluted as indicated in 5% Marvel in TBST and shaken with the membrane for 1 hour at room temperature, or overnight at 4°C, followed by 3 x 5 min washes in TBST. The membrane was then incubated in a 1:1000 dilution of HRP-conjugated secondary antibody in 5% Marvel in TBST for 1 hour at room temperature. Following 3 x 5 min washes in TBST, specific bands were detected by addition of 1 ml ECL mix (freshly mixed ECL I and ECL II) for 1 min and exposure of the membrane to auto-radiographic film.

2.2.8 Immunofluorescence of transfected and infected cells

Glass coverslips within 24 well plates were seeded with $1x10^5$ BHK cells per well and the next day transfected for 18 hours with 0.5 µg indicated plasmids by lipofection (section 2.2.1.4). Alternatively, coverslips of cells were infected with 5 p.f.u./cell of the indicated virus (section 2.2.4.3) for 6 hours.

Cells were washed twice in PBS and then fixed for 10 minutes in 1 ml formaldehyde fix. The monolayers were thoroughly washed in PBS and 1 ml permeabilisation solution added for 10 min. The cells were washed again in PBS and coverslips that had been infected with HSV-1 blocked for 30 minutes with 10% human serum in PBS (to block IgG binding). Coverslips were placed cell-side down on to appropriate primary antibodies, diluted to the indicated concentrations in PBS/1% FCS, for one hour at room temperature. The coverslips were then washed 3 x 5 min face-down and 3 x 5 min face-up in PBS/1% FCS with very gentle agitation. The appropriate FITC- or Cy5- conjugated secondary antibodies were added in the same way and the coverslips incubated face-down for one hour at room temperature. After 6 further washes in PBS/1%FCS, the coverslips were rinsed in H_2O and air-dried. Dry coverslips were mounted on glass slides using AF-1 mounting agent and examined using a Zeiss LSM 510 confocal microscope. Laser lines with excitation

wavelengths of 488 nm, 545 nm and 633 nm were used to detect the FITC, TRITC and Cy5 fluors respectively and images were compiled in Adobe Photoshop.

2.2.9 Purification of the UL32 protein

2.2.9.1 Infection of Sf21 cells

175 cm^2 flasks of *Sf*21 cells at approximately 50% confluency were infected at a multiplicity of 5 p.f.u./cell in 20 ml *Sf*21 growth medium and incubated at 28ºC for two days. The cells were pelleted at 835 x g for 5 min and then resuspended in 1 ml buffer A (containing protease inhibitor tablets) per flask. Insoluble protein was removed by ultra-centrifugation at 44,000 x g for 20 minutes at 4ºC. The supernatant (soluble protein) was collected and stored at -70ºC.

2.2.9.2 MonoQ ion-exchange chromatography

All chromatography was carried out using the AKTA 900 purification system. Soluble extracts of protein were filtered through a 0.45 µm filter and separated by anion exchange chromatography using a 1 ml MonoQ 5/50 GL column (Amersham). The column was prepared by equilibration with 5 column volumes buffer A at a flow rate of 1 ml/min. The protein was loaded onto the column and washed with 5 column volumes buffer A. Proteins were eluted with a salt gradient by gradually increasing the proportion of buffer B applied to the column so as to increase the NaCl concentration from 50 mM to 1 M over a 60 ml gradient. Fractions of 0.5 ml were collected and stored at -70ºC. 20 µl each fraction was added to 10 µl 3 x SDS PAGE sample buffer and the proteins separated on an 8% SDS-PAGE gel which was stained with Coomassie (sections 2.2.7.1 and 2.2.7.2) or western blotted (section 2.2.7.3) to identify peak fractions containing UL32.

2.2.9.3 Measurement of protein concentration

The concentration of total protein in the fractions collected from the MonoQ column was determined by Bradford assay (Bradford, 1976). 5 µl each sample was mixed with 250 µl protein dye (BioRad) in the wells of a 96-well plate and the absorbance measured at 560 nm. The concentration of protein was calculated from a standard curve for BSA samples of known concentration.

2.2.9.4 Superose 12 size exclusion column

A 24 ml Superose 12 HR 10/30 column (Amersham) was used to determine the size of UL32. Buffer A was used to equilibrate the column at a flow rate of 0.2 ml/min for 10 column volumes. IgG (160 kDa), BSA (67 kDa) and ribonucleaseA (13.7 kDa) were used as molecular markers, and these were pooled and diluted to a final concentration of 2 mg/ml each in buffer A and filtered. A further 0.2 column volumes buffer A were added to the column, and a 200 µl aliquot of the diluted markers was applied to the column at a flow rate of 0.25 ml/min and eluted in 1 column volume buffer A. The elution point of each marker was identified from the UV trace. Peak fractions from the MonoQ column were then pooled and 200 µl injected onto the Superose 12 column and fractionated using identical conditions to the markers. 0.5 ml fractions were collected and stored at -70°C, before being analysed by SDS-PAGE and Coomassie staining or western blot as before.

2.2.10 Generation of UL32 rabbit antisera

2.2.10.1 Preparation of immunogen and immunisation

UL32-containing fractions from multiple MonoQ fractionations were pooled and the total protein quantified (section 2.2.9.3). The protein used as an immunogen had a concentration of approximately 1.5 mg/ml (total protein) in buffer A. The purity of the UL32 protein in this sample was estimated as approximately 40% by density analysis of the protein bands from a Coomassie stained gel (using BioRad QuantityOne software). The total protein sample was emulsified in Freund's complete adjuvant (FCA) for immunisation by Dr Susan Graham (MRC Virology Unit), and two rabbits were immunised and sera collected by Colin Hughes (University of Glasgow). A pre-immune bleed was taken from each rabbit prior to immunisation. The primary immunisation contained 50-100 µg total soluble protein in FCA. This was followed by a boost after four weeks and then two further boosts at two week intervals, all containing 50-100 µg protein emulsified in Freund's incomplete adjuvant (FIA). Sera from test bleeds collected one week after the third boost were prepared as in section 2.2.10.2 and tested along with the pre-immune sera by western blotting for reactivity to the UL32 protein (sections 2.2.7.1 and 2.2.7.3). The rabbits were then given a final fourth boost of 100 µg protein in FIA and bled one week later for the final antisera.

2.2.10.2 Collection and preparation of antisera

Final bleeds of approximately 50 ml were taken from rabbits R1 and R2 and allowed to clot at 4°C overnight. The serum was removed from the clot and centrifuged at 835 x g for 10 min to remove any remaining red blood cells. The supernatants were kept and used as the UL32 antisera, named R1 and R2. These were stored in aliquots at -20°C and were tested for reactivity against UL32 by western blot and immunofluorescence.

2.2.11 Co-immunoprecipitation of baculovirus-expressed proteins

$2x10^6$ *Sf*21 cells were infected with the appropriate baculoviruses at 2.5 p.f.u./cell in suspension in a total volume of 2 ml in *Sf*21 growth medium and plated out into 35 mm dishes. After 48 hours at 28°C, cells were scraped into the medium and harvested by centrifugation at 835 x g for 5 min. Cells were resuspended in 1 ml PBS, pelleted in a microfuge for 10 sec and the supernatant discarded. The pellets were resuspended in 500 µl EZ buffer by vortexing and incubated on ice for 20 minutes. Insoluble protein was removed by ultra-centrifugation at 44,000 x g for 20 min and the supernatant (soluble protein) retained. 40 µl of this supernatant was mixed with 40µl H_20 and 40µl 3 x SDS PAGE sample buffer (total extracted protein sample). For the immunoprecipitation, 150 µl of the soluble supernatant protein was incubated with 2 µl appropriate antibody, rotating end-over-end at 4ºC for 2 hours. 50 µl protein-A-sepharose beads (50% slurry in PBS) was added and incubated on a rotator at 4ºC for a further hour. Immune complexes were collected by centrifugation at 14,100 x g for 30 sec and washed four times with 0.5 ml EZ buffer (the final wash being in a fresh tube).The washed beads were resuspended in 60 µl 1 x SDS PAGE sample buffer and boiled for 10 min in a waterbath. 20 µl each sample (and 20 µl of each total extracted protein sample) was analysed by SDS-PAGE and western blotting (sections 2.2.7.1 and 2.2.7.3).

2.2.12 Generation of HSV-1 recombinant expressing HA-tagged UL32

The approach taken involved the rescue of the UL32 null mutant *hr*64 with a DNA fragment encoding UL32 tagged near to its N-terminus with a tag derived from the influenza haemagglutinin (HA).

2.2.12.1 Preparation of *hr*64 genomic DNA

175 cm^2 flasks of UL32-5 cells were infected with *hr*64 at 5 x 10^5 p.f.u./flask and incubated at 31°C for 3 days. The infected cells were tapped into the medium and centrifuged at 835 x g for 10 min. The supernatant was centrifuged again at 21,860 x g for 3 hours and the pellet containing the cell released virus particles was resuspended in 1 ml TE+RNase by pipetting and sonication. 40 µl 0.25 M EDTA, 25 µl 20% SDS and 50 µl 20 mg/ml proteinase K were added and incubated for 30 min at 50°C. DNA was purified following the addition of 32 µl 4 M NaCl/0.5 M EDTA by sequential extraction with phenol and chloroform:isoamyl alcohol. The aqueous phase containing the viral DNA was dialysed once against 1 litre 1 x TE for 16-20 hours at 4°C, followed by further dialysis against 1 litre 1 x TE for 2 hours.

2.2.12.2 Transfection

The construction of plasmid p33-HA-32 is described in section 5.3.1. p33-HA-32 was digested with *Nde*I and *Xho*I and the fragment containing 33-HA-32 was gel purified (section 2.2.3.6). 35 mm plates of BHK cells were transfected with 0.5 µg *hr*64 genomic DNA and 0.5 µg 33-HA-32 fragment by the calcium phosphate method as described in section 2.2.1.3. Cells were incubated in EC5 at 37°C for 3 days to allow recombination and replication to occur. Once infection was evident in the plates, cells were scraped into the media, sonicated, and the virus progeny titrated on BHK cells as described in section 2.2.4.2.

2.2.12.3 Plaque purification and growth of HA-HSV-1 stock

Serial two-fold dilutions of the above harvested virus were made and each was used to infect 12 wells of a 96-well plate of BHK cells, covering the range 128 p.f.u/well to $3.9x10^{-3}$ p.f.u./well. The plate was incubated at 37°C for 4 days and then the cells from four wells each containing a single plaque were scraped into the medium. 50 µl from each of these wells was used to infect a 35 mm dish of BHK cells overnight. The infected cells were then scraped into the medium and divided into two samples. One sample was lysed, separated by SDS-PAGE and checked for expression of HA-tagged UL32 by western blotting using mouse anti-HA antibody (sections 2.2.7.1 and 2.2.7.3). Once presence of the HA tag had been confirmed for a single plaque, the other half of this sample was used to

infect 175 cm^2 flasks of BHK cells to generate a virus stock named HA32EP (section 2.2.4.1).

2.2.13 Generation of a HSV-1 UL32 null mutant by recombination in *E. coli*

The new HSV-1 UL32 null mutant, ΔUL32EP, was generated using the Counter-Selection BAC modification kit (GeneBridges), which utilises the Red/ET homologous recombination enzymes. The kit was used according to the manufacturer's instructions.

2.2.13.1 Growth of DH10B *E. coli* and expression of recombination enzymes

E. coli DH10B cells (GeneHogs) containing the BAC, fHSV-1Δpac, and pSC101-BAD-gbaA^{tet} (encoding the Red/ET recombination enzymes) were cultured overnight in LB containing tetracycline (3 µg/ml) and chloramphenicol (50 µg/ml) at 30°C, 225 rpm and used to inoculate 30 ml fresh LB + cam/tet. The culture was incubated at 30°C, 225 rpm for approximately two hours until the OD_{600} reached 0.3. The expression of the genes mediating the Red/ET recombination was induced by addition of 3 ml 30% L-arabinose and a temperature switch to 37°C. After one hour at 37°C, the cells were made competent for transformation as follows. The culture was centrifuged at 835 x g for 15 min at 4°C and the pellet resuspended gently in 30 ml ice-cold H_20, and centrifuged again. This was repeated three times, reducing the volume of ice-cold H_20 by half each time. Finally, the cells were resuspended in 0.5 ml 10% ice-cold glycerol and used for electroporation of rpsL-neo-32, as described below.

2.2.13.2 Insertion of rpsL-neo-32 PCR cassette into BAC

The cassette for recombination was the rpsL-neo fragment flanked by homology arms to UL32 gene. This cassette was generated by PCR (section 6.12) and was designed so that the rpsL-neo sequences replaced nucleotides 202 to 1599 of UL32. 2 µl of the rpsL-neo-32 PCR product were transformed into 40 µl of the above electrocompetent DH10B cells containing fHSV-1Δpac (as in section 2.2.2.1). 1 ml LB was added and the cells incubated at 37°C and 225 rpm for 70 min before plating onto a LB-agar plate containing cam (50 µg/ml) and kan (15µg/ml) overnight at 37°C.

The resulting colonies picked were also plated on kan/cam/strep plates for 48 hours to confirm they had the strep^S phenotype expected from successful insertion of the rpsL-neo containing cassette.

2.2.13.3 Preparation of BAC DNA and confirmation of the disruption of the UL32 gene

BAC DNA for screening was prepared from 5 ml overnight cultures of clones with the phenotype cam^R, kan^R and strp^S by the alkaline lysis method (Sambrook & Russell, 2001a). Two aliquots of each DNA sample (approx 1 µg each) were digested with 5 U *Eco*RI each for 6 hours at 37°C. The reactions were stopped by addition of 5 x loading dye and the samples were run on duplicate 0.8% agarose gels in 0.5 x Loening's Buffer at 20 V overnight. The gels were Southern blotted (sections 2.2.6.3) and probed for the presence of either the kanamycin cassette or the UL32 gene using ^{32}P labelled probes generated by random priming (section 2.2.6.4).

One clone with the correct kanamycin positive Southern blot profile (UL32 negative and kanamycin positive) was identified and BAC DNA was prepared for transfection into mammalian cells using the Qiagen Midi Kit (Tip 100) (section 2.2.3.3). After isopropanol precipitation the DNA pellet was resuspended in 200 µl H_20. 1/10 volume 3 M NaOAc and 2 ½ volumes EtOH were added and the DNA was precipitated at -20°C overnight. Finally, the DNA was pelleted and resuspended in 50 µl TE+RNase.

2.2.13.4 Transfection of mutated BACs into UL32-5 cells

35 mm dishes of UL32-5 cells were set up the day before transfection. 2 µg mutated BAC DNA and 2 µg *Bam*HI cleaved pGX2 DNA (containing the HSV-1 *Bam*HI K fragment to repair the *a* sequence deleted from fHSV-1Δpac) were transfected using the calcium phosphate method (section 2.2.1.3). The cells were incubated in EC5 for 3 days and then scraped into the medium and sonicated. One half of the sonicate was added to a new 35 mm dish of UL32-5 cells and incubated for 48 hours at 37°C. Once CPE was established, after 3 days, the cells and virus from this plate were scraped into the medium and stored at -70°C before titration of the viral yield and large scale production of virus stock, named Δ32EP (sections 2.2.4.1 and 2.2.4.2).

2.2.14 Pulsed Field Gel Electrophoresis

2.2.14.1 Preparation of agarose embedded cell suspensions

Duplicate 35 mm plates of BHK cells were infected at a multiplicity of 5 p.f.u./cell as described in section 2.2.4.3 and harvested after 18 hours by scraping into the medium and centrifugation at 835 x g for 5 min. Pelleted cells from each plate were resuspended in 200 µl PFGE cell suspension buffer, pooled, and equilibrated to 50ºC. 200 µl melted 2% CleanCut Agarose was added, mixed well and 4 x 100 µl samples from each infection were added to BioRad plug moulds and set at 4º.

2.2.14.2 Preparation of total DNA and restrictions enzyme digestion in agarose blocks

Agarose blocks were incubated at 50ºC overnight in proteinase K reaction buffer containing 1 mg/ml proteinase K. Blocks were then washed 4 x 30 min in 0.5 ml PFGE WASH

The agarose blocks were washed twice in 0.1 x PFGE WASH to reduce the EDTA concentration and incubated for 30 min in 200 µl of the appropriate 1 x restriction enzyme buffer at 37ºC. The blocks were then digested with 40 U of enzyme in fresh restriction buffer overnight, and washed twice in 0.5 ml PFGE WASH.

2.2.14.3 Electrophoresis and Southern blotting of PFGE samples

One gram of PFGE certified agarose was melted in 100 ml 0.5 x TBE, allowed to cool and poured into the CHEF-DR II casting mould. Each agarose block was placed in one well of this gel, ensuring there were no air bubbles. The wells were then sealed by filling with 1% CleanCut Agarose. The gel was placed in the CHEF-DR II electrophoresis tank containing 2 litres of 0.5 x TBE pre-cooled to 14ºC. DNA was separated using run parameters of 6 V/cm for 16 hours at 14ºC with a ramped switch time of 1 – 15 sec. After electrophoresis the gel was stained in 0.5 µg/ml ethidium bromide in dH_20 for 20 min, examined by UV light and photographed.

The gel was soaked in 0.25 M HCl for 15 min and then the DNA Southern blotted as described in section 2.2.6.3. HSV-1 DNA was detected by hybridisation to fHSV-1pac+ BAC DNA, ^{32}P labelled by nick-translation (Rigby *et al.*, 1977; Sambrook *et al.*, 1989).

2.2.15 Electrophoresis Mobility Shift Assay for DNA binding

Simultaneous large scale infections of *Sf*21 cells with AcUL32 and pac6 were carried out in 175 cm^2 flasks and extracts prepared (section 2.2.9.1). Equivalent fractions were collected following MonoQ column fractionation of these extracts (section 2.2.9.2) and used for the DNA binding experiments described below. A 20 µl sample of each fraction was analysed by SDS-PAGE and Coomassie staining to identify fractions containing UL32 (sections 2.2.7.1 and 2.2.7.2).

2.2.15.1 3' end-labelling of double-stranded DNA

DNA fragments were excised from plasmids by restriction enzyme digestion and purified from agarose gels (2.2.3.6). The sticky ends of these fragments were filled in using DNA pol I Klenow fragment and a radiolabelled nucleotide as follows. Approximately 400 ng DNA was incubated in a 30 µl total reaction with 5 U Klenow, 1 x polymerase buffer, 0.3 ul each of dATP, dTTP, dGTP (1 mM stocks) and 2 µl (20 µCi) α-^{32}P dCTP for 15 min at 37ºC. The enzyme was inactivated at 75°C for 15 min and the DNA stored at -20°C.

2.2.15.2 Gel Electrophoresis

The labelled DNA was diluted in H_2O and approximately 4 ng DNA incubated in a total reaction volume of 30 µl with 1 x buffer M and 10 µl MonoQ column fraction for 30 min at room temperature. 6 µl loading buffer was added and the samples resolved by electrophoresis on a large 8% non-denaturing polyacrylamide gel in 0.5 x TBE at 200 V for 5 hours. The gel was then dried onto a piece of DE81 for 2 hours at 80ºC. The dried gel was exposed to a phosphorimage screen which was processed using a Personal Molecular Imager (BioRad) and analysed using Quantity One software.

2.2.16 Zinc binding assay

2.2.16.1 Preparation of protein samples

Simultaneous large scale infections of *Sf*21 cells with AcUL32 and pac6 were carried out in 175 cm^2 flasks with the addition of 10 µM zinc acetate to the growth medium, and harvested after 48 hours (section 2.2.9.1). Soluble protein extracts were prepared and dialysed 4 times for one hour each against buffer A at 4°C to remove unbound zinc. These samples were fractionated through the MonoQ column and equivalent fractions from the two infections collected (section 2.2.9.2). A 20 µl sample of each fraction was analysed by SDS-PAGE and Coomassie staining to identify those containing UL32 (sections 2.2.7.1 and 2.2.7.2). Protein concentrations of the fractions were determined using the Bradford assay (section 2.2.9.3).

2.2.16.2 Zinc binding

Zinc binding was measured by release of bound zinc into solution upon addition of p-chloromercuribenzoic acid (PCMB) as follows. Duplicate 200 µl protein fractions were mixed with 100 µM 4-(2-pyridylazo) resorcinol (PAR), with and without 2 mM (PCMB) in a total volume of 300 µl. These were transferred to the wells of a 94-well microtitre plate and absorbance measured at 492 nm using a Titertek Multiskan Plus plate reader. The difference in absorbance between the samples with and without PCMB is indicative of the amount of zinc released by each protein sample. The zinc released was determined by comparison with a standard curve for known zinc concentrations processed in the same way.

2.2.17 Computer software

PSIpred (Jones, 1999)	- http://bioinf.cs.ucl.ac.uk/psipred/
Expasy Translate (Gasteiger *et al.*, 2003)	- http://www.expasy.org/tools/dna.html
PSORT (Nakai & Horton, 1999)	- http://psort.ims.u-tokyo.ac.jp/

3 Generation of rabbit antisera reactive with the UL32 protein

3.1 Introduction

The planned experiments for the initial characterisation of UL32 had a requirement for a UL32 antiserum, particularly one which could detect UL32 from samples of HSV-1 infected and transfected BHK cells on western blot. This chapter describes the testing of four already available sera and subsequent partial purification of the UL32 protein and generation of new polyclonal rabbit antisera. These antisera were then employed in many of the experiments described later in this thesis

3.2 Testing of UL32 anti-peptide antibodies

Four UL32 anti-peptide sera already available in the laboratory were first tested for their ability to recognise UL32. These had been generated by Dr. Arvind Patel (MRC Virology Unit), from rabbits immunised with branched peptides from either the N- or C- terminus of UL32. The sequences of these peptides are listed below.

Antibodies N9 and N10: peptide 1025B – MATSPPGVLASVAV (residues 1-14 of UL32)

Antibodies C11 and C12: peptide 1017D – RHSISLLSLEHTL (residues 580-592 of UL32)

The ability of the anti-peptide antibodies to recognise UL32 was examined by western blotting. Firstly, UL32 expressed from recombinant baculovirus-infected cells was analysed to confirm the size and expression of the UL32 protein. A recombinant baculovirus expressing the UL32 protein (AcUL32) was provided by Dr. Patel. AcUL32 contains the UL32 ORF (HSV-1 nucleotides 69159 to 67201) and expressed under the control of the polyhedrin promoter.

*Sf*21 cells were infected with 5.p.f.u/cell AcUL32 or the parental baculovirus pac6, which is identical to AcUL32 except that it expresses the lacZ protein rather than UL32. The cells were harvested after 48 hours and lysed by boiling in the presence of SDS (1 x SDS PAGE

sample buffer). Samples were separated by electrophoresis on 8% polyacrylamide gels and proteins detected by staining with Coomassie (2.2.7.1 and 2.2.7.2). The resultant gel is shown in figure 3.1A.

A strong band of slightly larger than 66 kDa was present in the AcUL32 infected lane (lane 2) which was absent from the pac6 infected sample (lane 1). This band represents the UL32 protein, as the reported size of UL32 is 67 kDa (Chang *et al.*, 1996). The pac6 infected sample in contrast, showed a strong staining band corresponding to the lacZ protein expressed by the pac6 baculovirus (which has a reported size of 116 kDa).

To examine whether UL32 could be detected by western blotting using the anti-peptide antisera, BHK cells were transfected with 1 µg pUL32 using the calcium phosphate method (section 2.2.1.3) or infected with 5 p.f.u./cell wt HSV-1 or *hr*64 (section 2.2.4.3) for 18 hours. *Sf*21 cells were infected at a multiplicity of 5 p.f.u./cell with AcUL32 or the parental baculovirus pac6 as described above. The cells were harvested and lysed and samples were separated by electrophoresis on duplicate 8% polyacrylamide gels before being transferred onto PVDF membranes and blocked using blocking solution (section 2.2.7.1). The membranes were incubated with the anti-peptide antibodies (diluted 1:500). This was followed by incubation with HRP-conjugated protein-A (1:1000) and the proteins detected using an ECL substrate (section 2.2.7.3).

Representative membranes of samples immunoblotted with antibodies C12 and C11 are shown in figure 3.1, panel B. Both C12 and C11 recognised a protein in the lysate from AcUL32 infected *Sf*21 cells (lane 1), which was absent from pac6 infected cells (lane 2). This band corresponded in size to the UL32 band in the Coomassie stained gel in figure 3.1 A. Thus both antibodies are capable of specifically recognising UL32. Although UL32 was readily apparent in AcUL32-infected cells it could not be detected in transfected BHK cells (lane 3). This is likely to result from a combination of the lower efficiency of transfection compared to infection, and that the polyhedrin promoter drives higher level expression than the HCMV major immediate early promoter. The transfection efficiency in these experiments was approximately 20% as determined by transfection with pE*lacZ* and counting blue-stained cells, expressing β-galactosidase (section 2.2.1.5). In addition, neither C11 nor C12 could detect the UL32 expressed from wt HSV-1 infected cells (lane 4). Similarly both N9 and N10 specifically detected UL32 from *Sf*21 but not transfected or HSV-1 infected BHK cells (data not shown).

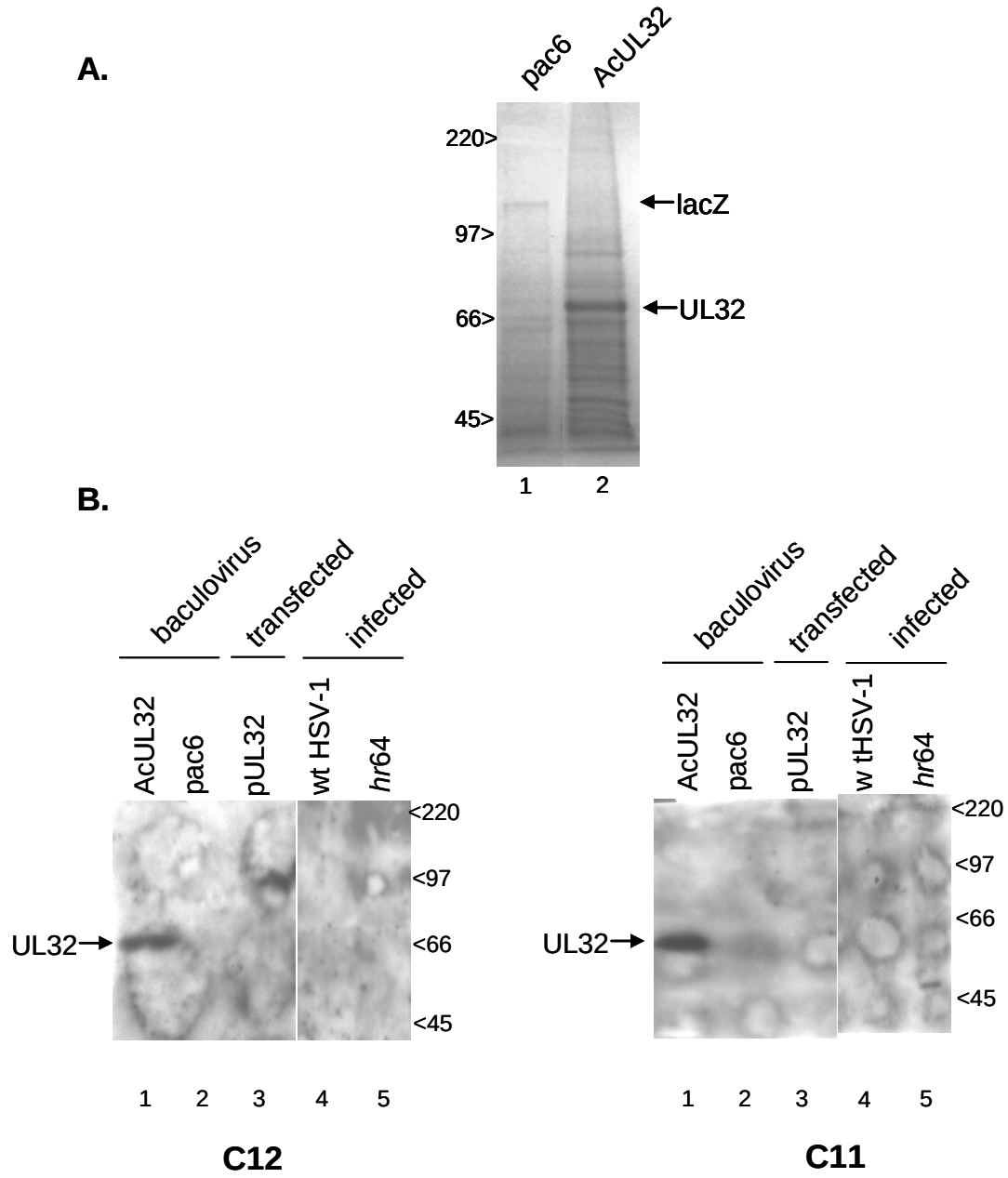

Figure 3.1: Testing UL32 anti-peptide antibodies in western blot.

A. *Sf*21 cells were infected with 5 p.f.u./cell AcUL32 or pac6 and harvested at 48 hours post infection. Cell lysates were prepared and separated by electrophoresis on 8% polyacrylamide gels and stained with Coomassie.

B. BHK cells were transfected with 1 µg pUL32 by the calcium phosphate procedure (lane 3), or infected with 5 p.f.u./cell wt HSV-1 or *hr*64 (lanes 4 and 5) and harvested after 18 hours. *Sf*21 cells were infected with 5 p.f.u./cell AcUL32 or pac6 and harvested at 48 h.p.i. (lanes 1 and 2). Cell lysates were prepared and separated on polyacrylamide gels and transferred to a PVDF membrane. The membranes were probed with either C12 or C11 antibodies at 1:500 followed by HRP-conjugated protein-A (1:1000), and developed with ECL. The positions of markers are indicated (kDa).

I therefore concluded that the anti-peptide antisera were probably insufficiently potent to be useful in further experiments and decided to generate an antiserum against the full-length native protein.

3.3 Expression of UL32 protein from baculovirus

The expression levels and solubility of UL32 in AcUL32-infected *Sf*21 cells were analysed at different time points to optimise infection conditions for the production of protein for use as an immunogen. *Sf*21 cells were infected with 5 p.f.u./cell AcUL32, for 24, 48 or 72 hours. After the specified time, the cells were harvested and resuspended in buffer A. An aliquot of the resuspended cells was retained as the total protein sample. The remainder was centrifuged to obtain a soluble extract (supernatant fraction). Samples of the total proteins and soluble extracts were analysed by SDS-PAGE and the gel stained with Coomassie.

Figure 3.2 shows that UL32 was undetectable as 24 hours post infection (lane 2) but a strong band corresponding to UL32 was detected in large amounts at 48 and 72 hours post infection (lanes 3 and 4). In addition, UL32 was efficiently recovered in the soluble extracts at these later times (lanes 6 and 7). The slightly greater amount of soluble UL32 at 72 hours post infection was not reproducibly observed, and it was decided to use a 48 hour infection to minimise problems with possible protein breakdown products.

3.4 Partial purification of UL32 using anion exchange chromatography

Anion exchange chromatography was used in an attempt to enrich the extract from AcUL32-infected cells for the UL32 protein prior to immunisation. This procedure separates proteins based upon their charge and so should allow partial purification of UL32 from a number of other baculovirus-expressed and cellular proteins with different properties.

Five 175 cm^2 flasks of *Sf*21 cells were infected with 5 p.f.u. per cell AcUL32 and harvested 48 hours post infection into 5 ml total buffer A (containing protease inhibitors)

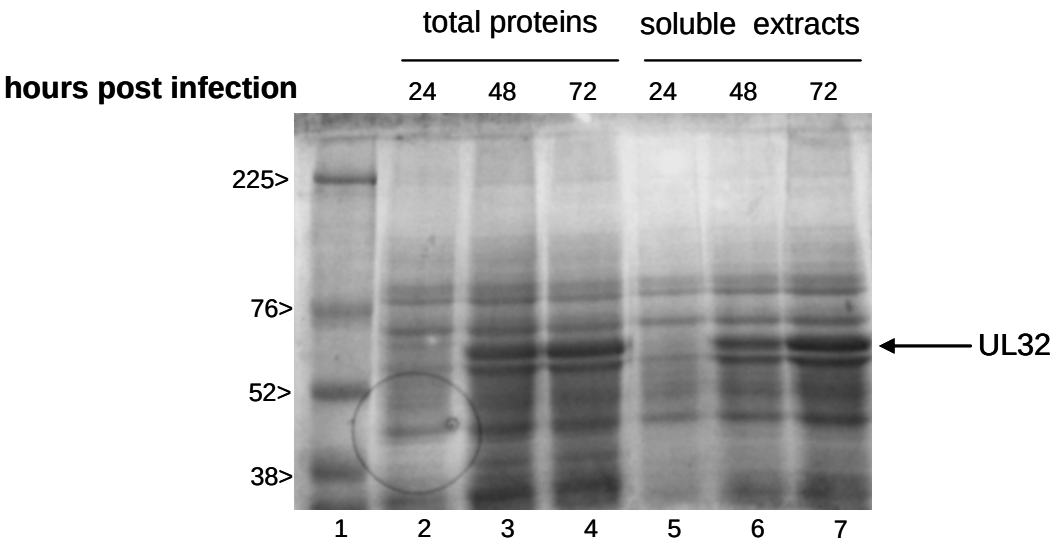

Figure 3.2: Expression of UL32 protein from AcUL32-infected *Sf*21 cells at 24-72 hours post infection.

*Sf*21 cells were infected with 5 p.f.u./cell AcUL32 and harvested at 24, 48 and 72 hours post infection. Total proteins were harvested and soluble extracts prepared by centrifugation. The samples were separated on an 8% acrylamide gel and stained with Coomassie. The position of the UL32 protein is indicated. Lane 1 contains marker proteins of the indicated sizes (kDa).

(section 2.2.9.1). Insoluble proteins were removed by ultra-centrifugation and the samples filtered through 0.45 µm filter. 20 µl soluble protein extract was analysed by SDS-PAGE followed by Coomassie staining to confirm good expression of the UL32 protein (data not shown).

The chromatography was carried out using the AKTA 900 purification system and a 1 ml MonoQ 5/50 GL column (Amersham). The column was equilibrated with buffer A and the filtered protein sample applied to the column. The column was washed and the protein eluted with a salt gradient from 50 mM NaCl to 1 M NaCl over 60 ml (section 2.2.9.2). 0.5 ml fractions were collected throughout the gradient.

Figure 3.3 shows a representative trace of the UV absorbance, corresponding to protein concentration, for the purification. The large peak between 0-10 ml contains the flow-through proteins that did not bind to the MonoQ column. SDS-PAGE analysis and Coomassie staining showed no detectable UL32 in these fractions (data not shown), confirming that UL32 protein bound efficiently to the MonoQ column. Various peaks can be seen as proteins are eluted at different salt concentrations. All fractions were analysed by SDS-PAGE and Coomassie staining, which demonstrated that the UL32 peak was eluted over fractions B13-C6, at approximately 0.3 M NaCl. Figure 3.4A shows the Coomassie stained gel of these peak fractions, demonstrating the presence of UL32 in these fractions. The identity of UL32 was confirmed by western blotting using the C12 antibody (figure 3.4B). Inspection of figures 3.4A and B revealed that fractions B15-C2 were most highly enriched for the UL32 protein. An equivalent MonoQ fractionation of soluble proteins expressed from the pac6 baculovirus showed an almost identical elution profile with the exception that the peak corresponding to UL32 at 27 ml was absent (data not shown).

This experiment confirmed that UL32 could be successfully enriched using anion exchange chromatography. However, as the UL32 was to be injected into rabbits, any toxic compounds needed to be removed. Therefore, the purification was repeated in the absence of the detergent, NP40. Soluble protein from AcUL32-infected *Sf*21 cells was prepared and applied to the MonoQ column as before, but NP40 was omitted from the buffers used for washing and elution. Examination of the resulting fractions yielded results essentially indistinguishable from those obtained in the presence of NP40 (data not shown).

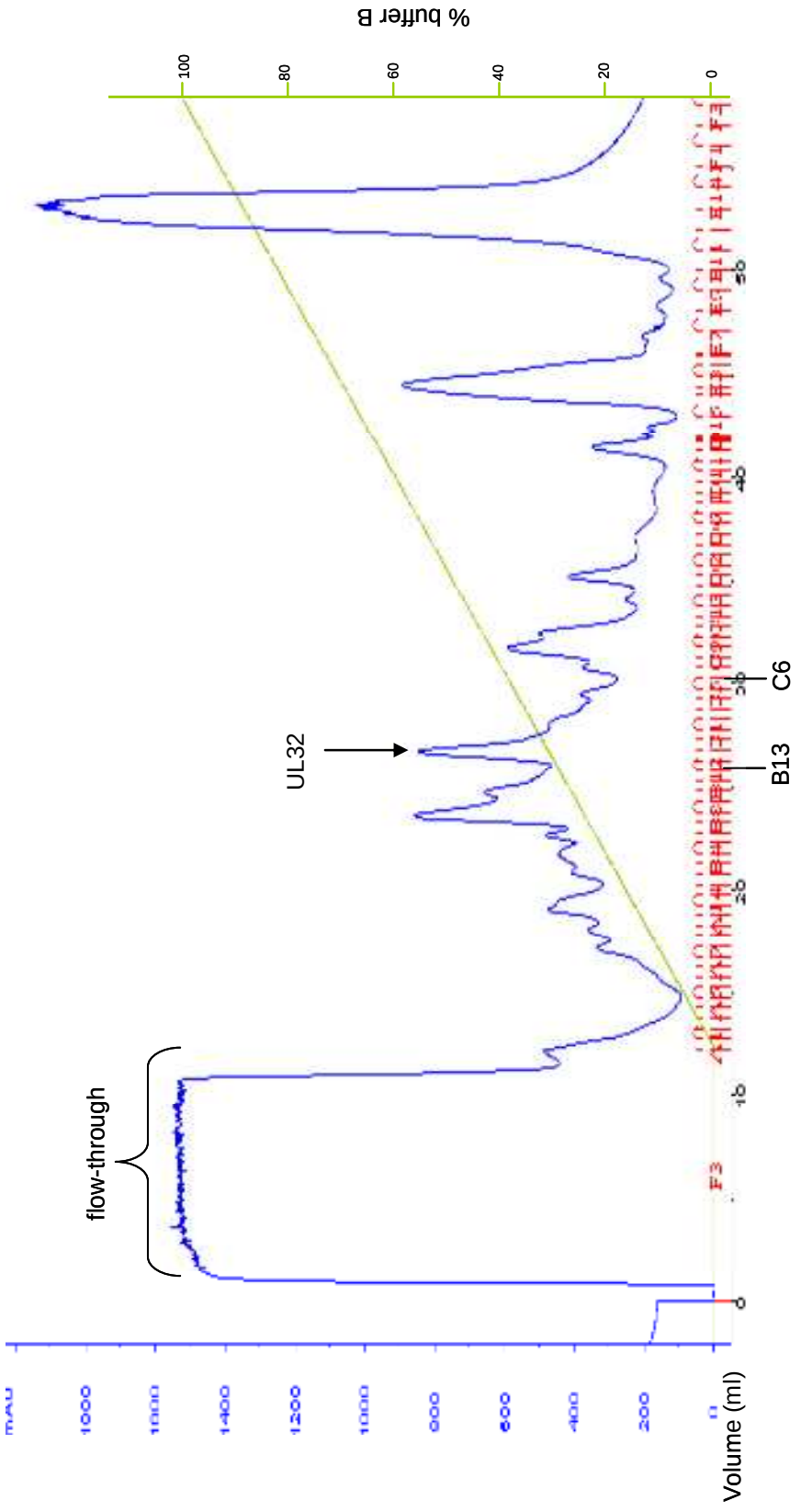

Figure 3.3 : Partial purification of UL32 using a MonoQ anion exchange column.
*Sf*21 cells were infected with 5 p.f.u./cell AcUL32 and the soluble proteins harvested and filtered. These proteins were loaded onto a MonoQ column and eluted with a NaCl gradient (50 mM–1 M). 0.5 ml fractions were collected. This trace shows the UV absorbance of fractions eluted from the MonoQ column. The volume of buffer through the column is shown at the bottom, and the fractions collected are shown in red. The green line shows the concentration of buffer B (0-100%), indicating the NaCl gradient. The position of the flow-through proteins is shown and the UL32 peak (along with the corresponding fractions) is labelled.

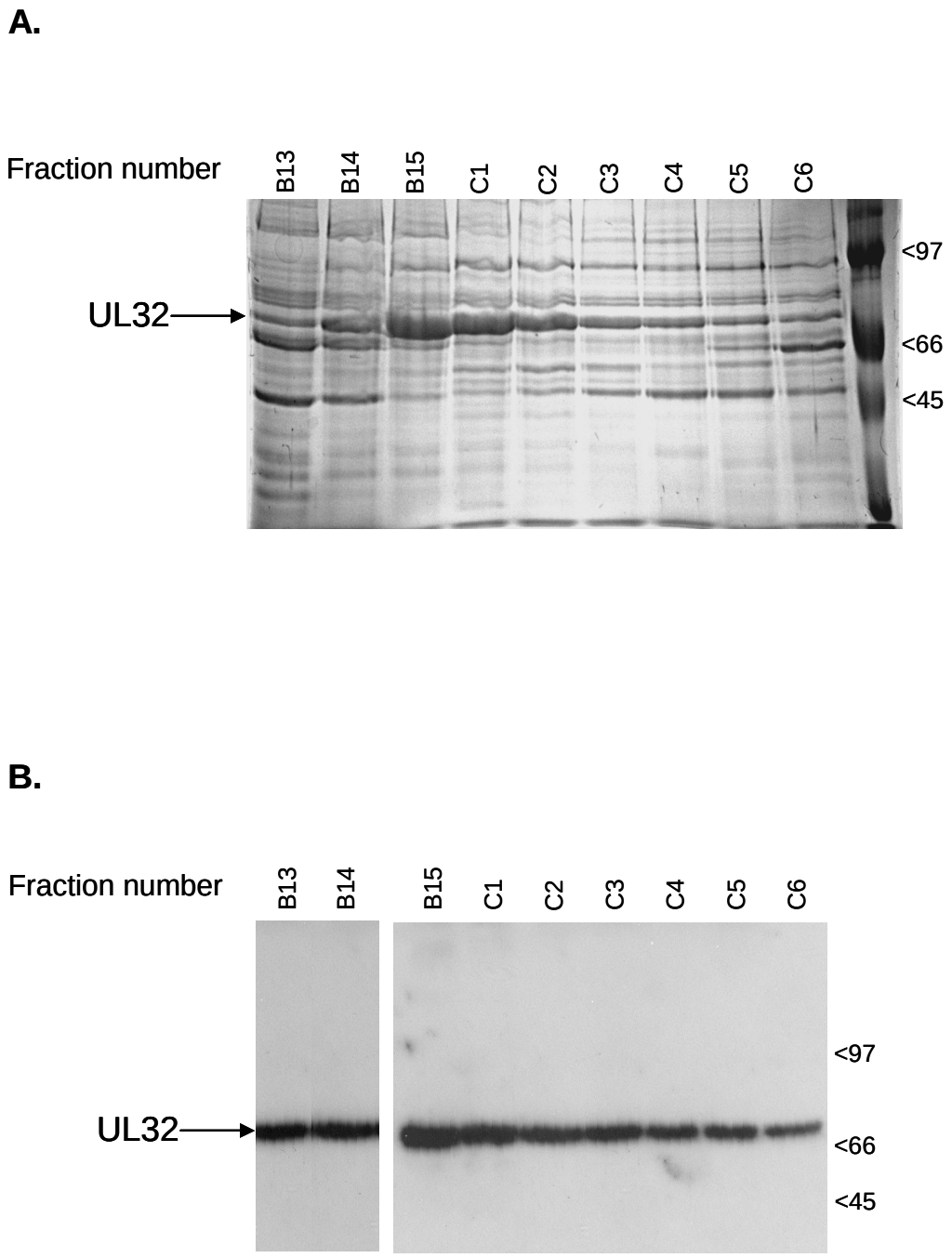

Figure 3.4: Confirmation of the presence of UL32 in peak fractions from anion exchange purification.
*Sf*21 cells were infected with AcUL32 and the cell extract purified through a MonoQ column (see figure 3.3). Fractions were collected and analysed by SDS-PAGE and either Coomassie staining (A) or western blotting with anti-peptide antibody C12 (1:500) followed by HRP-conjugated protein-A (1:1000) (B). Only fractions B13-C6, corresponding to the UL32 peak, are shown. Positions of size marker proteins are indicated (kDa).

3.5 Production of UL32 antisera

Three separate samples of protein were applied to the MonoQ column in the absence of NP40 and the peak fractions from each (seven fractions in total) pooled for use as immunogen. The total protein concentration was determined by Bradford assay as approximately 1.5 mg/ml (section 2.2.9.3). The purity of UL32 in this sample was estimated following SDS-PAGE analysis and Coomassie staining. Analysis of the gel using the "lane" function (Bio-Rad Quantity One) indicated that the UL32 peak corresponded to approximately 40% of the protein present in the whole lane.

The protein sample was emulsified in adjuvant by Dr. Susan Graham (MRC Virology Unit) and two rabbits immunised and sera collected by Colin Hughes (University of Glasgow). The immunisation schedule is described in methods, section 2.2.10.1.

3.6 Testing pre-immune and test-bleed sera

A pre-immune bleed was taken from each rabbit prior to immunisation to confirm that the rabbits had no pre-existing antibodies that reacted against proteins of a similar size to UL32 that may interfere with the recognition of UL32, and also to act as a negative control for the recognition of UL32 by the immune sera.

A test bleed of 5ml was taken from each rabbit one week after the third UL32 protein boost to ensure that the antisera produced after immunisation was able to recognise UL32.

Both the pre-immune and test-bleed sera were harvested by clotting overnight at 4°C, removing the serum and then separating this from any remaining red blood cells by centrifugation (section 2.2.10.2). These sera were split into small aliquots and stored at -20°C, and the pre-immune named R1-PI and R2-PI, with the test bleeds named R1-TB and R2-TB. All of these were then examined for reactivity against UL32 in western blots. The pre-immune sera were used at a much higher concentration (1:6) than the antisera to ensure that even low levels of pre-existing reactivity were detected.

3.6.1 Western blot using R1 and R2

BHK cells were transfected with 1 µg pUL32 or pCMV10 using the calcium phosphate method and harvested after 18 hours. Alternatively BHK cells were infected with wt HSV-1 or *hr*64 at a multiplicity of 5 p.f.u. per cell or mock infected for 18 hours. For further testing of the pre-immune sera, *Sf*21 cells were also infected with 5 p.f.u. per cell AcUL32 and harvested 48 hours post infection. 20 µl samples of each were separated by electrophoresis on an 8% acrylamide gel and transferred to PVDF membranes. The membranes were immunoblotted with either R1-PI or R2-PI pre-immune sera at a 1:6 dilution, or R1-TB or R2-TB antisera at a 1:500 dilution. This was followed by incubation with HRP-conjugated protein-A and detection using the ECL substrate. The results are shown in figure 3.5.

The pre-immune serum R1-PI (panel A) recognised two protein bands of between 45 and 66 kDa in all lanes. However, these proteins are both smaller than UL32, which migrates at 67 kDa, and so should not interfere with the recognition of UL32 by the final antisera. Furthermore, there are no extra bands seen in the samples containing UL32 (lanes 3, 4 and 6), confirming that R1-PI doesn't react against UL32. In contrast, antiserum R1-TB (shown in figure 3.5, panel B) clearly reacts against a protein corresponding to the reported size of UL32 of 67 kDa in the sample from cells transfected with pUL32 (lane 11), but not in cells transfected with pCMV10 (lane 12). R1-TB also detects a specific band of the same size in wt HSV-1 infected cells (lane 9), that is not present in cells that are infected with UL32 null mutant *hr*64 (lane 8) or mock infected (lane 7). This confirms that antiserum R1 reacts specifically against the UL32 protein in western blots.

Pre-immune serum R2-PI (figure 3.5C) again showed two bands between 45 and 66 kDa in all lanes, but showed no reaction against the UL32 protein in lanes 14 and 15. R2-PI did however, react against a number of extra proteins in the baculovirus-infected sample (lane 17) at least one of which was a similar size to UL32. Antiserum R2-TB (figure 3.5D) reacted similarly to R1-TB, recognising UL32 protein from cells transfected with pUL32 (lane 22) and infected with wt HSV-1 (lane 20) but showing no reaction to the samples not containing UL32. However, the recognition of the UL32-containing samples by R2-TB was somewhat weaker than that of R1-TB. These results show that both antisera can specifically recognise the UL32 protein in western blot.

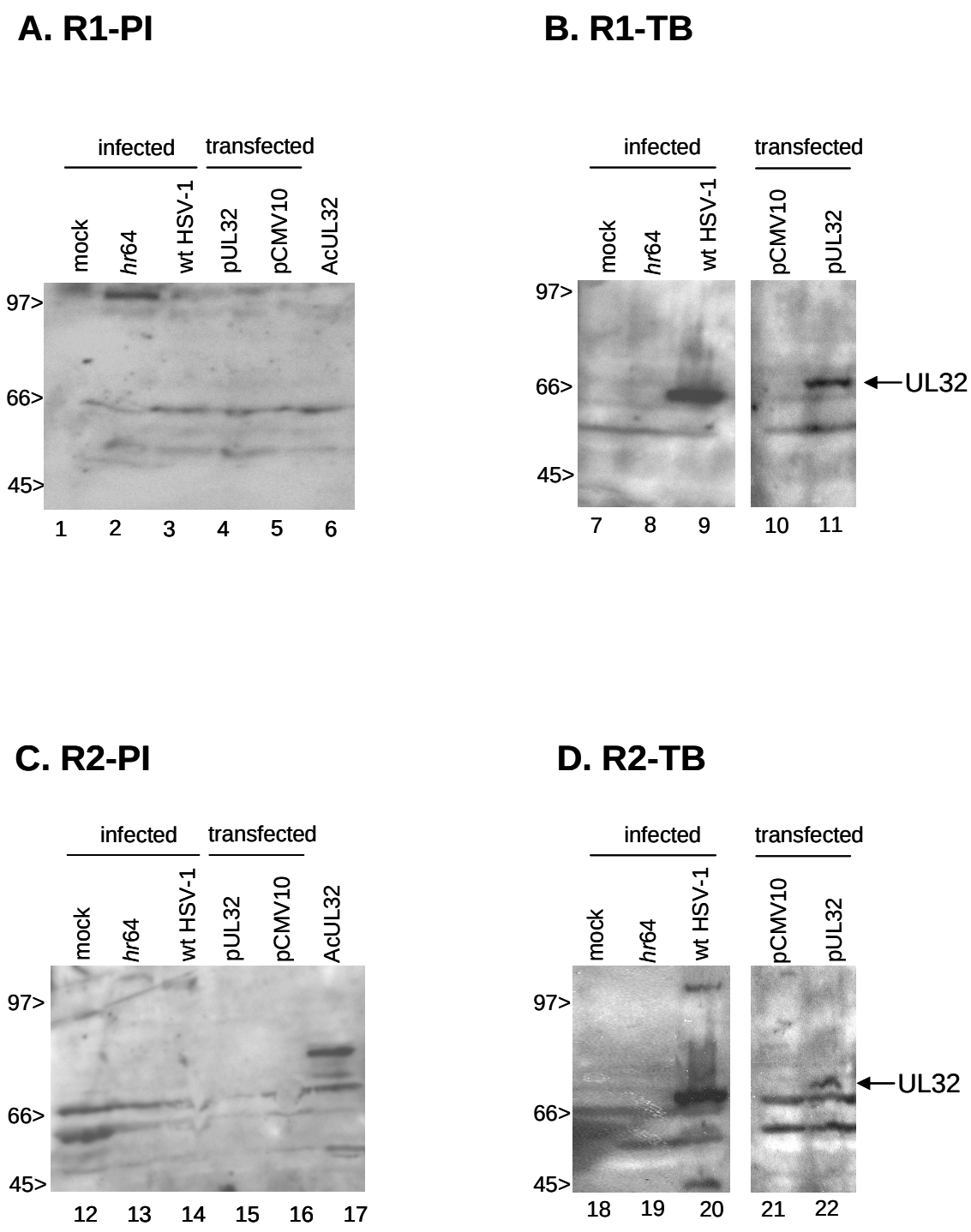

Figure 3.5: Testing pre-immune sera and test-bleed antisera for reaction against UL32.

BHK cells were infected with 5 p.f.u./cell wt HSV-1 or *hr*64 or mock infected, or transfected with 1 µg pUL32 or pCMV10 and harvested after 18 hours. *Sf*21 cells were infected with AcUL32 at 5 p.f.u./cell for 48 hours. All samples were separated by SDS-PAGE and immunoblotted using a 1:6 dilution of R1-PI (A) or R2-PI (C), or a 1:500 dilution of R1-TB (B) or R2-TB (D) as indicated. This was followed by incubation with HRP-conjugated protein-A (1:1000) and detection using ECL. Positions of size markers are indicated (kDa)

3.6.2 Immunofluorescence using R1 and R2

The two antisera were next tested for their ability to recognise UL32 by immunofluorescence in transfected cells. Duplicate glass coverslips of BHK cells were transfected with 0.5 µg pUL32 or pCMV10 using Lipofectamine 2000 (section 2.2.1.4). 18 hours post transfection the coverslips were treated with formaldehyde fix and permeabilisation solution (section 2.2.8). The cells were incubated with antibodies R1-TB or R2-TB (1:500 dilution) followed by r-FITC (FITC-conjugated goat anti-rabbit IgG) (1:200) and examined by confocal microscopy. Representative images are shown in figure 3.6.

Both R1-TB and R2-TB antisera showed bright fluorescence in the cytoplasm of cells transfected with pUL32. In contrast, when the cells were transfected with the vector control pCMV10, no fluorescence was seen in any cells within a whole field of view, even though β-galactosidase expression from cells transfected with pELacZ confirmed a high transfection efficiency. This indicates that both antisera can specifically detect UL32 in an immunofluorescence assay.

As the test bleeds showed good reactivity to UL32, both rabbits were given one final boost before final bleeds of approximately 50 ml were taken. These were harvested as previously described and named R1 and R2. These antisera were analysed for reactivity against UL32 in the same assays as the test bleeds. Both final bleeds reacted in an identical way to the test bleeds, specifically recognising the UL32 protein in both western blot and immunofluorescence. Again, R1 showed a stronger reaction against UL32 than R2 in the western blots. The antisera were stored in aliquots at -20°C.

3.7 Titration of R1 antiserum in western blot

Since R1 appeared to give a stronger UL32 signal and lower background than R2 it was chosen as the main antiserum against UL32, and titrated to find the optimum concentration for use in western blots.

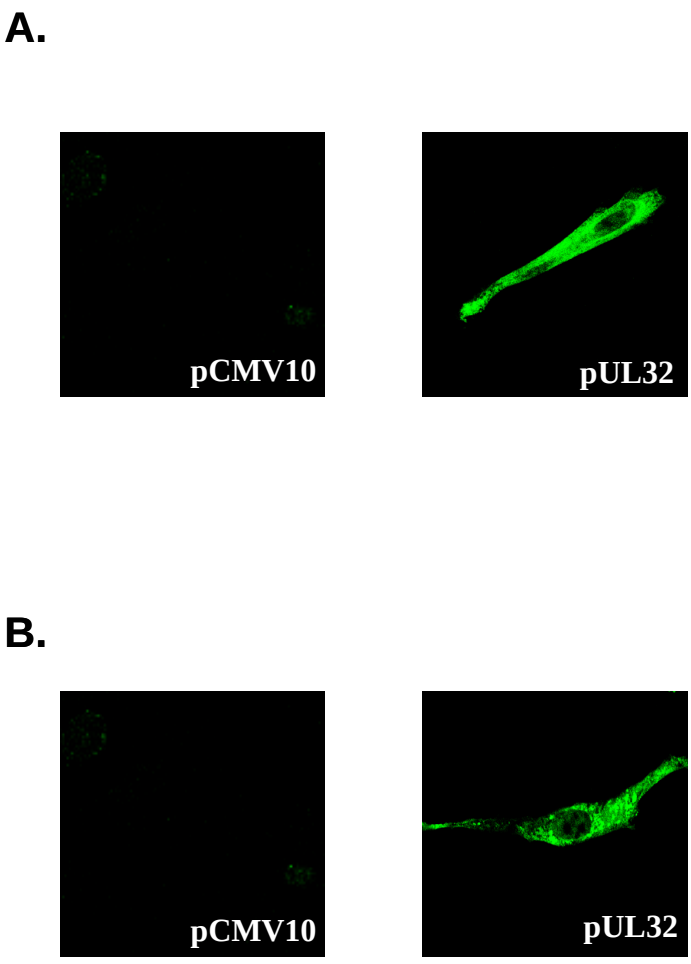

Figure 3.6: Testing R1 and R2 antisera for their ability to recognise UL32 by immunofluorescence.

0.5 µg pUL32 or pCMV10 was transfected into BHK cells on glass coverslips using Lipofectamine 2000. 18 hours post transfection, cells were fixed with formaldehyde and permeabilised with NP40. Coverslips were then probed with R1 (A) or R2 (B) at 1:500 dilution followed by FITC (1:200) and examined by confocal microscopy. All images represent the same exposure.

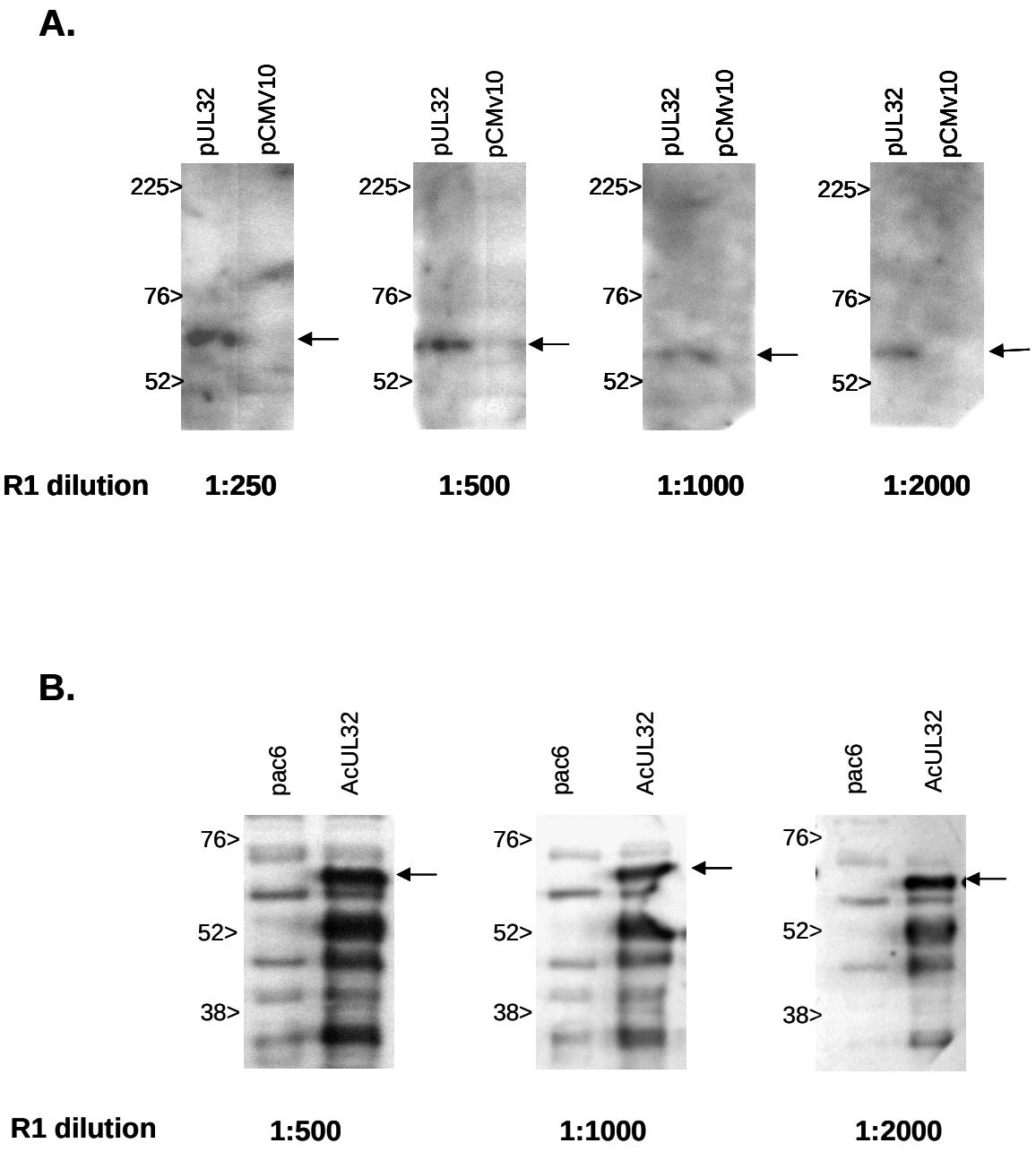

Figure 3.7: Titration of R1 antibody in western blot.

A. BHK cells were transfected with 1 µg pUL32 or pCMV10 using the calcium phosphate method. 18 hours post transfection, cells were harvested and lysed and samples separated by SDS-PAGE and western blotted. Membranes were incubated with R1 at the indicted dilutions, followed by HRP-conjugated protein-A sepharose. The positions of size markers are indicated and UL32 is denoted with an arrow.

B. *Sf*21 cells were infected with 5 p.f.u./cell pac6 or AcUL32 recombinant baculoviruses for 48 hours. Soluble protein extracts were prepared and separated by electrophoresis on an SDS-PAGE gel and immunoblotted with R1 at the indicated dilutions. The positions of size markers are indicated and UL32 is denoted with an arrow.

BHK cells were transfected with 1 µg pUL32 or pCMV10 and harvested after 18 hours. Samples were separated by SDS-PAGE and western blotted and the membranes immunoblotted using R1 at the concentrations indicated in figure 3.7A. A band corresponding to UL32 was detected at all four antibody concentrations. This band was most prominent at the 1:250 and 1:500 dilutions, and much weaker when the antiserum was diluted to 1:1000 and 1:2000. However, a slightly higher background signal was present at the 1:250 dilution (as seen in the samples transfected with pCMV10). It was therefore decided to use R1 at a 1:500 dilution in western blots of transfected cells for the remainder of this work.

The reactivity of R1 with extracts of baculovirus-infected insect cells was also examined. *Sf*21 cells were infected with 5 p.f.u. per cell AcUL32 or pac6 for 48 hours. Soluble extracts were prepared as previously described and duplicate samples separated by SDS-PAGE and western blotted. Membranes were then immunoblotted with R1 at the concentrations indicated in figure 3.7B. The R1 antibody recognised a number of bands in the AcUL32 sample, many of which were also present in the pac6 samples. This is not surprising since the UL32 preparation used for immunisation was known to contain many other proteins of cellular and/or baculovirus origin, a proportion of which were likely to have been recognised as foreign antigens by the rabbits. These additional proteins were most prominent at the higher concentrations of R1 (1:500 and 1:100 dilution). The UL32 protein is the largest band unique to the AcUL32 sample, corresponding to the reported size of 67 kDa. A number of smaller bands can also be seen between the sizes of 30-50 kDa in the UL32 samples that are not present in the pac6 samples. These are likely to be breakdown products of the UL32 protein, which are also recognised by the R1 antiserum. At the 1:2000 dilution, full-length UL32 was readily detected, with a reduction in the intensity of some of the other bands, and therefore this dilution was chosen for western blots of baculovirus-expressed UL32.

3.8 Discussion

This chapter described the partial purification of UL32 and the production of two new antisera raised against UL32.

These new antisera were required because the anti-peptide antibodies against UL32 available in the laboratory were very weak, and large amounts of protein were required for detection on western blot. Thus baculovirus-expressed protein but not UL32 from transfected or HSV-1 infected cells could be detected.

Anion exchange chromatography provided a convenient method for the partial purification of UL32 from other baculovirus-expressed and cellular proteins on the basis of charge. This method did not completely remove other proteins, but resulted in a protein preparation that was approximately 40% pure, with UL32 as the predominant protein, which was suitable for use as an immunogen.

Two antisera were produced, both of which specifically reacted against UL32 in western blots and were potent enough to achieve the initial aim of detecting UL32 in transfected and HSV-1 infected cells. The R1 antibody was selected for main use due to its stronger reactivity against UL32 relative to background signal. When used in western blots of baculovirus-expressed UL32, the antibodies showed reactivity against many other proteins, although this may be expected as other proteins were present in the immunogen sample injected into the rabbit. However, by using the parental control baculovirus, pac6, it was easy to identify bands corresponding to full-length UL32 and its breakdown products in a western blot.

The new antisera also recognised UL32 in immunofluorescence assays and showed that UL32 localises to the cytoplasm of transfected cells. This is not surprising since HSV-1 UL32 lacks any obvious nuclear localisation sequence (NLS) and is too large to be able to diffuse through the nuclear pore. A putative NLS has been identified within HCMV UL52 which does localise to the nucleus of transfected cells (Borst *et al.*, 2008), and the PSORT II sub-cellular localisation prediction program identifies a putative NLS in a number of other UL32 homologues within the *Betaherpesvirinae* (Nakai & Horton, 1999). However, such a sequence is absent from HSV-1 UL32 and known homologues within the *Alphaherpesvirinae*.

The recognition of UL32 in immunofluorescence of transfected cells by the new antisera confirms that these polyclonal antisera can recognise the native form of UL32 as well as the denatured form in western blots. These antisera may therefore be useful for other techniques using native proteins, such as immunoprecipitation (IP).

4 Mutagenesis of UL32

4.1 Introduction

Although previous work has identified UL32 as a protein essential for genomic DNA packaging, its precise role within this pathway is still unclear. Furthermore, no large-scale mutagenic analysis of the protein has been carried out to identify essential regions. Thus far, bioinformatic analysis of the UL32 sequence has not yielded any information about the potential function of UL32 based on sequence similarity to other known proteins, whether viral or non-viral.

This chapter describes the generation and characterisation of a panel of insertional mutants throughout the length of the UL32 protein. The ability of each mutant to support the growth and DNA packaging of a virus lacking UL32 (*hr*64) was investigated in order to identify regions of the UL32 protein essential for function.

Further data presented in this chapter describe site-directed mutagenesis of conserved amino acids within UL32 and a similar analysis of the mutated proteins.

4.2 Generation of UL32 insertional mutants

4.2.1 Transposon-mediated mutagenesis

Random transposon-mediated insertional mutagenesis is an extremely useful tool for studying relatively uncharacterised proteins. It enables rapid generation of a panel of mutants with insertions scattered throughout the protein to allow identification of regions essential for growth and function.

The mutagenesis of UL32 was carried out using the Mutation Generation System kit from Finnzymes. This kit employs the transposition machinery of the bacteriophage Mu to insert a 1,131 bp artificial transposon (*Entransposon*) encoding a kanamycin resistance (kan^R) gene into the target plasmid at random sites in a cell-free reaction (figure 4.1). The DNA is

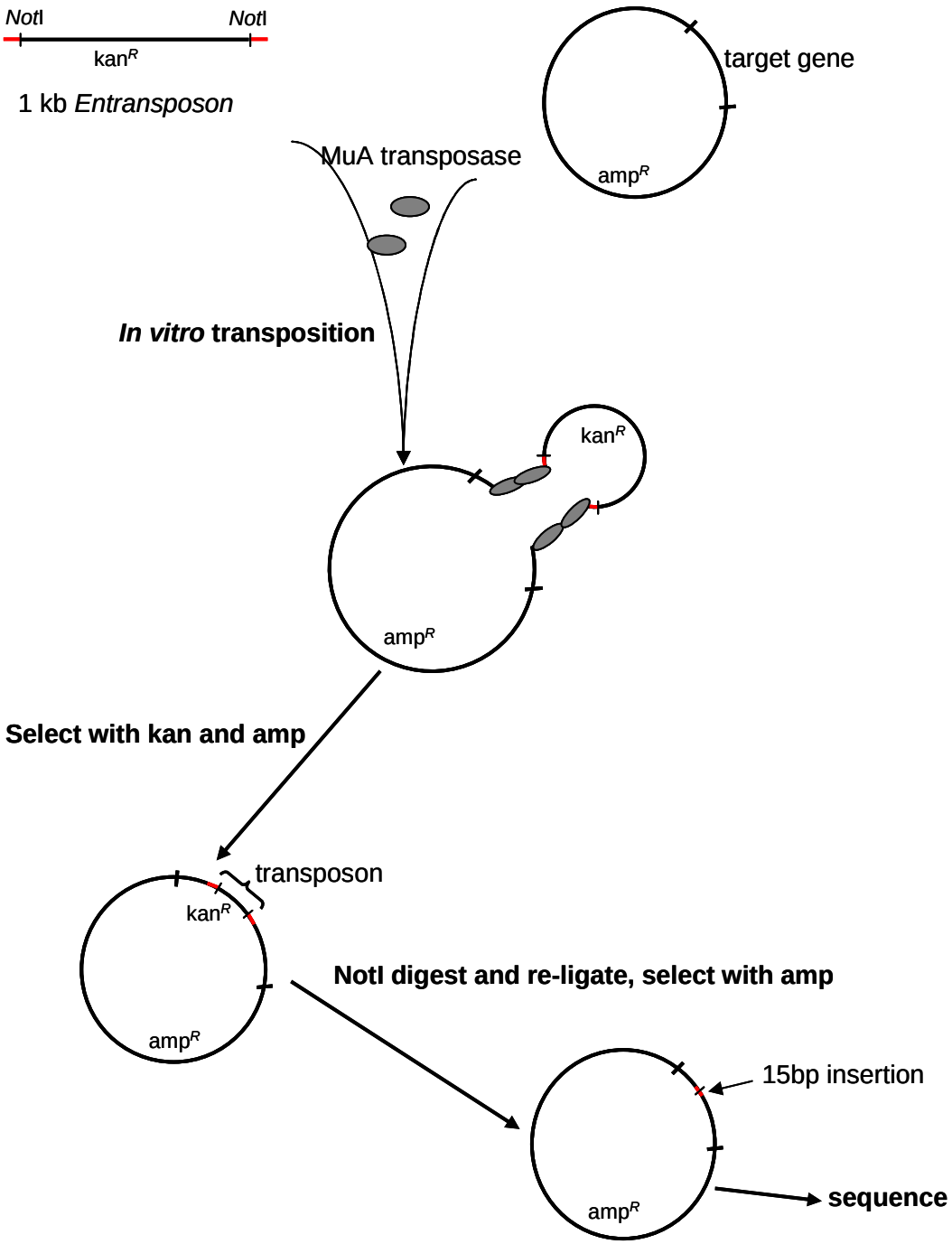

Figure 4.1: Principles of the Mutation Generation System.

An *in vitro* reaction catalysed by the MuA transposase results in the insertion of a 1,131 bp *Entransposon* (encoding kan^R and containing *Not*I sites at either end) into the amp^R target plasmid. This insertion may be within the target gene (as indicated here) or the plasmid backbone. Colonies are selected by resistance to kanamycin and ampicillin and plasmid DNA isolated from individual colonies. This DNA is digested with *Not*I and re ligated to remove the bulk of the transposon leaving a 15 bp insertion. The plasmid DNA is retransformed back into *E. coli* and amp^R colonies selected. Plasmid DNA from individual colonies is analysed by restriction digest and DNA sequencing to determine the position and nature of the insertions.

then transformed into bacteria and those plasmids that have the *Entransposon* selected by growth in the presence of kanamycin. The DNA is isolated and the kanamycin resistance gene excised using *Not*I sites situated at each end of the *Entransposon.* The DNA is recircularised resulting in a 15 bp insert consisting of 10 bp derived from the *Entransposon* (encoding a novel *Not*I site) and a 5 bp duplication of the target site (figure 4.2).

Insertions of 15 bp will not disrupt the reading frame of the protein and the resultant product should be identical to the wildtype protein except for the insertion of 5 amino acids. The inserted sequences do not encode a stop codon in any of the three frames, ensuring that none of the mutated proteins will be truncated.

4.2.2 Mutagenesis of UL32 protein

Plasmid pUL32 was generated by Arvind Patel (MRC Virology Unit). It contains an HSV-1 fragment comprising nucleotides 69159 to 67201 cloned as an *Nco*I to *Eco*47III fragment into the *Sma*I site of pCMV10. Within pUL32, the UL32 ORF is encoded by 1791 nucleotides (69162 – 67372 of HSV-1) and is under the control of the HCMV major immediate-early promoter.

pUL32 was incubated in a cell-free transposase reaction for one hour as described in section 2.2.3.10 and the reaction transformed into electrocompetent *E. coli* DH10 cells (GeneHogs; Invitrogen Ltd.). Plasmids containing the transposon were selected by growth in the presence of ampicillin and kanamycin. 293 colonies were picked and DNA prepared by the boiling lysis method (section 2.2.3.2).

As the inserted *Entransposon* is 1,131 bp, digestion with *Xba*I and *Kpn*I, which cleave near to either end of the UL32 gene, was used to screen whether the insert was within the UL32 gene or the plasmid backbone. Figure 4.3A shows the positions of the *Kpn*I and *Xba*I sites in pUL32. Integration of the *Entransposon* into the backbone should generate fragments of 4954 and 1973 bp, whereas integration into the UL32 containing fragment should result in fragments of 3823 and 3104 bp.

Figure 4.3B is a representative gel of this screen and the different restriction profiles obtained upon insertion of the Entransposon into either the plasmid backbone or the UL32 gene. Of these nine plasmids, the two marked with asterisks (lanes 3 and 9) generated

A.

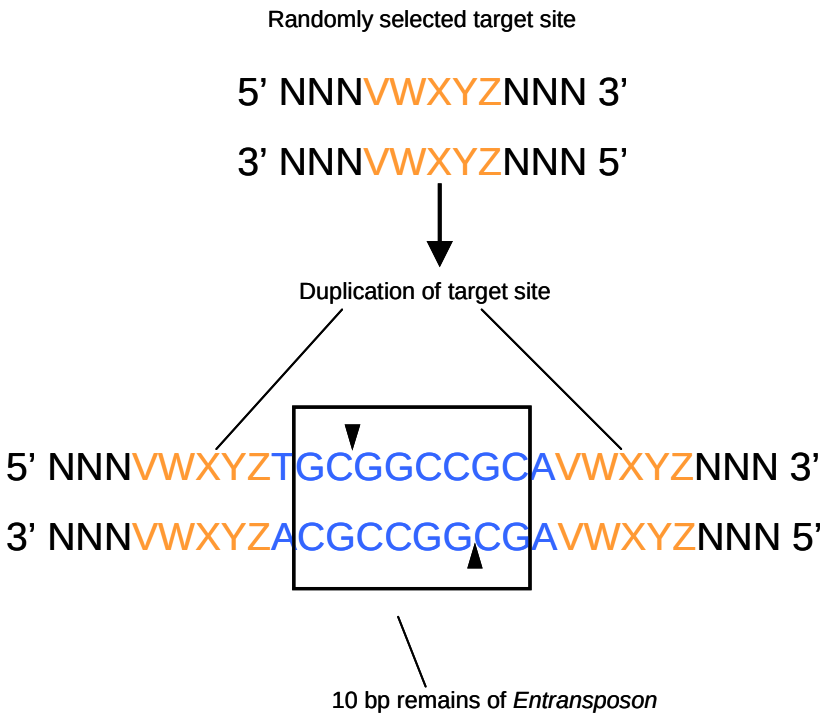

B.

Frame1:	NVW	XYZ	TGC	GGC	CGC	AVW	XYZ	NNN
	X	X	Cys	Gly	Arg	A	X	X
Frame 2:	NNV	WXY	ZTG	CGG	CCG	CAV	WXY	ZNN
	X	X	Leu Met Val	Arg	Pro	His Gln	X	X
Frame 3:	NNN	VWX	YZT	GCG	GCC	GCA	VWX	YZN
	X	X	X*	Ala	Ala	Ala	X	X

A = Ile, Met, Thr, Asn, Lys, Ser, Arg

X = any amino acid

X* = any amino acid except Gln, Glu, Lys, Met, Trp

Figure 4.2: Sequence of insertions generated by the MGS.

A. The randomly selected 5 bp target site is shown in orange and is duplicated during the transposition reaction. After *Not*I digestion, 10 bp of the *Entransposon* remains forming the short insert (blue). The box indicates the inserted *Not*I site, with the arrows indicating where the enzyme cleaves and the DNA is re ligated.

B. The frame in which the *Entransposon* is inserted and the sequence of the target DNA will determine the precise sequence of amino acids inserted. This table shows the 15 bp insert and translation of this in all three frames.

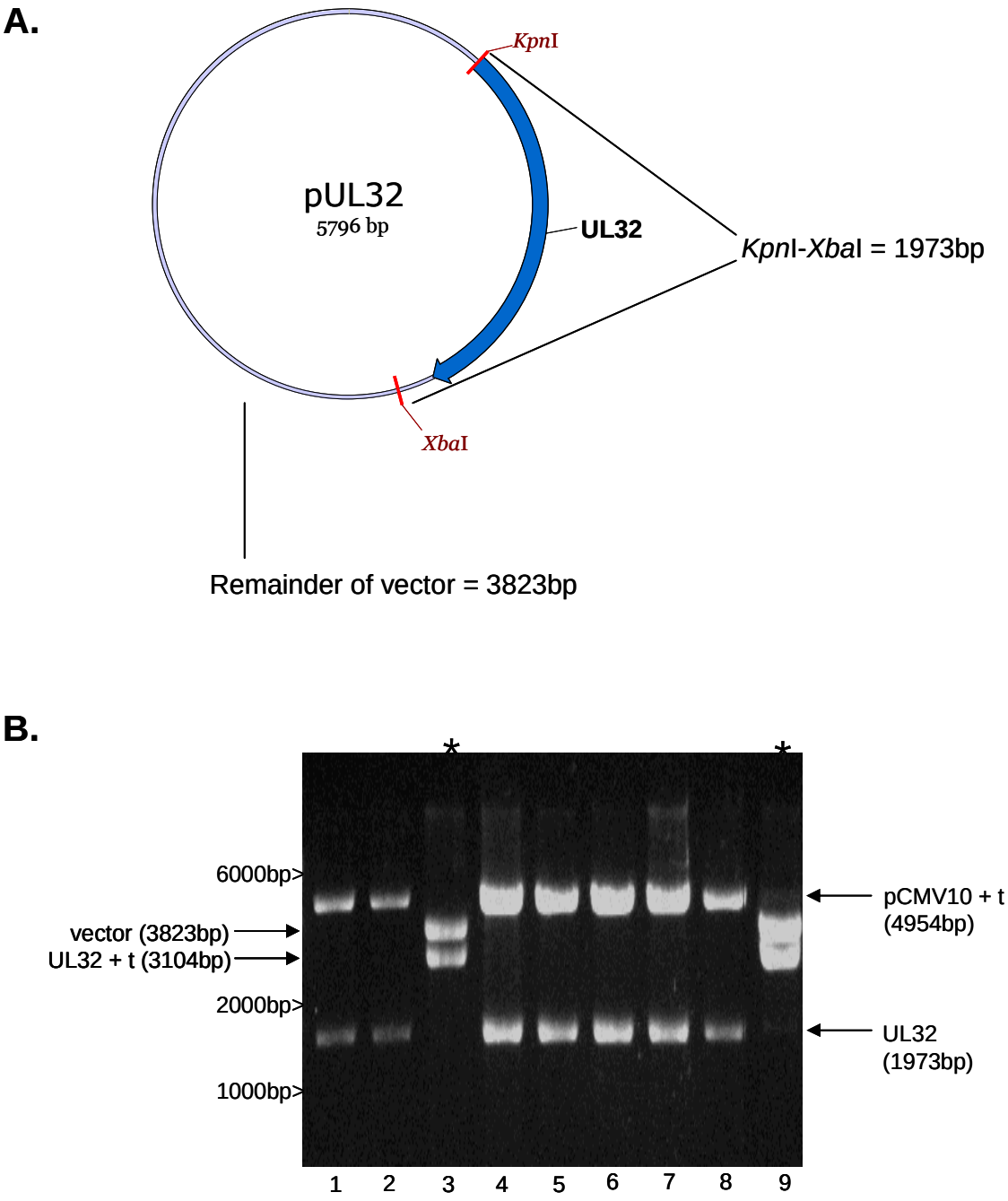

Figure 4.3 : Screening for transposon insertions within pUL32.

A. Plasmid map of pUL32, showing the positions of *XbaI* and *Kpn*I sites and the sizes of fragments generated in a double digest with these enzymes.

B. A representative 0.8% agarose gel of transposon-containing plasmid DNAs digested with *Kpn*I and *Xba*I, showing two populations, in agreement with the fragments predicted above. The size and identity of each fragment is indicated and the positions of DNA markers are shown.

fragments consistent with the predicted of sizes 3823bp and 3104bp, for the 1131bp transposon inserted within the UL32 gene. The remaining seven plasmids generated fragments consistent with the transposon inserted within the vector. In total 39 plasmids were identified with the *Entransposon* inserted within the UL32 fragment. An aliquot of each of these 39 plasmids was digested with *Not*I to excise the *Entransposon* and then re-ligated before being transformed into *E. coli* DH10 cells. Colonies were selected with ampicillin, picked and final DNA plasmid preparations made by boiling the lysis method as before.

4.2.3 Position of insertions within UL32

The approximate positions of insertions within the UL32 gene were first determined by digestion of the transposon-containing plasmids with *Not*I and *Xba*I. The *Xba*I site is 176 bp downstream from the 3' end of the UL32 ORF. This digest should generate 3 fragments; the 1,131 bp transposon, a fragment of up to 2 kb indicating the distance of the insertion from the *Xba*I site near the 3' end of the UL32 fragment, and a third fragment of between 3.8 and 5.8 kb containing the vector backbone. Figure 4.4 shows a representative gel of 15 mutants digested with *Xba*I and *Not*I. Lane 1 shows pUL32 which is linearised with *Xba*I but not cleaved by *Not*I. The *Entransposon* can be seen in all other lanes and the location of the transposon relative to the 3' end of the UL32 gene is shown by the smaller of the two other fragments, with the larger being the vector backbone. This enabled the approximate position of all 39 inserts to be determined.

Six primers (5240, UL32F1, UL32F2, UL32F3, UL32F4, and UL32R1) were designed to span the entire length of the UL32 gene and the positions and sequences of these primers are shown in figure 4.5. The appropriate primer was used to sequence the region of each final mutant plasmid from which the *Entransposon* had been excised. Once it had been established that each mutant contained the expected 15 bp insertion, the full UL32 sequence of each mutant was determined using all six sequencing primers.

In each case a 15 bp insertion was present consisting of a duplication of the target sequence and the 10 bp sequence TGCGGCCGCA derived from the *Entransposon*. The position and sequence of each insert within the UL32 gene is shown in figure 4.6. For consistency the first nucleotide of the 15 bp insertion is considered as the T residue of the sequence TGCGGCCGCA with the target sequence duplication being at the 3' end of the insert.

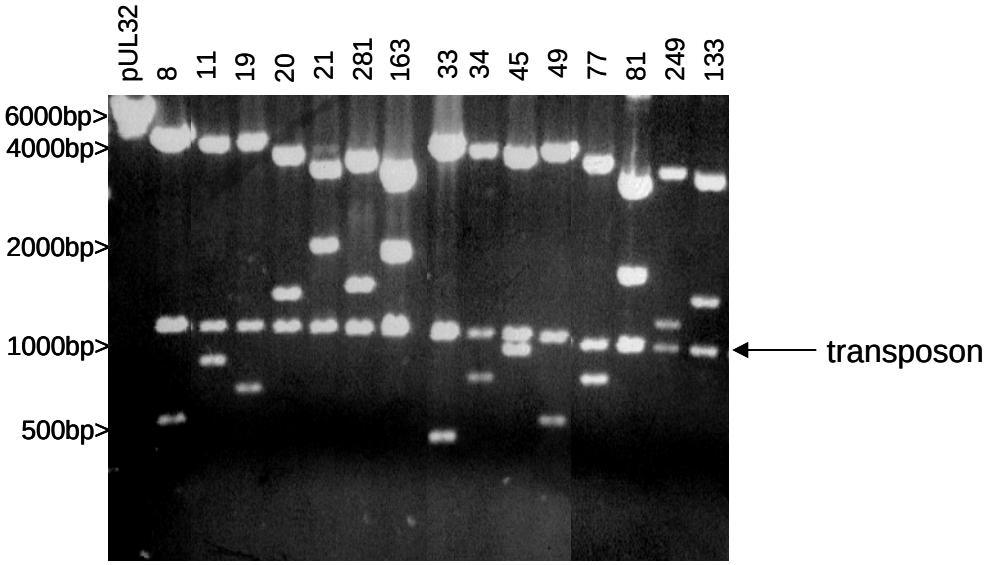

Figure 4.4: Mapping the position of insertion of transposon into pUL32 mutants.

Plasmid DNA of pUL32 and all mutants prior to excision of the transposon was digested with *XbaI* and *Not*I and fragments separated on a 0.8% agarose gel and visualised under UV light. This is a representative gel showing the position of the transposon within a selection of clones. The positions of the transposon is shown and positions of size markers are indicated.

A.

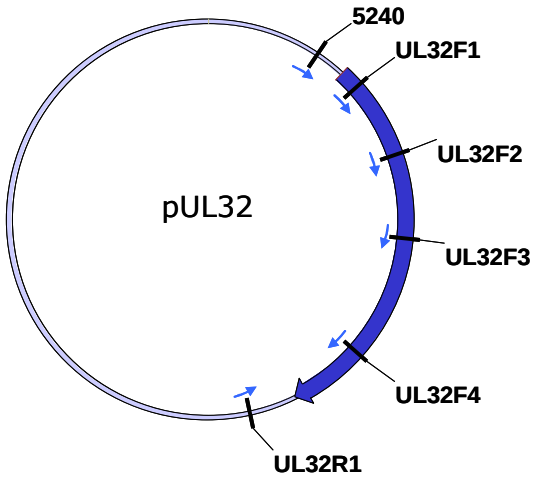

B.

	5' - 3' sequence
5240	CCATTGACGCAAATGGGC
UL32F1	CGTATGTGGCCTTCGATCC
UL32FR	TCTCTGTGCCAAATGCCTGG
UL32F3	GCTGATGAACTGGAAGGATTGC
UL32F4	GTTTGTGAGCCTGCTTCG
UL32R1	CACCACAGAAGTAAGGTTCC

Figure 4.5: Position and sequence of primers used for sequencing of UL32 mutants.

A. Plasmid map of pUL32 showing the positions of the six primers used to sequence the whole of the UL32 gene for all of the UL32 transposon mutants

B. 5’ – 3’ sequences of these sequencing primers. All primers give reads corresponding to the sense strand except UL32R1, which is complementary.

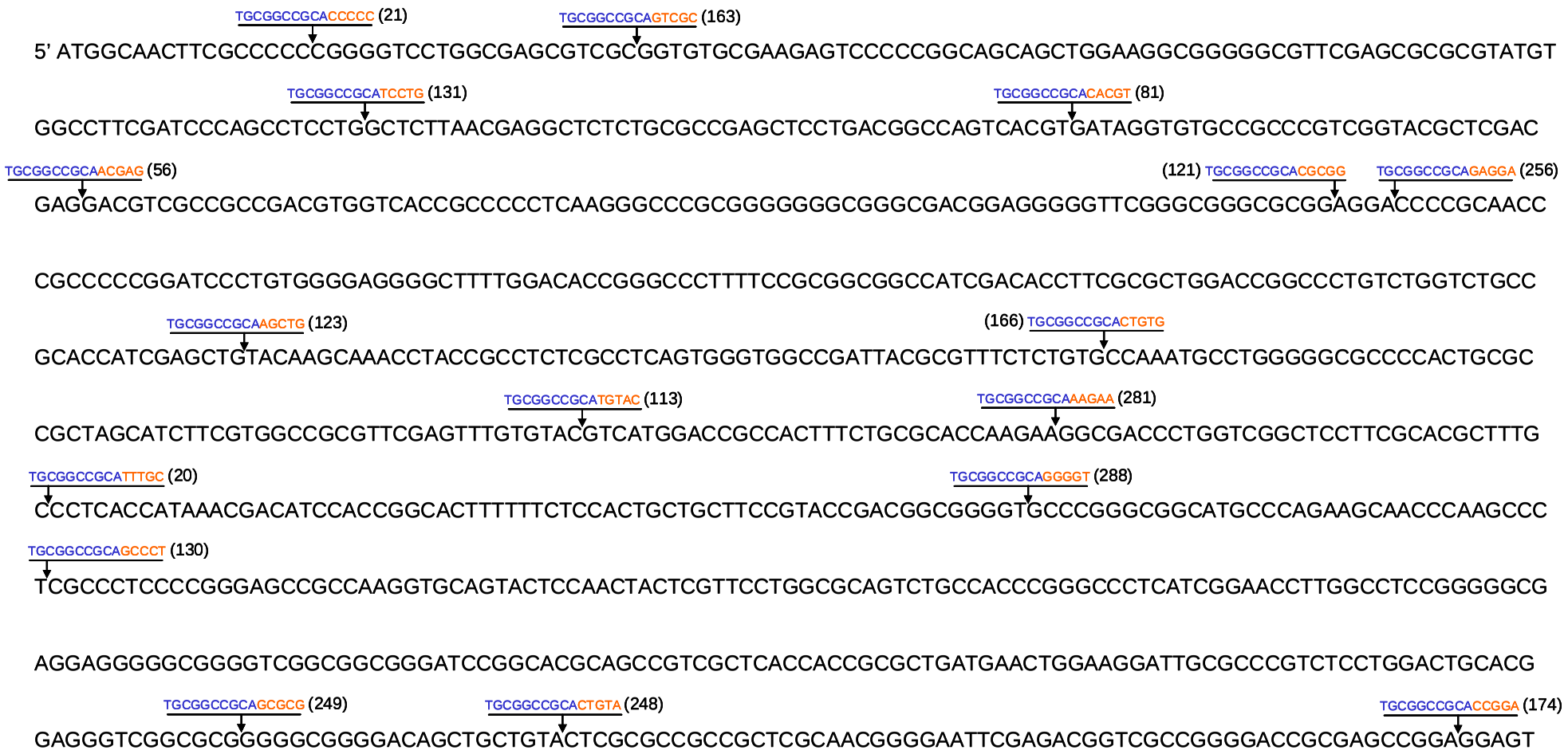
TGCGGCCGCACCCCC (21)
TGCGGCCGCAGTCGC (163)
5’ ATGGCAACTTCGCCCCCCGGGGTCCTGGCGAGCGTCGCGGTGTGCGAAGAGTCCCCCGGCAGCAGCTGGAAGGCGGGGGCGTTCGAGCGCGCGTATGT
TGCGGCCGCATCCTG (131)
TGCGGCCGCACACGT (81)
GGCCTTCGATCCCAGCCTCCTGGCTCTTAACGAGGCTCTCTGCGCCGAGCTCCTGACGGCCAGTCACGTGATAGGTGTGCCGCCCGTCGGTACGCTCGAC
TGCGGCCGCAACGAG (56)
(121) TGCGGCCGCACGCGG
TGCGGCCGCAGAGGA (256)
GAGGACGTCGCCGCCGACGTGGTCACCGCCCCCTCAAGGGCCCGCGGGGGGGCGGGCGACGGAGGGGGTTCGGGCGGGCGCGGAGGACCCCGCAACC
CGCCCCCGGATCCCTGTGGGGAGGGGCTTTTGGACACCGGGCCCTTTTCCGCGGCGGCCATCGACACCTTCGCGCTGGACCGGCCCTGTCTGGTCTGCC
TGCGGCCGCAAGCTG (123)
(166) TGCGGCCGCACTGTG
GCACCATCGAGCTGTACAAGCAAACCTACCGCCTCTCGCCTCAGTGGGTGGCCGATTACGCGTTTCTCTGTGCCAAATGCCTGGGGGCGCCCCACTGCGC
TGCGGCCGCATGTAC (113)
TGCGGCCGCAAAGAA (281)
CGCTAGCATCTTCGTGGCCGCGTTCGAGTTTGTGTACGTCATGGACCGCCACTTTCTGCGCACCAAGAAGGCGACCCTGGTCGGCTCCTTCGCACGCTTTG
TGCGGCCGCATTTGC (20)
TGCGGCCGCAGGGGT (288)
CCCTCACCATAAACGACATCCACCGGCACTTTTTTCTCCACTGCTGCTTCCGTACCGACGGCGGGGTGCCCGGGCGGCATGCCCAGAAGCAACCCAAGCCC
TGCGGCCGCAGCCCT (130)
TCGCCCTCCCCGGGAGCCGCCAAGGTGCAGTACTCCAACTACTCGTTCCTGGCGCAGTCTGCCACCCGGGCCCTCATCGGAACCTTGGCCTCCGGGGGCG
AGGAGGGGGCGGGGTCGGCGGCGGGATCCGGCACGCAGCCGTCGCTCACCACCGCGCTGATGAACTGGAAGGATTGCGCCCGTCTCCTGGACTGCACG
TGCGGCCGCAGCGCG (249)
TGCGGCCGCACTGTA (248)
TGCGGCCGCACCGGA (174)
GAGGGTCGGCGCGGGGGCGGGGACAGCTGCTGTACTCGCGCCGCCGCTCGCAACGGGGAATTCGAGACGGTCGCCGGGGACCGCGAGCCGGAGGAGT

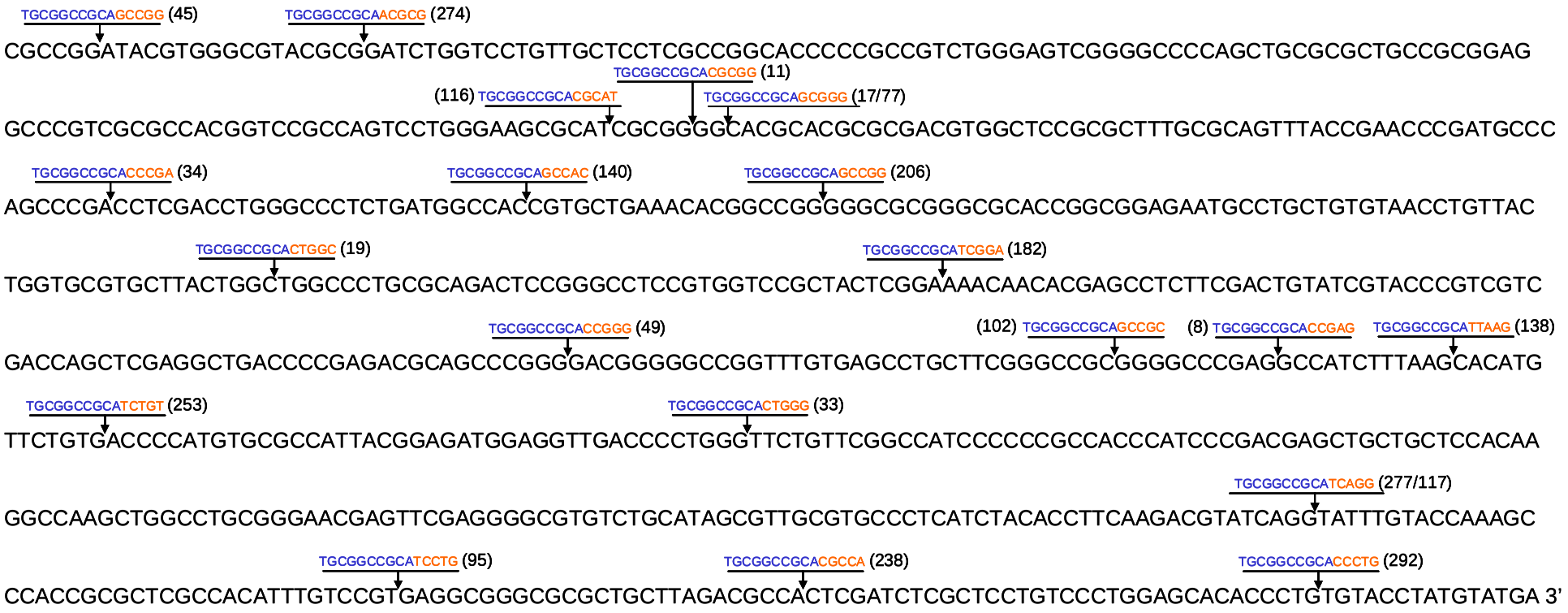

Figure 4.6: DNA sequence of HSV-1 UL32, showing the positions of DNA insertions.

Nucleotides 1 - 1791 of UL32 ORF (comprising nts 69162 - 67372 of HSV-1 sequence) are shown. The full DNA sequences of each of the insertional mutants was determined by sequencing and the position and sequence of each insert is shown. Mutants are indicated by clone number in brackets and where clonally identical insertions were present, both clones have been numbered. For clarity, the 10 bp insertion is shown in blue and the 5 bp target site duplication is indicated in orange at the 3' end of each insertion.

Apart from the 15 bp insert, the full DNA sequence of each clone was identical to that of the wt UL32 gene of pUL32.

Each DNA sequence was next translated using the Expasy Translate program and compared to the wt UL32 protein sequence using the ClustalX alignment programme to identify the position and sequence of each 5 amino acid insertion. As the insertion can be in any of the three frames and also involves the duplication of part of the target sequence, there is variation between the inserted amino acids in different mutants. The sequence of the amino acid insertion within each mutant protein is shown in table 4.1. Each mutant was named according to the last unaltered amino acid before the insertion and will be referred to as such for the remainder of this thesis. Clones 17 and 77, and 117 and 277 had identical insertions at the same points in the protein and only one clone of each pair (17 and 277 respectively) was selected for further characterisation. The positions of each insertion within the UL32 protein are shown in figure 4.7.

After sequencing of all of the mutants, 1 µg of each was again digested with *Not*I and *Xba*I and separated on a gel to confirm that the inserted *Not*I site was in the expected position and that the transposon had been excised. Figure 4.8 shows the digest patterns for a selection of clones with inserts between amino acids 378 and 485. As expected, the nearer the insertion to the C-terminus of UL32 the smaller the *Not*I-*Xba*I fragment.

4.2.4 Expression of UL32 mutant proteins

Having verified the DNA sequences of the insertional mutants, it was important to check that the encoded proteins were of a similar size to wt UL32 and expressed at similar levels.

1 µg each plasmid was transfected into BHK cells by the calcium phosphate method as described in section 2.2.1.3. 18 hours post transfection, cells were harvested and lysed and the proteins separated on an 8% polyacrylamide gel. These were transferred to PVDF membranes which were reacted with R1 antibody against UL32, followed by HRP-coupled protein-A and developed using ECL as previously described. To verify similar amounts of sample were loaded in each well, the membranes were stripped and reprobed with a monoclonal antibody recognising actin (AC-40), followed by HRP-conjugated goat anti-mouse IgG.

Clone number	Inserted amino acids	Mutant designation
21	PAAAP	in5
163	AAAAV	in12
131	CGRIL	in40
81	VAAAH	in55
56	CGRNE	in67
121	GAAAR	in93
256	CGRRG	in95
123	CGRKL	in136
166	VRPHC	in155
113	CGRMY	in177
281	NAAAK	in187
20	AAAAF	in198
288	VAAAG	in220
130	LRPQP	in232
249	VRPQR	in302
248	MRPHC	in309
174	DAAAP	in328
45	VRPQP	in332
274	CGRNA	in338
116	GAAAR	in376
11	CGRSG	in377
17	CGRSG	in378
77	CGRSG	NONE
34	DAAAP	in398
140	TAAAA	in407
206	CGRSR	in414
19	LRPHW	in435
182	DAAAS	in449
49	CGRTG	in475
102	AAAAA	in486
8	CGRTE	in490
138	CGRIK	in494
253	CGRIC	in498
33	VRPHW	in512
277	VRPHQ	in558
117	VRPHQ	NONE
95	CGRIR	in572
238	HAAAR	in580
292	CGRTL	in592

Table 4.1: Position of each insertion and sequence of amino acid insertion.

The position of the inserted DNA sequence for each clone was determined by sequencing and compared to the sequence of the UL32 gene in pUL32 (figure 4.6). The full DNA sequences for each clone were then translated to the protein sequence using Expasy Translate program. The inserted amino acids for each clone are listed. Each protein mutant was renamed according to the last unaltered amino acid. Those shown in red contained exactly the same insertion in the same position as another mutant.

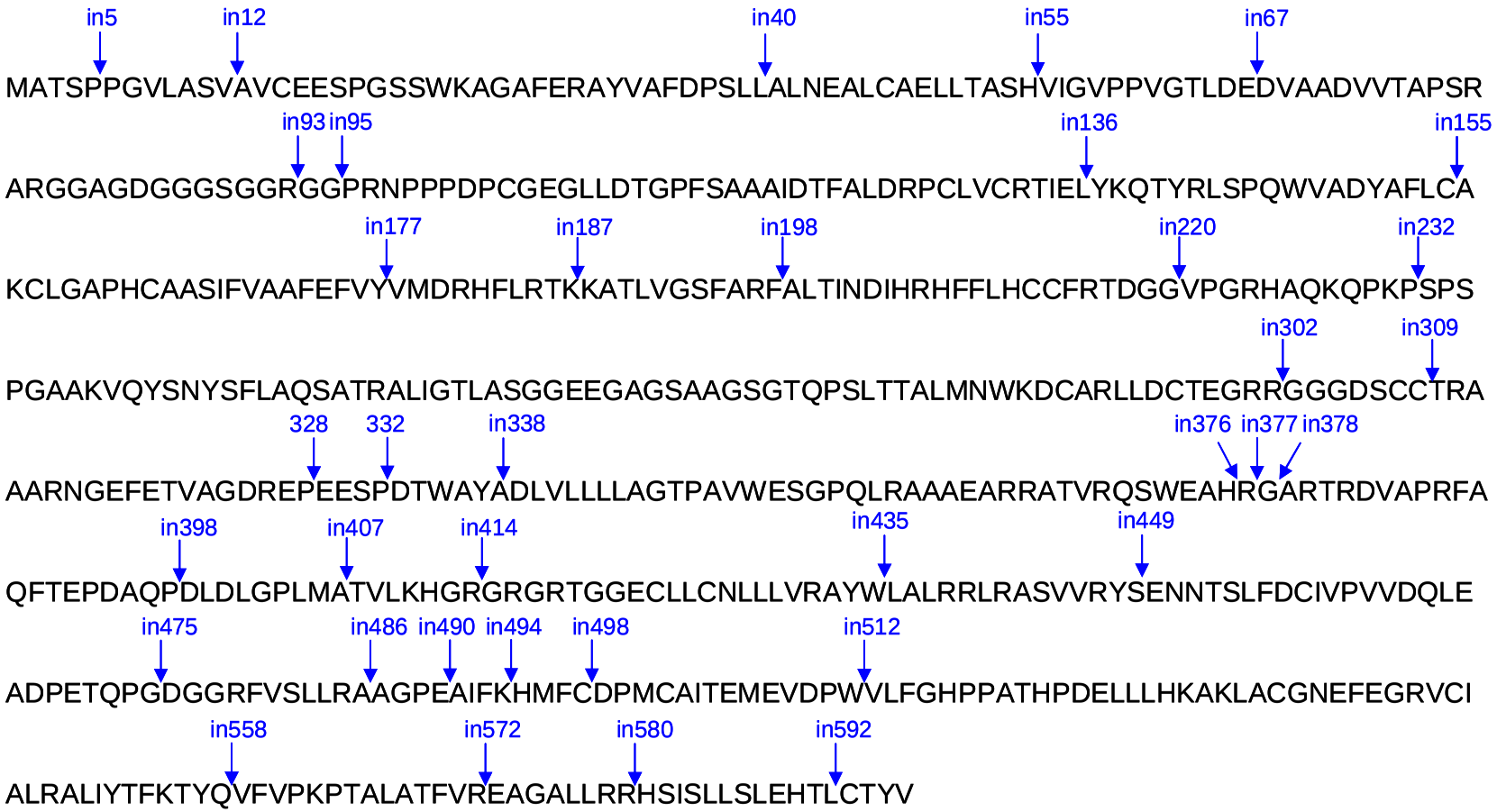

Figure 4.7: Positions of insertions within UL32 protein.

The amino acid sequence of each mutant was determined by translation of the full DNA sequences using the Expasy Translate program. These sequences were compared to that of the wt UL32 protein using the ClustalX alignment programme to determine the sequence and position of each mutation (see table 4.1). The new name and position of each insertion throughout the UL32 protein is shown.

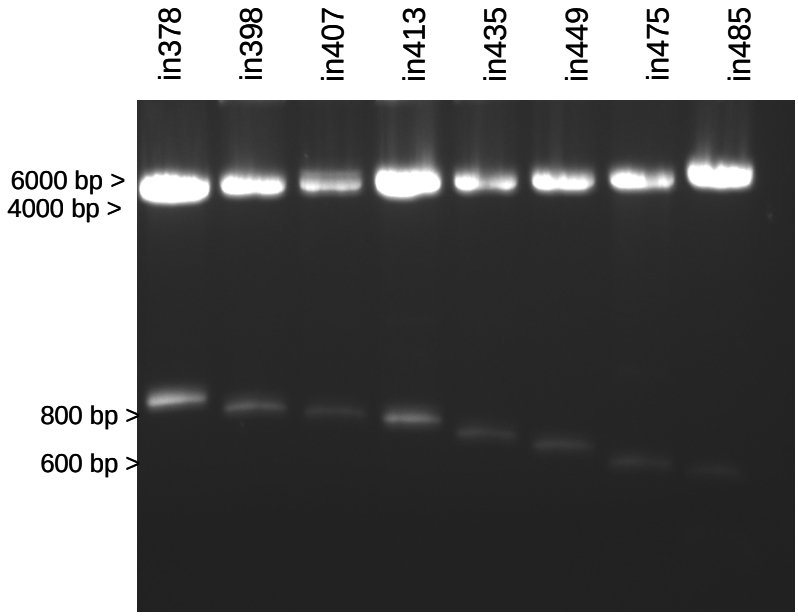

Figure 4.8: Position of insertions within UL32 mutant plasmids.

A representative gel showing the positions of the insertion in mutant plasmids in378 to in485. 1 µg each plasmid was digested with *Xba*I and *Not*I and separated on a 0.8% agarose gel. The small fragment liberated in each lane indicates the distance between the insert and the end of the UL32 gene, with decreasing size showing the insertion lies further towards the 3' end of the gene. Positions of size markers are indicated.

Figure 4.9 shows the western blots of cells transfected with each of the 37 mutants. As previously seen, R1 reacts with a protein of approximately 67 kDa, which is not seen in the cells transfected with pCMV10 empty vector. All of the insertional mutants produced a protein of the expected size and accumulated to similar levels to wt UL32 in transfected cells, indicating that their stability is not significantly affected. The actin staining confirms that similar amounts of protein were loaded in each well.

4.2.5 Localisation of UL32 mutant proteins

The localisation of transfected wt UL32 and all of the mutants was examined by immunofluorescence to determine whether any of the mutants differed in their localisation compared to wt UL32. BHK cells on coverslips were transfected with 0.5 µg pUL32, pCMV10 or each mutant plasmid using Lipofectamine 2000 (section 2.2.1.4). 18 hours post transfection the coverslips were fixed and permeablilised with formaldehyde and NP40 as previously described. The cells were incubated with antibody R1 followed by r-FITC (FITC-conjugated goat anti-rabbit IgG) and examined by confocal microscopy. Images are shown in figure 4.10. As previously shown, wt UL32 localises to the cytoplasm of transfected cells. No fluorescence was seen in the cells transfected with the empty vector, pCMV10 (figure 4.10A). Again, each of the mutant plasmids clearly expressed protein and all of these showed similar cytoplasmic localisation to wt UL32 (figure 4.10B).

4.3 Ability of mutants to complement growth of *hr*64

The functionality of the mutated proteins was first assessed by analysis of their ability to complement the growth of the mutant virus *hr*64 in a transient complementation assay (section 2.2.5). BHK cells were transfected with 1µg of plasmids pUL32, pCMV10 or the insertional mutants using the calcium phosphate method. Six hours post transfection, the cells were superinfected with 5 p.f.u. per cell *hr*64. After one hour, the virus that had not penetrated the cells was neutralised with an acid glycine wash. 18 hours post infection, the cells and media were harvested and sonicated. The viral progeny were titrated on the complementing cell line, UL32-5. The plates were incubated for 4 days at 37°C, stained and plaques counted. This assay was repeated for each mutant and the ability of each to complement the growth of *hr*64 determined by comparison of the yields obtained to that

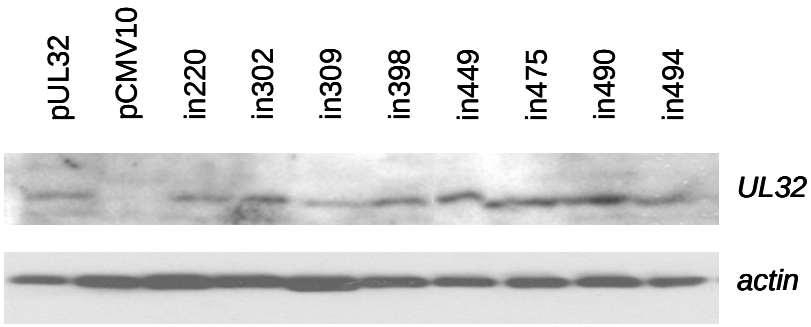
pUL32
pCMV10
in220
in302
in309
in398
in449
in475
in490
in494
UL32
actin

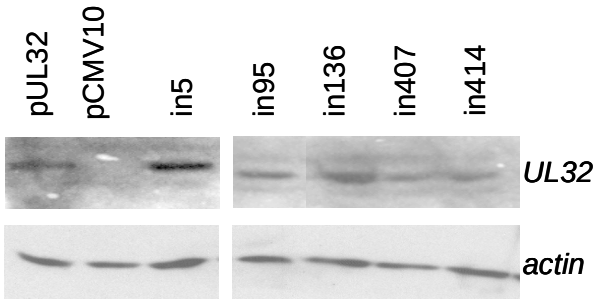
pUL32
pCMV10
in5
in95
in136
in407
in414
UL32
actin

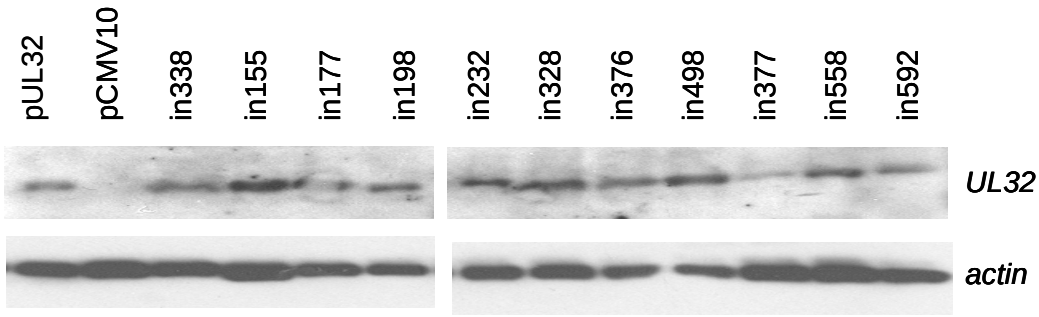
pUL32
pCMV10
in338
in155
in177
in198
in232
in328
in376
in498
in377
in558
in592
UL32
actin

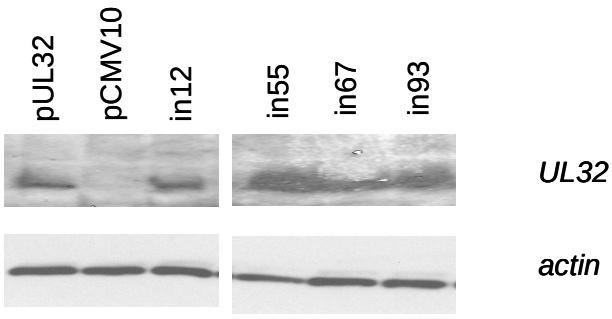
pUL32
pCMV10
in12
in55
in67
in93
UL32
actin

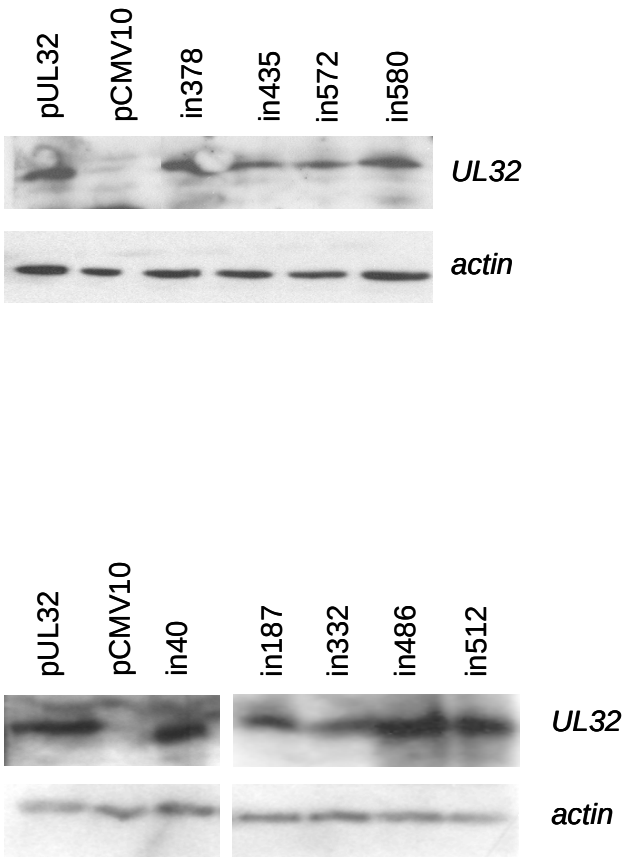

Figure 4.9: Expression of insertion mutants.

BHK cells were transfected with 1 µg pUL32, pCMV10 or plasmids encoding the insertional mutants by the calcium phosphate method. 18 hours post transfection cells were harvested and the lysates resolved by electrophoresis on 8% polyacrylamide gels. Samples were transferred to PVDF membranes and blotted with antibody R1 (1:500) followed by HRP-couple protein-A (1:1000), and developed with ECL. Membranes were then stripped and reprobed with a monoclonal antibody recognising actin (AC-40; 1:500) and HRP-conjugated goat anti-mouse IgG (1:1000) to confirm equal loading in each lane.

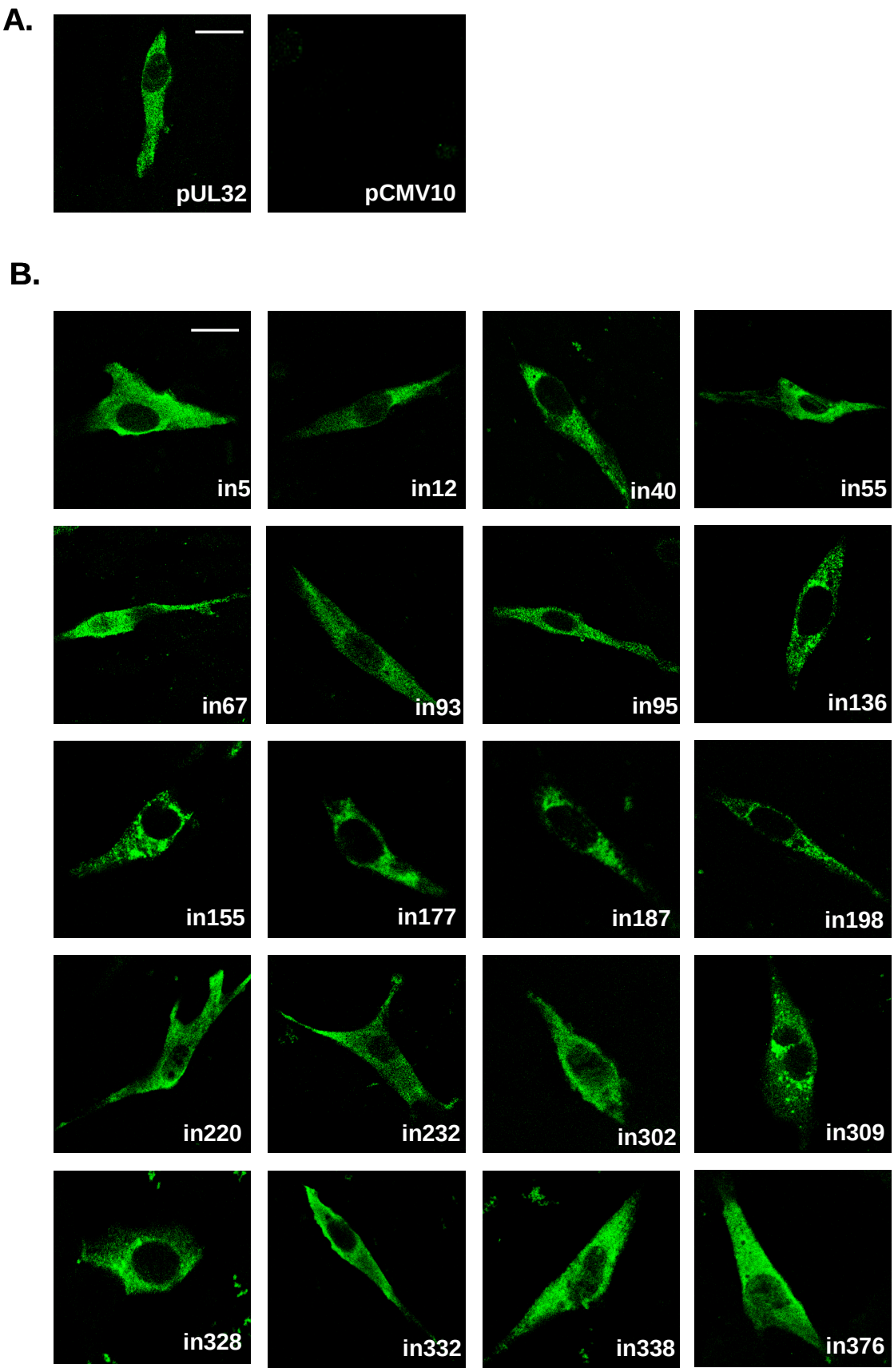
A.
pUL32
pCMV10
B.
in5
in12
in40
in55
in67
in93
in95
in136
in155
in177
in187
in198
in220
in232
in302
in309
in328
in332
in338
in376

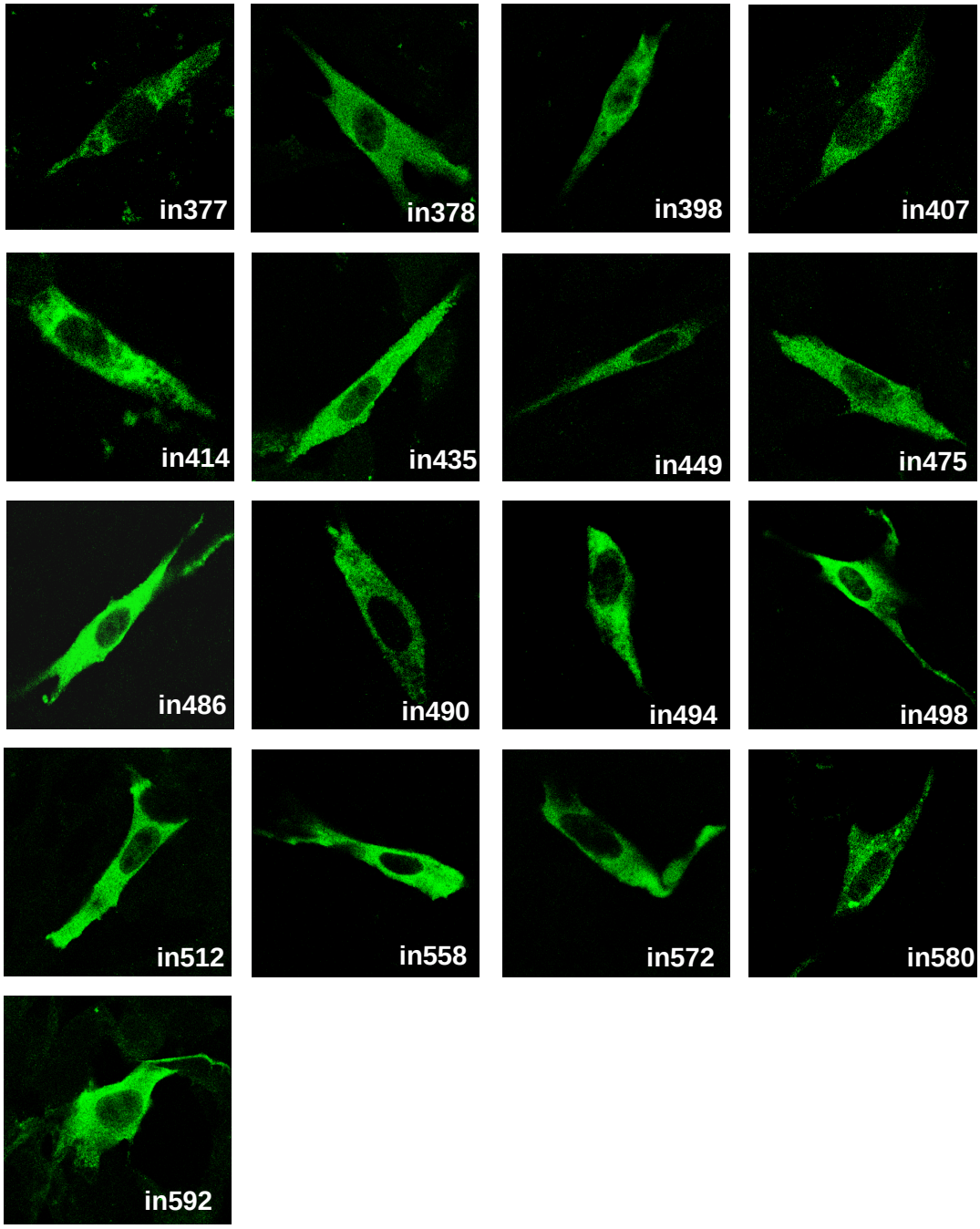

Figure 4.10: Localisation of UL32 insertion mutants within transfected cells.

0.5 µg the indicated plasmid DNA was transfected into BHK cells using Lipofectamine 2000. 18 hours post transfection, cells were fixed with formaldehyde and permeabilised with NP40. Coverslips were then probed with antibody R1 (1:500) followed by r-FITC (1:200) and were then examined by confocal microscopy. Scale bar = 20 µm.

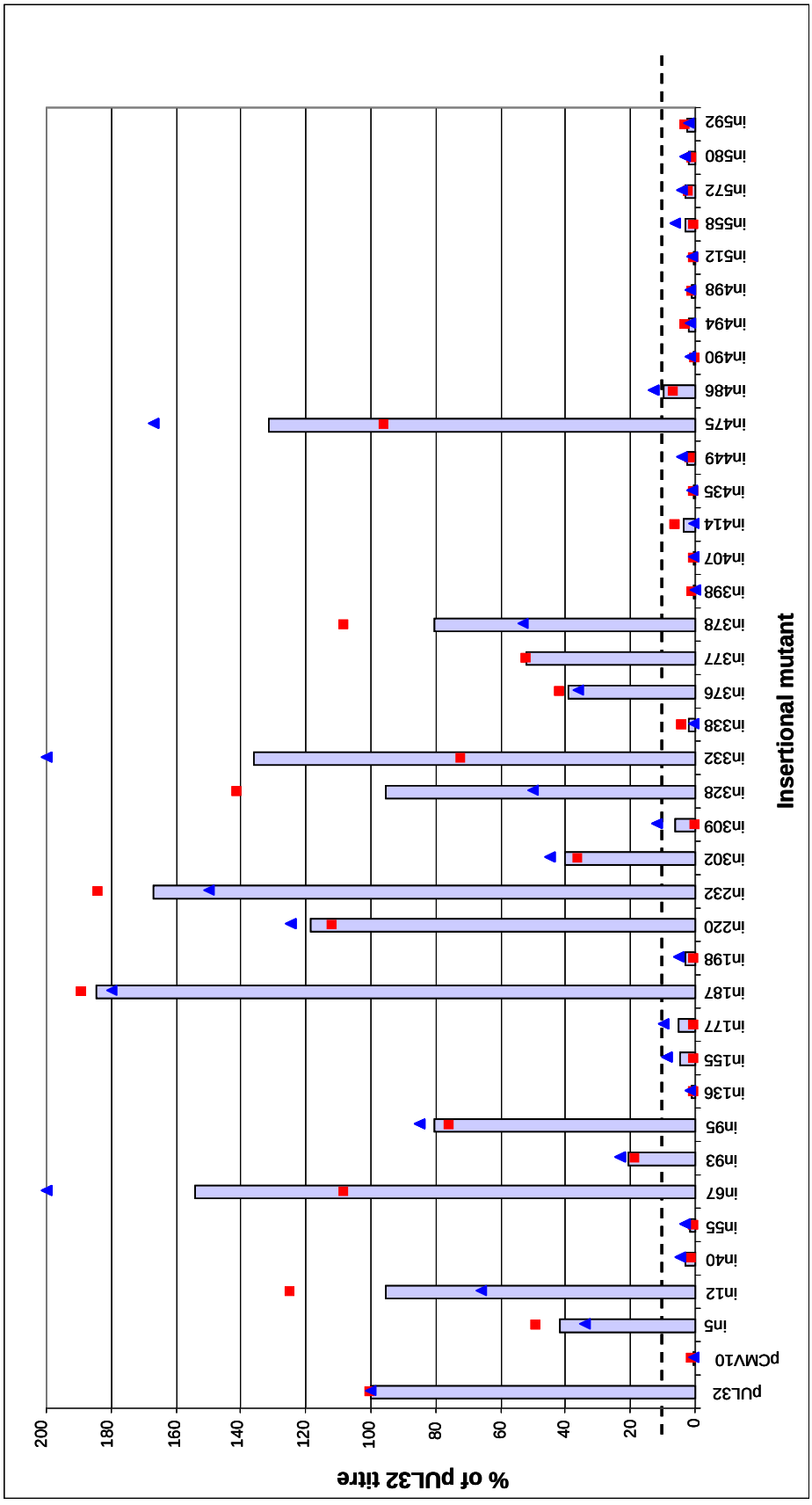

Figure 4.11 : Ability of insertional mutants to complement growth of *hr64*.

BHK cells were transfected with 1µg pUL32, pCMV10 or the indicated mutant plasmids by calcium phosphate. 6 hours post transfection they were superinfected with 5 p.f.u./cell *hr64*. 18 h.p.i., viral progeny was collected and titrated on UL32-5 cells for 4 days at 37ºC. Cells were stained and plaques counted. Titres from repeated experiments were taken and expressed as a percentage of the titre given with pUL32. The red squares and blue triangles show the results from duplicate experiments, and the light blue bars show the mean values. The dashed line shows a cut-off value of 10% compared to pUL32 titres.

obtained with pUL32. The mean value for each mutant is shown in figure 4.11, expressed as a percentage of the mean yield obtained with pUL32.

The empty vector pCMV10 was not able to support growth of *hr*64 on BHK cells, giving very low background titres of virus. Plasmid pUL32 complemented the growth of *hr*64 efficiently, giving titres ranging from 1.3×10^4 to 9.2×10^4 p.f.u., which were over 100 fold greater than those with pCMV10. 15 of the 37 mutants showed clear complementation of *hr*64, all giving yields of over 10% compared to pUL32. Nine of these, mutants in5, in12, in93, in95, in302, in328, in376, in377 and in378 gave values between 20-100% of wt UL32. Six of the mutants (in67, in187, in220, in232, in332 and in475) gave titres that were above those seen with pUL32, but none of these differences were greater than two-fold and are probably insignificant. The remaining 22 mutants did not complement the growth of *hr*64, having titres of less than 10% of that of pUL32. These were mutants in40, in55, in136, in155, in177, in198, in309, in338, in398, in407, in414, in435, in449, in486, in490, in494, in498, in512, in558, in572, in580 and in592. This lack of complementation was unlikely to be due to low levels of UL32 expression as the repeat experiments were performed on different occasions with different batches of cells, which should rule out any differences in expression levels.

These results show, that there is variation in the ability of the mutants to complement the growth of *hr*64 and identify essential regions throughout the protein. Of the 10 insertions within the N-terminal portion of the protein (residues 1-177), 5 generated functional proteins. 9 of the 12 insertions in the central portion (residues 187 – 378) were tolerated. In contrast, only 1 of 15 mutations (in475) in the C-terminal portion (residues 398 – 592) was functional in this assay. This suggests that the C-terminal third of the protein is particularly critical for its function, although mutants that disrupted function were present in other parts of the molecule.

4.4 Ability of mutants to complement DNA packaging

4.4.1 Amplicon packaging assay

The ability of each mutant UL32 protein to support DNA encapsidation was next tested using an amplicon packaging assay. This assay makes use of an amplicon plasmid (pSA1)

containing a minimal packaging signal (Uc-DR1-Ub) and HSV-1 origin of replication ori_S (Stow *et al.*, 1983). These features allow the amplicon to be replicated as a concatemer and packaged in the presence of wt HSV-1 helper virus. The amplicon plasmid is transfected into cells, and wt or mutant HSV-1 superinfected to provide the helper functions. Total and DNase resistant DNA samples are harvested from these cells, digested, Southern blotted and probed for the presence of the amplicon using ^{32}P labelled DNA. All of the replicated amplicon DNA will be detected in the total DNA samples, whereas only packaged amplicon DNA, which is protected from DNase treatment by the viral capsid and so will be present in the DNase-treated samples.

In addition, unreplicated input pSA1 can be cleaved into small fragments by *Dpn*I since the plasmid DNA is fully *dam* methylated. Following replication in mammalian cells this methylation is lost and the DNA becomes resistant to *Dpn*I thereby allows essentially zero background signal levels from input molecules to be obtained (Hodge & Stow, 2001; Nasseri & Mocarski, 1988).

Figure 4.12 shows the result of a packaging assay confirming that provision of wt UL32 is required for packaging of amplicon DNA by *hr*64. BHK monolayers were transfected with 1 µg pUL32 or pCMV10 along with 0.5 µg pSA1 using the calcium phosphate method as described. Six hours post transfection the cells were infected with 5 p.f.u./cell *hr*64 or wt HSV-1. Total and DNase resistant DNA were harvested as described in section 2.2.6.2. These samples were digested with *Eco*RI and *Dpn*I and separated on a 0.8% agarose gel. The gel was Southern blotted and probed using ^{32}P labelled pAT153, which is the parental vector for pSA1. The *Eco*RI digestion linearises pSA1, producing a band of approximately 4.4 kbp.

Lane 1 shows cells that were transfected with pUL32 but not superinfected, and therefore neither replication nor packaging of pSA1 is seen. Infection with wt HSV-1 allowed both replication and packaging of the amplicon DNA (lane 2). As expected, pSA1 was replicated to equivalent levels in the *hr*64 infection in the presence of either the empty vector or pUL32, confirming that *hr*64 does not have a defect in DNA replication (lanes 3 and 4). In contrast, packaged amplicon DNA was detected in the cells that received pUL32 but not the empty vector pCMV10.

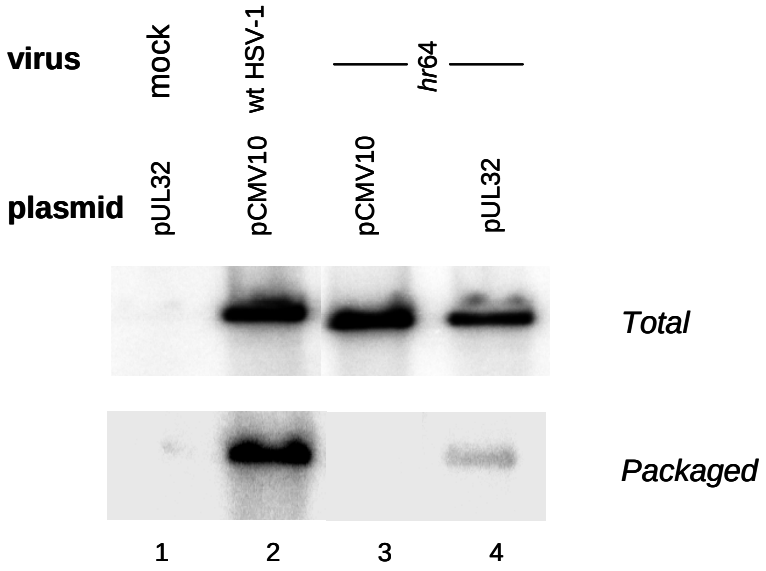

Figure 4.12: Packaging of amplicon DNA in the presence of *hr*64.

BHK cells were transfected with 0.5 µg pSA1 along with 1 µg either pUL32 or pCMV10 using the calcium phosphate method. The cells were superinfected with 5.p.f.u./cell wt HSV-1 or *hr*64, harvested 18 h.p.i., and total and packaged DNA prepared. DNA was digested with *Eco*RI and *Dpn*I and separated by agarose gel electrophoresis before being Southern blotted. pSA1 was detected by probing with ^{32}P labelled pAT153.

4.4.2 Ability of mutants to support amplicon DNA packaging in *hr*64 infected cells

The ability of the mutants to support packaging of amplicon DNA was tested as above and the results are shown in figure 4.13. The amount of pSA1 packaged by each mutant was determined by densitometric analysis of the bands on the phosphorimage and compared to that packaged in the presence of wt UL32, and the values of repeated experiments are shown in table 4.2.

As before, packaged amplicon DNA was detected in *hr*64 infected cells transfected with pUL32 but not pCMV10 in each experiment. DNA replication was not affected in cells transfected with any of the UL32 mutants. 15 of the mutants supported packaging of the amplicon DNA, with values of packaged pSA1 over 50% of that shown with pUL32. These were the mutants in5, in12, in67, in93, in95, in187, in220, in232, in302, in328, in332, in376, in377, in378 and in475. The remaining 22 mutants did not support DNA packaging (values of less than 10% of wt UL32). Some mutants showed a faint band of DNase resistant DNA, for example mutant in309 and in407, due to the long phosphorimage. However, when quantified, these values were very low (less than 10% of that seen with pUL32) and repeated experiments with these mutants showed no significant packaging of DNA.

These results show there is complete correlation between the ability of mutants to support viral growth and their ability to package amplicon DNA.

4.4.3 Dominant negative inhibition of packaging in wt HSV-1 infected cells

It was possible that one or more of the mutants that were unable to package amplicon DNA or complement viral growth might act as a dominant-negative inhibitor of the DNA packaging pathway.

To investigate this possibility, BHK cells were transfected with 1 µg each UL32 plasmid and 0.5 µg pSA1 as before, but superinfected at 5 p.f.u. per cell with wt HSV-1. Total and

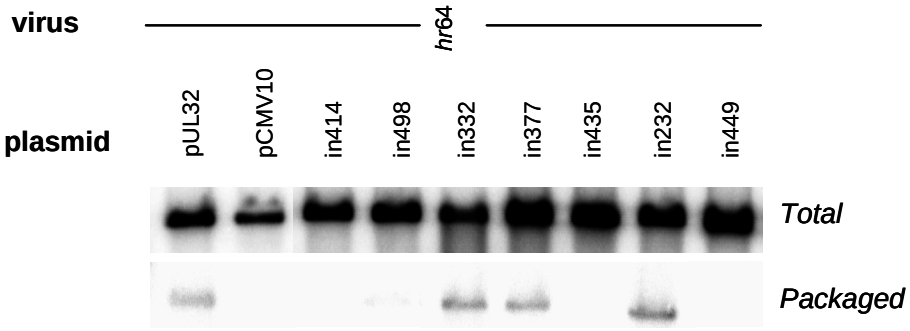
virus
hr64
plasmid
pUL32
pCMV10
in414
in498
in332
in377
in435
in232
in449
Total
Packaged

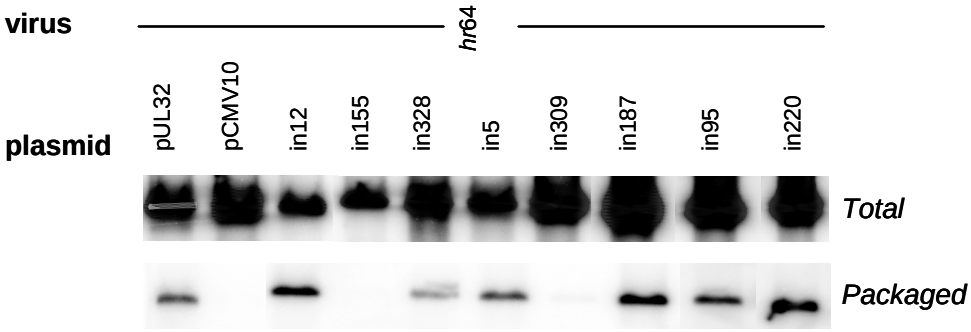
virus
hr64
plasmid
pUL32
pCMV10
in12
in155
in328
in5
in309
in187
in95
in220
Total
Packaged

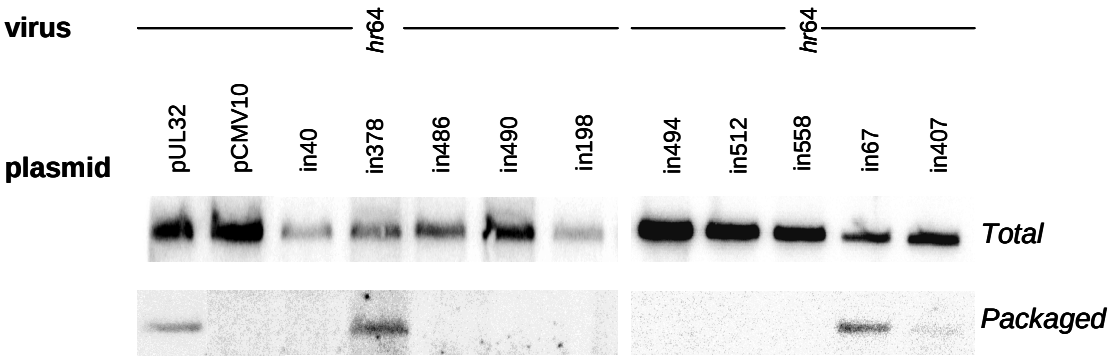
virus
hr64
hr64
plasmid
pUL32
pCMV10
in40
in378
in486
in490
in198
in494
in512
in558
in67
in407
Total
Packaged

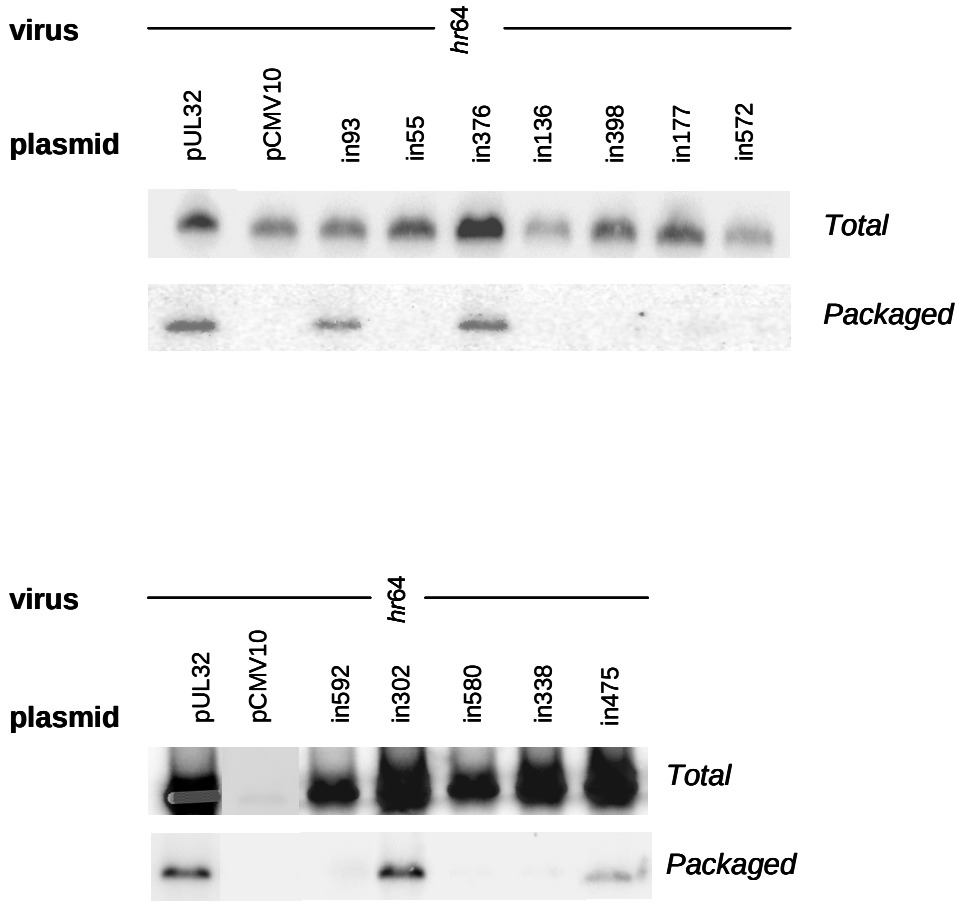

Figure 4.13: Ability of insertional mutants to package amplicon DNA.

BHK cells were transfected with 0.5 µg pSA1 and 1 µg of the indicated plasmid using the calcium phosphate procedure. Cells were superinfected with 5p.f.u./cell *hr*64, harvested 18 h.p.i. and total and packaged DNA prepared. DNA was digested with *Eco*RI and *Dpn*I and separated by agarose gel eletrophoresis before being Southern blotted. pSA1 was detected by probing with ^{32}P labelled pAT153.

	% packaged compared to pUL32		
mutants	Experiment 1	Experiment 2	Mean
pUL32	100	100	100.00
pCMV10	0.28	2.0	1.14
in5	99.3	109	104.15
in12	168	184.6	176.30
in40	6.9	6.6	6.75
in55	0.5	1.41	0.96
in67	45.2	100	72.60
in93	55.1	82	68.55
in95	56.4	136.6	96.50
in136	9.5	0.8	5.15
in155	1.1	0.2	0.65
in177	3.7	3.9	3.80
in187	183.3	189.3	186.30
in198	4.67	0	2.34
in220	187	80	133.50
in232	103	83.8	93.40
in302	51.5	108	79.75
in309	8.1	0	4.05
in328	56.9	59.7	58.30
in332	96	83.8	89.90
in338	7.5	0.8	4.15
in376	87	120	103.50
in377	110.4	85.6	98.00
in378	248.6	78.1	163.35
in398	4.95	2.05	3.50
in407	9.6	0.6	5.10
in414	8.3	2.4	5.35
in435	6.7	4	5.35
in449	2.3	8.4	5.35
in475	85.5	51.7	68.60
in486	0	4.55	2.28
in490	0.8	8.7	4.75
in494	1.15	0	0.58
in498	3.8	2.5	3.15
in512	1.45	0	0.73
in558	0.1	0	0.05
in572	0.4	0.8	0.60
in580	6.9	4.8	5.85
in592	0	0	0.00

Table 4.2: Quantification of the ability of mutants to package amplicon DNA.

Phosphorimages from 2 separate amplicon packaging experiments were quantified using Quantity One software. The amount of pSA1 packaged in each experiment was quantified according to total counts/mm^2 in each band of DNase resistant DNA. Each of these was expressed as a percentage of the values obtained when pUL32 was used to support DNA packaging.

DNase resistant DNA was prepared and the samples processed, Southern blotted and probed with ^{32}P-labelled pAT153 as above.

As shown in figure 4.14, transfection of the UL32 mutants did not greatly affect the replication levels of pSA1. Amplicon packaging was seen in cells infected with wt HSV-1, and addition of the plasmid encoding wt UL32 had no effect on packaging of pSA1. Although there was some variation in the levels of total and packaged amplicon it is clear that none of the mutant proteins is a potent inhibitor of the function of wt UL32 expressed by the superinfecting virus.

4.5 Site specific mutagenesis of conserved CxxC/CxxxC motifs

4.5.1 CxxC/CxxxC motifs

As discussed in the introduction, HSV-1 UL32 is a very cysteine rich protein with 22 Cys residues throughout its length. Many of these are highly conserved within the *Herpesviridae* (with seven being completely conserved), including three CxxC/CxxxC motifs which are present in almost all currently known herpesvirus UL32 sequences. The first of these motifs has the sequence CLVC in HSV-1 UL32 and corresponds to amino acids 127-130. The two cysteine residues are completely conserved in all herpesvirus sequences, and the residue at position three is always valine, leucine or isoleucine. The second CxxC motif has the sequence CLLC at amino acids 422-425 in HSV-1 UL32, and the cysteines and second leucine are completely conserved. The final motif is found at amino acids 497-501 in HSV-1 and has the sequence CDPMC. The first cysteine is conserved with the exception of murid herpesviruses 1 and 2. The aspartic acid and second cysteine are completely conserved, as is the proline, with the exception of the VZV homologue in which it is a leucine. The high degree of conservation of all of these residues suggests an important role in the function of the UL32 protein.

This section describes the site-specific mutagenesis of each of these conserved CxxC/CxxxC motifs in turn and the functional analysis of these mutants.

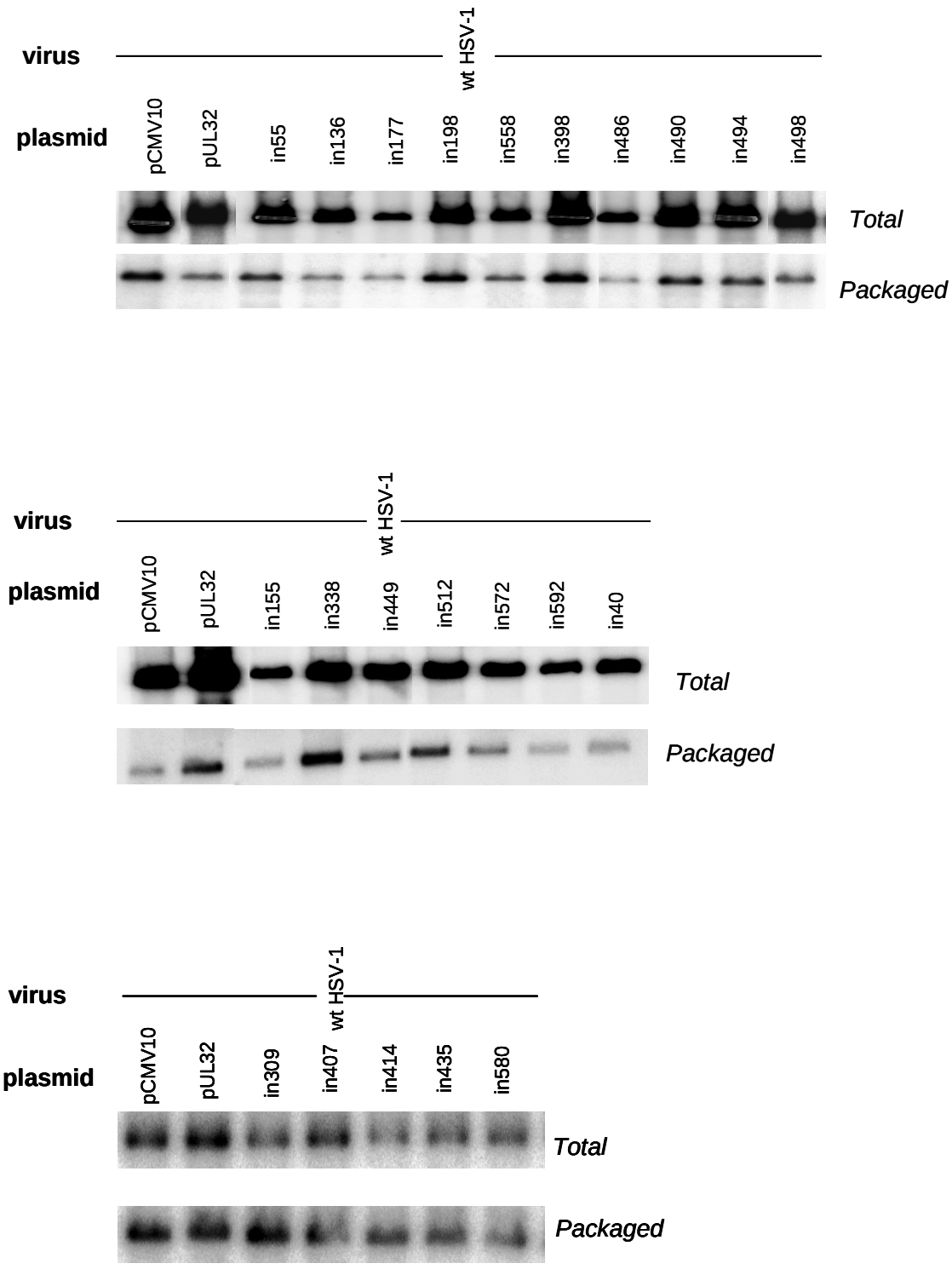

Figure 4.14: Ability of insertion mutants to act as dominant-negative packaging inhibitors.

BHK cells were transfected with pSA1 along with each indicated plasmid using the calcium phosphate method. Cells were superinfected with 5 p.f.u./cell wt HSV-1, harvested 18 h.p.i., and total and DNase resistant DNA prepared. Samples were digested, separated on an agarose gel and Southern blotted as described previously. pSA1 was detected by hybridisation to ^{32}P labelled pAT153 probe.

4.5.2 Construction of CxxC/CxxxC mutants

In order to easily create specific mutations in each of the CxxC/CxxxC motifs, a PCR-based approach was used, summarised in figure 4.15.

Two pairs of primers were designed for each motif, which encoded serines in place of the cysteines (SxxS/SxxxS), and introduced a novel restriction enzyme site to facilitate screening. These primers also spanned unique restriction sites at either end of the fragment for use in subsequent cloning steps (UL32CxxC1: *Pml*I and *Nhe*I, UL32CxxC2: *Xho*I and *Nhe*I, UL32CxxxC3: *Xho*I and *Pst*I). The sequences of these primers are shown in table 4.3 below. First round PCRs using primer pairs F1-R1 and F2-R2 generated two fragments for each motif which overlapped at the mutated sequences. These fragments were annealed and amplified using the outside primers (F1 and R2) to generate a large fragment containing the mutated sequences. The large PCR products were inserted into pGEM T sub-cloning vector to facilitate further cloning, and white colonies (containing the PCR product) selected (section 2.2.3.9). These colonies were screened for the presence of the inserted novel restriction site. The fragments were then excised from the sub-cloning vector by cleavage with the appropriate restriction enzymes and ligated into pUL32 digested with the same enzymes. Plasmid DNA was prepared using a Qiagen QIAprep Spin Miniprep kit, screened for presence of the novel restriction enzyme site and sequenced to confirm that only the desired nucleotide substitutions were present.

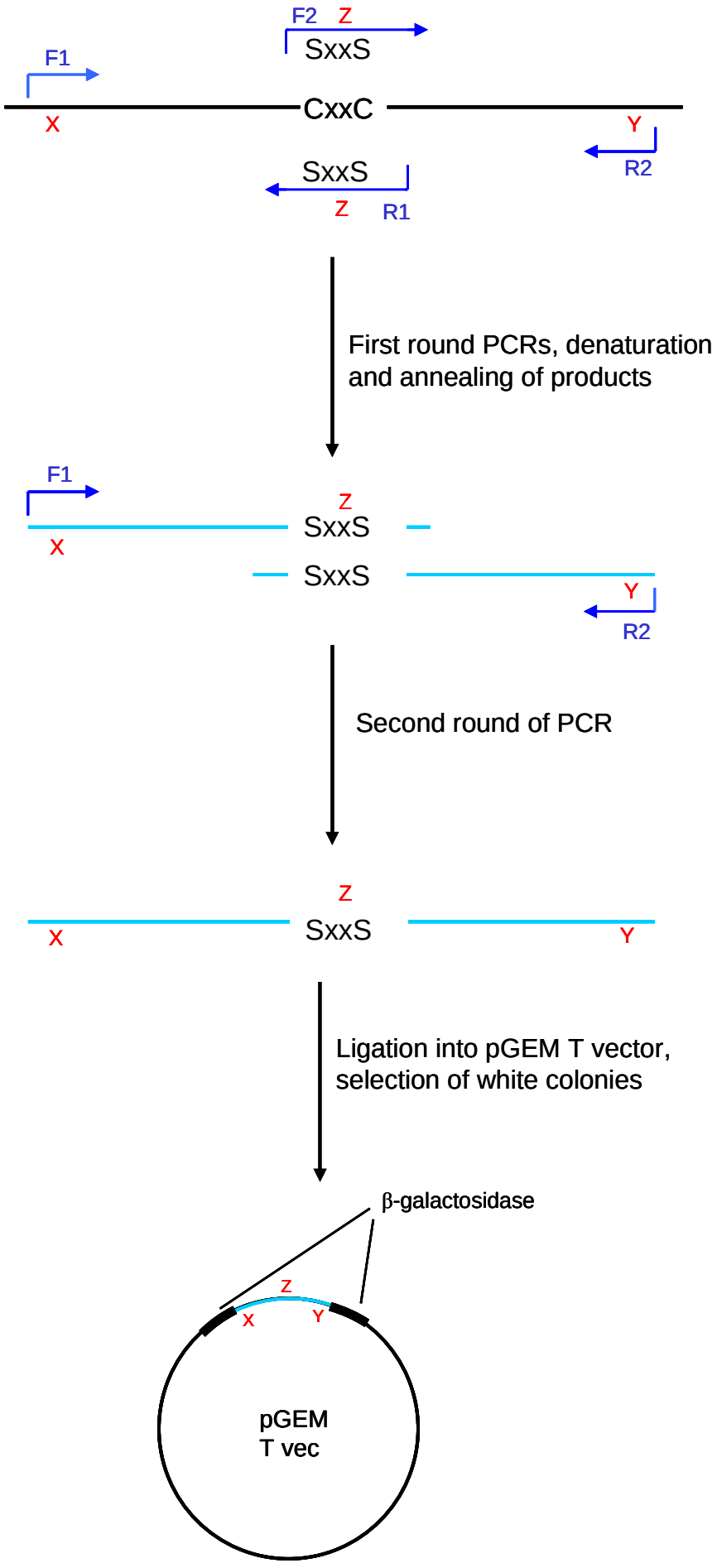
F2 Z
SxxS
F1
CxxC
X
Y
R2
SxxS
Z R1
First round PCRs, denaturation
and annealing of products
F1
Z
SxxS
X
SxxS
Y
R2
Second round of PCR
Z
SxxS
X
Y
Ligation into pGEM T vector,
selection of white colonies
β-galactosidase
Z
X
Y
pGEM
T vec

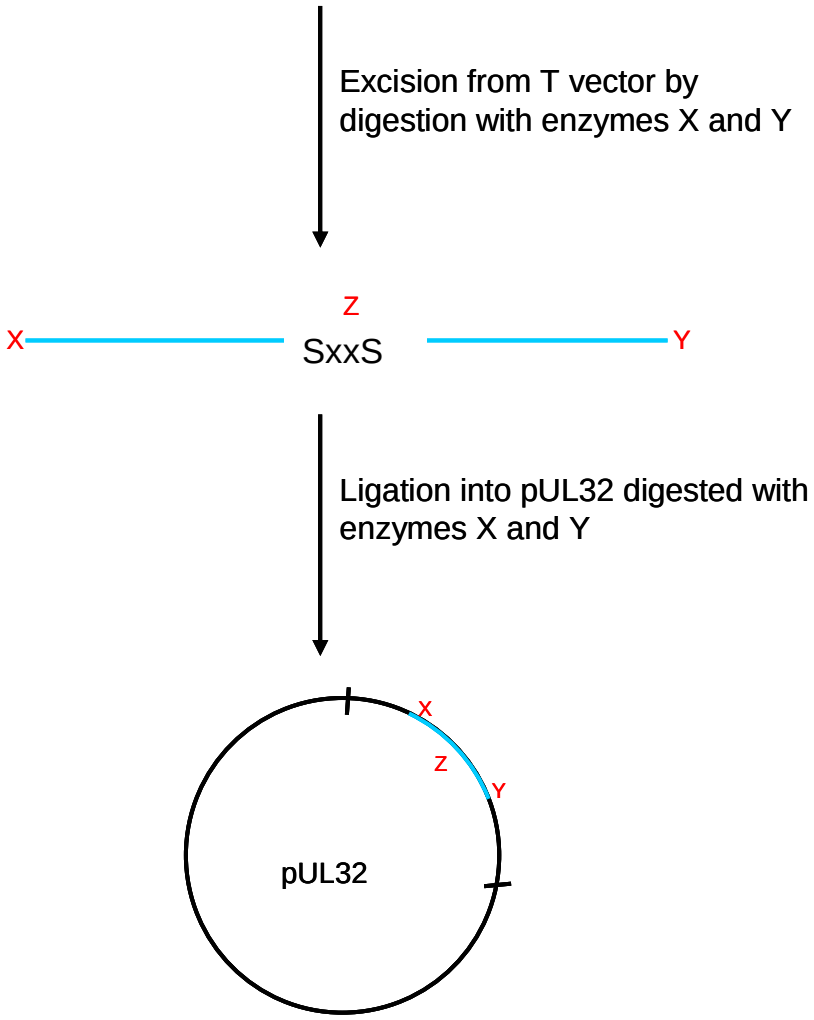

Figure 4.15: Generation of site-specific CxxC/CxxxC mutants.

Site specific mutations were introduced into the CxxC/CxxxC motifs by a two-step PCR approach. The first round of PCR used primer pairs F1-R1 and F2-R2. Primers F2 and R1 specified the mutated sequence to be inserted (SxxS/SxxxS), and a novel restriction site (Z). Primers F1 and R2 incorporated unique restriction sites at each end (X and Y). Two PCR products were generated which overlapped at the mutated sequences. These were dentaured and reannealed and amplified by PCR using the outside primers (F1 and R2) to produce a complete fragment with the mutated site. The PCR product was inserted into a sub-cloning vector (pGEM T vector) which was transformed into *E. coli* and colonies with the PCR insert distinguished by blue-white screening. The PCR product was then excised from the T vector by digestion with enzymes X and Y and ligated into pUL32 digested with the same enzymes. This was transformed back into *E. coli* and plasmid DNA from individual colonies prepared, screened for presence of the novel restriction site and sequenced.

	5' - 3' sequence	
UL32CxxC1		**inserted site**
CxxC1F1	CACGTGATAGGTGTGCCGCCCGTC	
CxxC1R1	GGTGCGGGAGACCAGGGAGGGCCGGTCTAGAGCGAAGGTGTCGATGGCCGC	*Xba*I
CxxC1F2	GCTCTAGACCGGCCCTCCCTGGTCTCCGGCACCATCGAGCTGTACAAGCAAACC	*Xba*I
CxxC1R2	CACGAAGATGCTAGCGGCGCAGTG	
UL32CxxC2		
CxxC2F1	CCCACTGCGCCGCTAGCATCTTCGTGGCC	
CxxC2R1	CAGGTTGGACAGCAGGGATTCTCCGCCGCTGCGCCCGCG	*Hinf*I
CxxC2F2	GGAGAATCCCTGCTGTCCAACCTGTTACTGGTGCGTGCTTACTGGCTGGCCC	*Hinf*I
CxxC2R2	GGGTCAGCCTCGAGCTGGTCGACGACGGG	
UL32CxxxC3		
CxxxC3F1	CGACCAGCTCGAGGCTGACCCCGA	
CxxxC3R1	AATGGCGGACATGGGATCCGAGAACATGTGCTTAAAGATGGCCTCGGGCCC	*Bam*HI
CxxxC3F2	ATGTTCTCGGATCCCATGTCCGCCATTACGGAGATGGAGGTTGACCCCTGG	*Bam*HI
CxxxC3R2	GATCCCAAGCTTGCATGCCTGCAGGTCGAC	

Table 4.3: Sequences of primers used for generating CxxC/CxxxC mutants.
5'-3' sequences of the primers designed for generation of CxxC/CxxxC mutants. The sequences encoding the mutated serine residues are shown highlighted in red. The novel restriction sites used for screening of the products are underlined and denoted in the right hand column. The unique restriction sites near the end of the PCR fragments used for further cloning are indicated in blue.

4.5.3 Expression and localisation of CxxC/CxxxC mutants

As with the transposon mutants, the expression level of each CxxC/CxxxC mutant was compared to wt UL32 in a transfection assay. BHK cells were transfected with 1 µg each plasmid by the calcium phosphate method and harvested at 18 hours. The samples were analysed by western blotting with antibody R1 and HRP-conjugated protein-A as before and the results shown in figure 4.16A. All three of the CxxC/CxxxC mutants express similar levels of polypeptides that are recognised by R1. Re-probing the blot with the actin antibody confirmed that similar levels of protein were loaded in each case.

The localisation of these mutant proteins in transfected cells was also examined compared to wt UL32. Coverslips of BHK cells were transfected with 0.5 µg each plasmid and

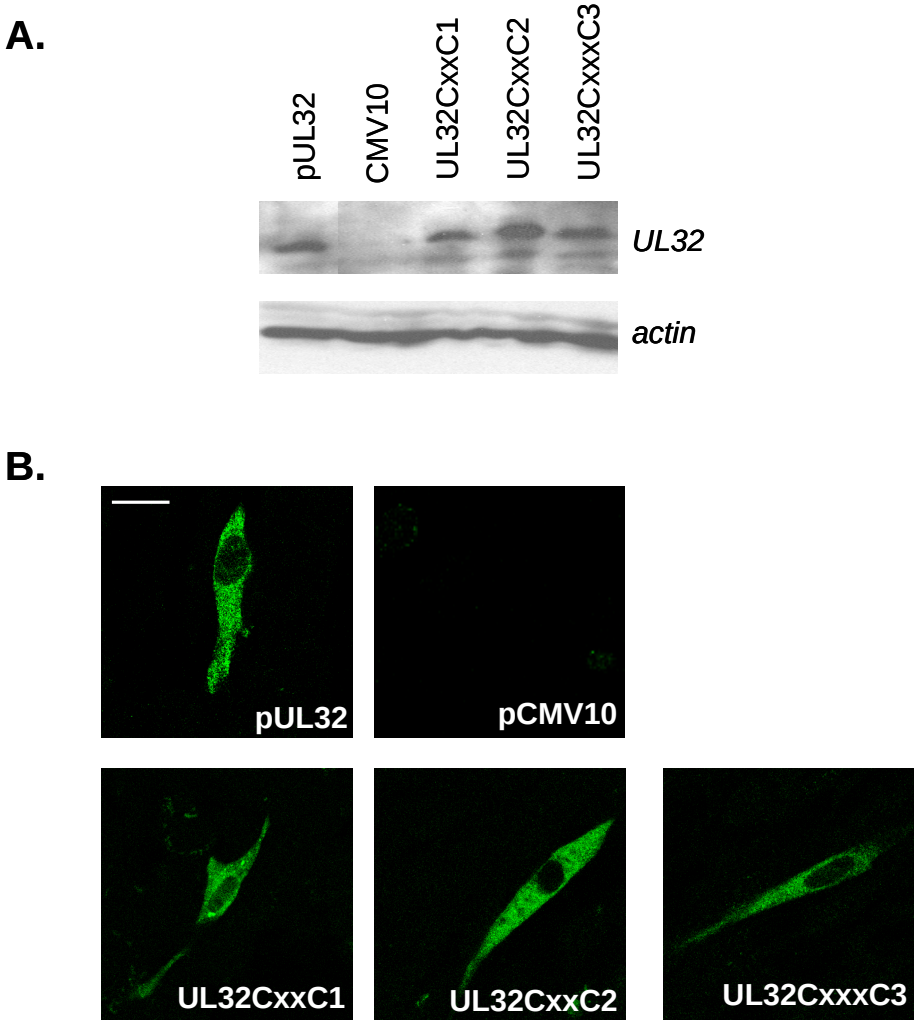

Figure 4.16: Transfection of CxxC/CxxxC mutants.

A. BHK cells were transfected with 1 µg pCMV10, pUL32 or mutant plasmid DNA using the calcium phosphate method. 18 hours post transfection, cell lysates were prepared and samples were separated by SDS-PAGE then western blotted as previously described. Membranes were probed with antibody R1 (1:500) followed by HRP-conjugated protein-A (1:1000). Blots were then stripped and reprobed for actin as a loading control.

B. 0.5 µg plasmid DNA was transfected into BHK cells using Lipofectamine 2000. 18 hours post transfection, cells were fixed with formaldehyde and permeabilised with NP40. Coverslips were then probed with R1 (1:500) followed by r-FITC (1:200) and examined by confocal microscopy. Scale bar = 20 µm.

processed at 18 hours post transfection as described previously. The coverslips were incubated with R1 followed by r-FITC, and analysed by confocal microscopy. The results are shown in figure 4.16B. Again, there seems to be no difference in the localisation of any of the CxxC/CxxxC mutants compared to wt UL32, with all four proteins localising throughout the cytoplasm.

4.5.4 Ability of CxxC/CxxxC mutants to complement growth of *hr*64

The ability of the CxxC/CxxxC mutants to support the growth of *hr*64 virus was examined using the complementation yield assay as previously described in section 4.3.

The results of duplicate experiments are shown in figure 4.17A. The values for each mutant are a mean of the duplicate experiments and are expressed as a percentage of that obtained with pUL32.

pUL32 complemented the growth of *hr*64, giving a mean titre of 6×10^5 p.f.u., compared to a value of 7×10^2 with the empty vector pCMV10. Mutants UL32CxxC1 and UL32CxxxC3 were not able to support viral growth significantly better than the empty vector, resulting in yields that were 1.1% and 1.9% of that obtained with pUL32, respectively. Interestingly, mutant UL32CxxC2 retained some function in this assay, giving titres of almost 18% of that obtained with pUL32.

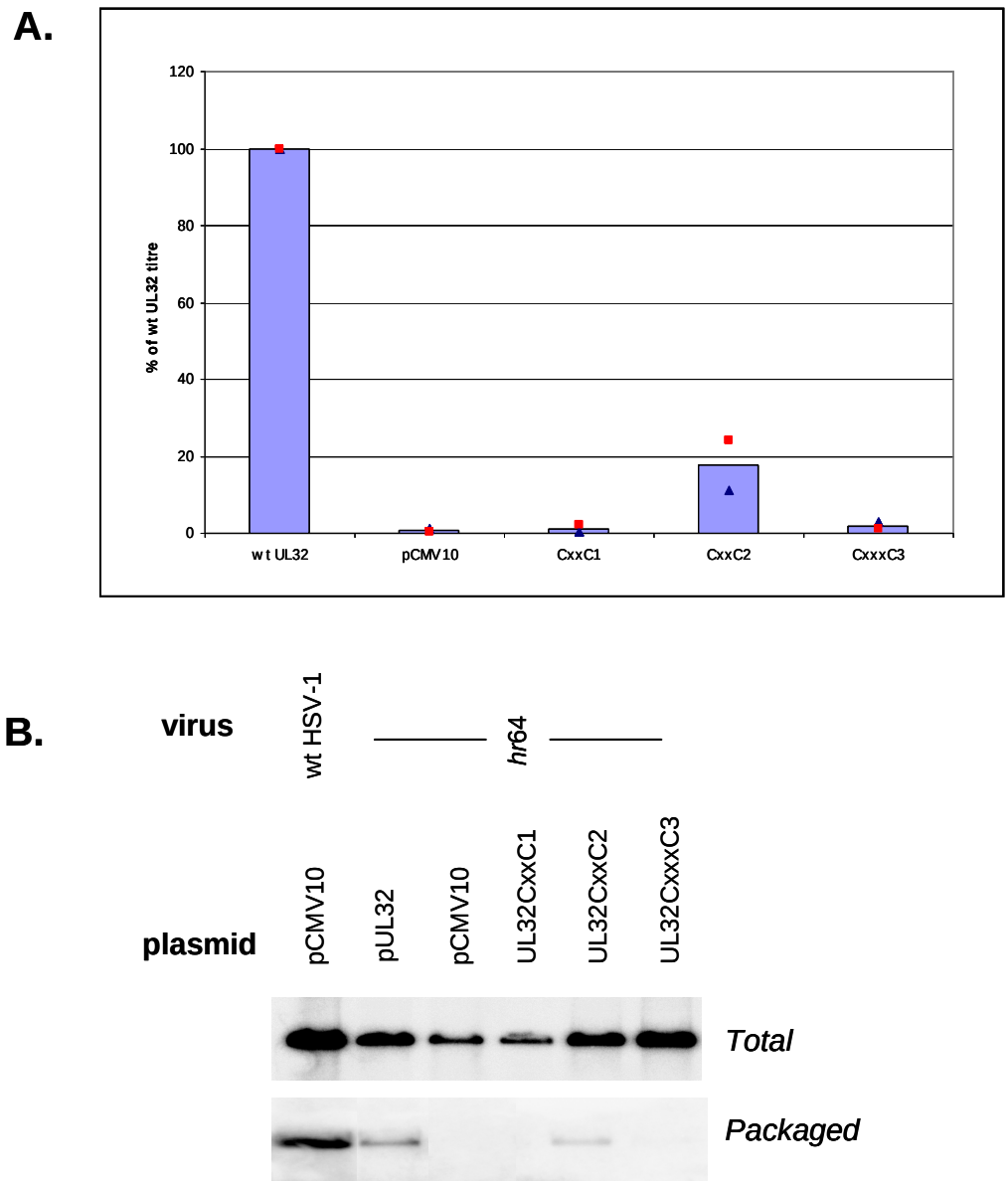

Figure 4.17: Function of CxxC/CxxxC mutants.

A. Complementation yield assay. BHK cells were transfected and superinfected as described in the legend to figure 4.11. 18 h.p.i., progeny was harvested and titrated on UL32-5 cells for 4 days. Plaques were counted and titres expressed as a percentage of those obtained with wt UL32. The red squares and blue triangles show the results from duplicate independent experiments, and the light blue bars show the mean values.

B. Amplicon packaging assay. Cells were transfected with the indicated plasmids and superinfected as described in the legend to figure 4.12. Total and DNase resistant DNA were prepared and processed as described in section 2.2.6.2 and pSA1 was detected by hybridisation to ^{32}P labelled pAT153.

4.5.5 Ability of CxxC/CxxxC mutants to support amplicon DNA packaging in *hr*64 infected cells

The three cysteine mutants were also tested for their functionality in the amplicon DNA packaging assay as previously described. The phosphorimage results are shown in figure 4.17B, and the mean values for two replicate packaging assays expressed as a percentage of the packaging in the presence of pUL32 are shown below:

	% packaged compared to wt UL32		
	Experiment 1	Experiment 2	Mean
pUL32	100	100	100
pCMV10	0.2	1.5	0.85
UL32CxxC1	0	11.5	5.75
UL32CxxC2	12.5	35.8	24.15
UL32CxxxC3	0	0.3	0.15

Table 4.4: Quantification of the ability of CxxC/CxxxC mutants to package amplicon DNA.
The amounts of packaged DNA from two separate experiments were quantified according to total counts/mm^2 in each DNA band from the phosphorimage. Each was expressed as a percentage of the values of packaged DNA seen in the cells where pUL32 was used to support DNA packaging.

As expected, DNA packaging occurred following infection with wt HSV-1 or *hr*64 infection in the presence of pUL32 but not pCMV10. Consistent with the complementation yield assay results, neither UL32CxxC1 nor UL32CxxxC3 supported DNA packaging. In contrast some packaged DNA was observed with UL32CxxC2. Quantitation of these results showed that UL32CxxC2 packaged pSA1 to a level of approximately 25% of that obtained with pUL32. This is consistent with the complementation yield results indicating that a protein mutated in the central CxxC motif retains limited function, suggesting that these highly conserved cysteine residues are not absolutely essential for UL32 function.

4.6 Deletion of the C-terminus of UL32 – UL32ΔC

One further site specific mutant was created, which contained a deletion of the C-terminal four amino acids of UL32. The extreme C-terminus has previously been implicated as

essential for the function of the homologous HCMV protein UL52 (Borst *et al.*, 2008). These workers constructed a BAC genome with an HA tag inserted immediately following the last codon of UL52 and found that the resulting DNA was non-infectious. In addition, this tagged UL52 protein had an altered localisation upon transfection of the BAC DNA into cells. Whilst wt UL52 was found to localise predominantly to the nucleus, the disruption of the C-terminus resulted in localisation throughout the cell, leading the authors to hypothesise that the C-terminus of HCMV UL52 is required for its correct sub-cellular localisation. I therefore wanted to examine whether the extreme C-terminus of HSV-1 UL32 was essential for its function.

4.6.1 Construction of UL32ΔC

The UL32ΔC mutant was constructed by a two-step PCR mutagenesis, using a similar method to that used for the CxxC/CxxxC mutants, summarised in figure 4.18. Primer pairs were designed that were complementary to the UL32 sequence except with deletion of the 12 nucleotides that encode the final four amino acids of the protein (CTYV). These primers also introduced a novel restriction enzyme site (*Hinf*I) for ease of screening. The sequences of the two primer pairs are shown in table 4.18C. The first round PCR used primer pairs F1-R1 and F2-R2 to generate two small fragments containing the mutated sequence in the overlap region. These were annealed and amplified in a second round of PCR using the outside primers (F1 and R2). The product was a 600 bp fragment flanked with *Hind*III and *Xho*I sites which had a deletion of the final four codons but retained the TGA stop codon. This PCR product was inserted into the pGEM T sub-cloning vector and screened for the presence of the novel *Hinf*I restriction site. The fragment containing the *Hinf*I site was excised by digestion with *Hind*III and *Xho*I, gel purified and inserted into pUL32 digested with the same enzymes. This plasmid, UL32ΔC was sequenced to confirm deletion of the final four codons.

4.6.2 Expression and localisation of UL32ΔC

The expression and localisation of UL32ΔC was compared to wt UL32 in transfected cells (figure 4.19). The western blot shows that UL32ΔC produced a polypeptide recognised by antibody R1 that was expressed at similar levels to wt UL32 protein. There was no visible size difference between wt UL32 and UL32ΔC, but this is not surprising, as the deletion of four amino acids is predicted to only reduce the molecular weight from 63.9 kDa to 63.6 kDa (figure 4.16A). In the immunofluorescence studies of transfected BHK cells, the

A.

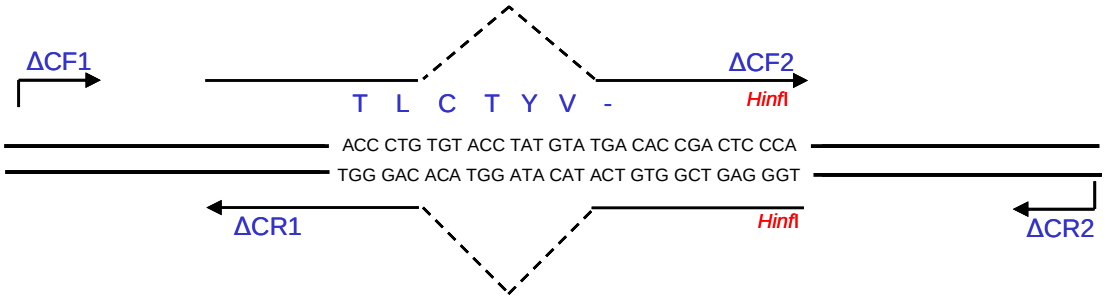

B.

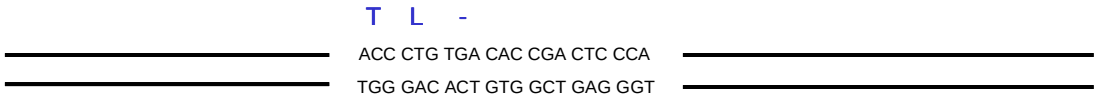

C.

	5' - 3' sequence
ΔCF1	CGACCAGCTCGAGGCTGACCCCGA
ΔCR1	TGGGAGTCGGTGTCACAGGGTGTGCTCCAGGGACAGGAGCGA
ΔCF2	TCGCTCCTGTCCCTGGAGCACACCCTGTGACACCGACTCCCA
ΔCR2	GAGCACACCCTGTGACACCGACTCCCATCGCCGCGGCTCCCC

Figure 4.18: Primers used for generation of UL32ΔC.

A. The positions of primer pairs ΔCF1 – ΔCR1 and ΔCF2 – ΔCR2 relative to the 3' end of UL32, showing the nucleotides deleted in the primer sequences. The positions of the introduced *Hinf*I sites are indicated in red.

B. The product generated by the PCR mutagenesis, with 12 nucleotides (coding for amino acids CTYV) deleted.

C. 5' – 3' sequences of primers designed for generation of UL32ΔC. The nucleotides complementary to the UL32 sequence are shown in blue and the introduced *Hinf*I sequences underlined.

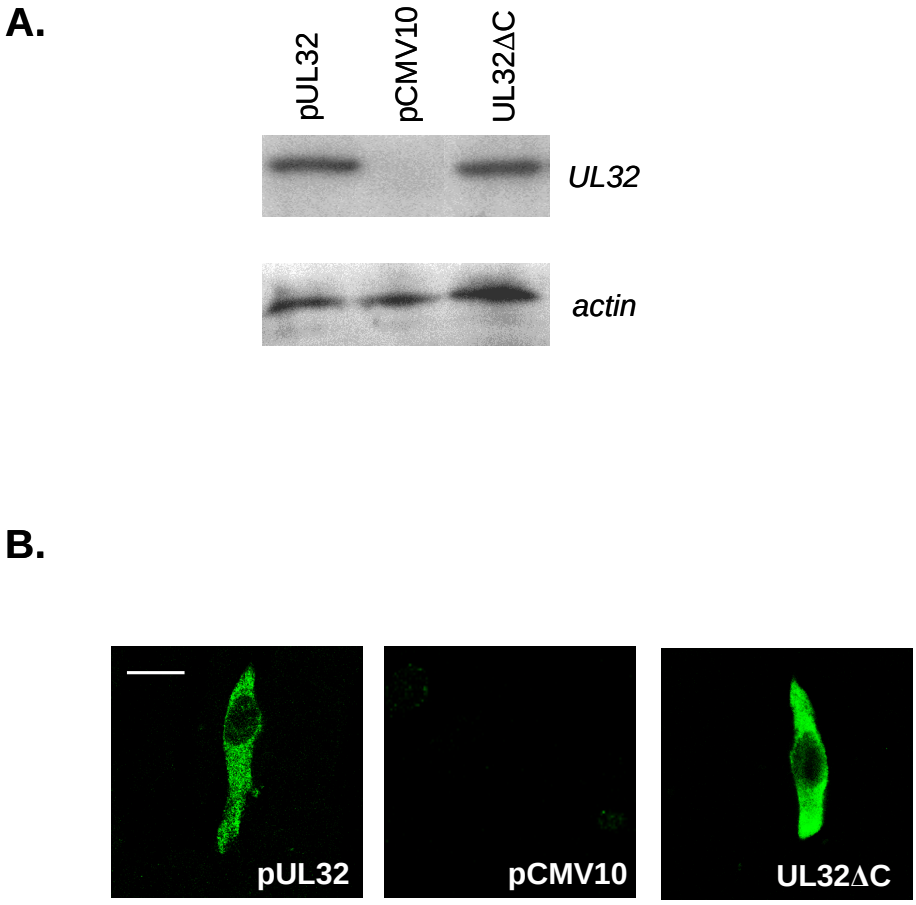

Figure 4.19: Expression and localisation of UL32ΔC in transfected cells.

A. BHK cells were transfected with 1 µg pCMV10, pUL32 or UL32ΔC plasmid DNA using the calcium phosphate method. 18 hours post transfection, cell lysates were prepared and samples were separated by SDS-PAGE then western blotted as previously described. Membranes were probed with antibody R1 (1:500). Blots were then stripped and reprobed for actin as a loading control.

B. 0.5 µg plasmid DNA was transfected into BHK cells using Lipofectamine 2000. 18 hours post transfection, cells were fixed with formaldehyde and permeabilised with NP40. Coverslips were then probed with antibody R1 (1:500) followed by r-FITC (1:200). These were then examined by confocal microscopy. Scale bar = 20 µm.

localisation of UL32ΔC was indistinguishable from that of wt UL32, both being distributed throughout the cytoplasm (figure 4.16B).

4.6.3 Ability of UL32ΔC to complement the growth and DNA packaging defects of *hr*64

UL32ΔC was then tested for functionality in the two assays examining the complementation of growth and DNA packaging of *hr*64.

Figure 4.20A shows that UL32ΔC was incapable of supporting virus growth in *hr*64 infected BHK cells. Furthermore, UL32ΔC did not support DNA packaging, and quantitation of duplicate experiments showed that UL32ΔC packaged DNA to a level of 4.78% of that obtained with wt UL32, not significantly more than the value of 3.15% obtained with the empty vector pCMV10 (figure 4.20B).

These results indicate that the C-terminal four amino acids of UL32 are essential for DNA packaging and virus replication.

4.7 Discussion

4.7.1 Creation of UL32 insertional mutants

Firstly, a panel of 37 insertional mutants was created using a random transposon based mutagenesis system. This approach was selected for the initial studies of UL32 because no previous work has been attempted to identify regions of the protein essential for its function. The identity of the mutants was confirmed by DNA sequencing and each expressed a full-length protein at similar levels to wt UL32. Like wt UL32, each protein localised to the cytoplasm of transfected cells. The insertions are generally well-spaced giving good coverage throughout the UL32 protein, except for a relatively small region between amino acids 232 and 301 with no insertions.

A further set of site specific mutants were created – UL32CxxC1, UL32CxxC2 and UL32CxxxC3. These substituted the highly conserved cysteine residues in each of these

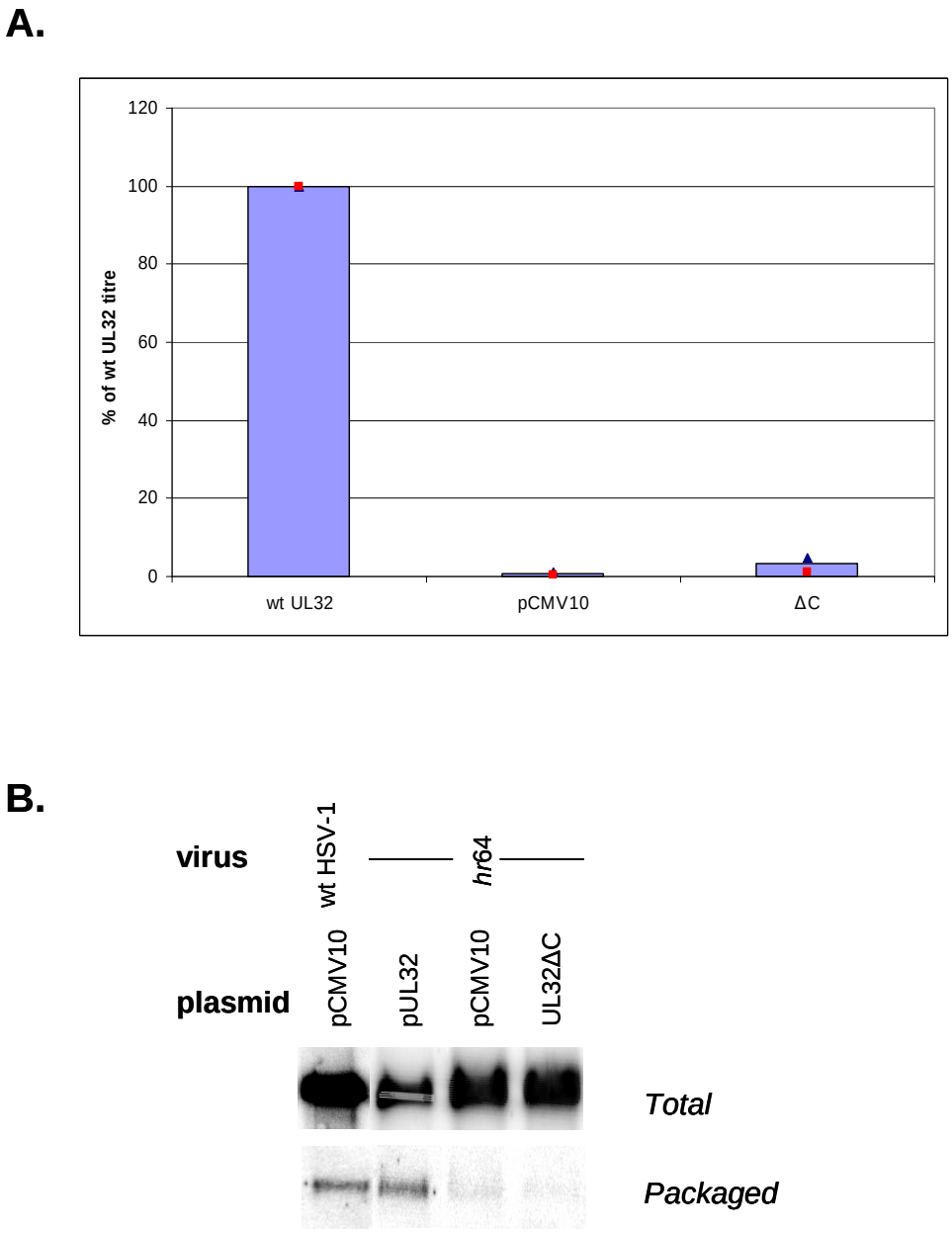

Figure 4.20: Functional analysis of ΔC mutant.

A. Complementation yield assay. BHK cells were transfected and superinfected as previously described. 18 h.p.i., viral yields were collected and titrated on UL32-5 cells for 4 days. Plaques were counted and titres expressed as a percentage of those obtained with wt UL32. The red squares and blue triangles represent duplicate independent experiments and the light blue bars show the mean values.

B. Amplicon packaging assay. Cells were co-transfected with pSA1 and either pCMV10, pUL32 or UL32ΔC and superinfected with wt HSV-1 or *hr*64 as previously described. Total DNAse resistant DNA were prepared and processed as described in section 2.2.6.2 and pSA1 was detected by hybridisation to ^{32}P labelled pAT153.

CxxC/CxxxC motifs with serines. Finally, the extreme C-terminus of UL32 (final four amino acids) was deleted, generating the UL32ΔC mutant.

4.7.2 Analysis of functionality of the UL32 mutants

The mutants were examined in two functional assays – their ability to complement the growth of the UL32 mutant virus *hr*64 and their ability to support DNA packaging by *hr*64.

An exact correlation was found between the ability of mutants to support viral growth and their ability to package DNA, both for the insertional mutants and the site-specific CxxC/CxxxC and UL32ΔC mutants. This suggests that the key function of UL32 in the viral life cycle is in initiation of DNA packaging. Were UL32 required at a later stage of the viral life cycle, another class of mutants might be expected that support DNA packaging but fail to complement growth of the mutant virus. This phenotype has been reported during mutational analysis of the UL25 protein, which is not required for the initiation of packaging, but is important for the termination of packaging and nuclear egress (O'Hara *et al.*).

4.7.3 Correlation between functionality of the mutant protein and conservation of the UL32 protein

Figure 4.21 shows a similarity plot (generated by Nigel Stow) constructed by extracting the UL32 protein sequences for the *Alphaherpesvirinae* from the RefSeq database. These were aligned with ClustalW and analysed using PlotSimilarity (GCG). The graph shows similarity plotted against amino acid number, with the peaks indicating regions of high conservation throughout these sequences and the troughs indicating poor conservation. Differences between the lengths of the proteins and the introduction of padding characters results in the alignment length being 720 amino acids compared to the 596 aa length of HSV-1 UL32. The positions of all of the insertional mutants are indicated on this alignment with the functional mutants (those giving over 10% packaging or growth complementation compared to wt UL32) shown in green and the non-functional (less than 10% of the values of wt UL32) in red. From the data, broad regions of the UL32 protein can be identified which have differing susceptibilities to disruption, which correlate with their conservation. The C-terminal portion of the protein shows a high degree of similarity and contains many highly conserved residues (C-terminal third). This region is intolerant

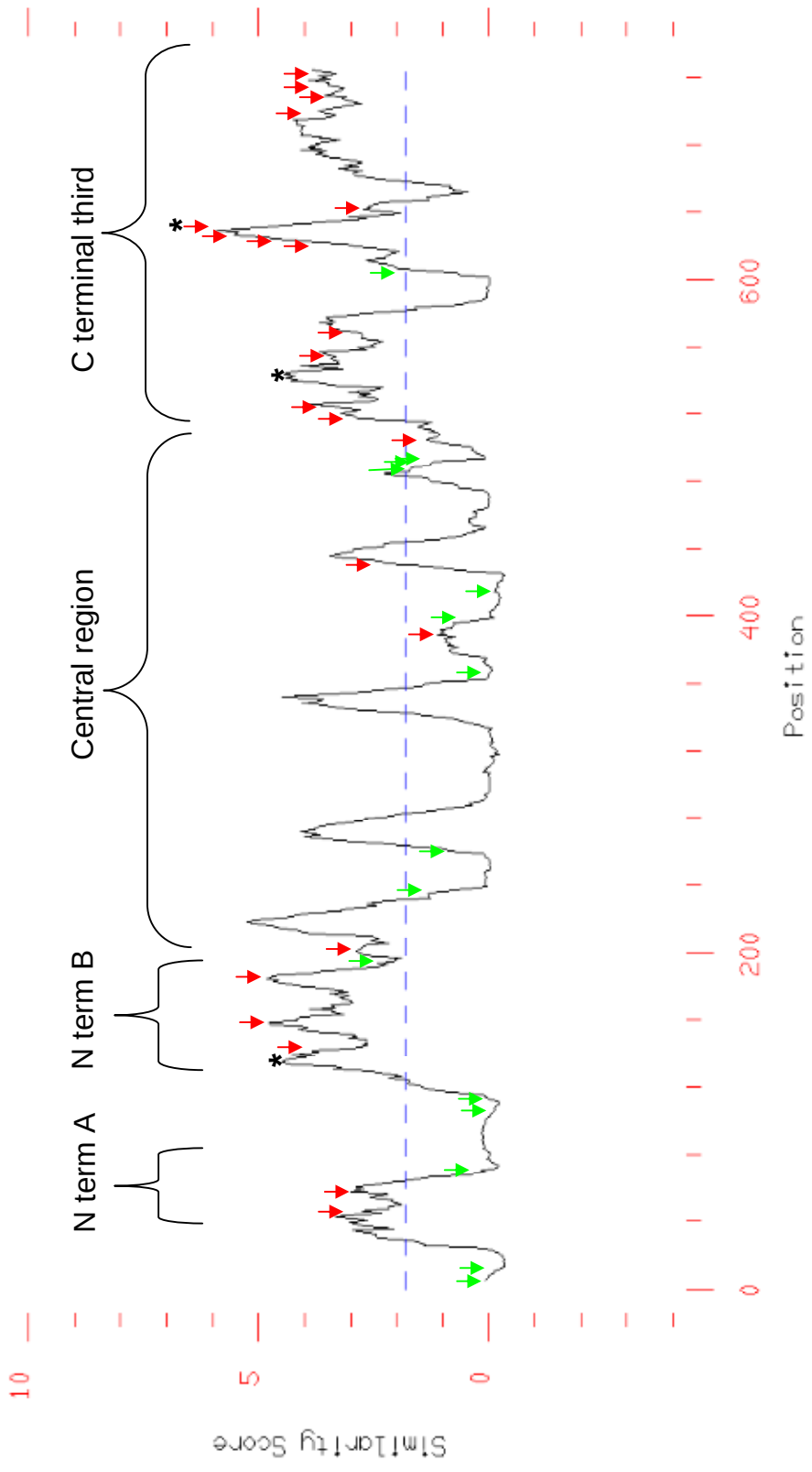

Figure 4.21: Positions of insertion mutants relative to the degree of conservation within the UL32 protein.

The available UL32 protein sequences from the *Alphaherpesvirinae* were extracted from the RefSeq database and aligned using the ClustalW programme and the similarity plot created using SimilarityPlot (GCG) . The peaks on the plot indicate regions that are highly conserved and the troughs regions of low conservation. The blue dashed line shows the mean similarity along the UL32 protein. The positions of the insertional mutants have been plotted, with the green arrows being the functional mutants, and the red arrows non-functional mutants. The positions of the conserved CxxC/CxxxC motifs are denoted with asterisks (*). The broad regions defined by the functional analysis of the insertion mutants are indicated.

of disruption, with all but one of the insertions after amino acid 398 generating a non-functional protein. The central portion (central region) of the protein is less well conserved and is much more tolerant of insertions, with 9 out the 12 mutants between amino acids 187 and 378 retaining functionality. The N-terminal third has two distinct regions of highly conserved residues and again, these correlate with the functionality of the mutants, with the mutants between amino acids 40 and 55 (N term A) and 136-177 (N term B) not supporting virus growth or DNA packaging of *hr*64.

Figure 4.22 shows another alignment of UL32 protein sequences from the *Alphaherpesvirinae*, this one created by aligning the same sequences using ClustalX. This gives a more detailed view of the conservation of individual amino acids within UL32 and also indicates completely conserved residues with an asterisk (*).

Again, the positions of all insertional mutants are indicated on this alignment with the functional mutants shown in green and the non-functional in red. A number of mutants have the insertion directly preceding or following a residue that is completely conserved within the *Alphaherpesvirinae* (mutants in40, in136, in155, in398, in435, in494, in498 in558, in580 and in592) or that is conservatively substituted (mutants in55, in177, in407 and in572). Furthermore, mutant in498 has the 5aa insertion within the third conserved CxxxC motif immediately after the first cysteine. All of these mutations render the protein non-functional, consistent with the completely conserved residues being essential for UL32 activity.

In contrast, mutant in475, which has an insertion directly before an aspartic acid (D) that is almost completely conserved within these sequences (with the exception of Suid herpesvirus 1), is fully functional. It is interesting to note that this aspartic acid is not well conserved in the UL32 sequences of the *Beta-* and *Gamma- herpesvirinae*. With the exception of mutant in475, the remaining mutants that retained function in the packaging and growth assays are all found within less conserved regions of UL32.

In general, insertions within those regions of UL32 that are the most highly conserved were non-functional, whereas the regions of lower conservation were more tolerant to the insertion of 5 amino acids. When looking at the similarity plot, 20 out of the 22 non-functional insertions were in regions above the mean similarity level of the UL32 protein, with 13 of the 15 functional insertions in regions of lower than average similarity.

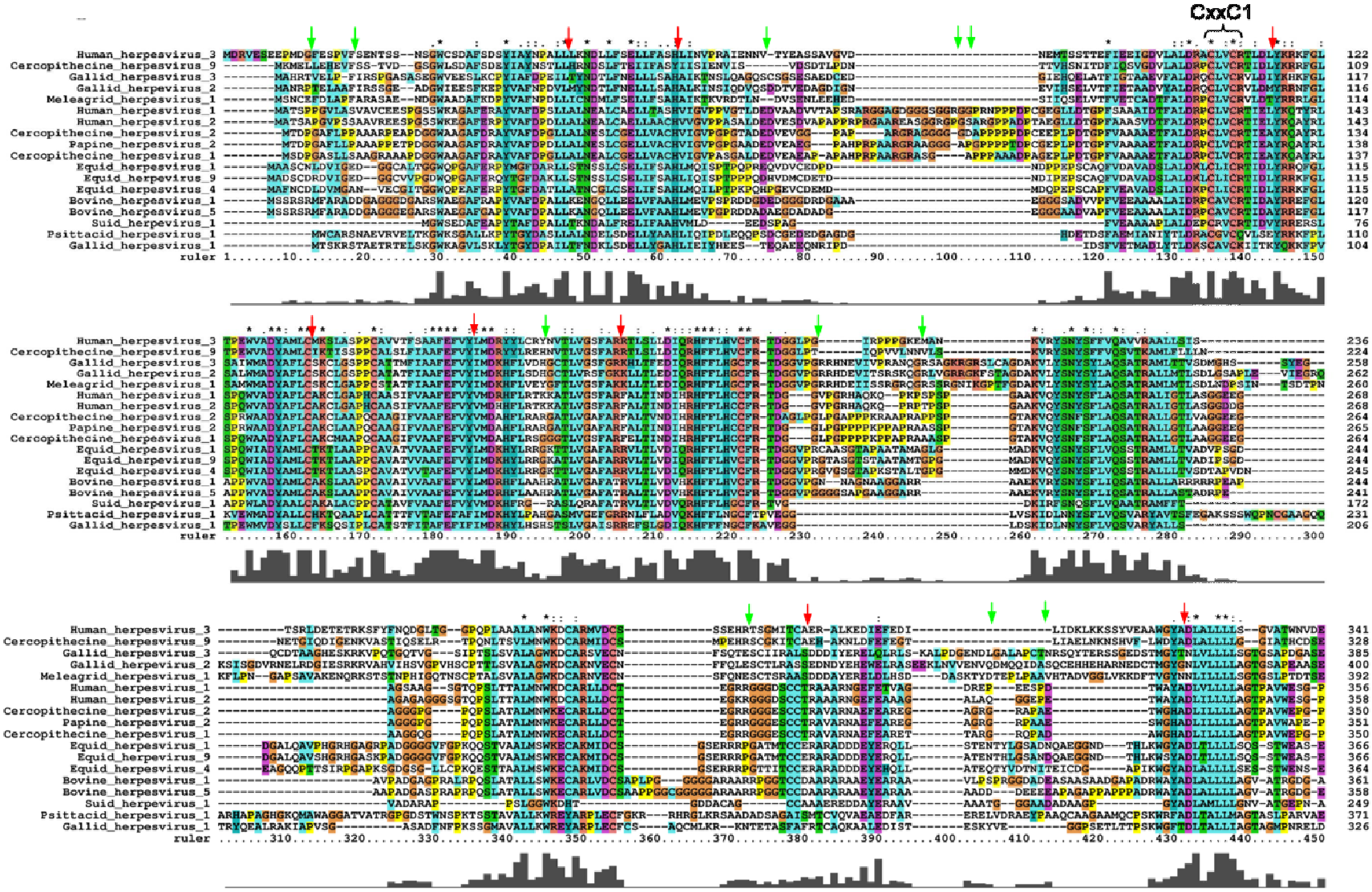
CxxC1
Human_herpesvirus_3
Cercopithecine_herpesvirus_9
Gallid_herpesvirus_3
Gallid_herpevirus_2
Meleagrid_herpesvirus_1
Human_herpesvirus_1
Human_herpesvirus_2
Cercopithecine_herpesvirus_2
Papine_herpesvirus_2
Cercopithecine_herpesvirus_1
Equid_herpesvirus_1
Equid_herpesvirus_9
Equid_herpesvirus_4
Bovine_herpesvirus_1
Bovine_herpesvirus_5
Suid_herpesvirus_1
Psittacid_herpesvirus_1
Gallid_herpesvirus_1
ruler

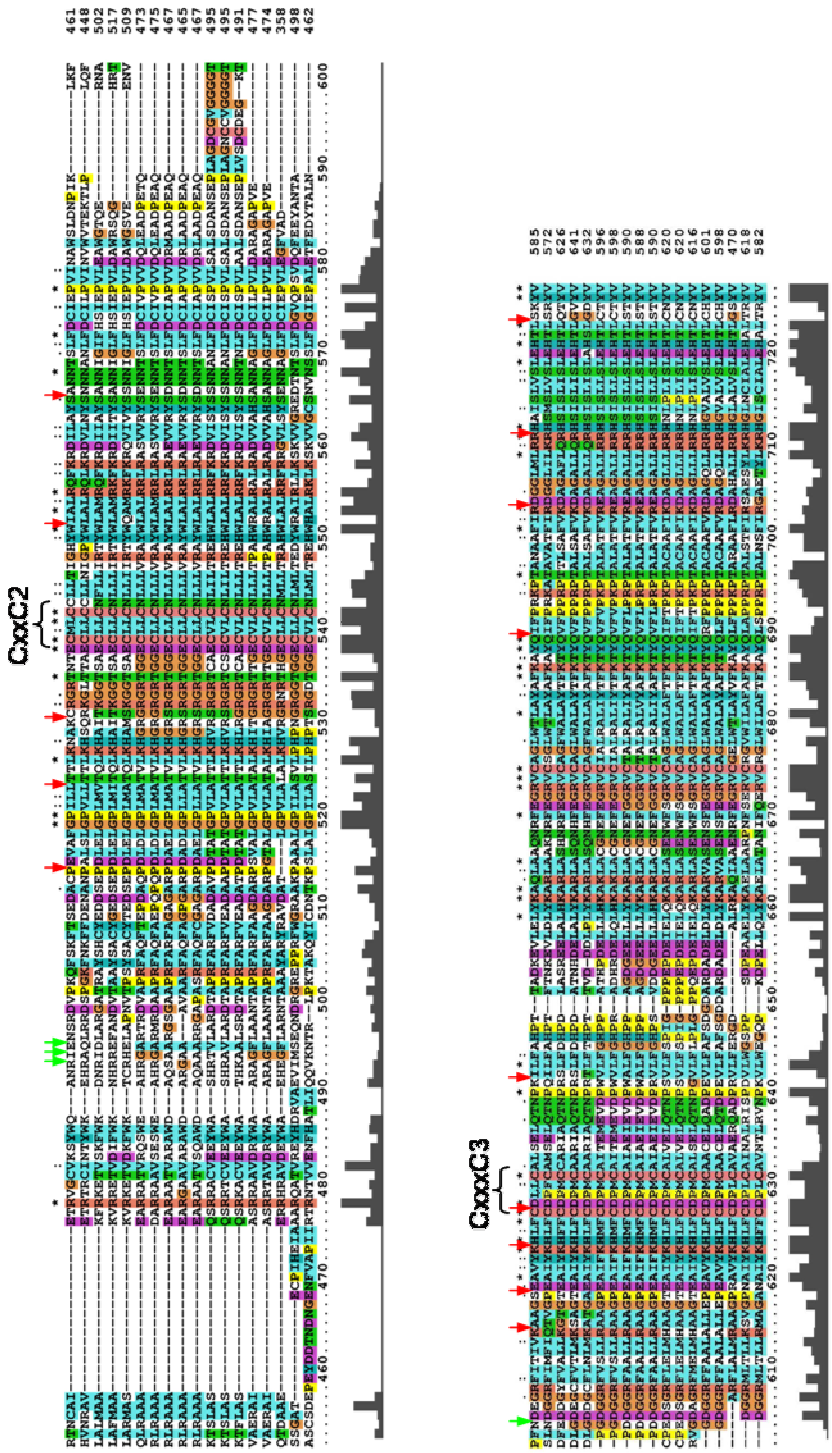

Figure 4.22: Alignment of UL32 sequences from all *Alphaherpesvirinae*.

Available UL32 sequences for *alphaherpesvirinae* were extracted from the RefSeq database and aligned using the ClustalX programme. The grey bars underneath each section of alignment show the relative sequence conservation and absolutely conserved amino acids are denoted with an * above the alignment. The colouring of the amino acids shows the nature and charge of conserved residues. The positions of the transposon mutants are indicated with arrows – green showing functional mutants, and red non-functional.

4.7.4 Correlation between function and predicted secondary structure

As there is no crystal structure of HSV-1 UL32 available, the position of mutants was compared to the secondary structure of UL32 predicted by the PSIPRED program (McGuffin *et al.*, 2000). The predicted secondary structure of UL32 is shown in figure 4.23, with positions of the functional mutants denoted in green and non-functional in red. The majority of mutants with insertions within predicted helices are non-functional, probably because they disrupt the structure of the helix. Conversely, most of the functional mutants lie within predicted unstructured regions of the protein. However, there are some mutants that do not follow this pattern, and mutants in12, in376, in377 and in378 all lie within helical regions but are able to complement the growth and packaging of *hr*64.

4.7.5 Site-specific mutants

Four further mutants were created to analyse highly conserved regions of the UL32 protein. The first set comprised three independent substitution mutations of the CxxC/CxxxC motifs replacing the cysteines with serines. Serine was chosen as the replacement amino acid because it has the same structure as cysteine apart from replacement of the –SH group with an –OH. This should however abolish the ability of the mutated residue to participate in disulphide bond formation and to coordinate zinc ions.

Mutation of the first and third CxxC/CxxxC motifs (CLVC and CDMPC) completely abrogated protein function, but substitution of the central pair of cysteines with serines resulted in a protein that retained partial ability to support growth and DNA packaging in cells infected with *hr*64. This was an unexpected result, as the CxLC sequence of this motif is completely conserved throughout all herpesvirus sequences.

CxxC motifs have been identified in a wide range of proteins, both viral and non-viral, which perform a variety of different functions. These motifs are found in proteins involved in formation and isomerisation of disulphide bonds, for example the thioredoxin superfamily, some of which can act as chaperones to aid folding of other proteins (Berndt *et al.*, 2008). It has previously been suggested that UL32 acts a redox chaperone, being involved in the correct folding and localisation of the VP19C capsid protein (S. Weller,

presented at International Herpesvirus Workshop, 2005), although these data have not been published. CxxC/CxxxC motifs are also important in zinc binding proteins and C-$X_{(2-4)}$-C sequences are found in many zinc finger (ZnF) containing proteins. ZnFs also often contain conserved histidines, and are divided into different classes based upon the organisation of the Cys and His residues and the secondary structure of these motifs. Many zinc binding proteins contain multiple zinc fingers throughout their length. Herpesvirus UL32 sequences do not contain these conserved histidine residues in the characteristic ZnF arrangement, but HSV-1 UL32 has previously been reported to bind zinc (Chang *et al.*, 1996) and this is likely to be through the CxxC/CxxxC motifs. Zinc binding proteins are implicated in a wide range of functions, including interactions with other proteins, folding/assembly of other proteins and interactions with nucleic acids. None of these functions has yet been assigned to UL32, but its role in DNA packaging could involve interactions with other capsid or packaging proteins.

The results presented here indicate that the central CxxC motif is not as critical for protein function as the first and third motifs. It is possible that the outer motifs function in zinc binding activity and the central motif is not involved in this activity. It could be envisaged that the first and third motifs, although far apart in the primary sequence of the protein, are in close proximity in the native protein, where they might be involved in zinc co-ordination. Alternatively, there may be a degree of redundancy, so that when the central CxxC is mutated, one of the other conserved motifs could partially overcome this mutation. However, this does not seem to be the case for the other CxxC/CxxxC motifs which are completely essential, and would presumably require changes to the overall conformation of the protein.

The other site specifically targeted was the extreme C-terminus of UL32 with a deletion of the C-terminal four amino acids (UL32ΔC). This deletion includes the C-terminal 2 amino acids which are completely conserved within the *Alphaherpesvirinae*, and not surprisingly, the mutation destroyed protein function. This is consistent with previous data showing that the extreme C-terminus is essential for protein function and correct localisation in UL52 of HCMV (Borst *et al.*, 2008). This is also in agreement with the phenotype of the insertional mutant in592, which has the insertion directly preceeding these four amino acids, and is non-functional. The final four amino acids of HSV-1 UL32 (CTYV) are found to fit the consensus for PDZ domain-binding sites (X-S/T-X-V). PDZ domains are among the most common domains found in proteins are involved in protein-protein interactions and the clustering and localisation of proteins, commonly binding consensus sequences at the C-

terminus of proteins (van Ham & Hendriks, 2003) . It remains to be determined whether the C-terminus of UL32 is involved in PDZ domain binding within the context of HSV-1 infection.

4.7.6 Inhibition of wt UL32 function

Each of the non-functional mutants was also tested in a transient packaging assay to determine whether they inhibited the function of wt UL32. A dominant negative phenotype is often seen if a mutated protein can still perform part of its function, for example binding to an interaction partner, but cannot carry out other functions. In this way, the mutated protein can sterically or otherwise inhibit the function of the wildtype protein. This property has been demonstrated with the HSV-1 DNA replication proteins, where mutant forms of the origin binding protein, ICP8 and UL8 all inhibit wt HSV-1 infection (Barnard *et al.*, 1997; Chen & Knipe, 1996; Stow *et al.*, 1993). Recently, it was also demonstrated that deletion of a NLS from the packaging protein UL15 created a dominant mutant able to inhibit HSV-1 replication (Yang *et al.*, 2007).

None of the UL32 mutants tested showed potent dominant negative inhibition of the packaging of wt HSV-1 in these assays. There may be a number of possible reasons for this. The UL32 protein may act as a monomer in HSV-1 packaging, for example having an enzymatic activity, so that as long as a wildtype form is present in cells, the mutant form has no effect. Alternatively the wt form of the protein may compete for binding of any potential partners more efficiently than the mutant proteins, or any interaction may be transient enough that the wt UL32 is still able to interact with its binding partners briefly even in the presence of the mutant protein.

One further possible reason why none of the mutants showed dominant-negative activity in this assay is that for some reason mutant UL32 expressed from a plasmid was unable to compete effectively with the wt protein expressed by wt HSV-1. An alternative approach to this assay might be to transfect three plasmids – the amplicon, pUL32 and the insertional mutant - and superinfect with *hr*64, to ensure that wt and mutant UL32 are similarly expressed in cells. A subset of the mutants have been tested again using this method and no dominant-inhibitory activity was seen, confirming the previous results (Dr Nigel Stow; data not shown).

4.7.7 Conclusions

This chapter describes the generation of a large panel of mutants within UL32, allowing functional characterisation of a substantial portion of the protein. Thus far, the precise role of UL32 within the DNA packaging pathway is not known, so the explanation for some of these mutants being non-functional remains unclear. Nevertheless, once specific functions for UL32 begin to emerge, these mutants should prove invaluable in identifying regions of the protein that contribute to such activities.

5 Investigation of potential interactions of UL32 with other HSV-1 proteins

5.1 Investigating the effect of UL32 on the localisation of HSV-1 capsids and capsid proteins in infected cells

HSV-1 DNA cleavage and packaging occurs in replication compartments (RCs) within infected cells, and many proteins involved in cleavage and packaging have been shown to localise to these sites. Lamberti and Weller (1998) reported that UL32 was required for the correct localisation of capsids to RCs in HSV-1 infected cells. They found that capsids were mis-localised throughout the nuclei (excluding the RCs) in cells infected with the HSV-1 UL32 mutant, *hr*64. However, these results have not been subsequently confirmed, and UL32 appears to be absent from B capsids or virions (Lamberti & Weller, 1998). I therefore decided to repeat these experiments to examine whether UL32 does have an affect on the localisation of capsids or capsid proteins.

5.1.1 The effect of UL32 on capsid localisation

Firstly the localisation of capsids was investigated using a rabbit anti-capsid antibody kindly provided by Dr David Pasdeloup (MRC Virology Unit). This antibody was raised against cytoplasmic capsids and as such recognises capsid and some tegument proteins (Dr Pasdeloup, personal communication). The presence of RCs were visualised with an antibody recognising ICP8, the HSV-1 single stranded DNA-binding protein.

BHK cells on coverslips were infected with 5 p.f.u. per cell wt HSV-1 or *hr*64 for six hours. Cells were then fixed and permeablilised using formaldehyde and NP40 and blocked with human serum (section 2.2.8). Coverslips were incubated with the anti-capsid antibody (1:1000) and M7381 (mouse-anti ICP8 IgG ;1:200). The cells were washed and then incubated with r-FITC (FITC-conjugated goat anti-rabbit IgG; 1:200) and m-Cy5 (Cy5-conjugated goat anti-mouse IgG; 1:500), to allow simultaneous detection of both ICP8 and capsids within infected cells. The coverslips were examined by confocal microscopy using lasers with excitation lines at 488 nm and 633 nm, corresponding to the excitation wavelengths of the FITC and Cy5 fluors respectively. The two channels were

scanned separately and the same settings maintained throughout. The results are shown in figure 5.1.

In both infections, the replication compartments are evident, as indicated by the staining of ICP8 within the nucleus (images B and E). As has been previously reported, capsids in wt HSV-1 infected cells localised predominantly to the RCs where they co-localised with ICP8 (images A and C). In contrast to the data from Lamberti and Weller, there was no significant difference in capsid localisation in the *hr*64 infected cells, with the majority of the capsids again colocalising with ICP8 in the RCs (images E and F). In both infections, a small portion of capsid staining can be seen at the outer edge of the cell, which may represent input capsids or cross-reactivity of the antibody with HSV-1 glycoproteins on the surface of the cell.

5.1.2 The effect of UL32 on the localisation of VP5 and VP19C

These results were furthered by examining the localisation of two specific capsid proteins, VP5 and VP19C, in the presence and absence of UL32. VP5 is the major capsid protein making up the hexons and pentons. VP19C is a triplex protein which has also been reported to be partially mis-localised and aggregated in the cytoplasm of cells infected with *hr*64 (S. Weller, presented at International Herpesvirus Workshop, 2005), although these results have not been published

BHK cells were infected and coverslips fixed and permeabilised as above. Coverslips were incubated with R515 (rabbit anti-ICP8 IgG; 1:500) together with either DM165 (mouse anti-VP5 IgG; 1:500) or M2040 (mouse anti-VP19C IgG; 1:500) antibodies. This was followed by incubation with r-FITC and m-Cy5 antibodies and examination of the coverslips by confocal microscopy. Resultant images are shown in figure 5.2. In all infections, ICP8 staining could be clearly seen in the nucleus, indicating that RCs had formed (images A, D, G and J). In agreement with the previous results using the anti-capsid antibody, VP5 showed the same localisation in cells infected with wt HSV-1 (image B) and *hr*64 (image E), colocalising with ICP8 in both instances (images C and F). VP19C also co-localised with ICP8 within RCs in cells infected with both wt HSV-1 (images H and I) and *hr*64 (images K and L).

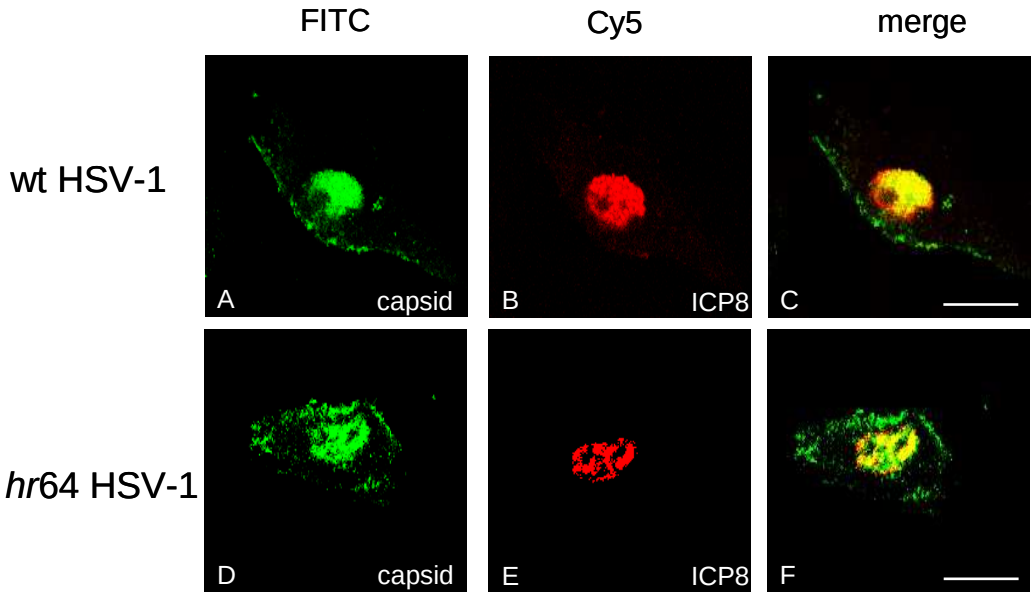

Figure 5.1: UL32 does not affect the localisation of capsids in HSV-1 infected cells.

BHK cells on coverslips were infected with 5 p.f.u./cell wt HSV-1 or *hr*64. 6 h.p.i. cells were fixed with formaldehyde and permeablilised with NP40, followed by blocking with human serum. Coverslips were incubated with M7381(mouse anti-ICP8; 1:200) and rabbit anti-capsid (1:1000) antibodies. This was followed by incubation with m-Cy5 (Cy5-conjugated anti-mouse; 1:500) and r-FITC (FITC-conjugated anti-rabbit; 1:200) and the examination of cells by confocal microscopy. Scale bar = 20 µm.

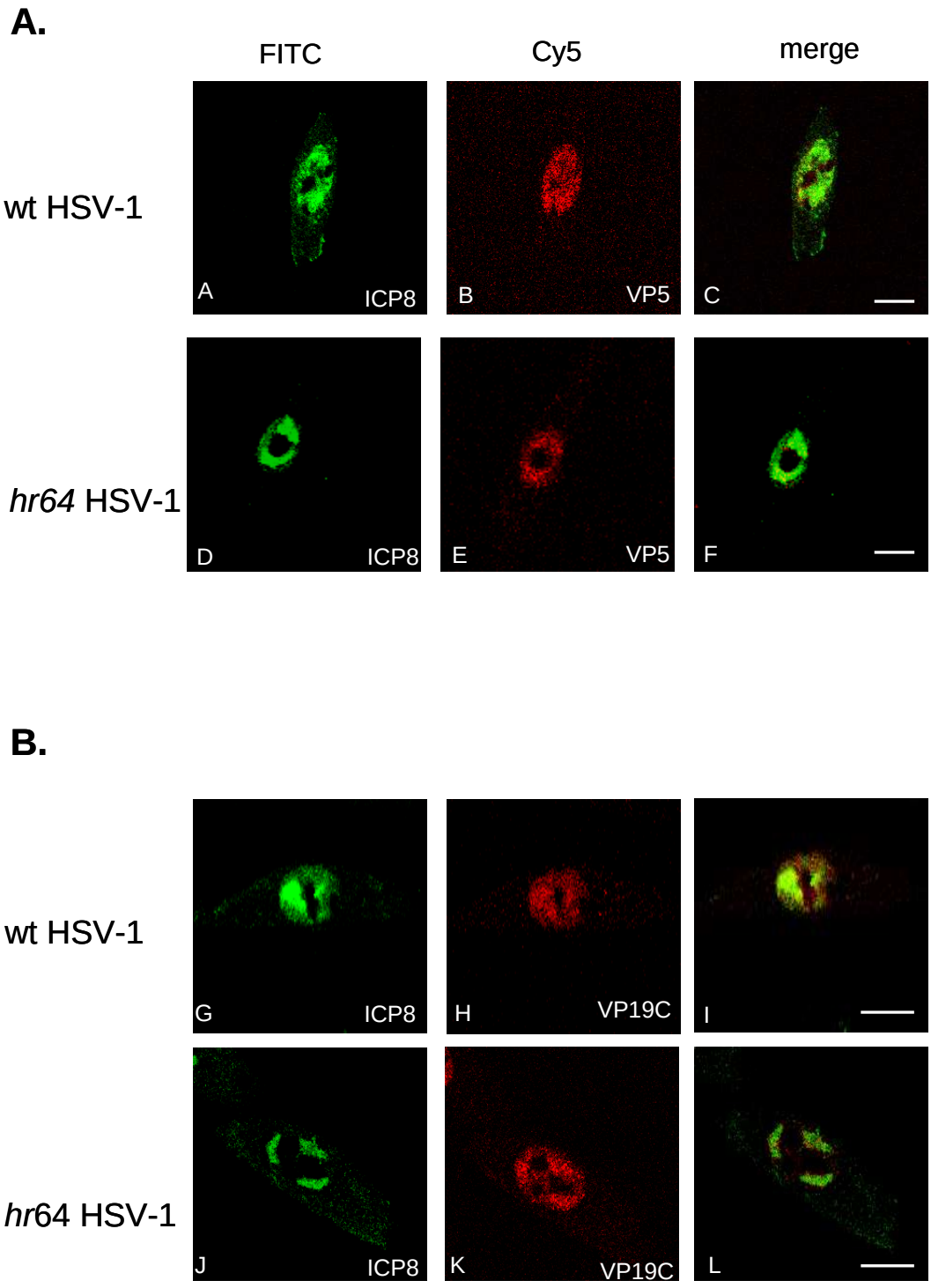

Figure 5.2: UL32 does not affect the localisation of capsids proteins in HSV-1 infected cells.

BHK cells on coverslips were infected with 5 p.f.u./cell wt HSV-1 or *hr*64. 6 h.p.i., cells were fixed, permeabilised and blocked. Coverslips were incubated with R515 (rabbit anti-ICP8 IgG; 1:500) and either DM165 (mouse anti-VP5 IgG; 1:500, panel A) or M2040(mouse anti-VP19C IgG; 1:500, panel B). These were then incubated with r-FITC and m-Cy5 and examined by confocal microscopy. Scale bar = 20 µm.

Together, these data suggest that UL32 is not required for the correct recruitment of capsids or the individual capsid proteins VP5 or VP19C to replication compartments prior to DNA packaging.

5.2 Generation of an HA-tagged UL32 construct

To further aid the studies examining the potential interactions of UL32 with other HSV-1 proteins, a plasmid expressing a tagged version of UL32 was generated. The tag used was the HA tag, which is a nine amino acid peptide derived from the haemagglutinin protein of influenza virus. High quality mouse monoclonal antibodies are available for the HA tag, which would allow this tagged version of UL32 to be visualised in immunofluorescence assays along with other HSV-1 proteins for which rabbit antisera are available in the laboratory.

5.2.1 Generation of plasmid pHA-UL32

It was decided to clone the HA-tag at the N-terminus of UL32 to avoid disruption of the very highly conserved extreme C-terminus. Furthermore, attempts by another group to add an HA tag to the C-terminus of the HCMV UL32 homologue, UL52, resulted in a non-functional protein. These authors were able to successfully introduce the tag at the N-terminus of the protein and generate a functional construct (Borst *et al.*, 2008). Another important factor to be considered when designing the tagged construct was the arrangement of UL32 and surrounding genes within the HSV-1 genome. The start codon (ATG) of UL32 overlaps in the opposite orientation with the start codon of the UL33 gene, as shown in figure 5.3A. UL32 is encoded by HSV-1 nucleotides 69162 to 67372 with UL33 encoded on the opposite strand from nucleotides 69161 to 69553. Therefore, if the tag was placed at the extreme N-terminus of UL32, this would interrupt the first codon of the UL33 gene. Instead, the tag was inserted between the second and third codons of UL32. This also ensured the Kozak consensus sequence for the initiation of translation of UL33 was not disrupted, and that the *Nco*I site was conserved, which could then be used for further cloning steps (section 5.3.1). In addition, the positioning of the tag would allow this construct to be used to introduce a tagged version of UL32 into the HSV-1 genome without disrupting the UL33 gene.

Figure 5.3: Primers used to generate pHA-UL32.

A. HSV-1 nucleotides 69175 to 69133 showing the overlap of the 5’ termini of the UL32 and UL33 genes. The N terminal amino acids of UL32 are shown in blue and UL33 in green.

B. Plasmid map of pUL32 indicating the positions of the primers HA-F and HA-R used to generate the HA-UL32 construct.

C. 5’-3’ sequences of primers used to generate pHA-UL32. The blue nucleotides show those that are complementary to the UL32 gene and the red nucleotides show those encoding the HA tag. The black nucleotides are complimentary to the plasmid backbone. The *Kpn*I and *Pml*I restriction endonuclease sites used for the cloning are underlined.

D. The nucleotide sequence of the 5’ end of the HA-tagged UL32 gene in plasmid pHA-UL32 and the corresponding protein sequence. Amino acids are shown in blue for the UL32 sequence and red for the HA tag. The *Kpn*I restriction endonuclease site is underlined.

A.

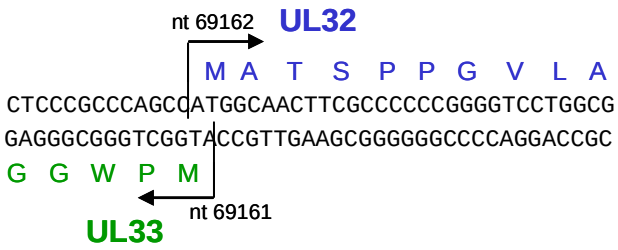

B.

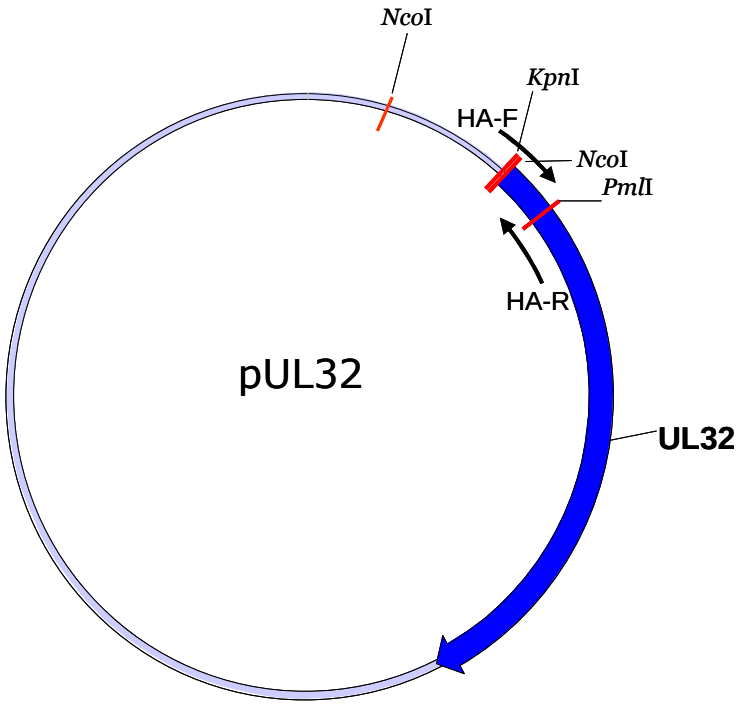

C.

HA-F:	5' GCTCGGTACCCCATGGCATACCCTT ACGACGTGCCTGACTACGCTACTTCGCCCCCCGGGGTCCTGGCG 3'
HA-R:	5' ACCTATCACGTGACTGGCCGTCAGGAGCTCGGC 3'

D.

M A Y P Y D V P D Y A T S P P G V L A

GG TAC CCC ATG GCA TAC CCT TAC GAC GTG CCT GAC TAC GCT ACT TCG CCC CCC GGG GTC CTG GCG

The tag was introduced into pUL32 using a PCR approach. Two primers were designed as shown in figure 5.3B and C. Primer HA-F encoded the first two codons of UL32, followed by the HA tag and then eight more UL32 codons (amino acids 3-11). This primer also included a *Kpn*I restriction endonuclease site that was used for further cloning. Primer HA-R was completely complimentary to the UL32 sequence approximately 150 nucleotides downstream from HA-F, and included a *Pml*I restriction site for further cloning. PCR using primers HA-F and HA-R generated a product of approximately 150 bp, flanked by *Pml*I and *Kpn*I restriction sites. The pUL32 plasmid was digested with these enzymes and the large fragment purified following gel electrophoresis. This was then ligated to the PCR fragment (also digested with *Pml*I and *Kpn*I) to generate plasmid pHA-UL32.

5.2.2 Expression and localisation of HA-UL32 protein in transfected cells

It was essential to verify that the plasmid pHA-UL32 did indeed express the HA-tag fused to the UL32 protein and that HA-UL32 could be detected using a commercial anti-HA antibody. This was done using western blots and immunofluorescence of cells transfected with pHA-UL32.

BHK cells were transfected with 1 µg pUL32 or pHA-UL32 using the calcium phosphate method. Cells were harvested 18 hours post infection, boiled in the presence of SDS and separated by electrophoresis on an 8% polyacrylamide gel. Samples were transferred to PVDF membranes and immunoblotted using a mouse anti-HA antibody (F-7; 1:500) followed by HRP-conjugated goat anti-mouse IgG (1:1000) and developed using ECL substrate. The resultant gel is shown in figure 5.4A. Lane 1 shows a band of the expected size for HA-UL32, indicating that the tag is able to be recognised by this antibody. A corresponding band was not present in the cells transfected with the untagged pUL32 (lane 2) confirming that this recognition is specific to the HA tag. The membrane was stripped and re-probed using R1 (anti-UL32) to confirm that a UL32 reactive protein migrated at the same position as the product recognised by the anti-HA antibody (lanes 3 and 4).

To investigate the localisation of HA-UL32 in transfected cells, BHK cells on coverslips were transfected with 0.5 µg pUL32 or pHA-UL32 using Lipofectamine 2000. 18 hours post transfection, cells were fixed and permeablilised with formaldehyde and NP40 and

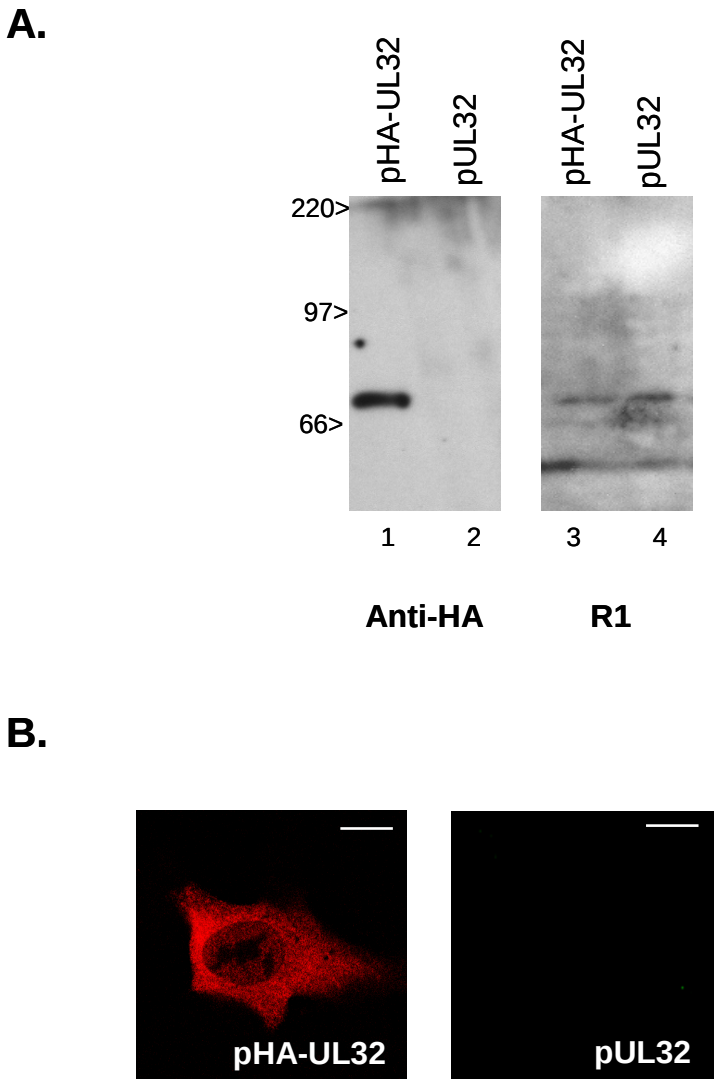

Figure 5.4: Expression and localisation of HA-UL32.

A. BHK cells were transfected with 1 µg pHA-UL32 or pUL32 using the calcium phosphate method. 18 hours post transfection, cell lysates were prepared and samples were separated by SDS-PAGE then western blotted as previously described. Membranes were probed with F-7 (mouse anti-HA; 1:500), followed by HRP-conjugated goat anti-mouse IgG (1:1000). The membranes were then stripped and re-probed with R1, followed by HRP-coupled protein-A.

B. 0.5 µg plasmid DNA was transfected into BHK cells using Lipofectamine 2000. 18 hours post transfection, cells were fixed and permeabilised. Coverslips were then probed with F-7 (mouse anti-HA; 1:500) followed by m-Cy5 (1:500) and examined by confocal microscopy. Scale bar = 20 µm.

incubated with F-7 (1:500) followed by m-Cy5. The coverslips were analysed by confocal microscopy and the images are shown in figure 5.4B. The anti-HA antibody shows bright fluorescence in the cytoplasm of those cells transfected with pHA-UL32 (image A) but no fluorescence was seen in the cells transfected with pUL32 (image B), again confirming the specificity of the antibody. HA-UL32 has the same localisation as untagged wtUL32 (figure 3.6), indicating that the addition of a small tag does not affect the localisation of the UL32 protein.

5.2.3 Functional analysis of pHA-UL32

It was also necessary to confirm that the tagged protein expressed from pHA-UL32 retained functionality. This was done by testing pHA-UL32 in the two assays already described in chapter 4 examining the complementation of growth and DNA packaging of the *hr*64 virus.

5.2.3.1 Complementation yield analysis

BHK cells were transfected with 1 µg pUL32, pCMV10 or pHA-UL32 and superinfected with *hr*64 as previously described (section 4.3). 18 hours post infection, the cells and media were harvested and viral progeny were titrated on the complementing cell line, UL32-5. Cells were stained and plaques counted, and the yields are shown in figure 5.5A. The value for pHA-UL32 is a mean of duplicate experiments and is expressed as a percentage of that obtained with pUL32.

As in previous experiments, pUL32 successfully complemented the growth defect of *hr*64, giving a mean titre of 6×10^5 p.f.u., compared to a value of 4.6×10^2 with the empty vector pCMV10. pHA-UL32 supported viral growth as efficiently as the untagged protein, with a mean titre of 6.6×10^5 p.f.u., 110% of that obtained with pUL32.

5.2.3.2 The ability of pHA-UL32 to support amplicon DNA packaging by *hr*64

The HA-tagged UL32 construct was also tested for its ability to support the DNA packaging of *hr*64 in the amplicon packaging assay. BHK cells were transfected with 1 µg pUL32, pCMV10 or pHA-UL32 along with 0.5 µg pSA1 and superinfected with wt HSV-1 or *hr*64 as described in section 2.2.6. Cells were harvested at 18 hours post infection and total and DNase resistant DNA samples prepared. The DNA samples were separated by

electrophoresis, Southern blotted and pSA1 was detected by hybridisation to ^{32}P-labelled pAT153 probe as described previously.

Figure 5.5B shows that pSA1 replication occurred in all samples. As expected, DNA packaging occurred following infection with wt HSV-1 (lane 1) or *hr*64 infection in the presence of pUL32 (lane 2) but not pCMV10 (lane 3). Consistent with the complementation yield assay results, pHA-UL32 was able to support DNA packaging of *hr*64 (lane 4). Quantification of the data from this and a repeat experiment revealed that pHA-UL32 supported pSA1 packaging to 80% and 105% of the levels observed with pUL32.

These results together confirm that a construct was successfully created that expressed the UL32 protein containing an HA tag and that this protein was indistinguishable from wt UL32 in assays examining its ability to support viral growth and DNA packaging of *hr*64.

5.3 Generation of an HSV-1 recombinant virus expressing HA-tagged UL32

An HSV-1 recombinant virus expressing the same HA-UL32 was then generated. The method used for this is described in section 2.2.12.

The approach taken was to rescue the *hr*64 mutation with a fragment containing the HA-UL32 gene. Since the HA tag lies very close to the end of the UL32-containing fragment in pHA-UL32, a plasmid, p33-HA-UL32, containing additional sequences from the UL33 gene to facilitate homologous recombination, was first constructed.

5.3.1 Generation of plasmid p33-HA-32

Figure 5.6 shows the cloning strategy used to generate plasmid p33-HA-32. Since the UL32 and UL33 initiation codons overlap within an *Nco*I restriction site (recognition sequence CCATGG) (figure 5.3A), this *Nco*I site can be used for convenient linking of the UL33 gene and the HA-tagged UL32 gene. Firstly, pHA-UL32 was digested using *Nco*I and *Nde*I, the fragments separated by agarose gel electrophoresis and the large fragment (containing HA-UL32 and a large section of the plasmid backbone) purified from the gel.

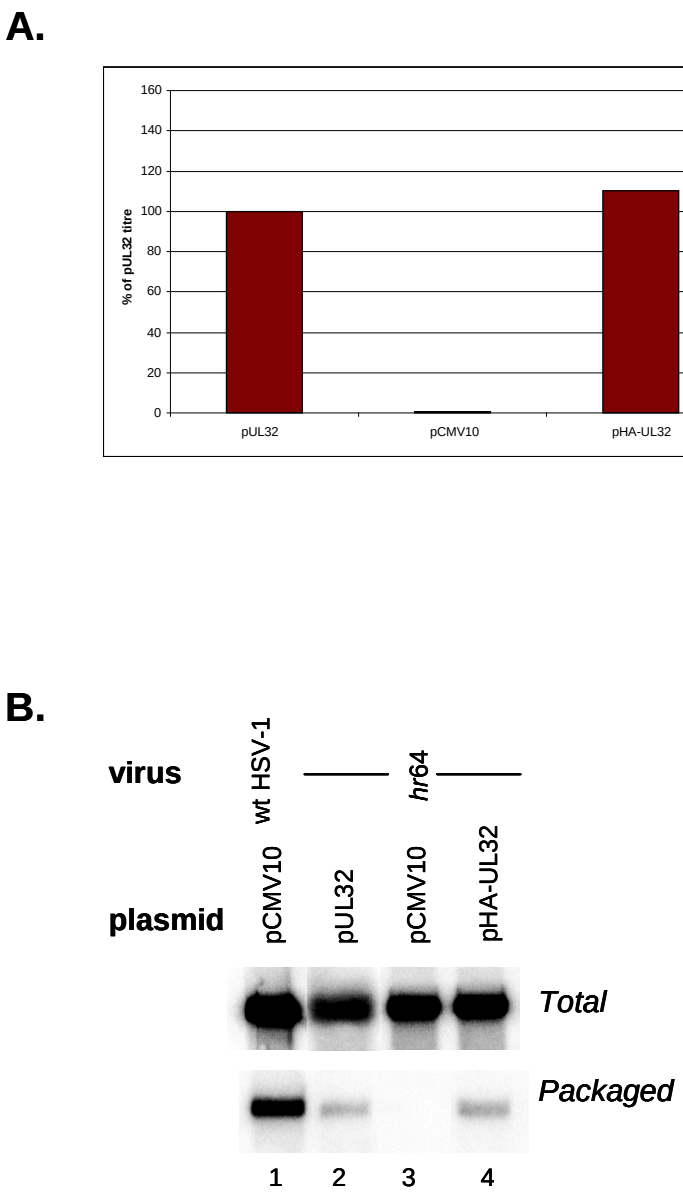

Figure 5.5: Functional analysis of pHA-UL32.

A. Complementation yield assay. BHK cells were transfected and superinfected as previously described in figure 4.11. 18 h.p.i., viral yields were collected and titrated on UL32-5 cells for 4 days. Plaques were counted and titres expressed as a percentage of those obtained with pUL32.

B. Amplicon packaging assay. Cells were co-transfected with pSA1 and either pCMV10, pUL32 or pHA-UL32 and superinfected with wt HSV-1 or *hr*64 as previously described in figure 4.12. Total and DNase resistant DNA were prepared and samples digested with *Eco*RI and *Dpn*I. DNA was separated by agarose gel electrophoresis and Southern blotted, and pSA1 was detected by hybridisation to ^{32}P labelled pAT153.

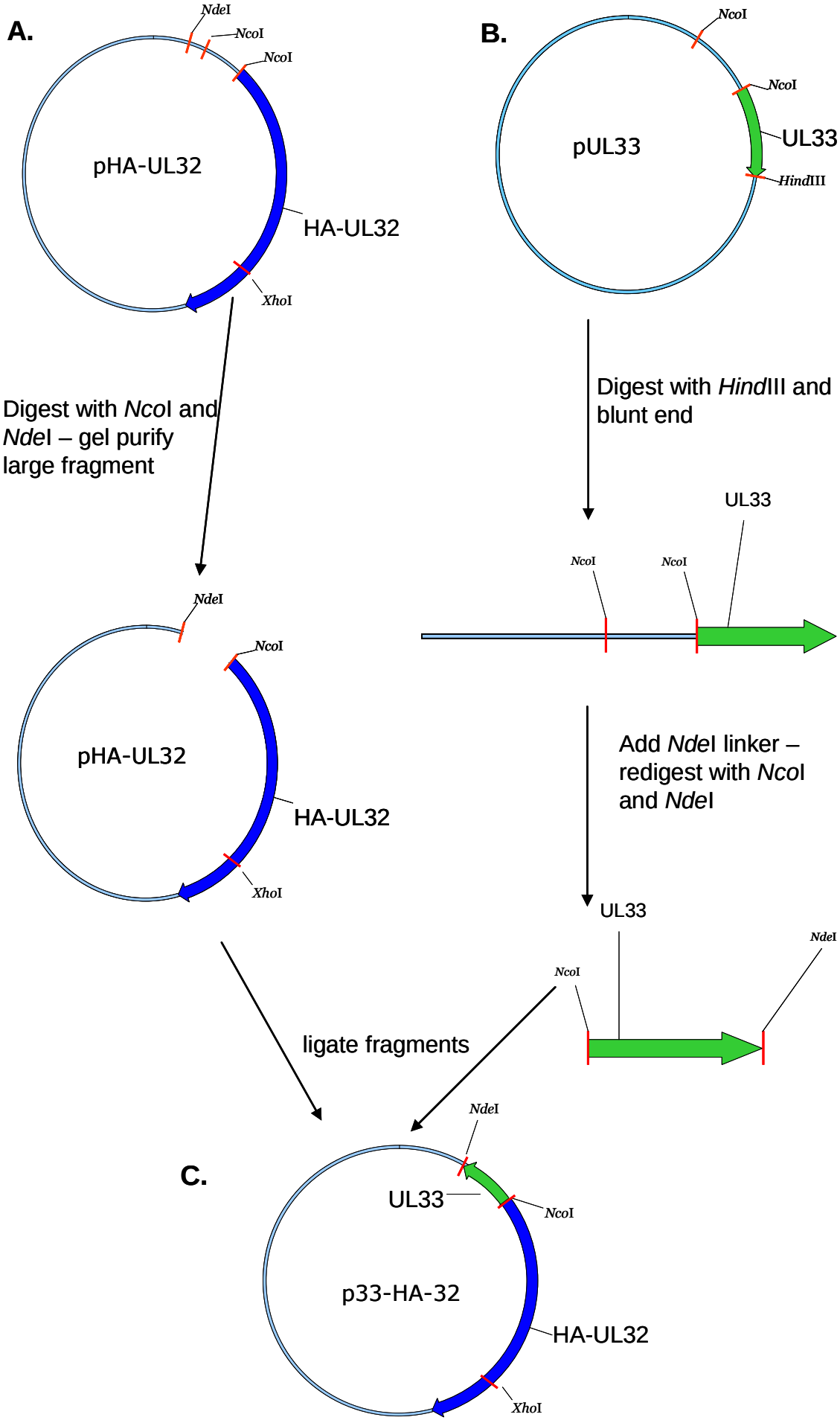
A.
NdeI
NcoI
NcoI
pHA-UL32
HA-UL32
XhoI
B.
NcoI
NcoI
pUL33
UL33
HindIII
Digest with HindIII and blunt end
Digest with NcoI and NdeI – gel purify large fragment
UL33
NcoI
NcoI
NdeI
NcoI
pHA-UL32
HA-UL32
XhoI
Add NdeI linker – redigest with NcoI and NdeI
UL33
NdeI
NcoI
ligate fragments
C.
NdeI
UL33
NcoI
p33-HA-32
HA-UL32
XhoI

D.

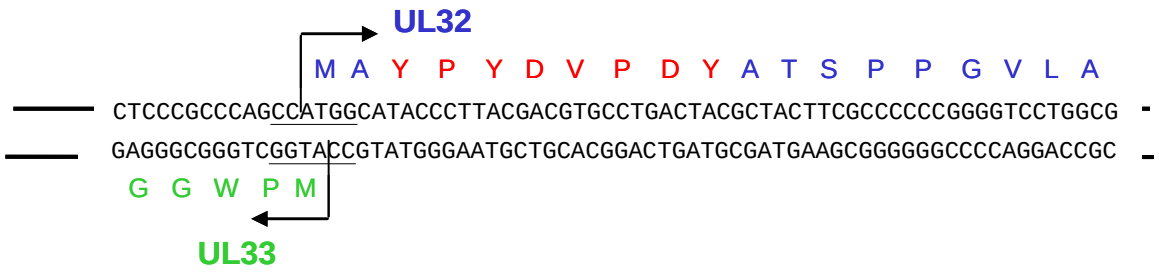

Figure 5.6: Generation of p33-HA-32.

A. pHA-UL32 was digested with *Nco*I and *Nde*I and the fragments separated by agarose gel electrophoresis. The large fragment containing the plasmid backbone and HA-UL32 was purified.

B. pUL33 was digested with *Hind*III and blunt-ended. An *Nde*I linker was added this was re-digested with *Nco*I and NdeI. The fragment containing UL33 was purified to yield a fragment containing the UL33 gene flanked by *Nco*I at its 5' end and *Nde*I downstream of the 3' end

C. The UL33 and pHA-UL32 fragments were ligated via the *Nde*I and *Nco*I restriction enzyme sites to generate plasmid p33-HA-32, containing HA-UL32 (blue) and UL33 (green) encoded in the opposite orientation to one another.

D. The nucleotide sequence of the 5' termini of UL33 and HA-UL32 within plasmid p33-HA-32. The start codon of each gene and the orientation are indicated by arrows. The amino acids of the UL33 protein are shown in green and UL32 in blue, with the HA tag shown in red. The shared *Nco*I restriction site is underlined

As pUL33 does not contain an *Nde*I site, the cloning strategy used to excise UL33 was slightly different. pUL33 was digested with *Hind*III and blunt-ended. An *Nde*I linker was added, the product re-digested with *Nde*I and *Nco*I and the UL33-containing fragment purified. This generated a fragment encoding UL33 with the *Nco*I site at the 5' end of the gene, and an *Nde*I site downstream of the 3' end of the gene. The two fragments (the UL33 fragment and the plasmid backbone containing HA-UL32) were then ligated and transformed into XL-1 blue cells. DNA of a resulting plasmid, p33-HA-32, was prepared using a Qiagen QIAquick Spin Miniprep kit and the sequence of the junction between UL33 and HA-UL32 confirmed by sequencing. The sequence was identical to that of wt HSV-1 except for the 45 nucleotide insertion coding for the HA tag. The insertion does not place any additional ATG codons upstream of the UL33 start codon and so should not affect the UL33 protein. The 33-HA-32 fragment was then excised from the plasmid by restriction digest using *Nde*I and *Xho*I to promote recombination with *hr*64 DNA in the marker rescue.

5.3.2 Marker rescue of *hr*64

For the marker rescue, *hr*64 genomic DNA was first prepared from infected UL32-5 cells as described in section 2.2.12.1. 0.5 µg *hr*64 DNA and 0.5 µg gel-purified 33-HA-32 fragment were co-transfected into duplicate 35 mm plates of non-complementing BHK cells, as described in section 2.2.12.2. One plate showed evidence of infection after incubation at 37°C for 3 days, and the cells and media were harvested. The progeny were titrated onto BHK cells to confirm that the virus could successfully replicate on non-complementing cells and to obtain a titre of this initial harvest.

Plaque purification of the initial harvested virus was performed, as described in section 2.2.12.3. Samples of two-fold serial dilutions covering the range 128 p.f.u/well to 3.9×10^{-3} p.f.u./well and used to infect microtitre wells of BHK cells. After 4 days incubation at 37°C, four wells were chosen containing single plaques were used to infect 35 mm dishes of BHK cells overnight. These virus-infected cells were harvested, the proteins separated by SDS-PAGE and the membranes were screened by western blotting using F-7 (anti-HA) to confirm that they expressed HA-UL32. Figure 5.7 shows that each harvested viral progeny produced a protein of the correct size that was recognised by the anti-HA antibody. Clone G7 was selected for use and the harvested cells used to infect 175 mm^2 flasks of BHK cells and generate a stock of virus, which was named HA32EP. This stock was also tested for the absence of the original *hr*64 virus by staining of infected cells for

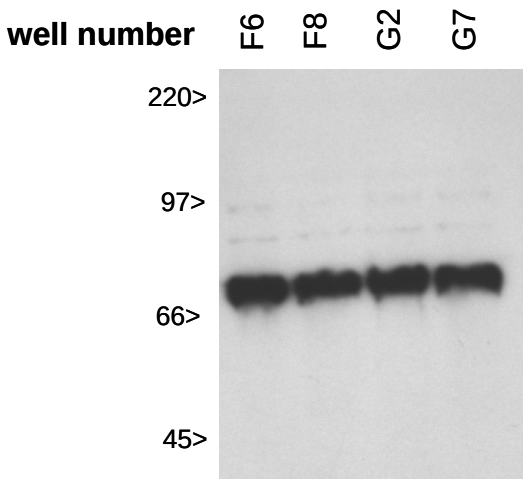

Figure 5.7: Screening of marker rescuants for the expression of HA-UL32.

Single wells from the serial dilution of marker-rescuant virus progeny were chosen and used to infect 35 mm dishes of BHK cells overnight. Cells were harvested and protein separated by electrophoresis on 8% polyacrylamide gels and western blotted. The membranes were probed with F-7 (mouse anti-HA), followed by HRP-coupled goat anti-mouse IgG. The positions of size markers are indicated (kDa).

β-galactosidase expression (from the lacZ cassette inserted into *hr*64). No β-galactosidase activity was seen, confirming that the virus stock contained only HA32EP HSV-1.

5.3.3 Growth curve of HA32EP on BHK cells

The above isolation of HA32EP confirmed that this virus was able to replicate in non-complementing BHK cells, and its growth was next compared to wt HSV-1 and *hr*64. 35 mm dishes of BHK cells were infected with 10 p.f.u. per cell wt HSV-1, *hr*64 or HA32EP. One hour after infection the cells were washed once with 0.14 M NaCl, exposed to acid glycine wash for one minute, then washed with EC5, followed by continued incubation in EC5 at 37°C. Cells were harvested at 4, 8, 12, 16, 20 and 24 hours post infection and the cells and media sonicated before being titrated onto BHK cells for 3 days (section 2.2.4.2). Plaques were counted and virus yields determined. This single-step growth analysis (figure 5.8) demonstrates that HA32EP replicates with similar kinetics to wt HSV-1, in contrast to *hr*64, which did not show any growth in BHK cells.

5.3.4 Investigating the ability of HA32EP to package HSV-1 DNA

The DNA packaging ability of HA32EP was investigated by using a viral DNA packaging assay. Duplicate monolayers of BHK cells were infected with 5 p.f.u. per cell wt HSV-1 or HA32EP. After one hour, cells were washed once with 0.14 M NaCl, exposed to acid glycine wash for one minute, then washed with EC5. One of each sample was harvested after this acid glycine wash and the cells pelleted and stored at -20°C (input). The other sample was incubated in EC5 at 37°C and harvested after 18 hours (18 hour). Total and DNase resistant DNAs were prepared from both input and 18 hour samples as described in section 2.2.6.2. These samples were digested with *Eco*RI and separated by electrophoresis on a 0.8% agarose gel. The gel was Southern blotted and hybridised to ^{32}P labelled pGX153, which contains the *Bam*HI P fragment of HSV-1 inserted into pAT153. Probing with pGX153 should detect 2 bands corresponding to the HSV-1 *Eco*RI N (2.4 kbp) and G and F fragments (16.1 and 16.2 kbp respectively, which migrate as one band).

Figure 5.9 shows that the amount of viral DNA in the input samples was insufficient to be detected in a short exposure (lanes 1, 3, 5 and 7). In contrast, wt HSV-1 and HA32EP DNA was readily detected at 18 hours post infection (lanes 2 and 4). Furthermore, both wt HSV-1 and HA32EP packaged the replicated viral DNA to a similar level (lanes 6 and 8).

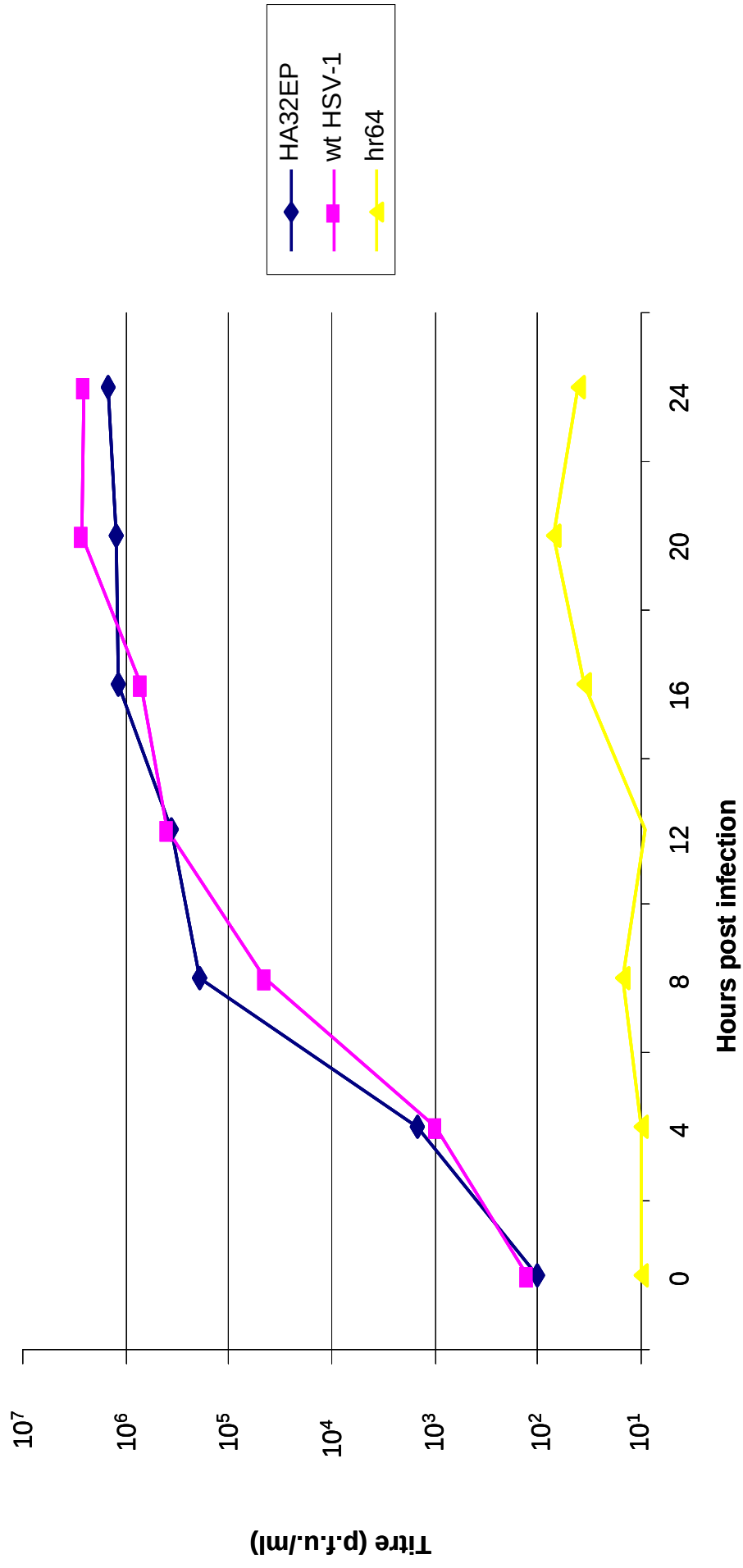

Figure 5.8: Comparison of the growth of wt HSV-1, HA32EP and *hr*64 in BHK cells.

Replicate plates of BHK cells were infected with 10 p.f.u./cell wt HSV-1, HA32EP or *hr*64. At the indicated times, cells were harvested and the progeny virus titrated onto BHK cells. Plaques were counted 3 d.p.i and the titres determined.

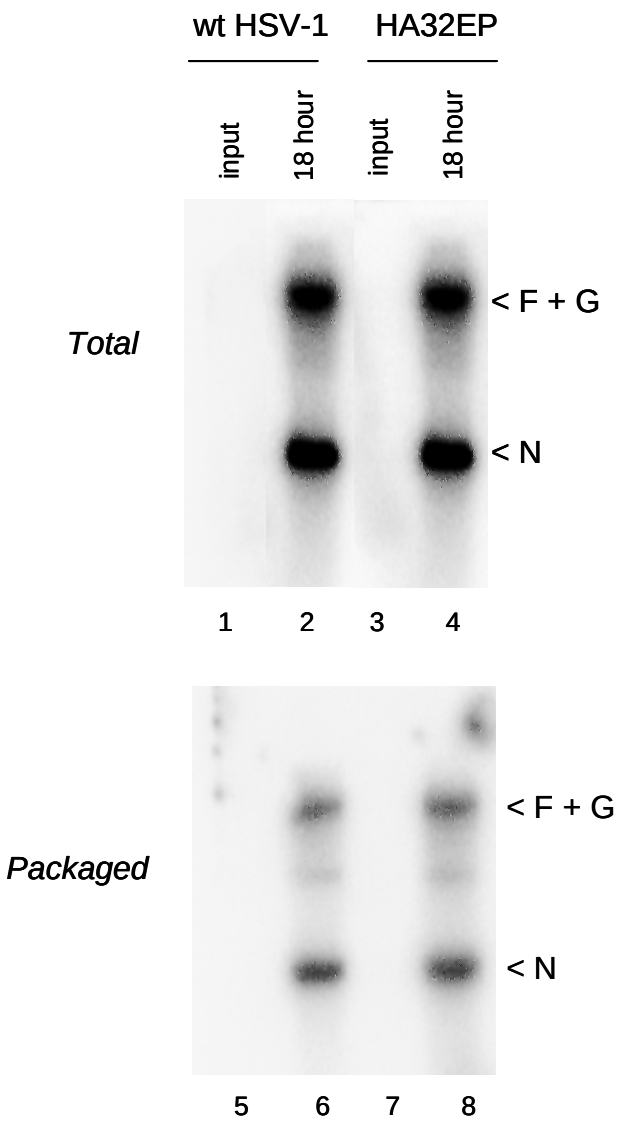

Figure 5.9: Packaging of viral DNA by wt HSV-1 and HA32EP.

BHK cells were infected with 5 p.f.u./cell wt HSV-1 or HA32EP and harvested at either 1 h.p.i. (input) or 18 h.p.i (18 hour). Total and packaged DNA were prepared and digested with *Eco*RI. DNA was separated by agarose gel electrophoresis, Southern blotted, and the membrane probed with ^{32}P labelled pGX153.The positions of the *Eco*RI F, G and N fragments are indicated.

The above assays confirmed that HA32EP replicates and packages DNA with similar efficiency to wt HSV-1 in BHK cells.

5.4 Localisation of HA-UL32 in HA32EP infected cells

Previous work concerning the localisation of UL32 within HSV-1 infected cells has yielded conflicting results. Chang et al (1996) reported that UL32 localised predominantly to the cytoplasm of infected cells in infection, using a rabbit antisera directed against UL32. Lamberti and Weller (1998) examined the localisation of UL32 by transfection of an epitope-tagged UL32 construct and superinfection using *hr*64. They found that although UL32 was predominantly cytoplasmic, there was a portion that localised to the replication compartments in the nucleus, colocalising with ICP8. The R1 antisera generated earlier in this work (see section 3) was incapable of specifically detecting UL32 in HSV-1 infected cells by immunofluorescence and gave very high levels of background staining throughout cells infected with *hr*64 (data not shown). Therefore HA32EP was used to investigate the localisation of HA-UL32 in HSV-1 infected cells.

BHK cells on coverslips were infected with 5 p.f.u. per cell HA32EP or wt HSV-1 for 6 hours. Cells were fixed and permeablilised and blocked using human serum, and the coverslips were incubated with F-7 (anti-HA) and R515 (rabbit anti-ICP8; 1:500) antibodies, followed by r-FITC and m-Cy5. The coverslips were examined by confocal microscopy and the images are shown in figure 5.10.

In the HA32EP infected cells, ICP8 staining was clearly visualised within the nucleus (image A). The HA-UL32 staining co-localised with ICP8 (images B and C). No HA staining was seen in cells infected with wt HSV-1 (image E), even though the ICP8 staining showed that the cells were efficiently infected (image D), confirming the specificity of the anti-HA antibody. Therefore, in contrast to other reports, this study shows that the UL32 protein localises entirely to the replication compartments within the nucleus of HSV-1 infected BHK cells.

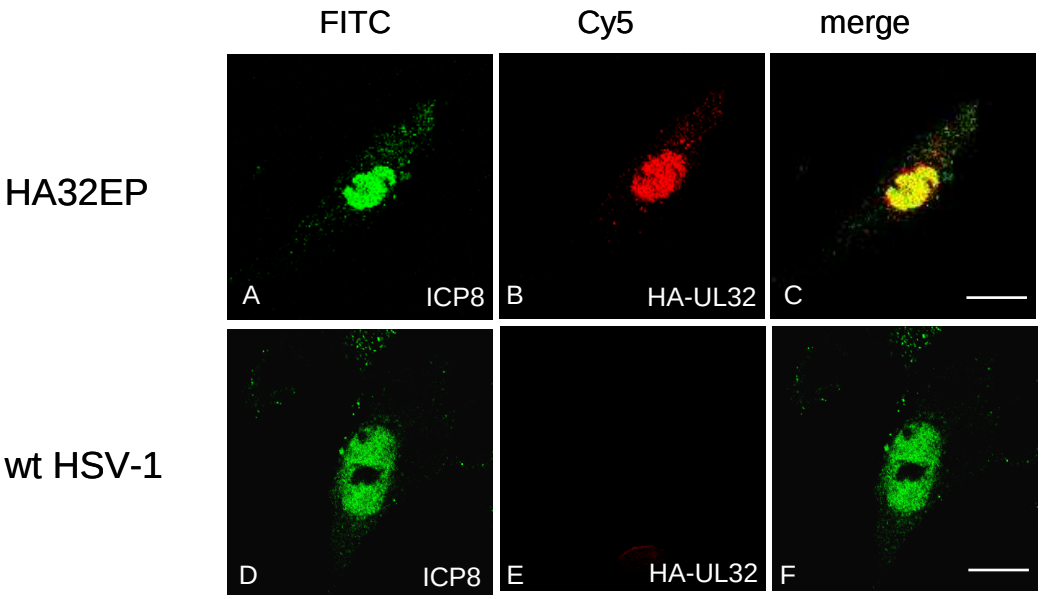

Figure 5.10: Localisation of HA-UL32 in HSV-1 infected cells.

Coverslips of BHK cells were infected with 5 p.f.u./cell HA32EP (A-C) or wt HSV-1 (D-E) for 6 hours. Cells were fixed and permeabilised using formaldehyde and NP40 and blocked with human serum. Coverslips were incubated with F-7 (mouse anti-HA; 1:500) and R515 (rabbit anti-ICP8; 1:500), followed by r-FITC (1:200) and m-Cy5 (1:500). Coverslips were mounted and examined by confocal microscopy. Scale bar = 20 µm.

5.5 Investigation of the interaction of UL32 with HSV-1 packaging proteins UL6, UL17 and UL25

No direct interactions have yet been reported between UL32 and any other HSV-1 protein, although it has recently been reported that UL32 may affect the localisation of UL25 in HSV-1 infected cells (Scholtes & Baines, 2009). It was therefore decided to analyse whether UL32 could interact with any other HSV-1 DNA cleavage/packaging protein. This section describes results obtained for UL6, UL17 and UL25. The analysis of possible interactions with the three components of the terminase is described in the following section (5.6).

5.5.1 Localisation of UL6, UL17 and UL25 in HSV-1 infected cells in the absence of UL32

As UL32 and all other packaging proteins localise to replication compartments in infected cells (along with the capsid proteins), I first examined whether UL32 plays a role in the correct localisation of UL6, UL17 and UL25 in HSV-1 infection .

BHK cells were infected with 5 p.f.u. per cell wt HSV-1 or *hr*64 and fixed at 6 hours post infection. Cells were processed as before and incubated with R335 (rabbit anti-UL25; 1:500), R992 (rabbit anti-UL6; 1:500) or R1218 (rabbit anti-UL17; 1:500), together with M7381 (mouse anti-ICP8). This was followed by incubation with m-Cy5 and r-FITC and examination by confocal microscopy. Representative images are shown in figure 5.11.

All cells infected with wt HSV-1 showed clear ICP8 staining in the nucleus, indicating that replication compartments had been formed (images B, H and N). As previously reported, all three proteins UL6, UL17 and UL25 were seen predominantly within the nucleus in these cells (images A, G and M) (Scholtes & Baines, 2009; Taus *et al.*, 1998) and co-localised with ICP8, confirming that they localise to replication compartments during wildtype infection (images C, I and O). In the *hr*64 infected cells, ICP8-stained replication compartments could again be visualised within the nucleus (images E, K and Q). UL6 and UL17 co-localised with the ICP8 foci, as in wt HSV-1 infection (images D and F; J and L). In contrast to the report from Scholtes and Baines, the localisation of UL25 in *hr*64

Figure 5.11: UL32 does not affect the localisation of packaging proteins UL6, UL17 or UL25 in HSV-1 infected cells.

Coverslips of BHK cells were infected with wt HSV-1 or *hr*64 at 5 p.f.u./cell for 6 hours. Cells were fixed and permeabilised and incubated with M7381 (mouse anti-ICP8) along with either R992 (rabbit anti-UL6; 1:500), R1218 (rabbit anti-UL17; 1:500) or R335 (rabbit anti-UL25; 1:500). This was followed by r-FITC and m-Cy5. The cells were examined by confocal microscopy. Scale bar = 10µm.

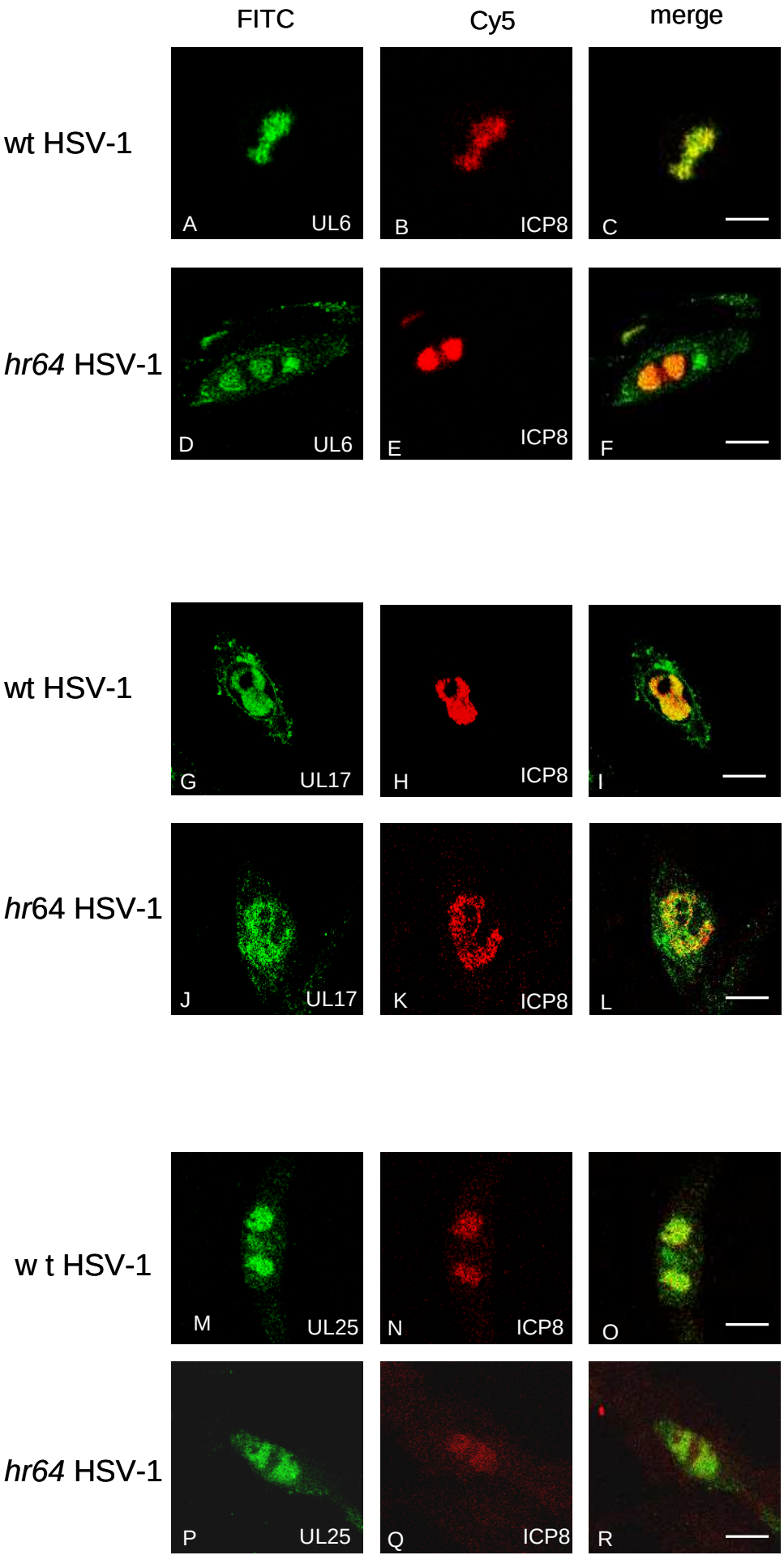
FITC
Cy5
merge
wt HSV-1
A UL6
B ICP8
C
hr64 HSV-1
D UL6
E ICP8
F
wt HSV-1
G UL17
H ICP8
I
hr64 HSV-1
J UL17
K ICP8
L
w t HSV-1
M UL25
N ICP8
O
hr64 HSV-1
P UL25
Q ICP8
R

infected cells was also indistinguishable from cells infected with wt HSV-1, with UL25 again colocalising with ICP8 (images P and R).

These results suggest that UL32 is not required for the localisation of UL6, UL17 or UL25 to the replication compartments in infected cells.

5.5.2 Co-localisation analysis of UL32 with UL6, UL17 or UL25 in transfected cells

To analyse whether UL32 might interact with UL6, UL17 or UL25 in the absence of other viral proteins, a co-transfection assay was used. For this assay, plasmids pAS30, pMH19 and pIM96 were used, encoding UL6, UL17 and UL25 respectively, each under the control of the HCMV IE promoter.

BHK cells were transfected with 0.5 µg pAS30, pMH19 or pIM96, either alone or in combination with 0.5 µg pHA-UL32, using Lipofectamine 2000. Cells were fixed and permeabilised 18 hours post transfection. Coverslips were reacted with F-7 and either R992, R1218 or R335, followed by staining with r-FITC and m-Cy5, as described above. Cells were examined by confocal microscopy and representative results are shown in figure 5.12.

As previously observed, HA-UL32 localised to the cytoplasm of transfected cells when expressed alone and no background signal was apparent in the FITC channel (images A-C). When expressed alone, UL6 was present solely in the nuclei of cells (images D-F), consistent with published results (White *et al.*, 2003). In cells co-expressing both proteins, UL6 remained in the nucleus while HA-UL32 remained cytoplasmic (images G-I). UL25 was present throughout the cell when expressed alone, predominantly in the cytoplasm, but also with a portion entering to the nucleus (images J-L). In co-transfected cells, neither UL25 or HA-UL32 was altered in its localisation (images M-O). The failure of UL25 to transport UL32 into the nucleus suggests the lack of a strong interaction between these proteins. Like HA-UL32, UL17 was found to localise exclusively to the cytoplasm when expressed alone (images P-R). In the co-transfected cells, both proteins remained diffusely distributed throughout the cytoplasm, and it is difficult to interpret whether any observed co-localisation is indicative of an interaction (images S-U).

Figure 5.12: Interaction of HA-UL32 with packaging proteins UL6, UL25 and UL17 in transfected cells.

BHK cells on coverslips were transfected with 0.5 µg of the indicated plasmids using Lipofectamine 2000. 18 hours post transfection, cells were fixed and permeabilised with formaldehyde and NP40 and incubated with either R992, R335 or R1218 (all at 1:500) along with F-7. This was followed by incubation with r-FITC and m-Cy5. Coverslips were mounted onto slides and examined by confocal microscopy. Scale bar = 20 µm

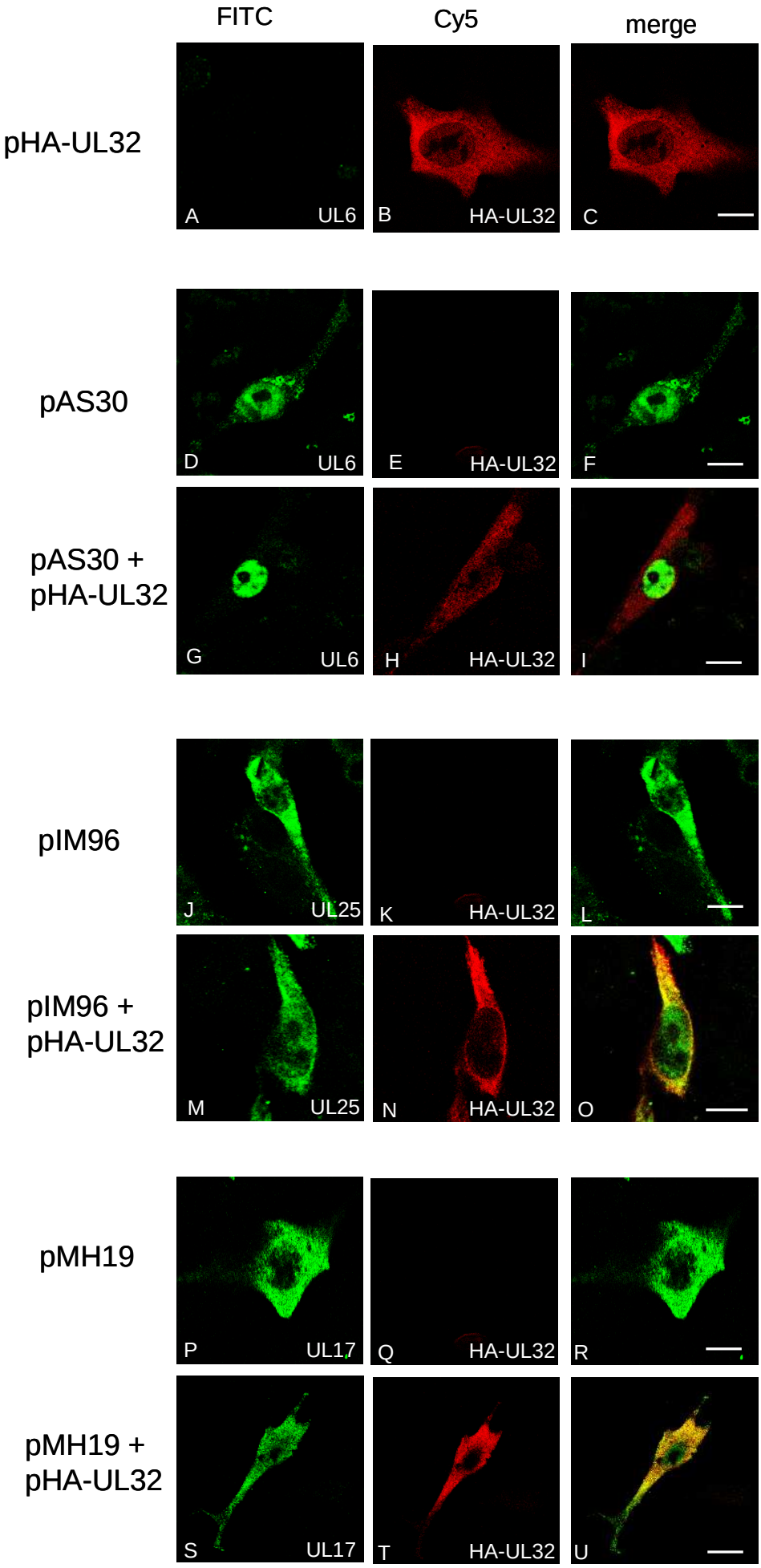
FITC
Cy5
merge
pHA-UL32
A UL6
B HA-UL32
C
pAS30
D UL6
E HA-UL32
F
pAS30 +
pHA-UL32
G UL6
H HA-UL32
I
pIM96
J UL25
K HA-UL32
L
pIM96 +
pHA-UL32
M UL25
N HA-UL32
O
pMH19
P UL17
Q HA-UL32
R
pMH19 +
pHA-UL32
S UL17
T HA-UL32
U

These results suggest that UL32 does not interact with packaging proteins UL6 or UL25 in the absence of other HSV-1 proteins in transfected mammalian cells, although it remains possible that an interaction with UL17 may occur.

5.5.3 Co-immunoprecipitation analysis of UL32 with UL6, UL17 or UL25

Possible interactions of UL32 with these three proteins were also examined using co-immunoprecipitation (co-IP) of recombinant baculovirus-expressed proteins.

5.5.3.1 Immunoprecipitation from baculovirus-infected cells

As no interactions have previously been reported for UL32, I first carried out a co-IP using two DNA packaging proteins with a well-established interaction as a positive control for the assay. For this, baculoviruses AcUL28 and AcUL15 (expressing proteins UL28 and UL15 respectively) were used. *Sf*21 cells were mock infected or infected with 2.5 p.f.u. per cell of each baculovirus alone, or together. Forty-eight hours post-infection cells were harvested and lysed, and insoluble proteins removed by centrifugation (section 2.2.11). An aliquot of each soluble extract was incubated with a rabbit antibody specific to UL28 (R123). Immune complexes were collected by further incubation with protein-A-sepharose followed by centrifugation and extensive washing. Soluble and immunoprecipitated samples were boiled in the presence of SDS and separated on an 8% polyacrylamide gel. The proteins were transferred to PDVF membranes reacted with antibodies specific to UL28 (R123) or UL15 (R605) followed by HRP-conjugated protein-A and detected using the ECL substrate. The resultant blots are shown in figure 5.13.

UL28 was not detected in mock infected cells or those infected with AcUL15 alone, but was expressed in cells receiving either AcUL28 alone, or together with AcUL15 (panel A; lanes 1-4). Similarly, UL15 was absent from cells that were mock infected or infected with only AcUL28, but could be detected in cells receiving AcUL15 both in the presence and absence of UL28 (panel A; lanes 5-8). UL28 was efficiently precipitated from cells infected with AcUL28 by its appropriate antibody (R123) (panel B; lanes 11 and 12). Furthermore, UL15 was co-immunoprecipitated by R123 in cells infected with both baculoviruses (panel B; lane 16). This was dependent on the presence of UL28, as no UL15 was precipitated in cells infected with AcUL15 alone (panel B; lane 14). These results confirm previous published reports that UL15 and UL28 interact in the absence of

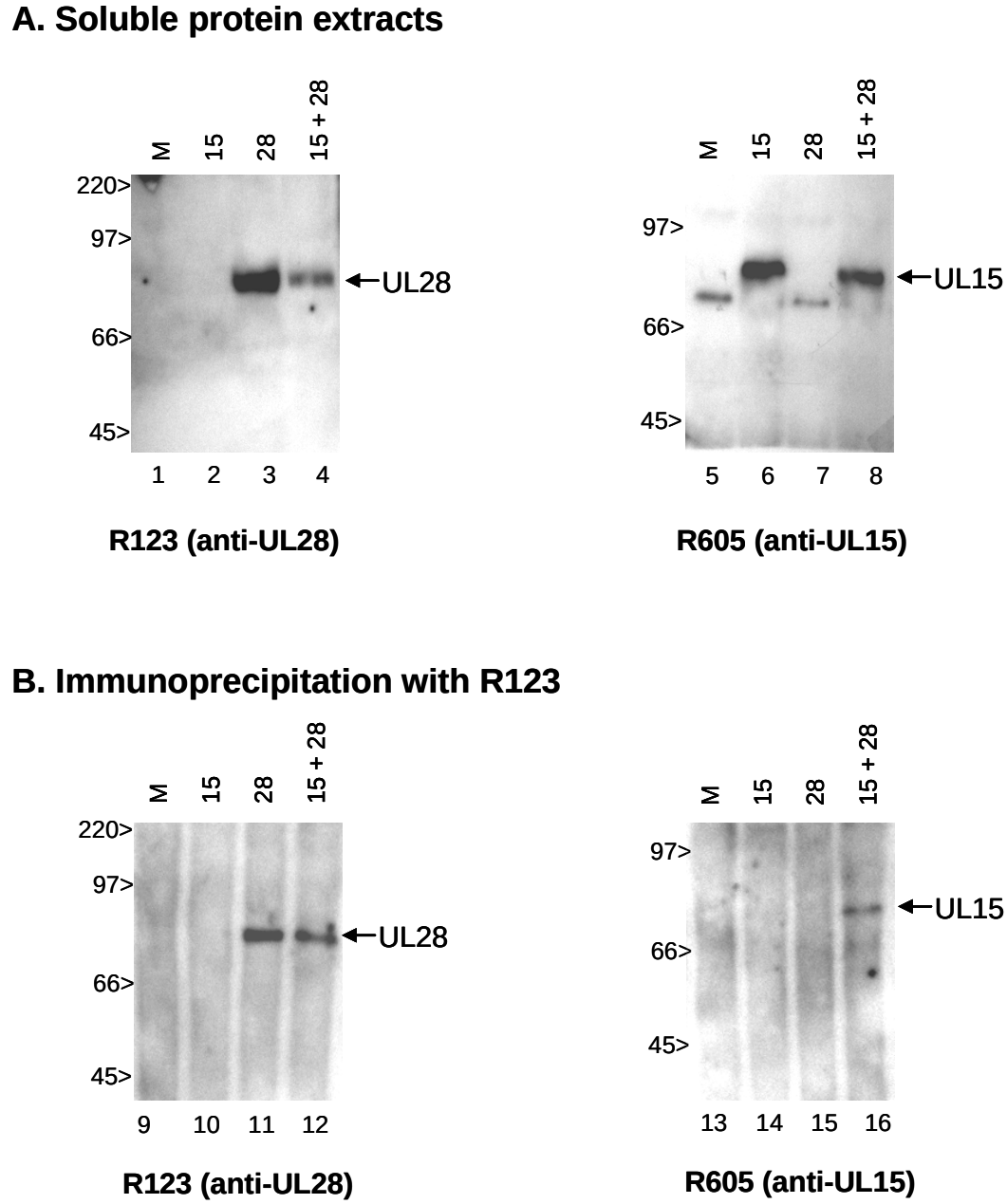

Figure 5.13: Immunoprecipitation of UL28 and UL15 from recombinant baculovirus-infected cells.

A. *Sf*21 cells were mock infected or infected with 2.5 p.f.u./cell of the indicated recombinant baculoviruses. 48 h.p.i., soluble protein extracts were prepared. Samples of these extracts were separated on an 8 % polyacrylamide gel and western blotted. The membranes were incubated with either R123 (anti-UL28; 1:500) (lanes 1-4) or R605 (anti-UL15; 1:500) (lanes 5-8). This was followed by incubation with HRP-conjugate protein-A and detection using (ECL substrate. The positions of size marker proteins are indicated (kDa).

B. Samples of the soluble protein extract were immunoprecipitated with R123 and the immune complexes harvested by incubation with protein-A-sepharose. These immunoprecipitated samples were separated by SDS PAGE and immunoblotted as above with either R123 (lanes 9-12) or R605 (lanes 13-16). The positions of size marker proteins are indicated (kDa).

other proteins (Abbotts *et al.*, 2000) and indicate that this protocol is appropriate for the detection of interaction between baculovirus-expressed proteins.

5.5.3.2 Co-immunoprecipitation of UL32 with UL25, UL17 or UL6

The above assay was then used to investigate whether UL32 interacts with UL25, UL17 or UL6, using the recombinant baculoviruses AcUL17, AcUL25 and AcUL6.

*Sf*21 cells were mock infected or infected with AcUL6, AcUL25 or AcUL17, either alone in the presence of AcUL32. Soluble extracts were prepared 48 h.p.i and an aliquot of each incubated with the appropriate antibody R335, R1218 or R992. The immune complexes were harvested and soluble extracts and immunoprecipitated samples separated by SDS-PAGE and western blotted as above. Membranes were incubated with either R1 (anti-UL32) or R335, R1218 or R992, followed by HRP-conjugated protein-A, and the resultant blots are shown in figure 5.14.

As shown in figure 5.14A, UL25 was expressed in cells infected with AcUL25 alone or in combination with AcUL32 (panel A; lanes 3 and 4). The anti-UL25 antibody R335 successfully precipitated UL25 from these cells (panel A; lanes 7 and 8). UL32 was detected in cells infected with AcUL32 alone, or co-infected with AcUL25 (panel A; lanes 10 and 12). However, UL32 did not co-precipitate with UL25 from cells that were dually infected with AcUL32 and AcUL25 (panel A; lane 16).

Similarly, both UL17 and UL6 could be specifically precipitated from baculovirus infected cells using their cognate antibodies, but not from mock infected cells or those receiving UL32 alone (panels B and C; lanes 1-4). Again, UL32 was not co-precipitated from the dually infected cells (panels B and C; lane 16), although probing of the soluble extracts confirmed that UL32 was efficiently expressed in these cells (panels B and C; lane 12).

In summary, the results of the co-localisation and co-immunoprecipitation experiments provide no evidence for an interaction between UL32 and UL25, UL6 or UL17.

Figure 5.14: Immunoprecipitation of UL32 and UL25, UL17 or UL6 from recombinant baculovirus-infected cells.

*Sf*21 cells were mock infected or infected with 2.5 p.f.u./cell of the indicated recombinant baculoviruses. 48 h.p.i., soluble protein extracts were prepared. Immunoprecipitations were carried out with R335 (A), R1218 (B) or R992 (C) and the immune complexes harvested by incubation with protein-A-sepharose. The soluble extracts and immunoprecipitated samples were separated by electrophoresis on 8 % polyacrylamide gels and western blotted. The membranes were immunoblotted using the antibodies indicated below each filter (all at 1:500 dilution), followed by HRP-conjugated protein-A and detected using ECL substrate. The positions of size marker proteins are indicated (kDa).

A. AcUL32 and AcUL25 – immunoprecipitated with R335

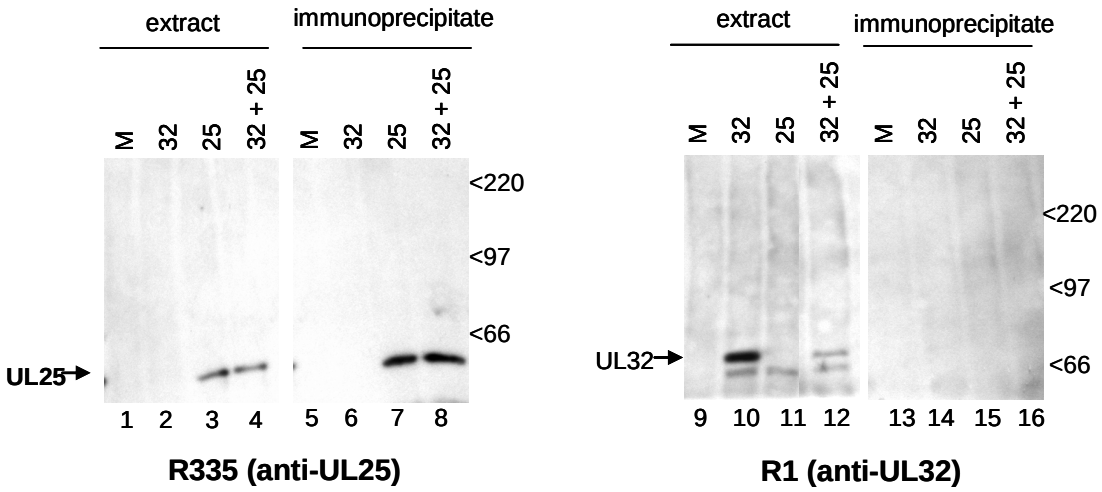

B. AcUL32 and AcUL17 – immunoprecipitated with R1218

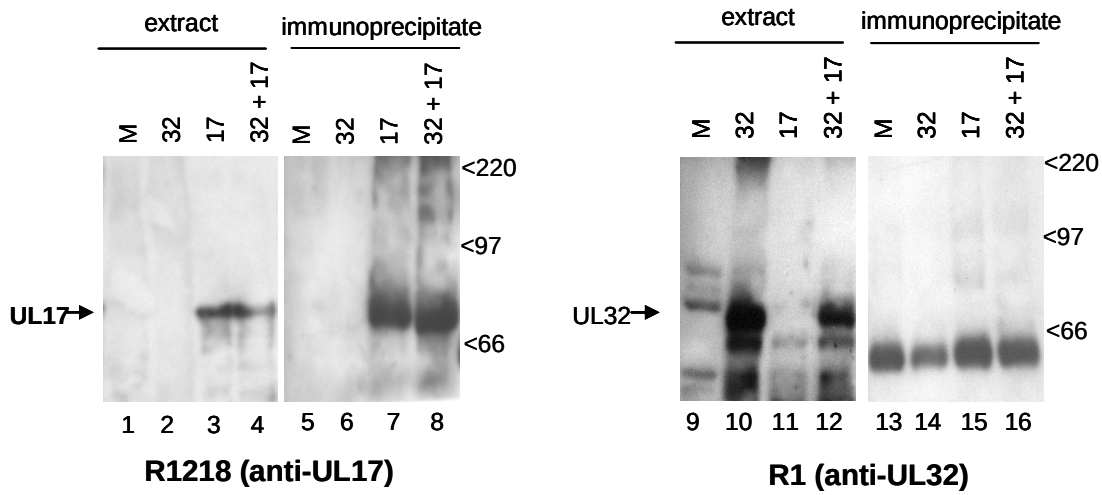

C. AcUL32 and AcUL6 – immunoprecipitated with R992

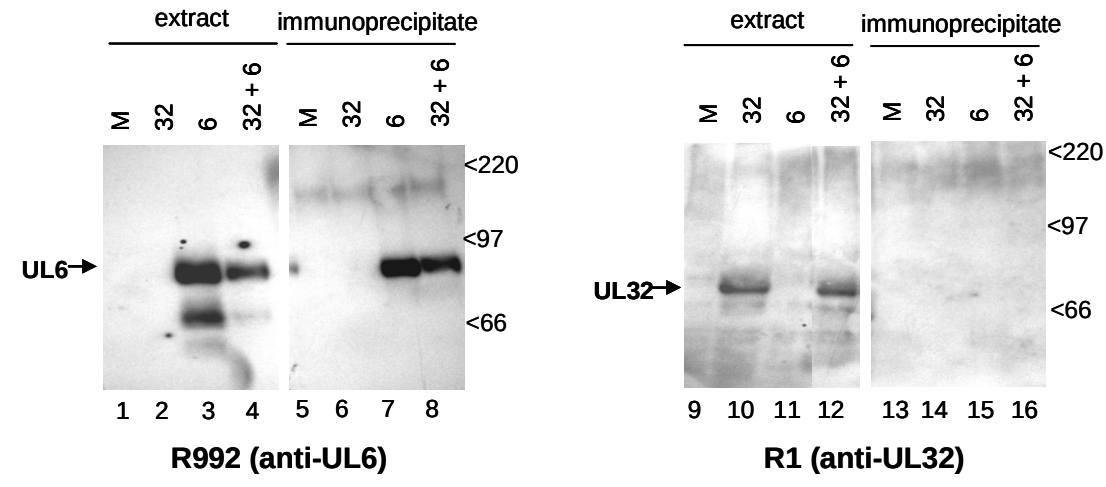

5.6 Investigation of the interaction of UL32 with the terminase components

Similar experiments were next performed to examine whether UL32 could interact with the components of the HSV-1 terminase UL15, UL28 and UL33.

5.6.1 Localisation of the terminase components in infected cells in the absence of UL32

Like the other packaging proteins, the terminase components localise to the replication compartments of infected cells. It has been reported UL15 is essential for the recruitment of UL33 and UL28 to RCs (Higgs *et al.*, 2008; Yang *et al.*, 2007). Firstly, it was investigated whether UL32 might also have any role to play in the correct localisation of these proteins during HSV-1 infection.

Coverslips of BHK cells were infected with 5 p.f.u. per cell wt HSV-1 or *hr*64. Six hours post infection, cells were fixed, permeabilised and blocked. Coverslips were incubated with M7381 to detect ICP8 along with R605 (anti-UL15), R123 (anti-UL28) or R148 (anti-UL33) rabbit antibodies. This was followed by incubation with r-FITC and m-Cy5 and examination of the cells by confocal microscopy. Images are shown in figure 5.15.

In each infection with either wt HSV-1 or *hr*64, ICP8 staining was visible in the nucleus, confirming efficient infection and that replication compartments had formed (images B, E, H, K, N and Q). In agreement with published results, UL15, UL33 and UL28 all predominantly localised to the nuclei of wt HSV-1 infected cells (images A, G and M). In all instances, this staining co-localised with ICP8 (images C, I and O). In the *hr*64 infected cells, the localisation of UL15, UL33 and UL28 was essentially unchanged, colocalising with ICP8 in RCs within the nuclei (images D and F; J and L; P and R). This suggests that UL32 is not involved in the localisation of the terminase components UL15, UL33 and UL28 in infected cells.

Figure 5.15: UL32 does not affect the localisation of terminase subunits UL15, UL33 or UL28 in HSV-1 infected cells.

Coverslips of BHK cells were infected with 5 p.f.u./cell wt HSV-1 or *hr*64 for 6 hours. Cells were fixed and permeabilised and incubated with anti-ICP8 (M7381) along with either R605 (anti-UL15; 1:500), R148 (anti-UL33; 1:200) or R123 (anti-UL28; 1:500) antibodies. This was followed by r-FITC and m-Cy5 antibodies. The cells were examined by confocal microscopy. Scale bar = 20 µm.

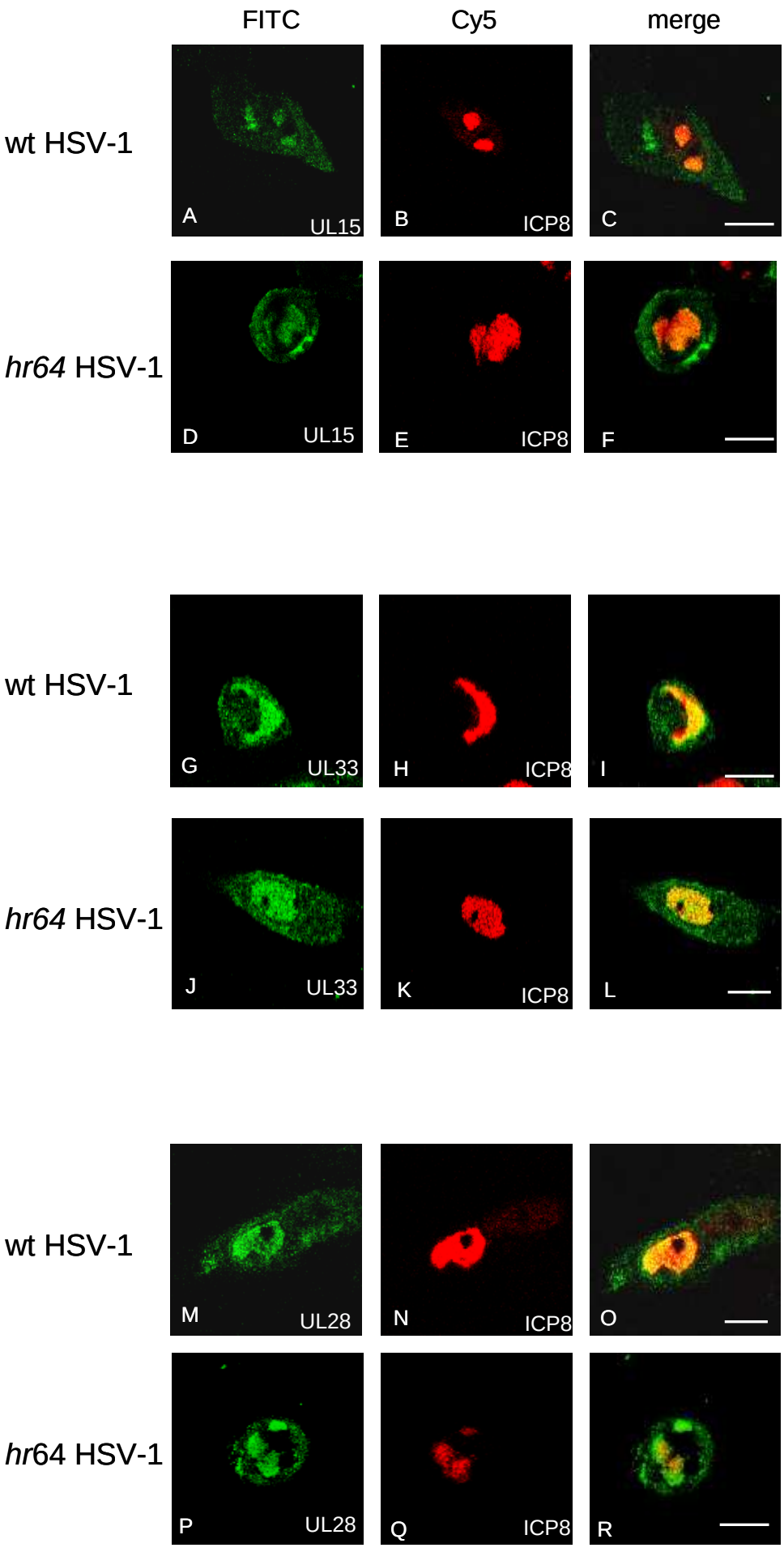
FITC
Cy5
merge
wt HSV-1
A
UL15
B
ICP8
C
hr64 HSV-1
D
UL15
E
ICP8
F
wt HSV-1
G
UL33
H
ICP8
I
hr64 HSV-1
J
UL33
K
ICP8
L
wt HSV-1
M
UL28
N
ICP8
O
hr64 HSV-1
P
UL28
Q
ICP8
R

5.6.2 Co-immunoprecipitation analysis of UL32 and the terminase components

To investigate whether UL32 could interact with any of the terminase components in the absence of other proteins, immunoprecipitations from baculovirus infected cells were carried out.

*Sf*21 cells were co-infected with AcUL32 and baculoviruses expressing UL15 (AcUL15), UL33 (AcUL33) or UL28 (AcUL28). Forty-eight hours post infection, cells were lysed and soluble protein extracts prepared. Extracts were immunoprecipitated using the appropriate rabbit antibody recognising UL28 (R123), UL15 (R605) or UL33 (R148). Immune complexes were collected by incubation with protein-A-sepharose and the soluble extracts and immunoprecipitated proteins separated by electrophoresis on 8% polyacrylamide gels (or 15% gels for the UL33 samples) and western blotted. Duplicate membranes were probed with anti-UL32 antibody (R1) and R123, R605 or R148 as appropriate.

As shown in figure 5.16, UL33 was expressed in cells infected with AcUL33 alone or dually infected with AcUL32, but could not be detected in cells that were mock infected or infected with only AcUL32 (panel A; lanes 1-4). UL32 was detected only in cells infected with AcUL32 alone or in combination with AcUL33 (panel A; lanes 10-12). The anti-UL33 antibody R148 successfully precipitated UL33 from cells in which this protein was expressed (panel A; lanes 7 and 8). However, UL32 was not co-precipitated from the cells that were dually infected with AcUL32 and AcUL33 (panel A; lane 16).

Similarly, both UL15 and UL28 could be specifically precipitated from baculovirus infected cells using their cognate antibodies, but not from mock infected cells or those receiving UL32 alone (panels B and C; lanes 5-8). Again, UL32 was not co-precipitated from the dually infected cells (panels B and C; lane 16), even though the soluble extracts confirm that UL32 was efficiently expressed in these cells (panels B and C; lane 12).

These results suggest that UL32 does not interact with the indicated proteins of the terminase complex in recombinant baculovirus-infected cells.

Figure 5.16: Immunoprecipitation of UL32 and UL33, UL15 or UL28 from baculovirus-infected cells.

*Sf*21 cells were mock infected or infected with 2.5 p.f.u./cell of the indicated recombinant baculoviruses. 48 h.p.i., soluble protein extracts were prepared. Immunoprecipitations were carried out by incubation with R148 (A), R605 (B) or R123 (C) and the immune complexes harvested by incubation with protein-A-sepharose. The soluble extracts and immunoprecipitated samples were separated on 8% or 15% polyacrylamide gels and western blotted. The membranes were immunoblotted using the antibodies indicated below each filter (all at 1:500 dilution), followed by HRP-conjugate protein-A and detected using ECL substrate. The positions of size marker proteins are indicated (kDa).

A. AcUL32 and AcUL33 – immunoprecipitated with R148

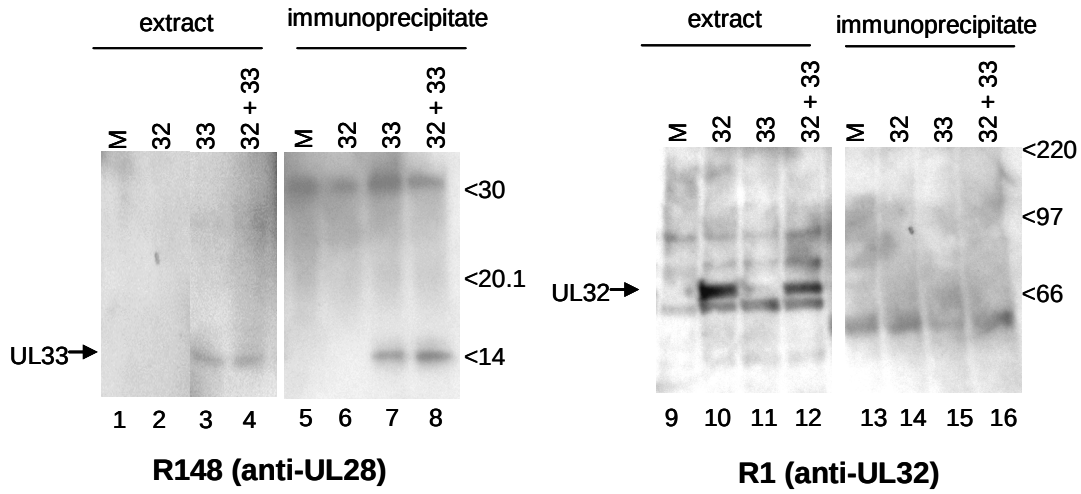

B. AcUL32 and AcUL15 – immunoprecipitated with R605

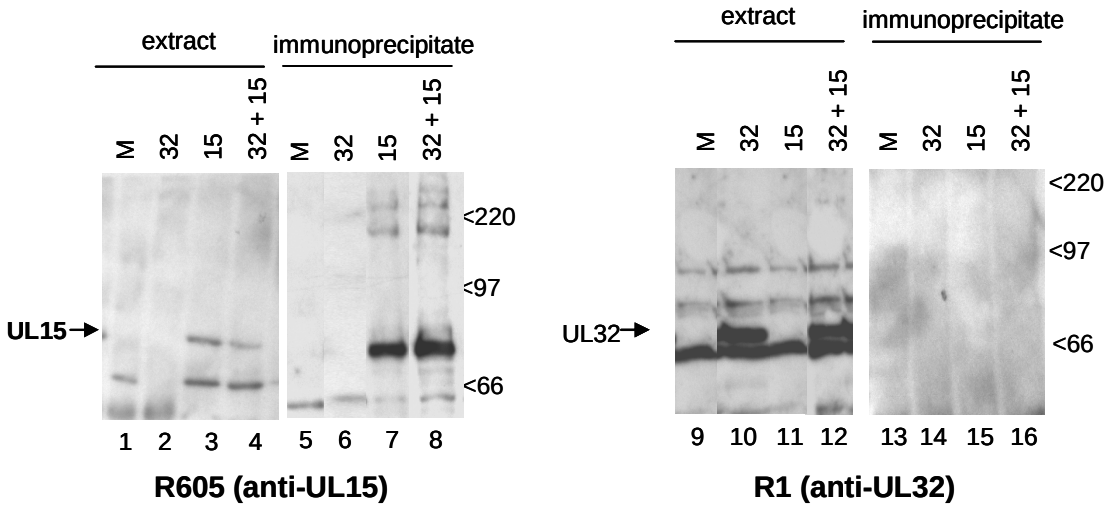

C. AcUL32 and AcUL28 – immunoprecipitated with R123

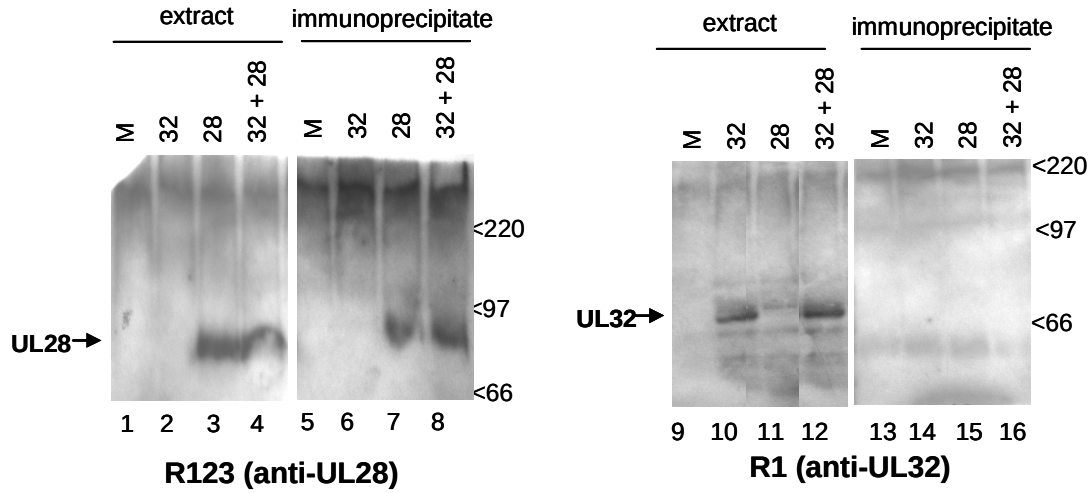

5.6.3 Immunofluorescence analysis of the interaction of wt UL32 and the terminase components in transfected cells

Finally the ability of UL32 to interact with the terminase components both individually and together was analysed by immunofluorescence using co-transfection assays.

5.6.3.1 Co-transfections with single terminase components

Coverslips of BHK cells were transfected as described in section 5.5.2 with pUL33 or pUL28 (encoding the UL33 and UL28 proteins respectively) either alone or in conjunction with pHA-UL32. Coverslips were fixed and permeabilised and incubated with F-7 along with R148 or R123, followed by FITC and Cy5-coupled secondary antibodies as before. The images from confocal microscopy are shown in figure 5.17.

As previously noted, HA-UL32 localised entirely to the cytoplasm of cells when transfected alone (images A-C). In contrast, UL33 was localised throughout the cell, both in the cytoplasm and nucleus when expressed alone (images D-F). In cells transfected with plasmids expressing both proteins, UL33 was again detected throughout the cell, whereas HA-UL32 remained within the cytoplasm (images G-I). Therefore, UL33 does not appear able to transport UL32 into the nucleus; however, this may not be significant if the presence of UL33 in the nucleus is simply a result of its ability to diffuse into the nucleus due to its small size.

UL28 showed a cytoplasmic localisation when transfected alone, similar to that seen with HA-UL32 alone (images J-L). It is difficult to interpret the result from the co-transfected cells, as both proteins remained in the cytoplasm (images M, N and O).

To investigate the interaction of UL32 with UL15, BHK coverslips were similarly transfected with pJM9 (encoding UL15) along with pHA-UL32 and processed as above. Coverslips were incubated with F-7 and R605, followed by r-FITC and m-Cy5 secondary antibodies. The images are shown in figure 5.18.

As in previous experiments, when expressed alone HA-UL32 localised in the cytoplasm of transfected cells (images A-C). UL15 was detected exclusively in the nuclei of cells when

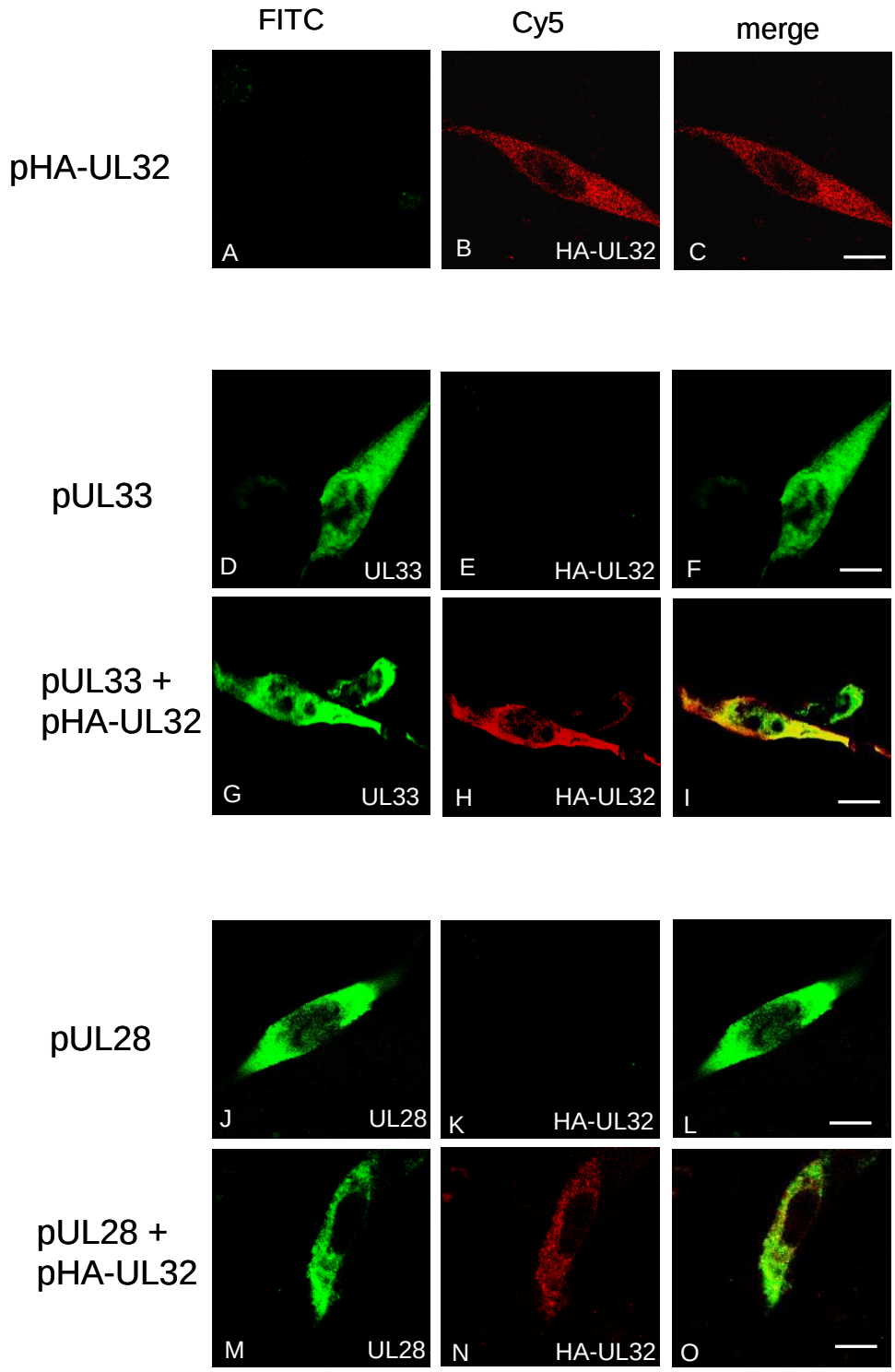

Figure 5.17: Interaction of HA-UL32 with terminase proteins UL33 and UL28 in transfected cells.

BHK cells on coverslips were transfected with 0.5 µg of the indicated plasmids using Lipofectamine 2000. 18 hours post transfection, cells were fixed and permeabilised and incubated with either R148 (anti-UL33) or R123 (anti-UL28) along F-7 (anti-HA) antibodies. This was followed by incubation with r-FITC and m-Cy5. Cells were mounted onto slides and examined by confocal microscopy. Scale bar = 20 µm.

transfected alone, in agreement with published data (Koslowski *et al.*, 1999). When the two proteins were expressed together, the results varied considerably. A small proportion of the cells (approximately 10%) showed the staining pattern seen in figure 5.18 panel 2, where UL15 remained in the nucleus (image G) and HA-UL32 was predominantly in the cytoplasm (image H). However the majority of the cells (approximately 60%) showed patterns similar to panel 3. In these cells, the UL15 staining remained within the nucleus (image J), whereas HA-UL32 was partially relocalised into the nucleus where it appeared to co-localise with UL15 (images K and L). Approximately 20% of cells showed complete recruitment of HA-UL32 to the nucleus, where it co-stained with the UL15 signal as shown in figure 5.18 panel 4 (images M-O). Figure 5.18 panel 5 shows the staining pattern seen in the small remainder of the cells, where HA-UL32 remained throughout the cytoplasm (image Q), while UL15 also appeared to be retained in the cytoplasm where it extensively co-localised with the HA-UL32 protein (images P and R).

To exclude the possibility that the partial colocalisation seen between HA-UL32 and UL15 might be due to some unexpected effect of the HA tag, the co-transfections were repeated using a tagged form of UL15 and untagged pUL32. The plasmid pJM19 encodes UL15 tagged with the pp65 epitope at the C-terminus, allowing the localisation of UL15 to be detected using an anti-pp65 antibody. Coverslips of BHK cells were transfected with pUL32 and pJM19 and processed as before. Coverslips were incubated with R1 and a mouse anti-pp65 antibody (1:500) followed by FITC and Cy5 conjugated secondary antibodies. The results are shown in figure 5.19.

As can be seen in panel 1, the pp65 tag did not affect the localisation of UL15, as UL15-pp65 was still detected solely in the nuclei of cells when transfected alone (images A-C). UL32 was detected in the cytoplasm of cells, as previously noted (images D-F). When cells were co-transfected with both plasmids, there was again a variation seen in the localisation of the proteins. In a small proportion of cells, no interaction was apparent between the two proteins with UL32 remaining in the cytoplasm and UL15-pp65 in the nucleus, as shown in figure 5.19 panel 2 (images G-I). Approximately 20-30% of cells showed the pattern represented in figure 5.19 panel 3, where UL15-pp65 remained in the nucleus, whereas UL32 was distributed throughout the cell. As with the previous transfections using HA-UL32 and UL15, the majority of the cells showed some degree of nuclear colocalisation of the two proteins. Approximately 70% of cells showed patterns similar to panels 4 and 5. In these cases, UL15-pp65 was localised in the nuclei of cells (images N and Q) with UL32

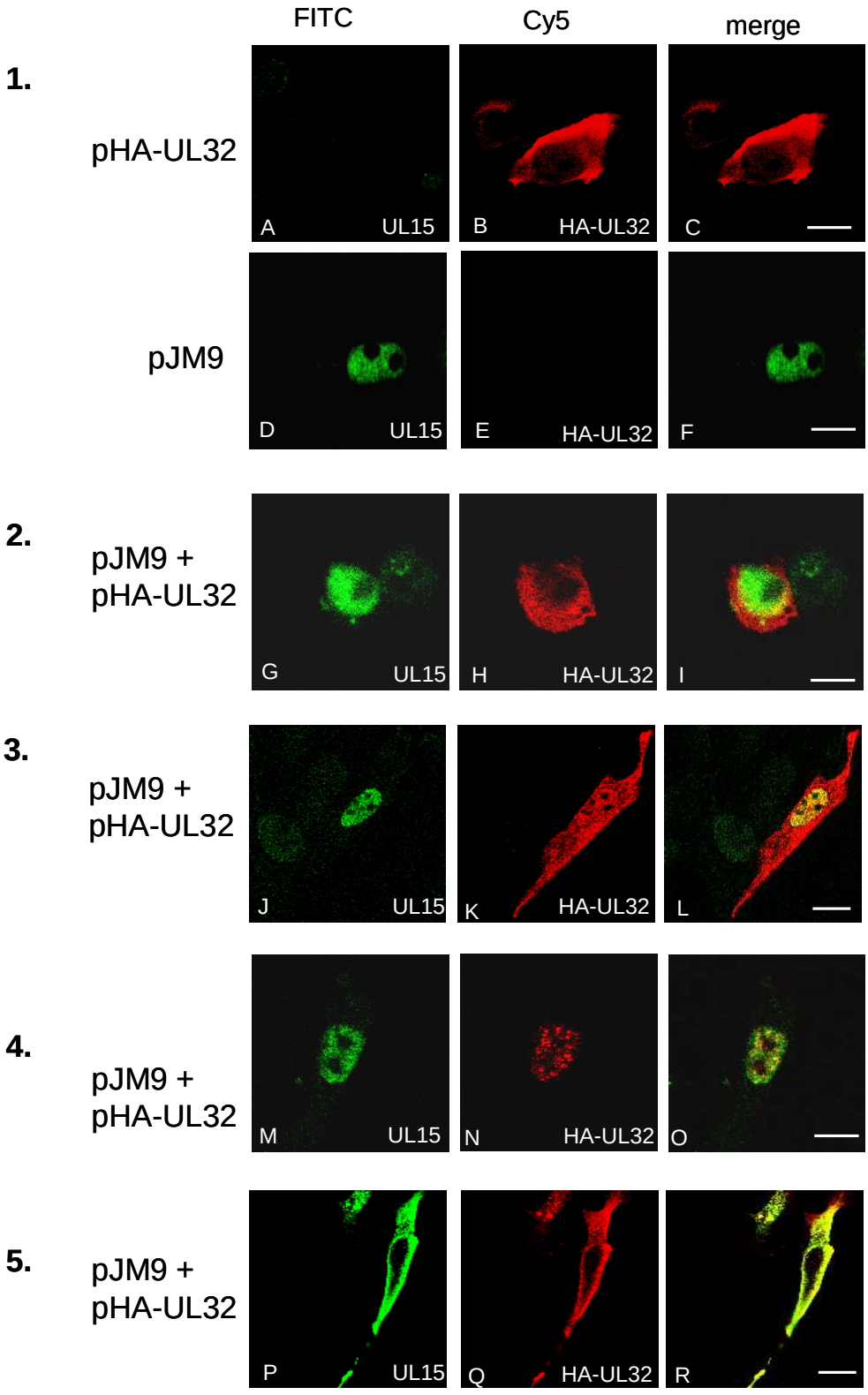

Figure 5.18: Interaction of HA-UL32 with UL15 in transfected cells.

BHK cells on coverslips were transfected with 0.5 µg of either pHA-UL32 or pJM9 or the two plasmids together using Lipofectamine 2000. 18 hours post transfection, cells were fixed and permeabilised and incubated with R605 (rabbit anti-UL15; 1:500) along with F-7 (mouse anti-HA; 1:500). This was followed by incubation with r-FITC and m-Cy5. Cells were mounted onto slides and examined by confocal microscopy. Scale bar = 20 µm.

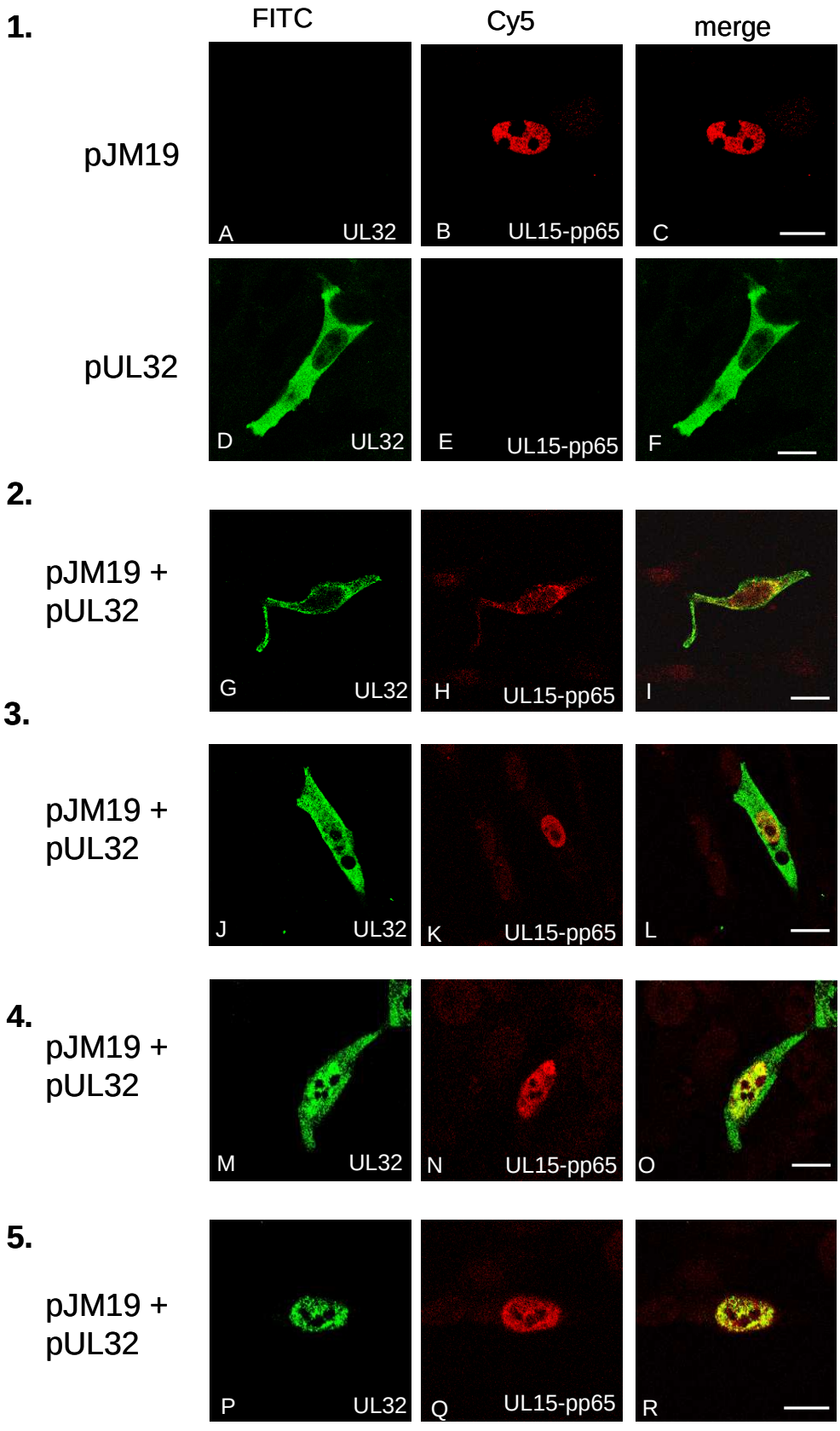

Figure 5.19: Interaction of UL32 with UL15-pp65 in transfected cells.

BHK cells on coverslips were transfected with 0.5 µg of either pUL32 or pJM19 (1) or the two plasmids together (2-5) using Lipofectamine 2000. 18 hours post transfection, cells were fixed and permeabilised and incubated with R1 (1:500) along with mouse anti-pp65 antibody (1:500). This was followed by incubation with r-FITC and m-Cy5. Scale bar = 20 µm.

either predominantly or completely relocalised to the nuclei (images M and P). When in the nucleus, UL32 co-localised extensively with the UL15-pp65 signal (images O and R).

These data confirm that the colocalisation of HA-UL32 and UL15 was not an artefact of the tags added to the proteins and suggest that there is some form of interaction between UL32 and UL15 in co-transfected cells. This interaction was not seen in all cells, and so it could be that other proteins are required to strengthen or stabilise the interaction between the two proteins.

5.6.3.2 Colocalisation of UL32 with the terminase in transfected cells

As UL15 is already known to be a component of the terminase along with UL28 and UL33, it was next examined whether UL32 could interact with the terminase complex and whether the presence of the other terminase proteins might influence its localisation.

Firstly, BHK cells were co-transfected with pUL33, pJM19 and pUL28-GFP (encoding the UL28 protein with a GFP tag inserted at the N-terminus) in the absence of UL32, to confirm that these proteins did indeed form a complex within the nucleus. Cells were processed as above and coverslips incubated with R148 (anti-UL33) and anti-pp65. This was followed by incubation with AlexaFluor antibodies A21428 (555-goat anti rabbit IgG; 1:1000) and A21050 (633-goat anti-mouse IgG; 1:1000). These were analysed by confocal microscopy using the laser wavelengths FITC (to detect UL28-GFP), Cy5 (to detect 633) and TRITC (to detect 555). A representative image is shown in figure 5.20 panel A.

UL28-GFP, UL15-pp65 and UL33 all completely co-localised in the nuclei of co-transfected cells (images A-D). This was observed consistently and it should be noted that in every cell where UL28 was relocalised to the nucleus by UL15, UL33 was also found in the nucleus. This confirms that the three proteins successfully form a complex which localises to the nuclei of cells. In the following experiments, four plasmids were co-transfected but only three of the proteins could be detected at any one time. Therefore, the localisation of UL33 was not examined, and the presence of both UL15-pp65 and UL28-GFP in the nucleus was taken to indicate that the terminase complex had been correctly formed and translocated to the nucleus of these cells.

The effect of all three terminase components together on the localisation of UL32 was then examined. Cells were transfected as above with pUL28-GFP, pJM19 and pUL33 along

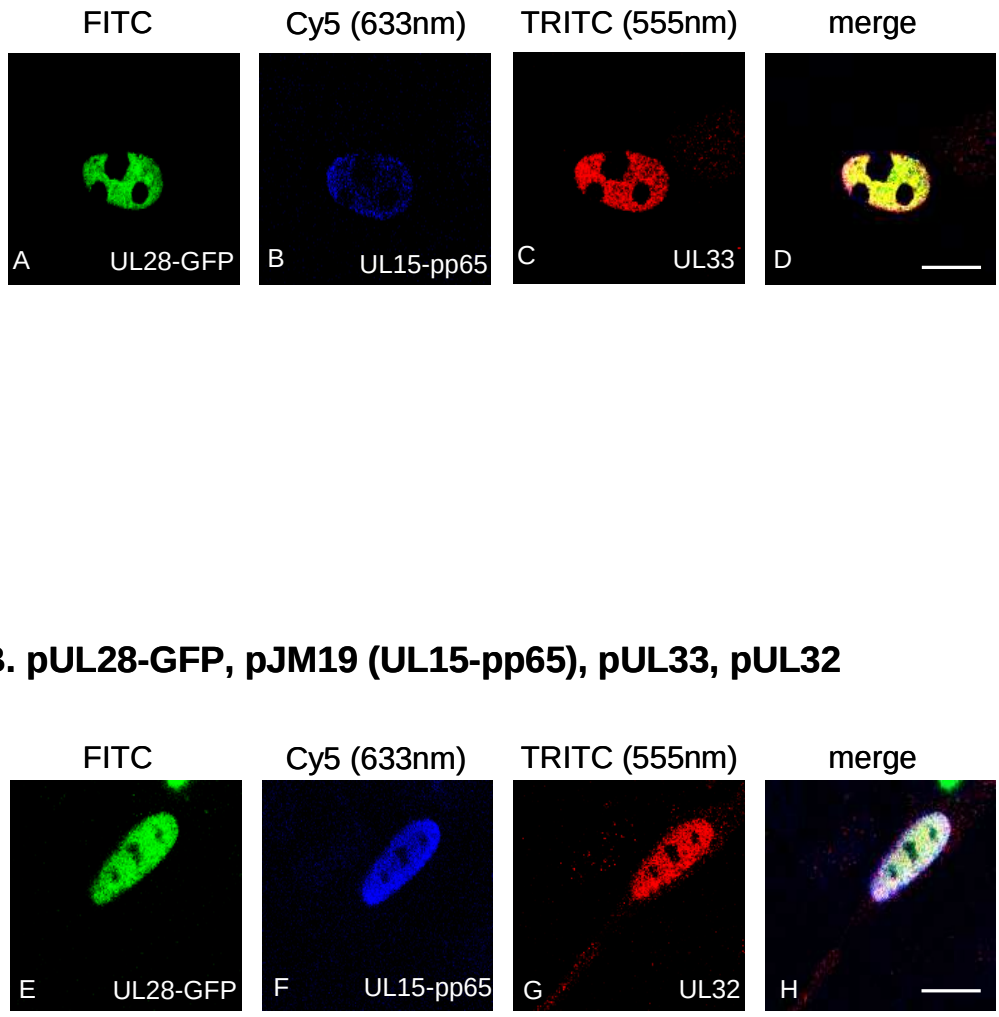

Figure 5.20: Interaction of UL32 with the putative terminase in transfected cells.

A. Coverslips of BHK cells were transfected with 0.5 µg pUL28-GFP, pJM19 and pUL33 using Lipofectamine 2000. Cells were fixed and permeabilised and incubated with mouse anti-pp65 and R148 (anti-UL33) antibodies followed by A21428 (AlexaFluor 555 goat anti-rabbit IgG; 1:1000) and A21050 (AlexaFluor 633 goat anti-mouse 633; 1:1000). Note the different colour for the Cy5 channel to that used in previous figures

B. BHK cells were transfected with 0.5 µg pUL28-GFP, pJM19 and pUL33 along with pUL32. Cells were fixed and permeabilised and incubated with anti-pp65 and R1 (anti-UL32) antibodies, followed by the secondary antibodies specified above. Scale bar = 10 µm.

with pUL32. They were incubated with anti-pp65 and R1, followed by A21428 and A21050 secondary antibodies. A representative result typical of virtually every cell expressing these proteins is shown in figure 5.20 panel B. In these cells, UL32 was completely relocalised to the nucleus (image G) where it co-localised with the UL28-GFP and UL15-pp65 staining (image H). This result suggests that UL32 can interact with the terminase complex resulting in its direction to the nucleus of transfected cells.

5.6.3.3 Which components of the terminase are essential for this interaction?

As the co-transfection of UL32 with all three terminase components resulted in the complete relocalisation of UL32 to the nucleus but co-transfection with UL15 alone resulting in only partial re-localisation of UL32, I next decided to determine which of the terminase components are essential for the complete nuclear relocalisation of UL32. These experiments were carried out by transfecting BHK cells with 0.5 µg each of plasmids pUL28-GFP, pUL33, pHA-UL32 and pJM19 in various combinations. Cells were processed as above and incubated with rabbit antibodies either recognising UL33 (R148) or UL32 (R1) along with either F-7 (mouse anti-HA) or mouse anti-pp65 antibodies as appropriate. This was followed by incubation with A21428 and A21050.

As seen in figure 5.21, transfection of pUL28-GFP, pJM19 and pUL32 resulted in all three of these proteins colocalising in the nucleus of cells (images A-D). This pattern was observed in all cells. In the absence of UL15, both UL28-GFP and UL33 were distributed throughout the cell (images E and G). This is consistent with UL33 and UL28 interacting directly, with UL15 required for the complete relocalisation of the proteins to the nucleus (Beard *et al.*, 2002; Koslowski *et al.*, 1999; Yang *et al.*, 2007). UL32 was found solely in the cytoplasm of these cells (image F). In cells co-transfected with pUL33-GFP, pJM19 and pHA-UL32, UL15 was entirely nuclear and UL33 was largely localised in the nucleus, probably by virtue of its interaction with UL15 (images I and J). In addition, UL32 was partially relocalised to the nucleus, with a small portion remaining in the cytoplasm (image K), similar to the predominant phenotype observed upon co-transfection of just UL15 and UL32 (figure 5.18).

Together these results confirm the observations made in section 5.6.3.1 that UL15 can influence the localisation of UL32, and indicate that UL15 is essential for the partial re-localisation to the nucleus. UL28 also plays an important role since its inclusion increases

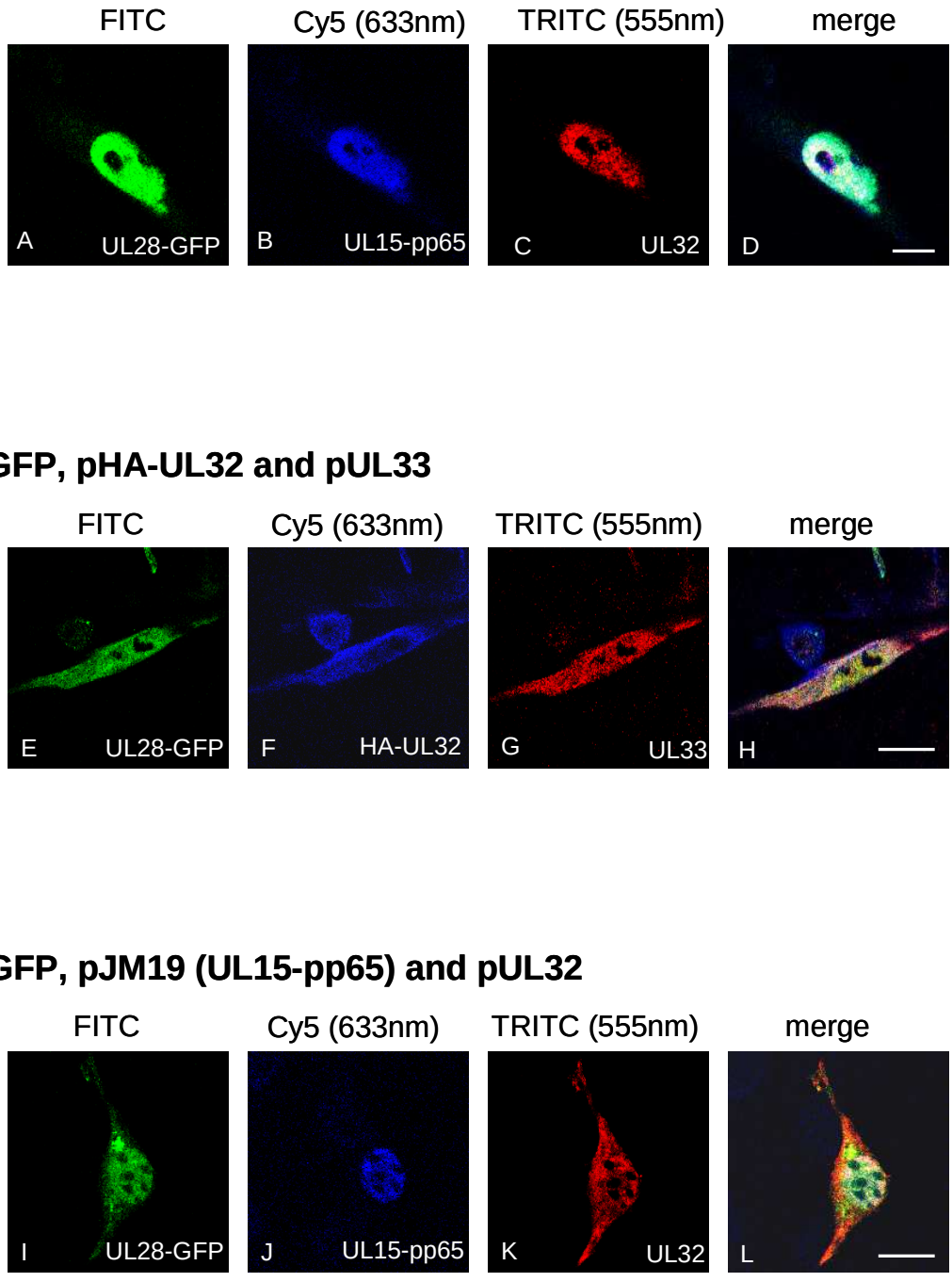

Figure 5.21: Localisation of the terminase proteins and UL32 in transfected cells.

BHK cells were transfected with the indicated plasmids using Lipofectamine 2000. 18 hours post transfection cells were fixed and permeabilised and incubated with primary antibodies anti-pp65, R1, F-7 (anti-HA) and R148 (anti-UL33) as appropriate. This was followed by incubation with AlexaFluor antibodies A21428 and A21050. Scale bar = 20 µm.

the efficiency of nuclear uptake of UL32. UL33 appears to have little effect on this process.

5.6.4 Interaction of mutated UL32 proteins with the terminase in transfected cells

The experiment described in section 5.6.3.2 was next used to investigate whether the insertional or site-specific mutants generated in section 4 interacted with the terminase in transfected cells. To do this, cells were transfected as above with 0.5 µg each of pUL28-GFP, pJM19 and pUL33 along with one of the UL32 mutants. Cells were processed and incubated with antibodies as in section 5.6.3.2 to detect the localisation of UL15-pp65 and the mutated UL32 proteins along with UL28-GFP. Images showing a selection of the UL32 mutants are presented in figure 5.22. When transfected alone each of these insertional mutants showed a cytoplasmic localisation, as reported in section 4.2.5 and figure 4.10. In the text below, those mutants that showed a positive result in the complementation yield and packaging assays in section 4 have been underlined.

Fifteen of the mutant UL32 proteins exhibited a phenotype similar to that of wt UL32, as represented by in302 and in95, with UL32 almost completely relocalised to the nucleus along with the terminase components. These were mutants in5, in12, in67, in93, in95, in187, in220, in232, in302, in332, in377, in378 and in475. This group also included the non-functional mutants in338 and in398 (also shown in figure 5.22). Eleven mutants showed an intermediate phenotype, with some UL32 detected in the nucleus but a portion remaining in the cytoplasm, as represented by in136, in155 and in558. These also included mutant proteins in55, in309, in328, in376, in414, in449, in494 and in498. Eleven insertional mutants were not affected by co-transfection with the terminase proteins and remained entirely cytoplasmic, suggesting that they did not interact with the terminase proteins. This phenotype is represented by in40 and in177 in figure 5.22, and also included mutants in198, in407, in435, in486, in490, in512, in572, in580 and in592.

The site-specific mutants were similarly analysed for their ability to interact with the terminase components in this assay. As can be seen in figure 5.22, UL32CxxC1 largely remained within the cytoplasm, whereas both UL32CxxC2 and UL32CxxxC3 were almost completely and partially relocalised to the nucleus, respectively. The mutant deleted at the extreme C-terminus, UL32ΔC, also showed partial nuclear co-localisation with the terminase.

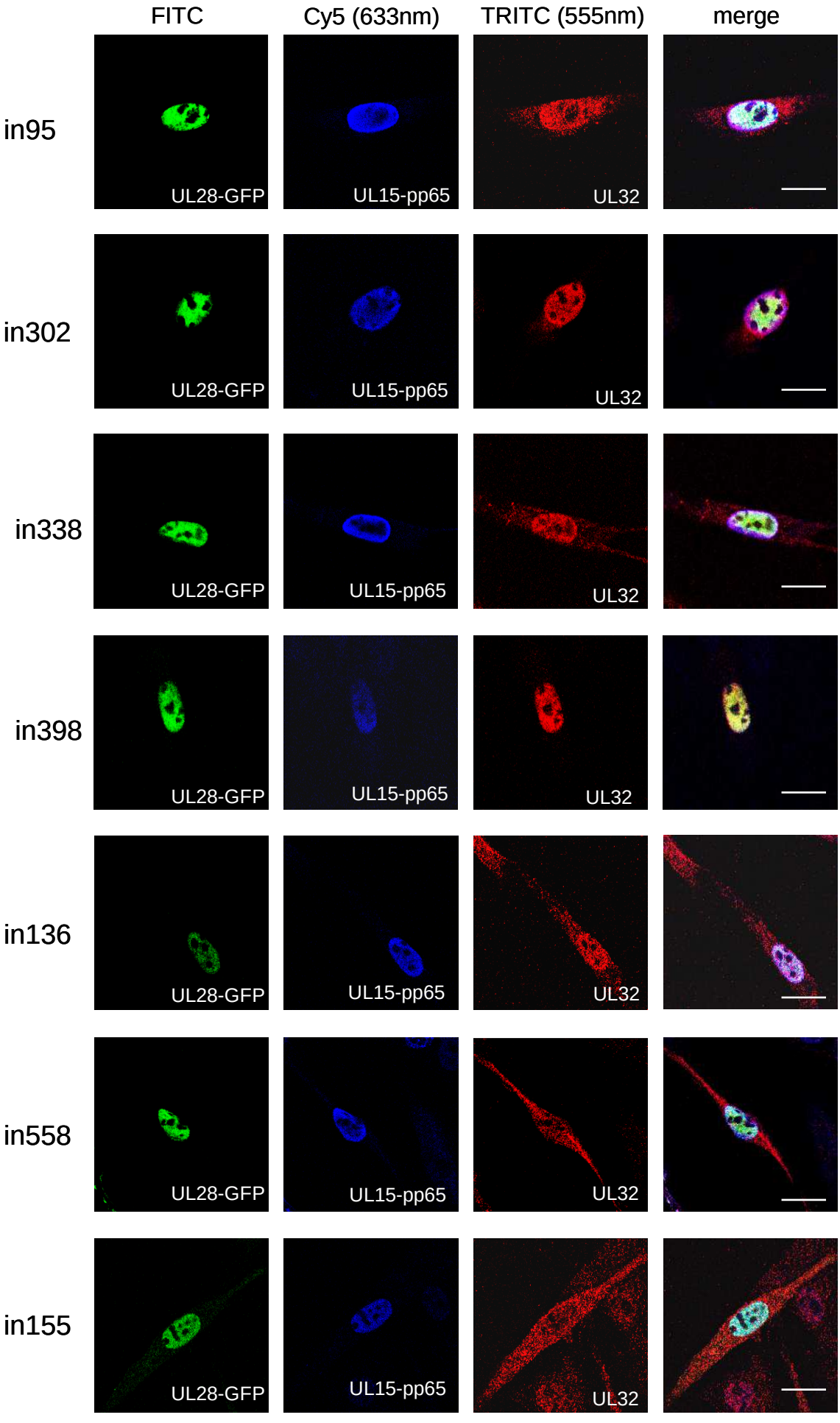
FITC
Cy5 (633nm)
TRITC (555nm)
merge
in95
in302
in338
in398
in136
in558
in155
UL28-GFP
UL15-pp65
UL32

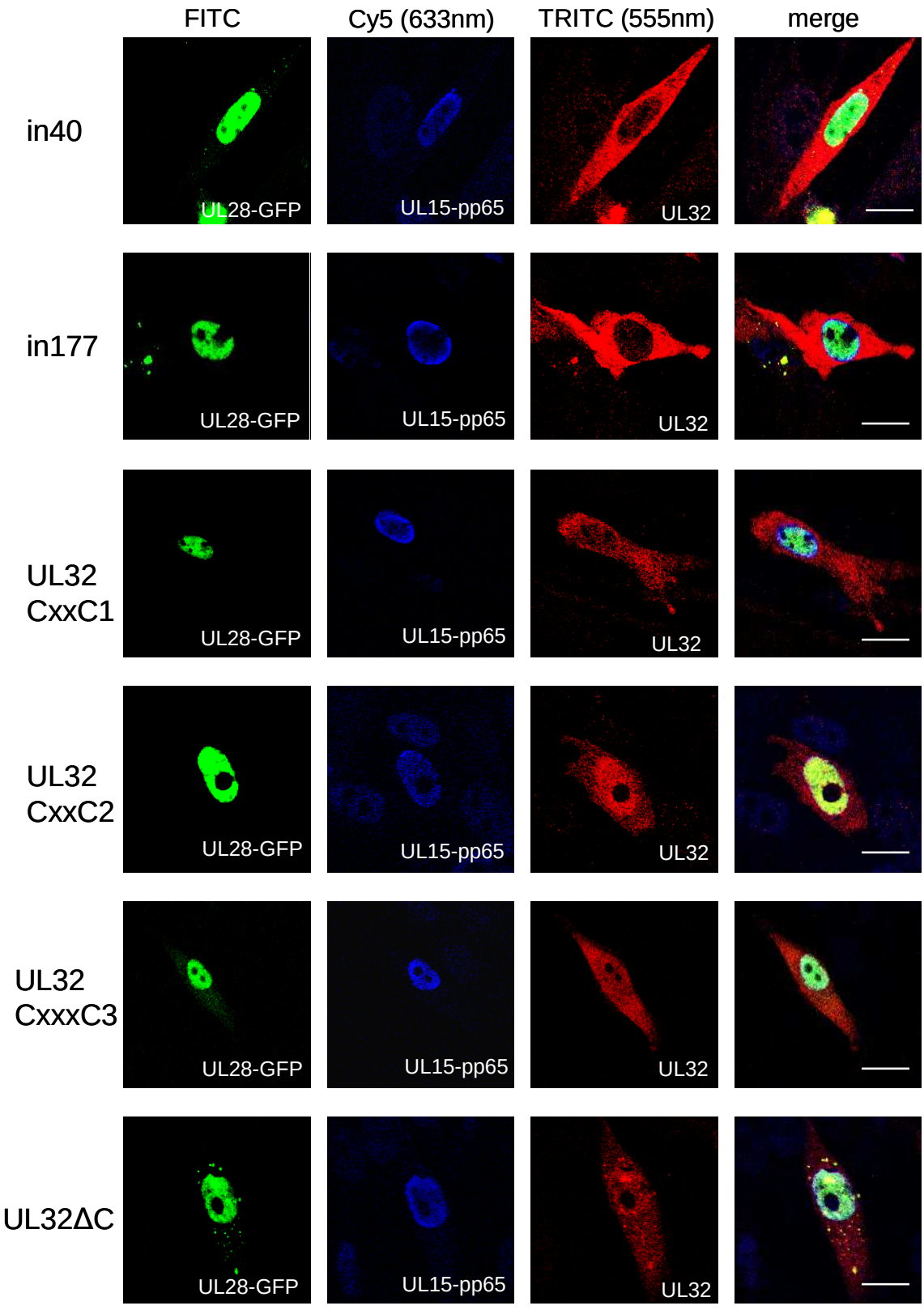

Figure 5.22: Interaction of UL32 mutants with the putative terminase in transfected cells.

BHK cells on coverslips were transfected with 0.5 µg pUL28-GFP, pJM19, pUL33 and the indicated UL32 mutant plasmids using Lipofectamine 2000 and processed as in the legend to figure 5.19 B. Scale bar = 20 µm.

Comparison of these results with the functional characterisation of these proteins carried out in sections 4.3 and 4.4 revealed that each of the mutants that could support the growth and DNA packaging of *hr*64 co-localised either partially or completely with the terminase components in this assay. However, there was variation in the localisation of the non-functional mutant proteins, with two still showing significant colocalisation with the terminase, nine showing partial colocalisation and the remaining eleven being unaffected in their localisation.

5.7 Discussion

This chapter describes the investigation of potential interactions between UL32 and various other HSV-1 DNA packaging proteins.

Many HSV-1 processes occur within replication compartments (RCs) in the cell nucleus, including DNA replication, late gene transcription and the cleavage and packaging of viral DNA. Many of the HSV-1 cleavage and packaging proteins, as well as HSV-1 capsids have previously been reported to localise to the RCs during HSV-1 infection. A single report had additionally proposed that UL32 is essential for the correct localisation of capsids to RCs (Lamberti & Weller, 1998). I therefore attempted to repeat these experiments but found that the presence or absence of UL32 had no effect on the localisation of capsids or capsid proteins VP19C or VP5.

To further investigate the localisation and interactions of UL32, an HA-tagged UL32 gene was constructed allowing expression both from a transfected plasmid and a recombinant HSV-1 virus. The HA tag, consisting of nine amino acids from influenza haemagglutinin, was added near to the N-terminus of UL32 to avoid disruption of the highly conserved C-terminus. Due to the overlapping arrangement of the UL32 and UL33 genes in HSV-1, the HA tag was inserted between the second and third codons of UL32 so that UL33 would also remain intact and its translation should be unaffected when the tag was introduced into virus. Functional analysis of both the plasmid, pHA-UL32, and the virus, HA32EP, confirmed that addition of the HA tag at the N-terminus of UL32 did not affect the ability of the protein to support viral growth and DNA packaging.

As previously discussed, there have been conflicting reports of the localisation of UL32 in infected cells, with different groups finding UL32 localised either entirely within the cytoplasm (Chang *et al.*, 1996) or predominantly cytoplasmic with a portion localising to RCs within the nucleus (Lamberti & Weller, 1998). This reported localisation is somewhat surprising given the known role of UL32 in DNA packaging and led Lamberti and Weller to suggest that UL32 may have an alternative/additional function. The UL32 homologue in HCMV, UL52, has been found to have a exhibit yet another pattern, being present within the nuclei of infected cells, but surrounding the replication compartments and not co-localising with them (Borst *et al.*, 2008).

My analysis using the HA-tagged UL32 protein expressed by the virus HA32EP demonstrated that HA-UL32 was localised entirely in the nuclei of infected cells at 6 hours post infection, where it co-localised with ICP8 in RCs. UL32 therefore shows the same sub-cellular localisation as all other packaging and capsid proteins. These results differ to those previously published, but there may be a number of explanations for this. Firstly, in contrast to Chang *et al.*, my work used an epitope-tagged UL32, and it is possible that the reactivity of the anti-HA antibody to its epitope is much stronger than that of their polyclonal antiserum to the UL32 protein. This might allow nuclear UL32 to be more readily detected (as reported by Lamberti and Weller, 1998) whilst decreasing the background signal. However, unlike Lamberti and Weller's studies, I introduced the HA-tagged protein into virus and employed a normal infection, rather than a transfection-superinfection assay. Therefore, the levels of HA-UL32 expressed in my experiment should be comparable to the normal levels of UL32 during HSV-1 infection, rather than expression driven from the strong ICP8 promoter in a plasmid. Furthermore, the other groups both examined the localisation of UL32 at very late times (18 hours and 20 hours) post infection, considerably after peak titres have been reached and when the cells exhibit considerable cytopathic effect. However, DNA packaging is readily detected much earlier, with DNase resistant DNA present, and the putative terminase subunits localised to RCs, at 6 hours post infection (Higgs *et al.*, 2008; Lamberti & Weller, 1998). My experiments were therefore carried out at early times (6 hours) post-infection to examine the localisation of UL32 while DNA packaging was occurring, and this may also account for some of the observed differences.

It is unlikely that the HA-epitope tag affected the localisation of UL32 since both the HA-UL32 plasmid and HA32EP virus behaved indistinguishably from corresponding

constructs expressing wt UL32 in functional assays. Furthermore, the proteins expressed from pHA-UL32 and pUL32 showed the same localisation in transfection assays.

My observations that UL32 is localised to the RCs within infected cells but is found solely within the cytoplasm when transfected alone, suggested that other HSV-1 proteins are involved in the correct localisation of UL32 during infection. The most obvious candidates for this were the other cleavage/packaging proteins. The potential interactions between UL32 and these proteins were therefore investigated.

At the commencement of my studies, no data indicative of an interaction between UL32 and any other HSV-1 protein had been published. However, a recent paper suggests that UL32 affects the localisation of UL25 during infection (Scholtes & Baines, 2009). These authors found that during infection in the absence of UL32, although UL25 was predominantly nuclear, significant levels were detected in the cytoplasm. They also noted that the ratio of soluble UL25 to UL17 was increased in lysates from these cells, but did not examine whether UL25 and UL32 might co-localise or physically interact. However, the data presented in this chapter fail to provide evidence that UL32 interacts with the packaging proteins UL6, UL17 or UL25. In contrast to Scholtes, I found that UL32 had no discernable effect on the localisation of UL25 in infected cells (figure 5.11). It is not clear why these results should differ, but my conclusion was supported by the failure to detect an interaction between UL32 and UL25 using either a co-transfection or co-immunoprecipitation assay. Similarly, UL32 did not show any interaction with either UL17 or UL6 in these assays.

Experiments with *hr*64 also showed that UL32 is dispensable for the correct localisation of the putative terminase components UL15, UL28 and UL33 during infection. UL32 showed no evidence of an interaction with either UL28 or UL33 alone, however, UL32 and UL15 influenced each others' localisation in co-transfected cells in the absence of other viral proteins. This is the first evidence indicative of an interaction between UL32 and a member of the putative terminase complex. As the effect was not seen in every cell, and many cells showed only a partial colocalisation of UL15 and UL32, it may represent a weak or transient interaction between the two proteins. The interaction could not be confirmed by co-immunoprecipitation of baculovirus-expressed proteins, which again suggests that it may be an indirect, weak or transient interaction. The UL15-UL32 interaction appears to be stabilised or strengthened by the addition of the other two putative terminase subunits, UL28 and UL33, as co-transfection of all four proteins consistently

caused almost complete relocalisation of UL32 to the nucleus. Co-transfection of UL32 with all possible combinations of the terminase components suggested that UL28 and UL15 were essential for maximum relocalisation of UL32 to the nucleus. These data also indicated that UL33 is probably not involved in any interaction between UL32 and the terminase complex.

The interactions between the putative terminase components are now well-established and it has been shown previously that UL15 is necessary for localisation of UL28 and UL33 to replication compartments during infection (Higgs *et al.*, 2008). It has also been shown that these three proteins first form a complex in the cytoplasm and then the nuclear localisation signal (NLS) within UL15 directs their localisation to the nucleus (Yang *et al.*, 2007). It is therefore possible that UL32 could bind stably to the assembled terminase complex in the cytoplasm and thereby be co-transported into the nucleus. In the context of an HSV-1 infection, this would provide a mechanism by which UL32 is localised to the RCs for correct DNA cleavage and packaging to occur. These results suggest that UL32 binds to UL15 weakly, but may also interact with the UL28 subunit, so that when these two proteins are assembled within the terminase complex, UL32 makes contact with both proteins, thereby stabilising the interaction. Alternatively, the binding of UL15 to UL28 may alter the conformation of UL15, allowing UL32 to bind more stably, possibly by exposing other binding sites within UL15.

It is important to note that although the immunofluorescence data indicate that UL15 (and potentially UL28) influence the localisation of UL32, it does not necessarily demonstrate a direct interaction. There are a number of ways in which one protein may influence the other in the absence of a direct physical interaction, for example, an interaction may be mediated by other (cellular) proteins or the presence of DNA. Alternatively, one protein may affect the localisation of another by altering post-translational modifications or signal sequences on the target protein.

Since a panel of mutants had previously been generated (chapter 4), each of these was analysed to determine whether they could interact with the terminase complex. The ability of each mutant UL32 protein to support viral replication and DNA packaging and to interact with the terminase is summarised in table 5.1. The interactions were classified into three types. In class 1 interactions, UL32 was entirely nuclear and completely co-localised with the terminase, in class 2, UL32 was distributed throughout the cell and appeared to

Table 5.1: The ability of UL32 mutants to interact with the terminase proteins in an immunofluorescence assay.

The ability of UL32 mutant proteins to co-localise with the terminase proteins in the immunofluorescence assay is displayed, along with previous data showing their ability to support DNA packaging and virus growth.

Y = Functional; ability to support growth and packaging to over 10% that obtained with pUL32.

N = Non-functional; ability to support growth and packaging to less than 10% of pUL32.

1 = complete colocalisation with the terminase (UL32 entirely nuclear).
2 = partial colocalisation with the terminase (UL32 nuclear and cytoplasmic).
3 = no colocalisation with the terminase (UL32 entirely cytoplasmic)

mutant	Ability to support DNA packaging and viral growth	Colocalisation with terminase
pUL32	Y	1
in5	Y	1
in12	Y	1
in40	N	3
in55	N	2
in67	Y	1
in93	Y	1
in95	Y	1
in136	N	2
in155	N	2
in177	N	3
in187	Y	1
in198	N	3
in220	Y	1
in232	Y	1
in302	Y	1
in309	N	2
in328	Y	2
in332	Y	1
in338	N	1
in376	Y	2
in377	Y	1
in378	Y	1
in398	N	1
in407	N	3
in414	N	2
in435	N	3
in449	N	2
in475	Y	1
in486	N	3
in490	N	3
in494	N	2
in498	N	2
in512	N	3
in558	N	2
in572	N	3
in580	N	3
in592	N	3
CxxC1	N	3
CxxC2	Y	1
CxxxC3	N	2
UL32ΔC	N	3

partially co-localise, and in class 3, UL32 remained cytoplasmic and its localisation was not affected by co-transfection of the terminase.

Virtually every mutant that supported the growth and DNA packaging of *hr*64 behaved indistinguishably from wt UL32 (class 1), being completely transported to the nucleus in the presence of the terminase. The only exceptions were mutants in328 and in376 which showed a partial nuclear localisation (class 2). Similarly, all mutants that failed to interact with the terminase (class 3) were defective in the functional assays. Nearly all of the other non-functional mutants exhibited only a partial relocalisation in the presence of the terminase (class 2; mutants in55, in136, in155, in309, in414, in449, in494, in498, in558 and UL32CxxC3). The observation that all the mutants defective in the interaction with the terminase components were also defective in growth and packaging suggests that this interaction is essential for the function of UL32 within the DNA packaging process. However, the interaction is not sufficient to allow packaging to occur. Two particularly interesting mutants (in338 and in398) showed the same localisation as wt UL32 but were non-functional, and therefore may have a further defect that prevents these from supporting viral growth and DNA packaging. The twelve mutants that were only partially re-localised by the terminase (class 2) may have weaker interactions with UL15 and/or UL28, or may exist in different forms or conformations, only some of which can interact with the terminase.

The regions of UL32 important for the interaction with the terminase do not map to a particular part of the protein, but are spread throughout. This perhaps supports the theory that UL32 binds to both UL15 and UL28, with different regions of the UL32 protein required for different interactions. Alternatively, the folding of UL32 may be such that these different regions are close to each other in the native protein, or some of the mutations may have long-range effects on the structure of the protein.

Ideally, the interaction between UL32 and the terminase needs to be confirmed within the context of virus infection, for example by co-immunoprecipitation of UL32 along with one or more of the terminase components from HSV-1 infected cells. The generation of HA32EP should prove useful for this, as the anti-HA antibody is extremely potent and can be used for immunoprecipitation. Furthermore, it would be interesting to examine the localisation of UL32 in infected cells in the absence of UL15, to determine whether the UL15-UL32 interaction is necessary for the correct localisation of UL32 in replication compartments. Unfortunately, the current lack of a potent antibody capable of specifically

recognising untagged UL32 in HSV-1 infected cells means that this is presently difficult. The introduction of a UL15 deletion into HA32EP should circumvent this problem.

6 Characterisation of the UL32 protein

This chapter describes a number of experiments undertaken to further characterise the UL32 protein, and attempt to identify its role within HSV-1 DNA packaging. Firstly, a new recombinant HSV-1 was created with an extensive deletion within UL32, to confirm the packaging defect of *hr*64. The ability of UL32 homologues from other herpesviruses to substitute for HSV-1 UL32 was also analysed. The UL32 protein itself was then examined in greater detail, to investigate the nature of the protein in solution, analyse and quantify its zinc-binding ability and investigate whether UL32 was capable of interacting with DNA.

6.1 Generation of a new UL32 null mutant

The UL32 mutant virus used in these studies up until now, *hr*64, was constructed by the insertion of an ICP6:lacZ cassette at amino acid 274 of UL32. None of the UL32 sequence was deleted from this virus, and *hr*64 was shown to express a 30 kDa protein corresponding to the N-terminus of UL32 (Lamberti & Weller, 1998). It is possible that this N-terminal fragment may affect the phenotype of *hr*64 and therefore it was decided to generate and analyse a new mutant HSV-1, with as much as possible of the UL32 gene deleted. Furthermore, *hr*64 is HSV-1 strain KOS mutant, whereas the parental UL32 gene used in my mutagenesis is derived from HSV-1 strain 17+. I therefore considered it would be useful to generate the new mutant in a strain 17+ background.

6.1.1 Red/ET recombination

The approach to generating the new UL32 deletion mutant employed the Counter-Selection BAC modification kit from GeneBridges, which utilises the Red/ET recombination enzymes. This kit induces homologous recombination *in vivo* in *E. coli* to introduce mutations into Bacterial Artificial Chromosomes (BACs). BACs are DNA constructs based on the fertility plasmid (F-plasmid) and so can replicate stably in *E. coli*. These BACs can harbour up to 300 kbp foreign DNA and so are suitable for cloning long DNAs such as the full-length 152 kbp HSV-1 genome. The BAC used in this study was fHSV-1Δpac, containing the complete HSV-1 strain 17 syn+ genome, but lacking the

packaging signals (Saeki *et al.*, 1998). The BAC vector also includes the selectable chloramphenicol resistance gene (cam^R).

In the Red/ET system, homologous recombination is mediated by two phage proteins Redα and Redβ, which act as an exonuclease and DNA annealing protein respectively. The plasmid pSC101-BAD-gbA^{tet} expresses the Redγαβ operon under the control of the arabinose inducible BAD promoter and confers tetracycline resistance (tet^R).

This recombination is used to recombine a specifically constructed cassette containing the rpsL and neo genes flanked by short regions of homology into the desired locus. By choosing homology arms corresponding to either end of the UL32 gene, the bulk of the gene will be replaced by DNA encoding the rpsL and neo genes. The presence of neo confers resistance to kanamycin (kan^R) whilst rpsL results in sensitivity to streptomycin ($strep^S$) which allow identification of the desired recombinant BAC.

6.1.2 Generation of mutant rpsL-neo cassette

In order to target the recombination to the UL32 gene in fHSV-1Δpac, a PCR product (rpsL-neo-32) containing the rpsL-neo cassette flanked by sequences homologous to UL32 was generated (figure 6.1). As UL32 overlaps with the 5' ends of both the UL33 and UL31 genes, the entire UL32 ORF could not be removed from fHSV-1Δpac without disrupting these genes. It was therefore decided to retain approximately 200 bp at each terminus of UL32, so that upstream regulatory sequences that may be needed for expression of UL33 or UL31 should not be affected. The sequences of the primers used to amplify the rpsL-neo cassette are listed in figure 6.1C. PCR was expected to produce a 1.4 kbp fragment, with nucleotides 151-201 and 1600-1650 of UL32 at either end. The rpsL-neo cassette replaced nucleotides 202 to 1599 of UL32.

6.1.3 Insertion of rpsL-neo cassette into fHSV-1Δpac BAC DNA

E. coli DH10B cells containing fHSV-1Δpac and pSC101-BAD-gbA^{tet} were cultured at 30°C overnight, and the Redα and Redβ recombination enzymes induced by addition of L-arabinose and a temperature switch to 37°C (section 2.2.13.1). The cells were made competent for transformation and the rpsL-neo-32 PCR product transformed into the cells using electroporation (section 2.2.13.2). To allow recombination to occur, the cells were

Figure 6.1: Generation of rpsL-neo cassette with homology arms for recombination.

A. rpsL-neo cassette. The 1319 bp cassette, encoding the rpsL and neo genes, was used as a template for PCR, using primers BAC-PCR-F and BAC-PCR-R. Each primer consisted of sequences complementary to the rpsL-neo cassette (shown in orange) and sequences homologous to the UL32 gene (blue).

B. PCR generated the rpsL-neo-32 cassette, of 1420 bp. This contained the rpsL-neo cassette with 50 bp homology to UL32 at the 5' and 3' ends (shown in blue) . The nucleotides positions of those sequences within the UL32 ORF are indicated. These homology arms then allowed the rpsL-neo-32 cassette to be recombined with fHSV-1Δpac DNA, with the rpsL-neo cassette replacing 1399 nucleotides of the UL32 gene.

C. 5' – 3' sequences of PCR primers used, indicating those sequences complementary to the rpsL-neo cassette in orange and those complementary to the UL32 gene in blue.

A.

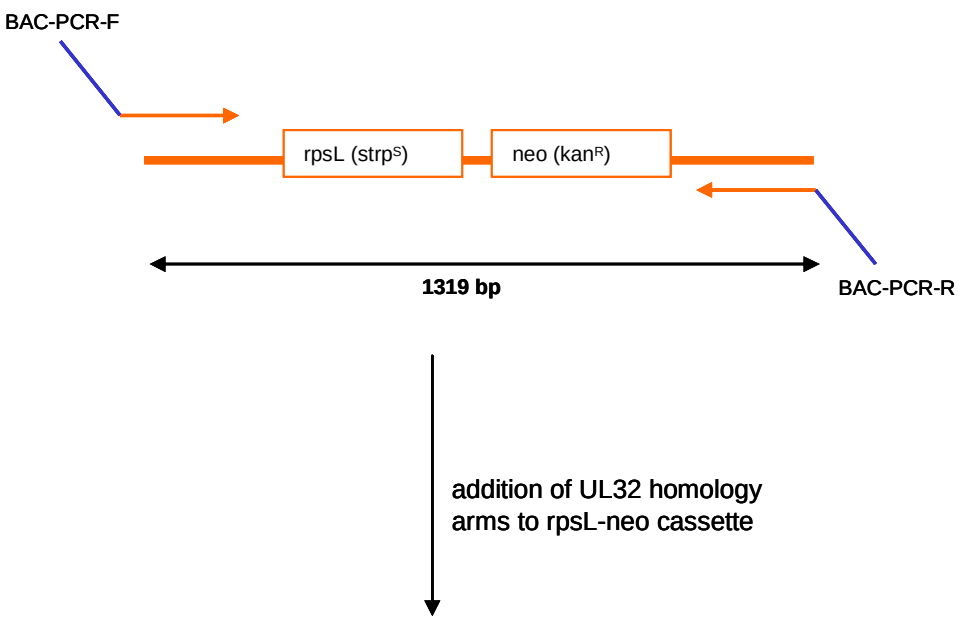

B.

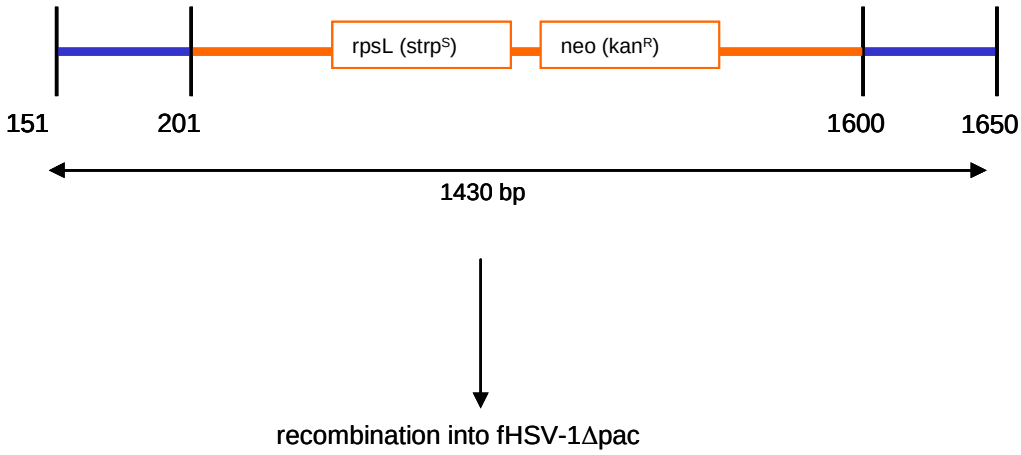

C.

	5' - 3' sequence
BAC-PCR-F	TGACGGCCAGTCACGTGATAGGTGTGCCGCCCGTCGGTACGCTCGA CGAGGGCCTGGTGATGATGGCGGGATCG
BAC-PCR-R	TGAGGGCACGCAACGCTATGCAGACACGCCCCTCGAACTCGTTCCCG CAGGTCAGAAGAACTCGTCAAGAAGGCG

incubated at 37°C for 70 min. Bacteria with the rpsL-neo-32 cassette integrated into fHSV-1Δpac should be $cam^R/kan^R/strp^S$ and so the bacteria were plated first onto LB-agar plates containing cam and kan. Ten colonies were picked and these were each further plated onto cam/kan/strp plates to confirm that the rpsL-neo-32 cassette was intact and conferred the strp sensitivity. Two colonies (fΔpacC and fΔpacG) showed the expected antibiotic resistance phenotype of $cam^R/kan^R/strp^S$, and therefore were analysed in further detail.

BAC DNA was prepared from overnight cultures of these clones and each was screened for the presence of the kanamycin resistance gene by Southern blotting as follows. The BAC DNA was digested with *Eco*RI, along with two other samples of BAC DNA to act as controls; BAC fHSV-1Δpac (the parental BAC) and BAC O (an fHSV-1Δpac derivative with the rpsL-neo cassette inserted into gene UL23 (Tong & Stow, 2010)). The DNA was separated by agarose gel electrophoresis and Southern blotted. The inserted rpsL-neo cassette was detected using ^{32}P labelled rpsL-neo, provided by Lily Tong. fΔpacC and fHSV-1Δpac BAC DNA was also similarly screened to confirm the deletion of the UL32 gene, but using ^{32}P labelled pUL32 as a probe.

Figure 6.2A shows the *Eco*RI sites around the UL32 locus in fHSV-1Δpac and fΔpacC/G (with the rpsL-neo cassette inserted), and indicates the expected sizes of fragments recognised by the kanamycin and pUL32 probes. *Eco*RI cuts the HSV-1 genome at nucleotides 64130, 68201 and 69697, and so pUL32 should hybridise to two fragments of approximately 4.1 kb and 1.5 kb if the UL32 gene is intact (as expected in fHSV-1Δpac). In this case, the kanamycin probe should not hybridise, as the rpsL-neo cassette has not been inserted. If, however, the UL32 gene has been replaced by the rpsL-neo cassette (which does not contain any *Eco*RI restriction sites), then only one fragment of 5.6 kb is expected from this region. This should be detected by both the kanamycin and pUL32 probes due to the presence of the rpsL-neo cassette and residual UL32 sequences at either end of the gene respectively.

The two Southern blot membranes are shown in figure 6.2B and C. The kanamycin probe did not hybridise to the fHSV-1Δpac DNA in lane 2, confirming that the parental BAC does not contain the kanamycin resistance gene. Lane 1 containing BAC O DNA, showed a single band of approximately 5 kbp, corresponding to the kam^R gene inserted into *Eco*RI N (Tong & Stow, 2010). The kanamycin probe also hybridised to a fragment of 5.6 kb from both fΔpacC and fΔpacG, confirming that the rpsL-neo-PCR cassette had been successfully inserted into these constructs. When probed with pUL32, fHSV-1Δpac (lane

Figure 6.2: Confirmation of the insertion of the rpsL-neo-32 cassette, and corresponding deletion of UL32 ORF in fΔpac DNA.

A. Diagrammatic representation of the region of fHSV-1Δpac and fΔpacC/G surrounding the UL32 gene. The UL32 gene is shown in blue with the HSV-1 nucleotides indicated above. The orange box represents the expected position of the rpsL-neo-32 cassette within fΔpacC/G . The red arrows show the positions at which the genome is cleaved by *Eco*RI, and the expected sizes of fragments generated by *Eco*RI digestion of the two BACs are indicated.

B. BAC DNA was prepared from bacteria containing the indicated BACs. The DNA was digested with *Eco*RI and separated by agarose gel electrophoresis. Samples were Southern blotted and the inserted cassette visualised by probing with α-32P labelled rpsL-neo. The positions of size markers (kb) are indicated.

C. BAC DNA from fΔpacC and fHSV-1Δpac was digested and separated by electrophoresis as above. The samples were probed using ^{32}P labelled pUL32 and the sizes of fragments generated are indicated.

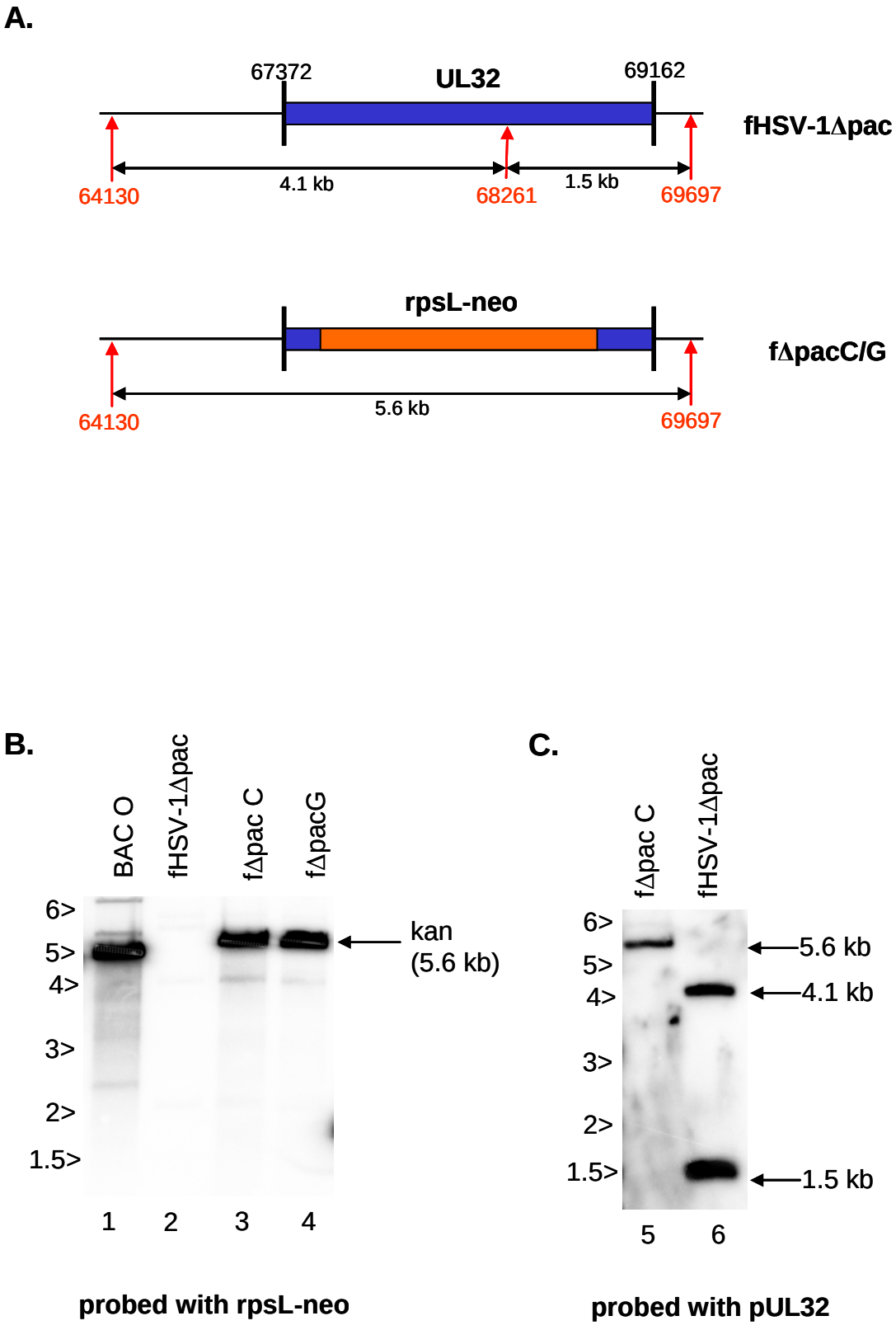
A.
67372
UL32
69162
fHSV-1Δpac
4.1 kb
1.5 kb
64130
68261
69697
rpsL-neo
fΔpacC/G
5.6 kb
64130
69697
B.
BAC O
fHSV-1Δpac
fΔpac C
fΔpacG
6>
5>
4>
3>
2>
1.5>
kan
(5.6 kb)
1
2
3
4
probed with rpsL-neo
C.
fΔpac C
fHSV-1Δpac
6>
5>
4>
3>
2>
1.5>
5.6 kb
4.1 kb
1.5 kb
5
6
probed with pUL32

6) and fΔpacC (lane 5) show the patterns expected for a wt genome and one in which the rpsL-neo cassette has been inserted into the UL32 gene, respectively.

6.1.4 Isolation of UL32 mutant virus

BAC DNA was prepared from clone fΔpacC for transfection into mammalian cells for generation of the UL32 mutant HSV-1. Monolayers of the UL32 complementing cell line, UL32-5, were transfected using the calcium phosphate method with 2 µg fΔpacC BAC DNA together with 2 µg *Bam*HI cleaved pGX2 (containing the HSV-1 *Bam*HI K fragment which is needed to repair the packaging signals deleted from fHSV-1Δpac). The cells were incubated at 37°C for 3 days, the cells and media harvested and then used to infect fresh plates of UL32-5 cells. After 48 hours, the plate showed clear evidence of CPE. The cells and media were harvested, and a stock of this virus (Δ32EP) prepared.

6.1.5 Characterisation of Δ32EP

The newly created Δ32EP virus was next characterised, to determine whether the phenotype was the same as *hr*64.

6.1.5.1 Growth curve for Δ32EP

The replication of Δ32EP on complementing and non-complementing cell lines was compared to wt HSV-1 and *hr*64 in a single-step growth curve. 35 mm dishes of BHK and cells were infected with 10 p.f.u. per cell wt HSV-1, *hr*64 or Δ32EP, and UL32-5 cells infected with *hr*64 or Δ32EP. One hour post infection, the cells were washed once with 0.14 M NaCl, exposed to acid glycine wash for one minute, then washed with EC5 or EFC5 as appropriate, followed by continued incubation in EC5 or EFC5 at 37°C. Cells were harvested at 4, 8, 12, 16, 20 and 24 hours post infection and the cells and media sonicated before being titrated on UL32-5 cells for 3 days. Plaques were counted and virus yields determined. This growth analysis (figure 6.3) indicated that Δ32EP did not replicate on non-complementing BHK cells, producing very low yields, comparable to those of *hr*64. However, provision of UL32 in the UL32-5 complementing cell line allowed Δ32EP to grow to titres comparable to wt HSV-1 and *hr*64 in these cells.

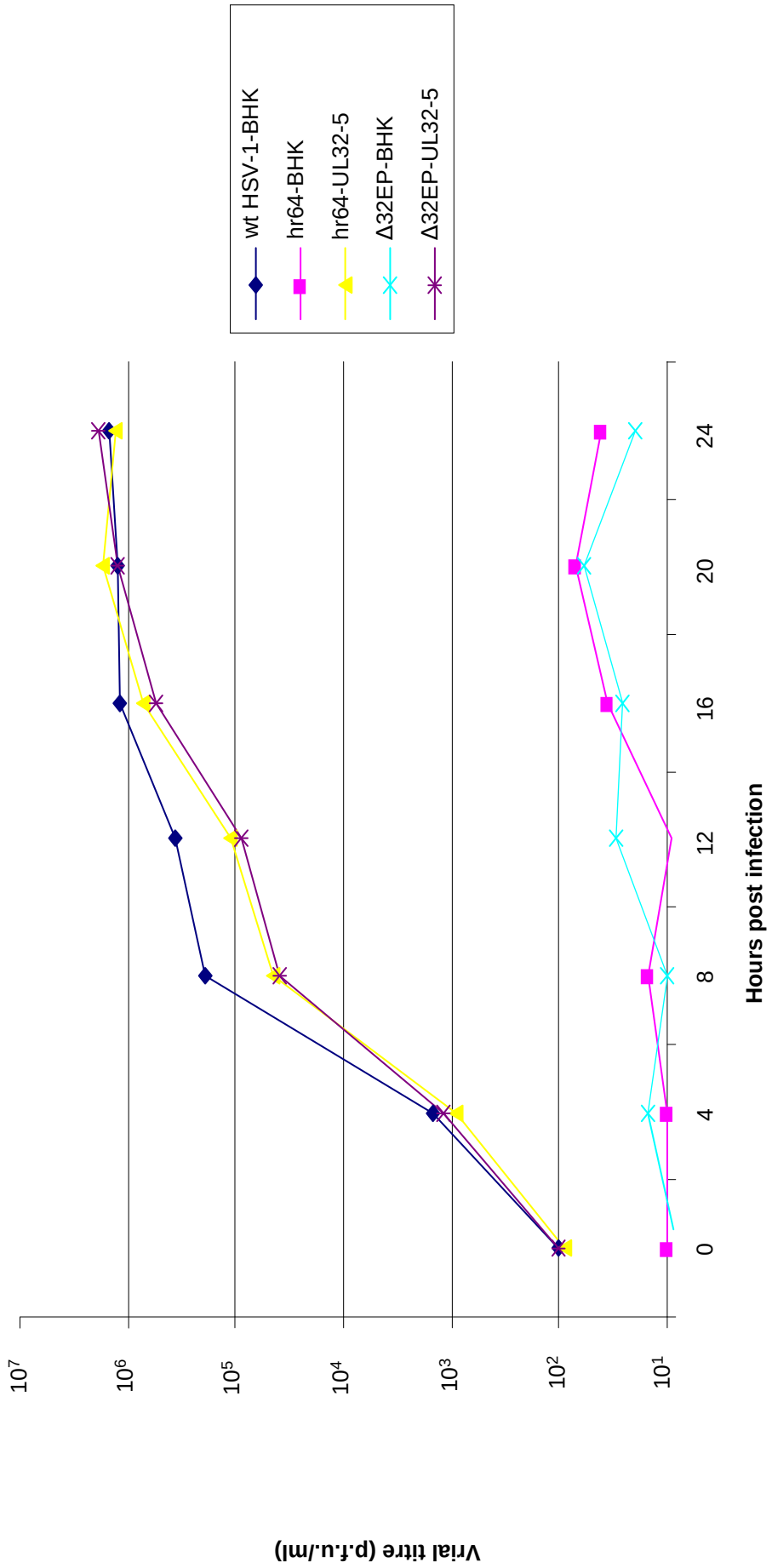

Figure 6.3: Comparison of the growth of wt HSV-1, Δ32EP and *hr*64 in BHK and UL32-5 cells.

Replicate plates of BHK or UL32-5 cells were infected with 10 p.f.u./cell wt HSV-1, Δ32EP or *hr*64. At the indicated times, cells were harvested and the progeny virus titrated in UL32-5 cells. Plaques were counted 3 d.p.i. and the titres determined.

6.1.5.2 Amplicon packaging assay

The ability of Δ32EP to support DNA packaging was also tested in a transient amplicon packaging assay. BHK cells were transfected with 1 µg pCMV10 or pUL32 along with 0.5 µg pSA1, and superinfected with 5 p.f.u. per cell wt HSV-1, *hr*64 or Δ32EP. Cells were harvested 18 hours post infection and total and DNase resistant DNAs prepared. The DNA samples were digested with *Eco*RI and *Dpn*I and separated on a 0.8% agarose gel. The gel was Southern blotted and probed using ^{32}P labelled pAT153, and the membrane is shown in figure 6.4. wt HSV-1 was able to efficiently replicate and package amplicon DNA, but as previously shown, *hr*64 could package DNA only in the presence of pUL32 (lanes 1-3). Δ32EP replicated DNA at levels similar to wt HSV-1, but was not able to package the replicated DNA in the presence of pCMV10 (lane 5). Addition of pUL32 restored the DNA packaging ability of Δ32EP (lane 4).

Together, these results all confirm that Δ32EP has a phenotype indistinguishable from *hr*64. The virus cannot replicate on non-complementing cells, or cleave and packaged DNA, but the provision of exogenous UL32 can repair these defects.

6.2 Testing the UL32 homologues of VZV and HCMV for their ability to complement Δ32EP

A number of reports have investigated the ability of the pseudorabies virus (PrV) and HSV-1 packaging proteins to functionally complement each other. It was found that HSV-1 UL32 was able to support the growth of a UL32-negative PrV, but this functional complementation was not reciprocal (Fuchs *et al.*, 2009).

I therefore examined whether Δ32EP could be complemented by the homologues of UL32 encoded by two other human herpesviruses, varicella-zoster virus (VZV; another alphaherpesvirus) and HCMV (a betaherpesvirus). The VZV homologue is a 585 amino acid protein, encoded by gene 26 (referred to here as VZV26). The HCMV homologue is a 668 amino acid protein, named UL52 (referred to here as HCMV52), and has previously

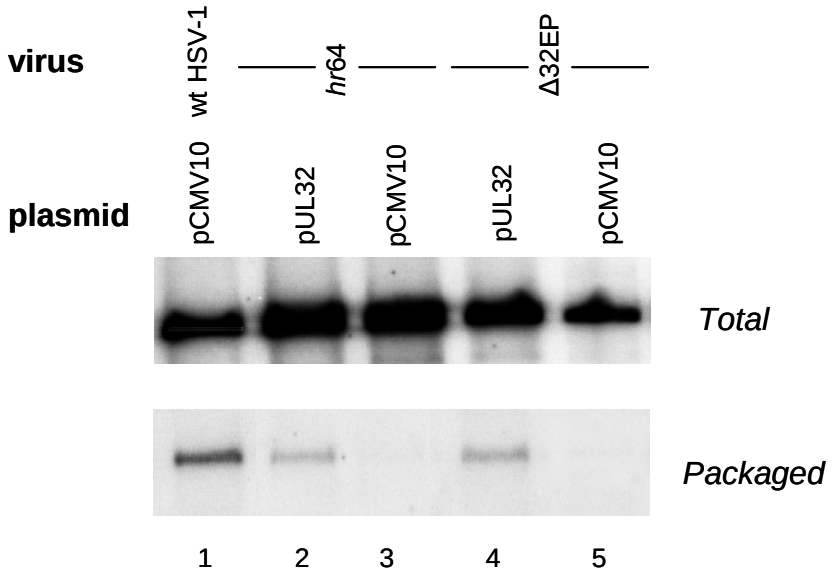

Figure 6.4: Amplicon packaging by Δ32EP.

BHK cells were transfected with 1µg pCMV10 or pUL32, along with 0.5 µg pSA1 using the calcium phosphate method, followed by superinfection with 5 p.f.u./cell wt HSV-1, *hr*64 or Δ32EP. 18 h.p.i., cells were harvested and total and DNase resistant DNA prepared. The DNA was digested with *Eco*RI and *Dpn*I and separated by agarose gel electrophoresis and Southern blotted. pSA1 was detected by probing the membrane with ^{32}P labelled pAT153.

been characterised as essential for virus growth and for cleavage and packaging of HCMV DNA (Borst *et al.*, 2008).

6.2.1 Generation of plasmids expressing HA-tagged versions of VZV26 and HCMV52

As no antibodies were available in the laboratory specific for VZV26 or HCMV52, constructs encoding HA-tagged proteins were generated by PCR. As with the generation of HA-UL32 (section 5.2), the primers were designed such that the HA tag was encoded between the second and third amino acids of VZV26 and HCMV52, generating constructs named HA-VZV26 and HA-HCMV52 respectively. The forward primers for each construct contained an introduced *Kpn*I site which was used during subsequent cloning as described below. The reverse primers for HA-VZV26 and HA-HCMV52 introduced *Xba*I and *Hind*III sites respectively, again used for further cloning. The primer sequences are listed in table 6.1.

The template for the PCR construction of the HA-tagged VZV-UL32 was plasmid pVZV-*Kpn*I f, which contains the *Kpn*I f fragment of VZV, spanning nucleotides 43943 to 49984 of the VZV genome, with gene 26 specified by nucleotides 44506 to 46263 (Davison & Scott, 1986). The template for the PCR construction of HA-HCMV52 was plasmid pHCMV-*Hind*III f containing the *Hind*IIII f fragment of HCMV strain AD169. This fragment spans nucleotides 65813 to 86163 with UL52 encoded from nucleotides 75087 to 77093.

	5' - 3' sequence	inserted site
HA-VZV26		
HA-VZV-F	GGGCGGTACCCCATGGATTACCCTTACGACGTGCCTGACTACG CTCGGGTAGAATCAGAAGAACC	*Kpn*I
VZV-R	CCGGCAGCTCTAGACCTAGACATACTTCGATAGGGTGTG	*Xba*I
HA-HCMV52		
HA-HCMV-F	GGGCGGTACCCCATGAATTACCCTTACGACGTGCCTGACTAC GCTCCGAGTACCCACGTGAGC	*Kpn*I
HCMV-R	CCGGGGTCGCCCAAGCTTGGGACGCTAGACATACTTGTCTACAC G	*Hind*III

Table 6.1: Sequences of primers used for generating HA-VZV26 and HA-HCMV52. 5'-3' sequences of the primers used for generation of HA-VZV26 and HA-HCMV52, showing the sequences encoding the HA tag in red and those complementary to the VZV26 and HCMV52 genes in blue. The introduced restriction sites are listed and underlined in the primer sequences.

Each PCR was carried out using the forward and reverse primers as described in section 2.2.3.8. The PCR fragments were then digested with the appropriate restriction enzymes (*Kpn*I and *Xba*I in the case of HA-VZV26; *Kpn*I and *Hind*III in the case of HA-HCMV52) and ligated into pCMV10 digested with the same enzymes, to generate pHA-VZV26 and pHA-HCMV52.

6.2.2 Functional analysis of pHA-VZV26 and pHA-HCMV52

Firstly, it was essential to verify that pHA-VZV26 and pHA-HCMV52 did indeed express the appropriate HA-tagged proteins. This was done by western blotting of transfected cells with F-7 (anti-HA). Figure 6.5A confirmed that each plasmid expressed a protein consistent with the predicted size of 64 kDa for VZV26 and 75 kDa for HCMV52.

The two proteins were next tested for their ability to complement the growth and DNA packaging of the UL32 null mutant Δ32EP, using a complementation yield assay and transient amplicon packaging assay as previously described.

As before, pUL32 supported the growth of Δ32EP in the complementation yield assay, giving a mean titre of 4.3×10^4, whereas pCMV10 did not, giving a titre of 40 (0.1% of the pUL32 value). Similarly, neither pHA-VZV26 nor pHA-HCMV52 could complement

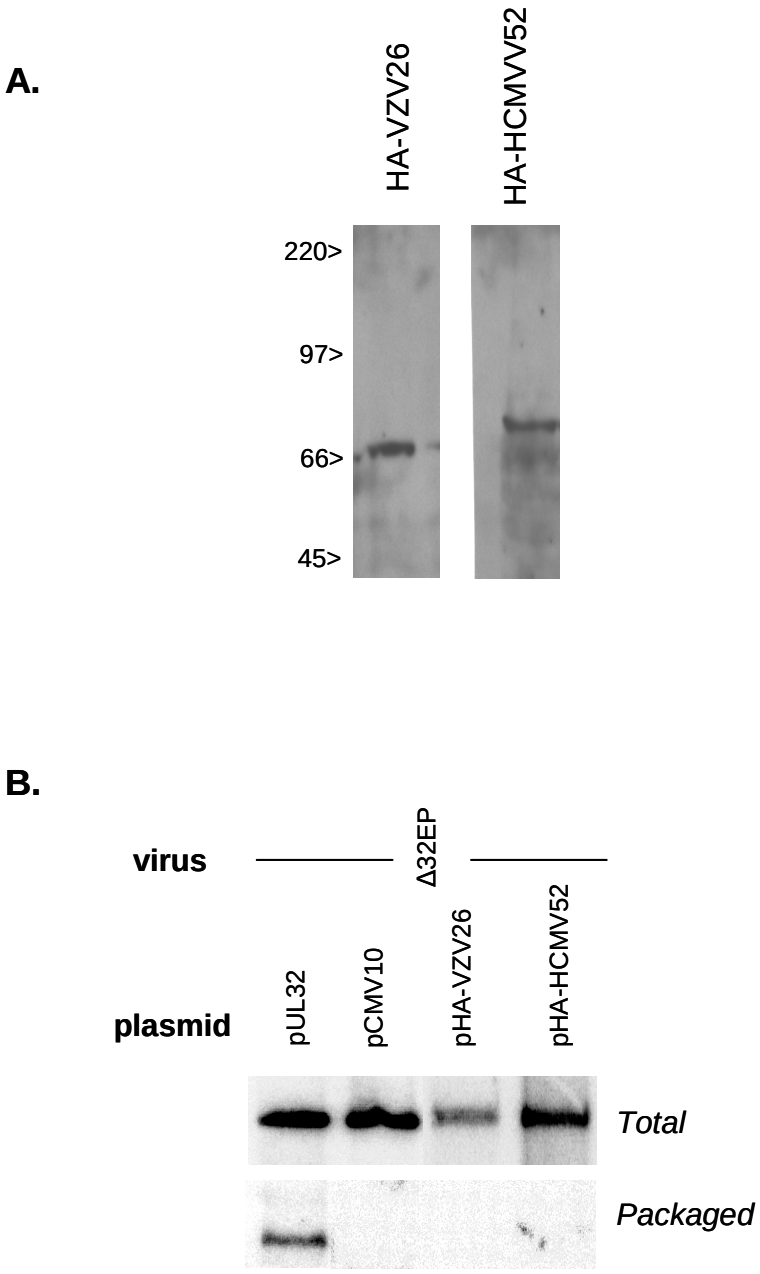

Figure 6.5: Expression of HA-VZV26 and HA-HCMV52, and analysis of their ability to support packaging of amplicon DNA by Δ32EP.

A. BHK cells were transfected with 1 µg pHA-VZV26 or pHA-HMCV52 using the calcium phosphate method and harvested after 18 hours. Cells were lysed and proteins separated by SDS-PAGE. Proteins were western blotted and the membranes immunoblotted with F-7 (anti-HA) followed by HRP-conjugated anti-mouse IgG and developed using ECL substrate.

B. BHK cells were transfected with 1 µg pCMV10, pUL32, pHA-VZV26 or pHA-HCMV52 along with 0.5 µg pSA1 using the calcium phosphate method, followed by superinfection with 5 p.f.u./cell Δ32EP. 18 h.p.i., cells were harvested and total and DNAse resistant DNA prepared and analysed as in the legend to figure 6.4.

Δ32EP, giving mean titres which were 0.1% and 0.15% of that obtained with pUL32 respectively.

The results of the amplicon packaging assay are shown in figure 6.5B. All samples showed similar levels of total (replicated) DNA, with packaged DNA seen in the samples containing pUL32 (lane 1) but not pCMV10 (lane 2). Neither pHA-VZV26 nor pHA-HCMV52 supported detectable packaging of amplicon DNA (lanes 3 and 4), with mean values from duplicate experiments of less than 0.1% of that packaged in the presence of pUL32.

These results together demonstrate that neither pHA-VZV26 nor pHA-HCMV52 can substitute for HSV-1 UL32 and functionally complement the defect of Δ32EP.

6.3 Investigation of a possible interaction of UL32 with UL12

As previously discussed, the HSV-1 UL12 gene encodes the alkaline nuclease, a protein involved in the resolution of branched structures in concatemeric viral DNA resulting from recombination during genome replication. Many bacteriophage also encode nucleases performing this function. One of these is endonuclease VII of phage T4, which is required at late points during infection to resolve branchpoints before packaging of DNA into the phage head (Kemper & Garabett, 1981; Kemper & Janz, 1976).

Endonuclease VII has been shown to have a modular organisation of structure and function, with the C-terminal portion providing the endonuclease and the N-terminal portion thought to be involved in the DNA binding properties of the protein (Giraud-Panis *et al.*, 1995). The N-terminal region contains four cysteine residues distributed in a CxxC pattern reminiscent of that in HSV-1 UL32. Endonuclease VII was also found to coordinate zinc atoms. This similarity between the N-terminal portion of endonuclease VII and UL32 led me to speculate whether UL32 could work in concert with UL12 to perform a similar function in HSV-1. For example, UL32 might encode the DNA binding subunit (analogous to the N-terminus of endonuclease VII) with UL12 being equivalent to the C-terminus and performing the nuclease function.

6.3.1 Co-immunoprecipitation analysis of UL32 and UL12 from baculovirus-infected cells

The possibility of a direct interaction between UL32 and UL12 was investigated by immunoprecipitation from insect cells infected with baculoviruses expressing these proteins. *Sf*21 cells were mock infected or infected with AcUL32 and AcUL12 (expressing the UL12 protein) either alone or together. Forty-eight hours post infection, soluble protein extracts were prepared. An aliquot of each of these was immunoprecipitated using monoclonal antibody Q1 (anti-UL12), followed by incubation with protein-A-sepharose. Soluble extracts and immunoprecipitates were separated by SDS-PAGE and immunoblotted using R1 or Q1 (1:500), followed by HRP-conjugated protein-A. The resultant western blot is shown in figure 6.6.

As shown in panel A, UL12 was expressed in cells infected with AcUL12 either alone (lane 3) or together with UL32 (lane 4), but not cells that were mock infected or infected with AcUL32 alone (lanes 1 and 2). Similarly, UL32 could be only detected in cells infected with AcUL32 alone or dually infected with AcUL12 (lanes 5-8). As would be expected, the UL12 antibody Q1 successfully precipitated the UL12 protein from infected cells (lanes 11 and 12). However, Q1 did not co-precipitate UL32 from the dually infected cells (lane 16). The reciprocal experiment, using R1 for the immunoprecipitation, gave the same result (data not shown). This indicates that UL32 and UL12 do not form a complex in baculovirus-infected cells.

6.3.2 Pulsed-field gel analysis of the structure of replicated DNA in Δ32EP infected cells

Gel electrophoretic techniques have previously been used to analyse the structure of replicative concatemers of HSV-1 DNA, and while conventional gel electrophoresis can resolve fragments of only approximately 40 kbp, pulsed-field gel electrophoresis (PFGE) enables resolution of much larger DNA molecules, of up to 2000 kbp in size. Previous work showed that replicative intermediates generated by wt HSV-1 remain in the wells of a pulsed-field gel, due to their branched structure, whereas the cleaved unit-length genomes can enter the gel. Restriction enzyme digestion followed by PFGE analysis of DNA from cells infected with a UL12 null mutant demonstrated that the replicative intermediates

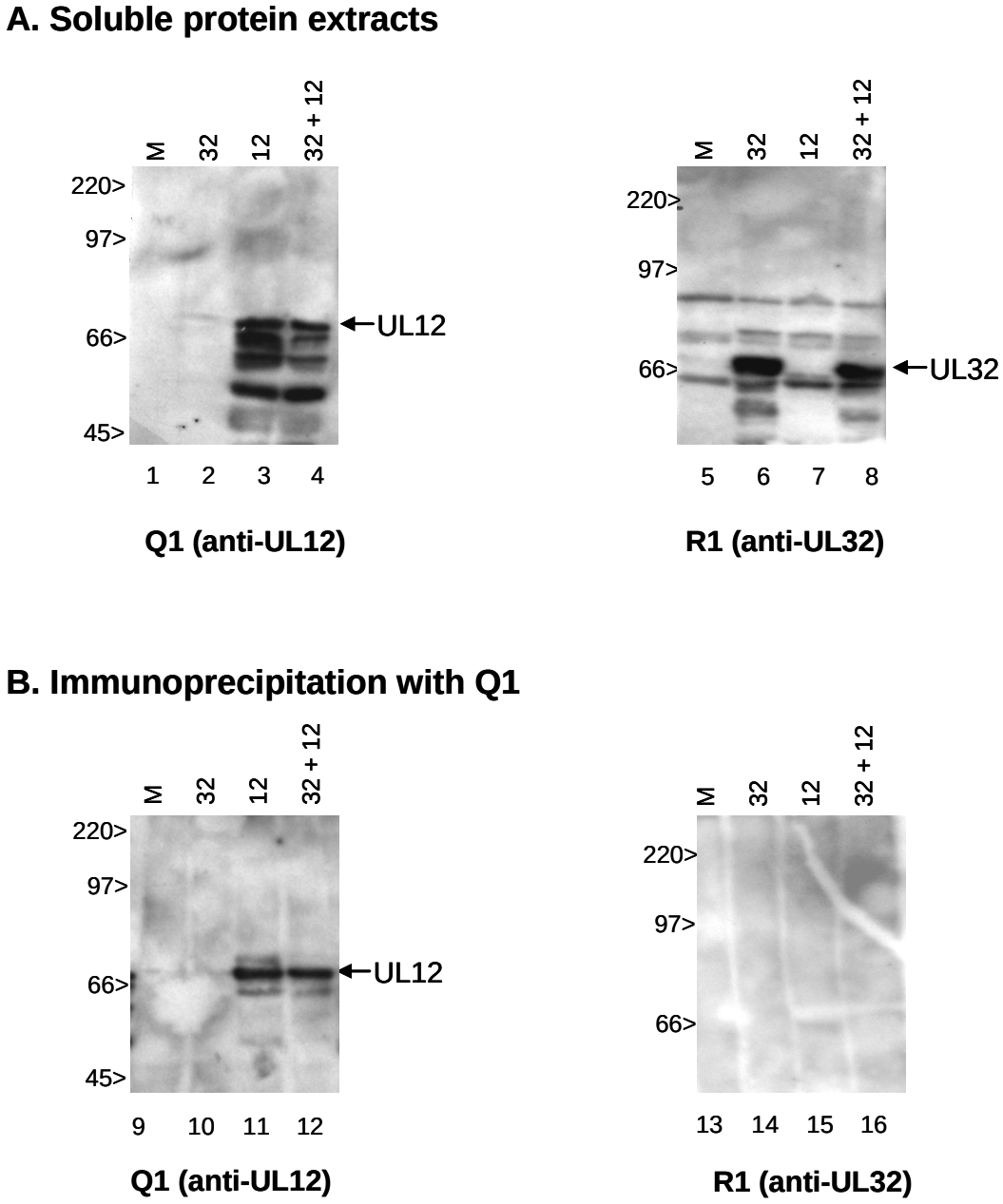

Figure 6.6: Immunoprecipitation of UL12 and UL32 from recombinant baculovirus-infected cells.

A. *Sf*21 cells were mock infected or infected with 2.5 p.f.u./cell of the indicated recombinant baculoviruses. 48 h.p.i., soluble protein extracts were prepared. Samples of these extracts were separated on an 8 % polyacrylamide gel and western blotted. The membranes were incubated with either Q1 (anti-UL12; lanes 1-4) or R1 (anti-UL32; lanes 5-8). This was followed by incubation with HRP-conjugated protein-A which was detected using ECL substrate. The positions of size marker proteins are indicated (kDa).

B. Samples of the soluble protein extract were immunoprecipitated with Q1 and the immune complexes harvested by incubation with protein-A-sepharose. These immunoprecipitated samples were separated by SDS PAGE and immunoblotted as above with either Q1 (lanes 9-12) or R1 (lanes 13-16). The positions of size marker proteins are indicated (kDa).

produced by this virus were more complex than those of wt HSV-1, and apparently contained a higher level of branched structures (Martinez *et al.*, 1996a).

It was therefore decided to carry out pulsed-field gel analysis of the replicated DNA produced by Δ32EP, to determine whether UL32 may, like UL12, be involved in the resolution of branched structures.

Duplicate plates of BHK cells were infected with 5 p.f.u. per cell wt HSV-1, Δ32EP or *amb*UL12, which contains an amber stop codon at position 129 of the UL12 ORF (Patel *et al.*, 1996b). 18 hours post infection, cells were harvested into the medium and the cells from each plate embedded in agarose blocks (as described in 2.2.14.1), so that the DNA could be manipulated *in situ* to avoid shearing high molecular weight molecules. Total DNA was prepared by incubation in proteinase K, and the plugs (corresponding to approximately 6.5 x 10^5 cells each) were incubated with either *Spe*I, *Xba*I, *Hind*III or left undigested. The DNA was then separated by electrophoresis in a 1% PFGE agarose/0.5 x TBE gel at 6 V/cm for 16 hours at 14ºC with a ramped switch time of 1 – 15 sec (section 2.2.14.3). The DNA was Southern blotted and HSV-1 DNA detected by hybridisation to ^{32}P labelled fHSV-1 pac+ BAC DNA (a recombinant BAC encoding the entire HSV-1 genome). The Southern blot is shown in figure 6.7.

As previously reported (Martinez *et al.*, 1996a), undigested DNA from wt HSV-1 infected cells produced two bands corresponding the released unit-length genomes of 152 kbp and the high molecular weight DNA that failed to enter the gel (lane 1). Neither *amb*UL12 nor Δ32EP produced detectable genomic length DNA, with most of the undigested DNA remaining in the wells (lane 2 and 3). This is consistent with the known inability of UL32 mutant HSV-1 to cleave concatemers and the reduced packaging of “poor quality” DNA by *amb*UL12 (Porter & Stow, 2004b; Sherman & Bachenheimer, 1987) .

*Spe*I cleaves the HSV-1 genome once. Complete digestion of concatemeric DNA with this enzyme is expected to produce three fragments of sizes 186 kbp, 152 kbp and 118 kb, due to the potential isomerisation of the genome (Martinez *et al.*, 1996a). These bands could be very faintly seen in the wt HSV-1 DNA sample, along with four prominent smaller bands generated from unit length genomes containing the L segment in either orientation. These were 80 and 70 kbp from the prototype orientation and 100 and 50 kbp from the inverted orientation (lane 4). In contrast to wt HSV-1, *Spe*I cleaved *amb*UL12 DNA was fully retained within the well, as the more branched nature of the DNA prevented fragments

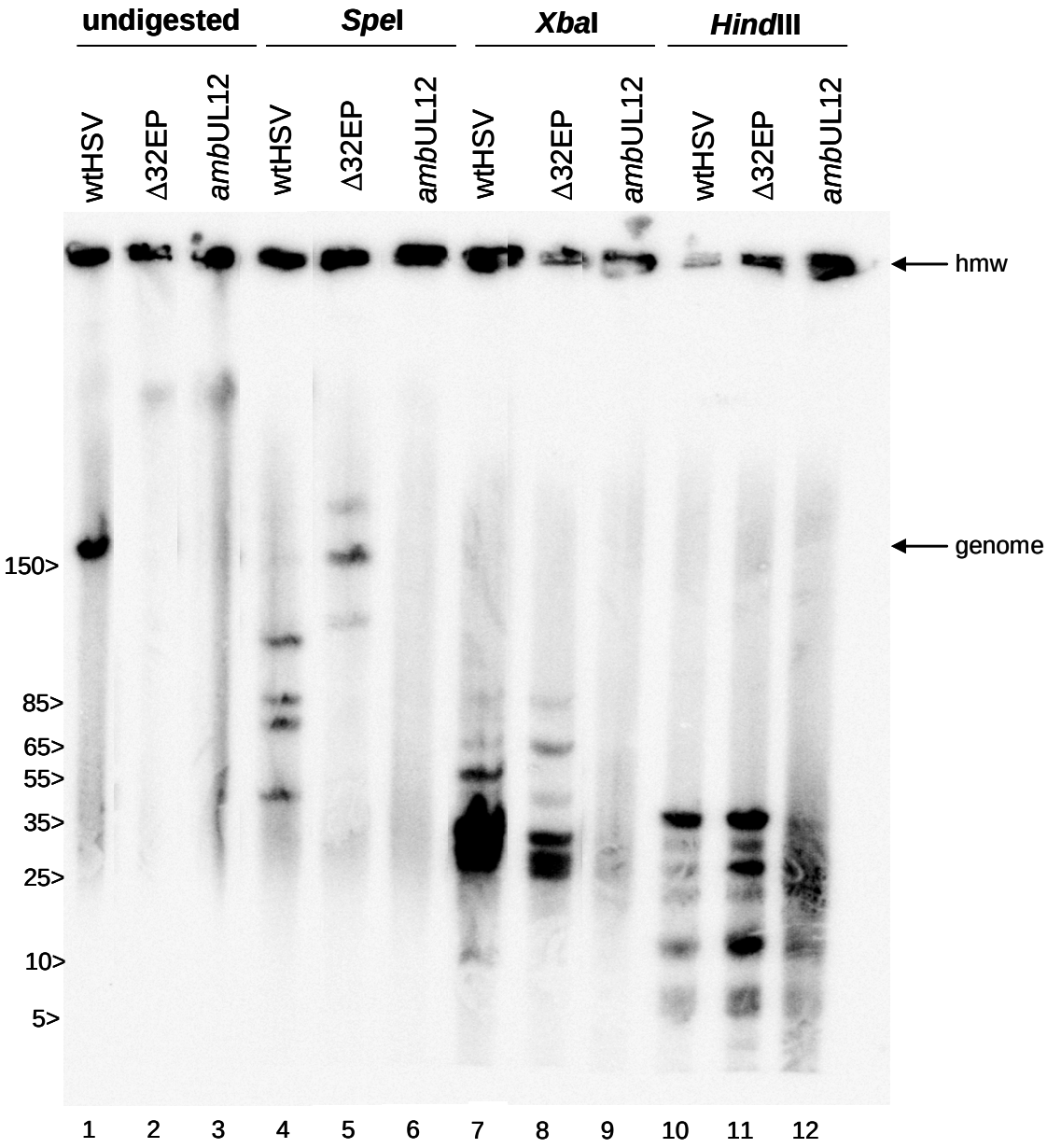

Figure 6.7: PFGE analysis of viral DNA from cells infected with wt HSV-1, Δ32EP or *amb*UL12.

BHK cells were infected with 5 p.f.u./cell wt HSV-1, Δ32EP or *amb*UL12 for 18 hours. Cells were harvested and embedded in agarose blocks. Total DNA was prepared in situ. The DNA within each block was digested with the indicated restriction endonuclease or left undigested. The samples were separated by PFGE using the following parameters: 1% PFGE agarose/0.5 x TBE gel at 6 V/cm for 16 hours at 14ºC with a ramped time of 1-15 sec. The gel was Southern blotted and the membrane probed with ^{32}P labelled fHSV-1 pac+ BAC DNA (encoding the HSV-1 genome). The positions of molecular markers are indicated (in kbp).

from entering the gel or running as discrete bands (lane 6). The DNA produced in the Δ32EP infection generated the three fragments predicted for wt concatemeric DNA, indicating that in this case the *Spe*I fragments generated from concatemers could enter the gel (lane 5).

Cleavage of unit length DNA with *Xba*I is predicted to produce seven fragments from the four possible isomers (11, 34, 25, 29, 55, 36 and 29 kbp). Concatemers should lack four of these, corresponding to terminal fragments (11, 55, 36 and 29 kbp), but yield three novel fragments (65, 84 and 47 kbp) resulting from L segment inversion within the concatemer.

The 84, 65, 55 and 11 kbp bands are clearly visible for the wt HSV-1 DNA in lane 7, along with an intense band falling within the predicted sizes of 25-47 kbp. Only a feint smear of DNA could be seen from *amb*UL12 infected cells rather than discrete bands, again showing that this DNA has a more complex structure than wt HSV-1 (lane 9). The Δ32EP DNA was similar to wt HSV-1, showing discrete bands, although the sizes were in some cases different because only concatemeric DNA was present in the Δ32EP infection (lane 8). A similar result was seen when the DNA was digested with *Hind*III, which is a more frequent cutting enzyme. Again, the wt HSV-1 DNA showed discrete bands of approximate sizes 4 to 40 (lane 10), whereas *amb*UL12 yielded fragments that were somewhat smeared and poorly resolved (lane 12). As before, the DNA from the Δ32EP infected cells behaved similarly to the wt DNA, yielding a similar set of discrete bands (lane 11).

This result confirms that the structure of *amb*UL12 is different to that of wt HSV-1 DNA, and that the frequency of cross-links or other abnormalities is sufficiently high that even when the DNA is cleaved into small fragments (e.g. by *Hind*III) sharp bands are not produced. In contrast, even though terminal fragments are not generated, the overall structure of Δ32EP DNA appears much more similar to wt HSV-1 DNA and discrete bands result from digestion with each of the three enzymes. Therefore, consistent with its lack of interaction with UL12, UL32 does not appear to be involved in resolution of branched structures prior to DNA encapsidation.

6.4 Estimation of the size of UL32 by size exclusion chromatography

Previous work presented in chapter 3 showed that baculovirus-expressed UL32 protein could be partially purified from other baculovirus and cellular proteins using anion exchange chromatography. It was decided to further this chromatography work to determine whether UL32 exists as a monomer or higher-order structure in solution. This was done using a 24 ml Superose 12 HR 10/30 column (Amersham).

Before the sizing of UL32, the column was first calibrated with standard proteins of known molecular weight; IgG (160 kDa), BSA (67 kDa) and ribonuclease A (13.7 kDa). The Superose column was equilibrated with buffer A and a filtered sample of the three proteins, each at a final concentration of 2 mg/ml was applied to the column. The proteins were eluted from the column with 24 ml buffer A. Examination of the UV absorbance trace showed that IgG, BSA and ribonuclease A eluted from the column at 11.41 ml, 11.98 ml and 15.78 ml respectively (data not shown). These standard sizes were then used as molecular markers for the sizing of UL32.

For the sizing of UL32, five flasks of *Sf*21 cells were infected with 5 p.f.u. per cell AcUL32. Forty-eight hours post infection, soluble protein extracts were prepared and filtered (section 2.2.9.1). This extract was applied to the MonoQ column and the fractions containing UL32 collected, as in section 3.4. The UL32 containing fractions were pooled and 200 µl applied to the Superose 12 column and eluted using exactly the same conditions as the markers. 0.5 ml fractions were collected for analysis. These samples were separated by SDS-PAGE and western blotted. UL32 was detected by incubation with R1 followed by HRP-conjugated protein-A and detection with ECL. The UV absorbance trace is shown in figure 6.8A, with the positions of the markers from the previous run marked.

This trace showed a number of discrete peaks. Analysis of all of the fractions on a Coomassie stained gel revealed that the majority of UL32 protein was in fractions B1-B11 (data not shown). A western blot of fractions A15-B13 immunoblotted with R1 is shown in figure 6.8B. Based on the elution of standard proteins, monomers and dimers of UL32 would be expected to elute at approximately fractions B10 and B8 respectively. Although some UL32 is present in these fractions, it is present in the largest amounts in fractions B1-B3 (equivalent to the peak at 7.79 ml) which correspond to the exclusion volume of this

Figure 6.8: Size exclusion chromatography of UL32.

UL32 protein was harvested from AcUL32-infected *Sf*21 cells and fractionated using a MonoQ column, as in the legend to figure 3.3. The peak UL32-containing fractions were pooled and 200 µl applied to a Superose 12 column. Proteins were eluted with 24 ml buffer A and 0.5 ml fractions collected.

A. UV absorbance trace of the Superose fractionation, showing the positions at which each peak was eluted from the column (ml). The positions at which standard molecular marker proteins were eluted from the column on an identical run are marked by the red arrows.

B. 20 µl samples from fractions A15-B13 were boiled in the presence of SDS and separated by electrophoresis on an 8% polyacrylamide gel and western blotted. The membrane was immunoblotted with R1. The position of UL32 is marked and the positions of size markers are indicated (kDa).

A.

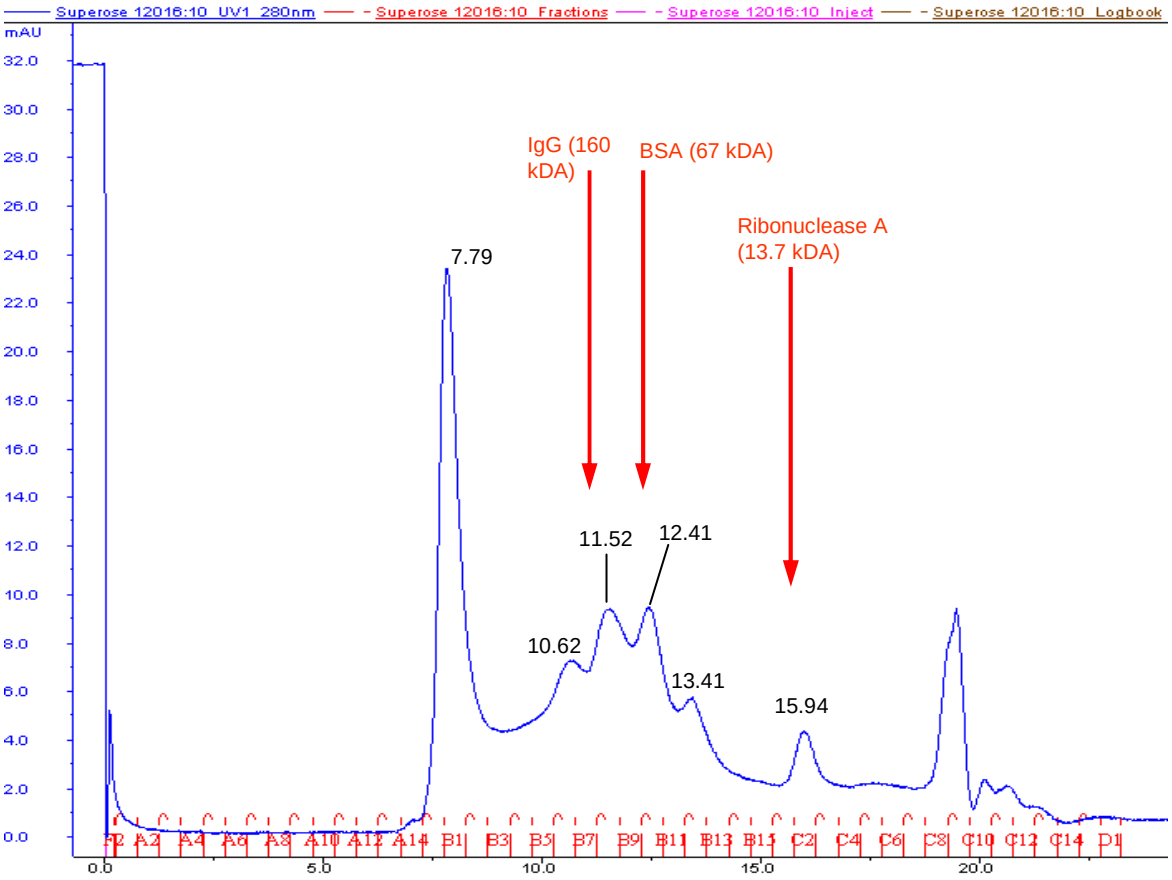
Superose 12016:10_UV1_280nm
Superose 12016:10_Fractions
Superose 12016:10_Inject
Superose 12016:10_Logbook
mAU
IgG (160 kDA)
BSA (67 kDA)
Ribonuclease A (13.7 kDA)
7.79
11.52
12.41
10.62
13.41
15.94

B.

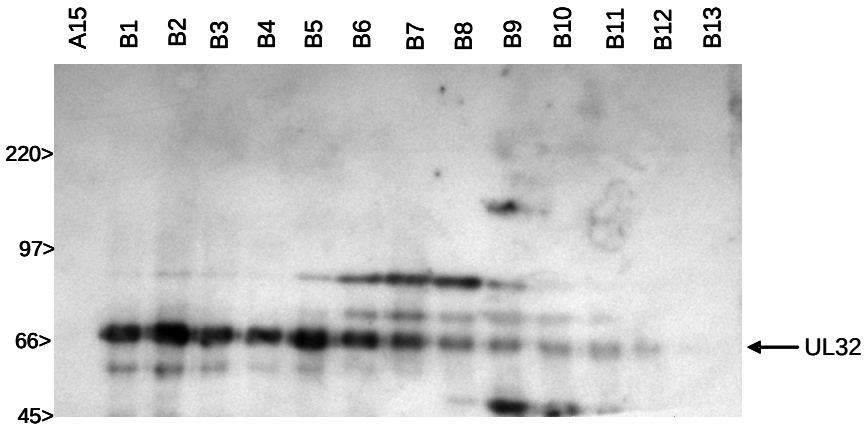
A15
B1
B2
B3
B4
B5
B6
B7
B8
B9
B10
B11
B12
B13
220>
97>
66>
45>
UL32

column. Since the exclusion limit of the Superose 12 HR 10/30 column is approximately $2x10^6$ kDa, this suggests that the UL32 protein exists predominantly as higher order multimers or aggregates which are too large to be separated by this column. However, a heterogeneous range of smaller complexes (monomers, dimers, trimers etc.) also appears to be present.

6.5 Analysis and quantification of the zinc binding properties of UL32

UL32 has CxxC/CxxxC motifs reminiscent of those in many zinc binding proteins and has previously been reported to bind to zinc (Chang *et al.*, 1996). However, the radioactive zinc blot assay used in this study required the electrophoresis of UL32 using a denaturing gel, transfer of the protein onto a blot, and renaturation before the zinc-binding ability could be analysed. It was therefore an indirect method which did not allow for quantification of the zinc-binding. For this reason, I decided to investigate the binding of UL32 to zinc in more detail and attempt to quantitate this interaction. This was done by means of spectroscopic measurement of the zinc displaced from UL32 by p-chloromercuribenzoic acid (PCMB). The concentration of the displaced zinc was determined by chelation with 4-(2-pyridylazo) resorcinol (PAR). PAR changes from a yellow to orange colour with increasing zinc concentrations which can be measured by absorbance at 492 nm (Giraud-Panis *et al.*, 1995; Hunt *et al.*, 1985; Hunt *et al.*, 1984)

6.5.1 Titration of zinc standard solutions

Firstly, it was necessary to determine the range of zinc concentrations over which a linear response was measured and also to confirm that the addition of PCMB had no affect on this reading. Duplicate samples of a range of zinc concentrations were made up and PAR added to a final concentration of 100 µM. One of each sample also included 2 mM PCMB (final concentration). 300 µl of each sample was transferred to the wells of a 96-well plate and read at 492 nm using a Titertek Multiskan Plus plate reader. Zinc concentrations were tested in the range 0-1 M zinc (final concentration), and it was found that the linear range for detection was 0-8 µM. A representative experiment covering this range is shown in figure 6.9.

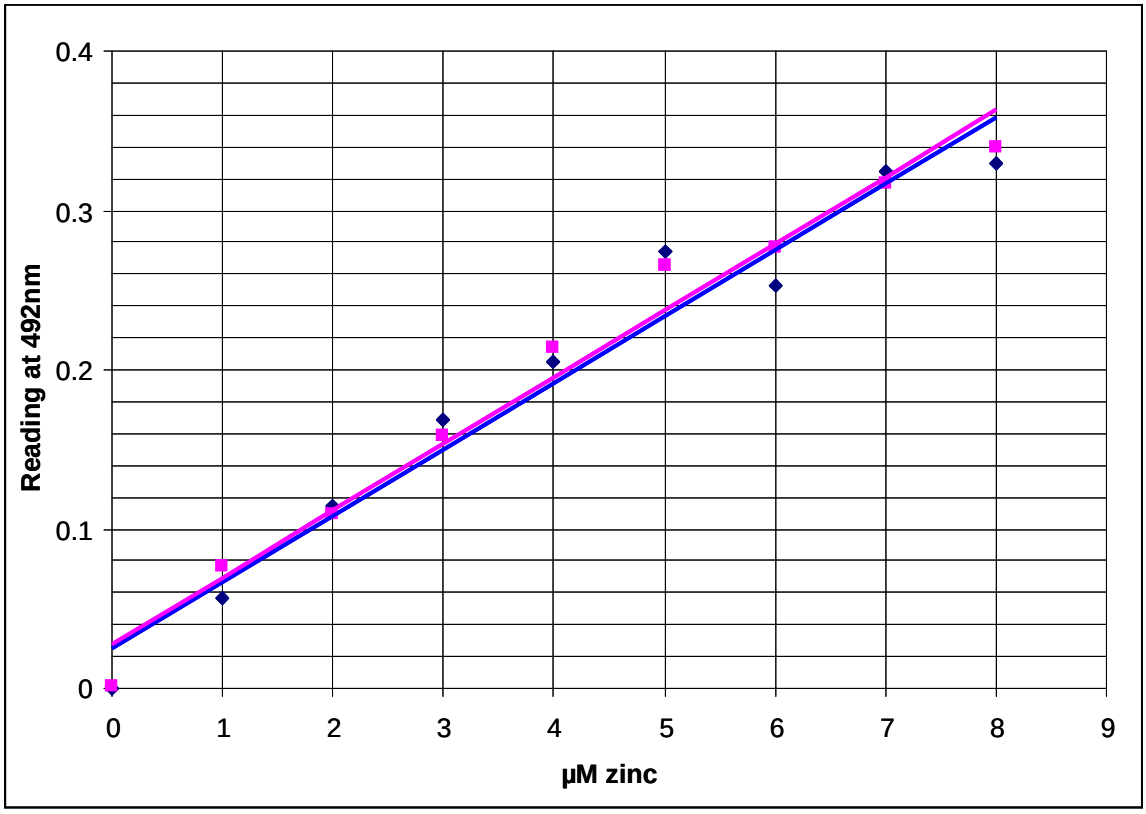

Figure 6.9: Titration of standard zinc chloride concentrations with PAR.

Duplicate samples were made up containing 100 µM PAR and the indicated final concentrations of zinc chloride, with and without 2 mM PCMB. 300 µl of each was transferred to the wells of a microtitre plate and the absorbance measured at 492 nm. Those samples with PCMB are shown in blue, and those without are shown in pink.

6.5.2 MonoQ fractionation of proteins expressed by AcUL32 and pac6 baculoviruses

Peak UL32-containing fractions from the MonoQ fractionation of baculovirus-expressed UL32 were used for the zinc-release assay. However, as this purification is incomplete and these fractions also contain other baculovirus and cellular proteins, an appropriate control needed to be included. This was the parental baculovirus pac6, which is indistinguishable from AcUL32 except that it encodes lacZ rather than UL32. Equivalent fractions eluted from MonoQ purification of protein extracts from AcUL32 and pac6 should differ only in the UL32 or β-galactosidase protein content. Therefore, any difference in zinc release found between the two samples should be due to the binding of zinc by UL32 protein. As the *Sf*21 growth medium used for culture of the *Sf*21 cells contained no additional zinc, the media was supplemented with zinc during the infections.

Ten 175 cm^2 flasks of *Sf*21 cells were infected with either AcUL32 or pac6 and incubated in growth medium supplemented with 10 µM zinc acetate for 48 hours (section 2.2.16.1). Cells were harvested and soluble protein extracts prepared as before, in a total volume of 10 ml buffer A. The protein samples were dialysed against buffer A to remove the unbound zinc from the medium. The two protein extracts were filtered and separately fractionated on a MonoQ column, with 0.5 ml fractions collected.

Figure 6.10 shows the two superimposed UV absorbance traces from the MonoQ fractionations. These are very similar in pattern but a clear peak can be seen in the UL32 sample (brown dashed line) eluted at approximately 0.3 M NaCl (approximately 35 ml), which is not present in the pac6 sample. The two traces are slightly offset relative to one another and so the equivalent fractions from each needed to be identified. This was done by comparing the peaks in the UV absorbance traces and also examination of the pattern of eluted proteins on Coomassie-stained gels for all fractions collected each sample. 25 fractions surrounding and including the UL32 peak, and the corresponding fractions from the pac6 gradient, were renumbered 1-25 and a Coomassie-stained gel of these fractions is shown in figure 6.11. The UL32 protein can be clearly seen in fractions 13 to 21 with the greatest amounts in fractions 13 to 16 (which corresponded to the peak seen at 35 ml on the UV absorbance trace).

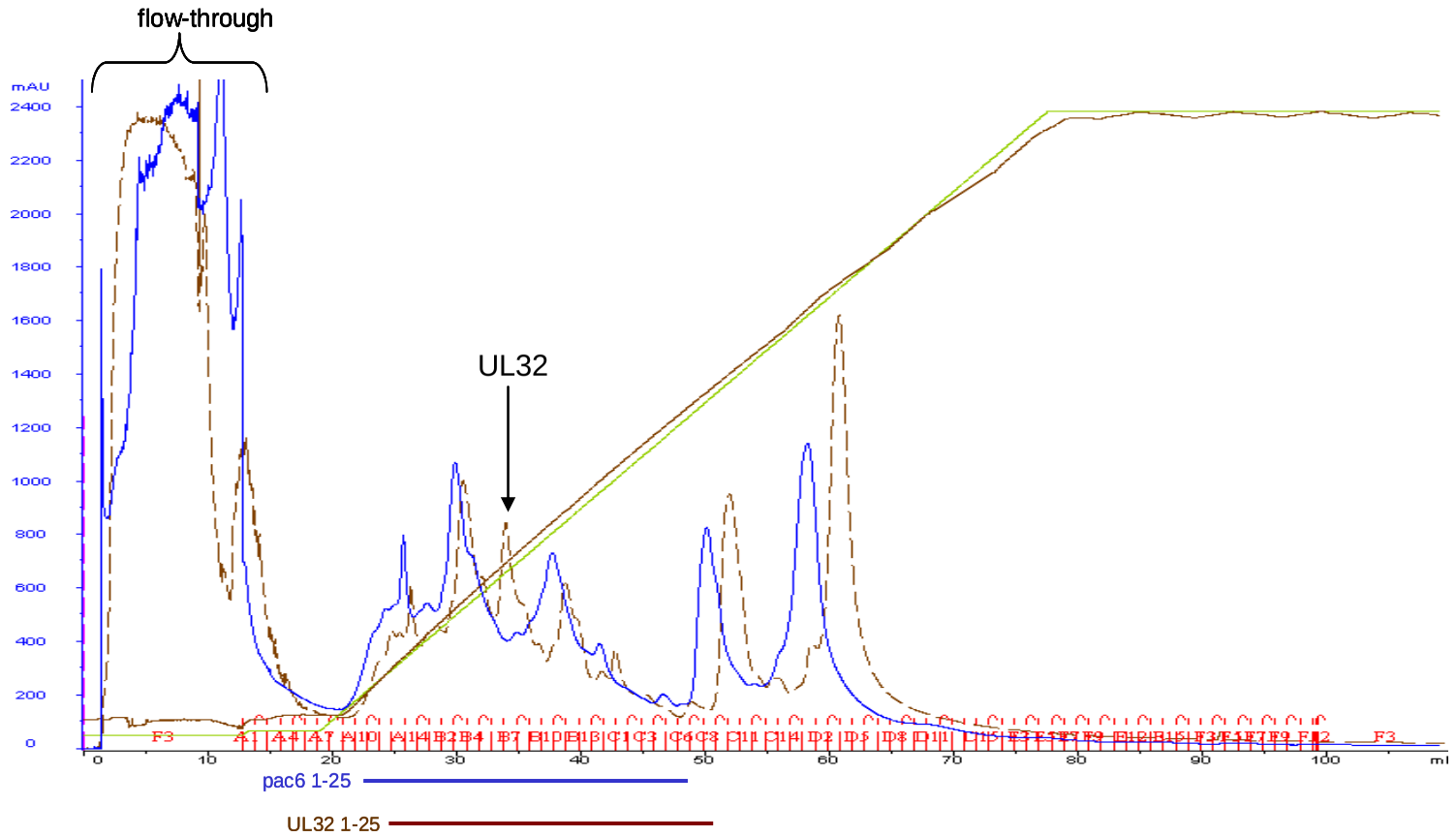

Figure 6.10: MonoQ fractionation of AcUL32 and pac6 protein extracts.

*Sf*21 cells were infected with 5 p.f.u./cell AcUL32 or pac6 and soluble protein extracts prepared 48 h.p.i. These samples were filtered and each applied to a MonoQ column and eluted with a NaCl gradient (50 mM-1 M). 0.5 ml fractions were collected. This trace shows the UV absorbance of UL32 (brown dashed line) and pac6 (blue line) fractions eluted from the column. The flow through for each sample is indicated and the peak corresponding to the UL32 protein is labelled. The green and solid brown lines show the NaCl gradient and conductivity respectively. The positions of the selected fractions (designated 1-25) for each sample are indicated beneath the trace. These samples are analysed in figures 6.11 and 6.12.

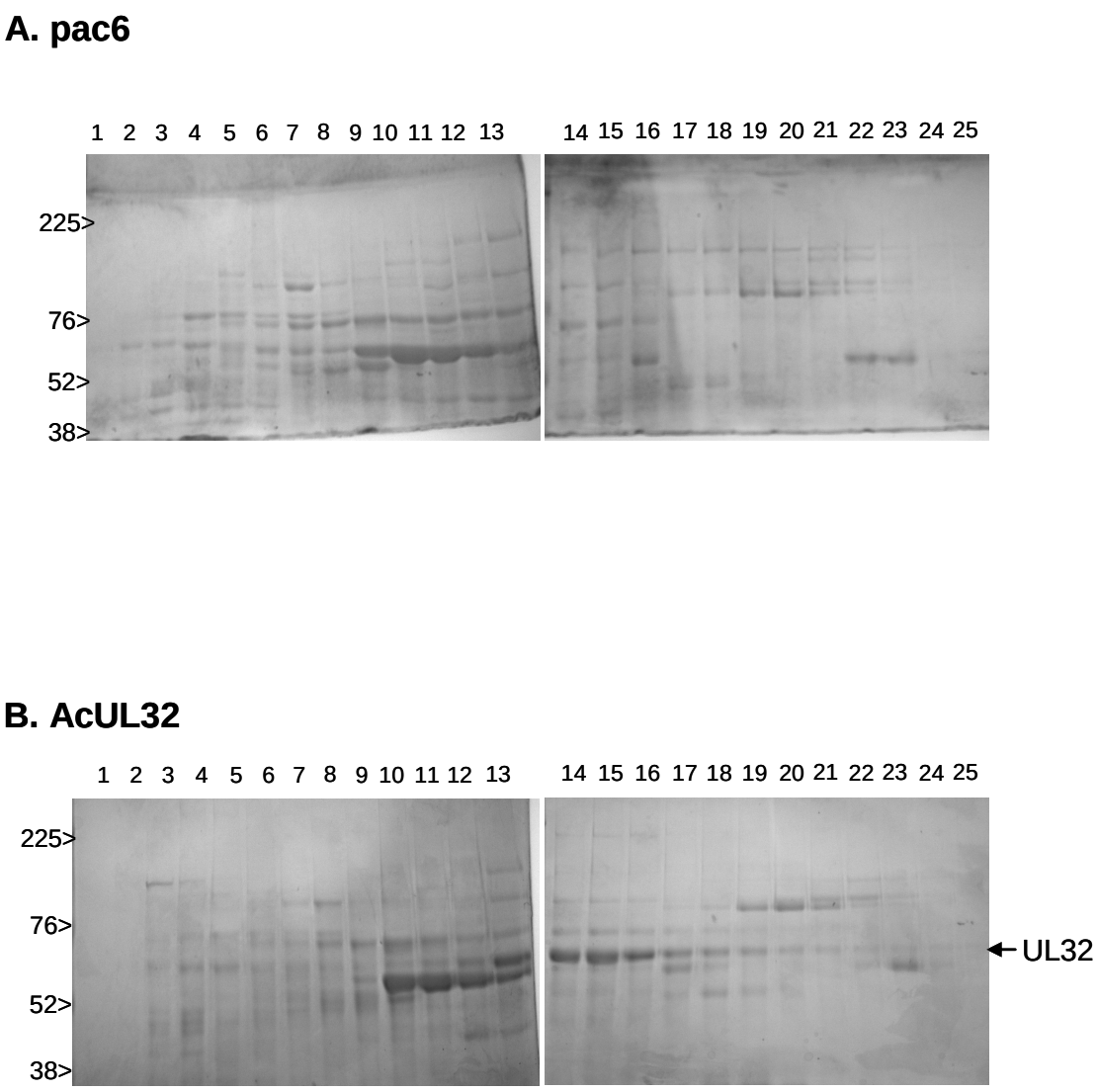

Figure 6.11: Coomassie gel of MonoQ fractionation of pac6 and AcUL32extracts.

UL32-containing fractions and the equivalent pac6 fractions eluted from the MonoQ fractionation shown in figure 6.10 were collected. 20 µl samples were boiled in the presence of SDS and separated by electrophoresis on an 8% polyacrylamide gel. Proteins were detected by staining with Coomassie. The positions of size markers (kDa) and the UL32 protein are indicated.

The total protein concentration of fractions 13-16 from both gradients was determined using a Bradford assay (section 2.2.9.3) and the concentration of UL32 protein in these fractions estimated by subtraction. The UL32 protein was approximately 20% pure and ranged between 100-300 µg/ml, equivalent to a molar concentration of approximately 1.5-4.5 µM UL32.

6.5.3 Quantification of zinc binding of UL32

Work by other groups using similar zinc-release assays has found that four molar equivalents of PCMB are required to remove 1 mole zinc from its bound protein if the zinc is chelated by four cysteine residues (Giraud-Panis *et al.*, 1995; Hunt *et al.*, 1984; Wojtyra *et al.*, 2003). However, as it was not known how much zinc was bound to the UL32 protein, or to any other proteins present in the AcUL32 and pac6 samples, I decided to use an excess of PCMB in these experiments to ensure that all of the zinc would be removed from the proteins, and available to chelate the PAR.

Duplicate 200 µl samples of each protein fraction, 1-25, were mixed with 100 µM PAR, with and without 2 mM PCMB in a total volume of 300 µl, as described in section 2.2.16.2. The absorbance was measured at 492 nm after 5 minutes. The amount of zinc released by each protein sample was determined by comparison with a standard zinc curve. The results from fractions 1-25 are shown in figure 6.12, with the zinc release from the UL32 samples shown in blue and from the pac6 samples shown in pink. A clear peak can be seen in the zinc release from the UL32 gradient fractions 13-16 that is not present in the equivalent pac6 fractions. These are the fractions containing the greatest amount of UL32, and confirm that UL32 does indeed bind to zinc. The stoichiometry of zinc in the UL32 protein was calculated for each of these fractions and is listed in the table below:

Fraction	Concentration of UL32 protein (nmoles)	Concentration of zinc released (nmoles)	Ratio zinc:UL32
13	1.08	1.2	1.11
14	1.22	1.26	1.04
15	0.81	0.93	1.15
16	0.54	0.81	1.5

Table 6.2: Concentration of zinc released from UL32.
The zinc released from samples collected from the fractionation of AcUL32 and pac6 was measured as described in figure 6.12. The zinc released specifically from the UL32 protein was determined by the difference between the UL32 and pac6 values for each equivalent fraction.

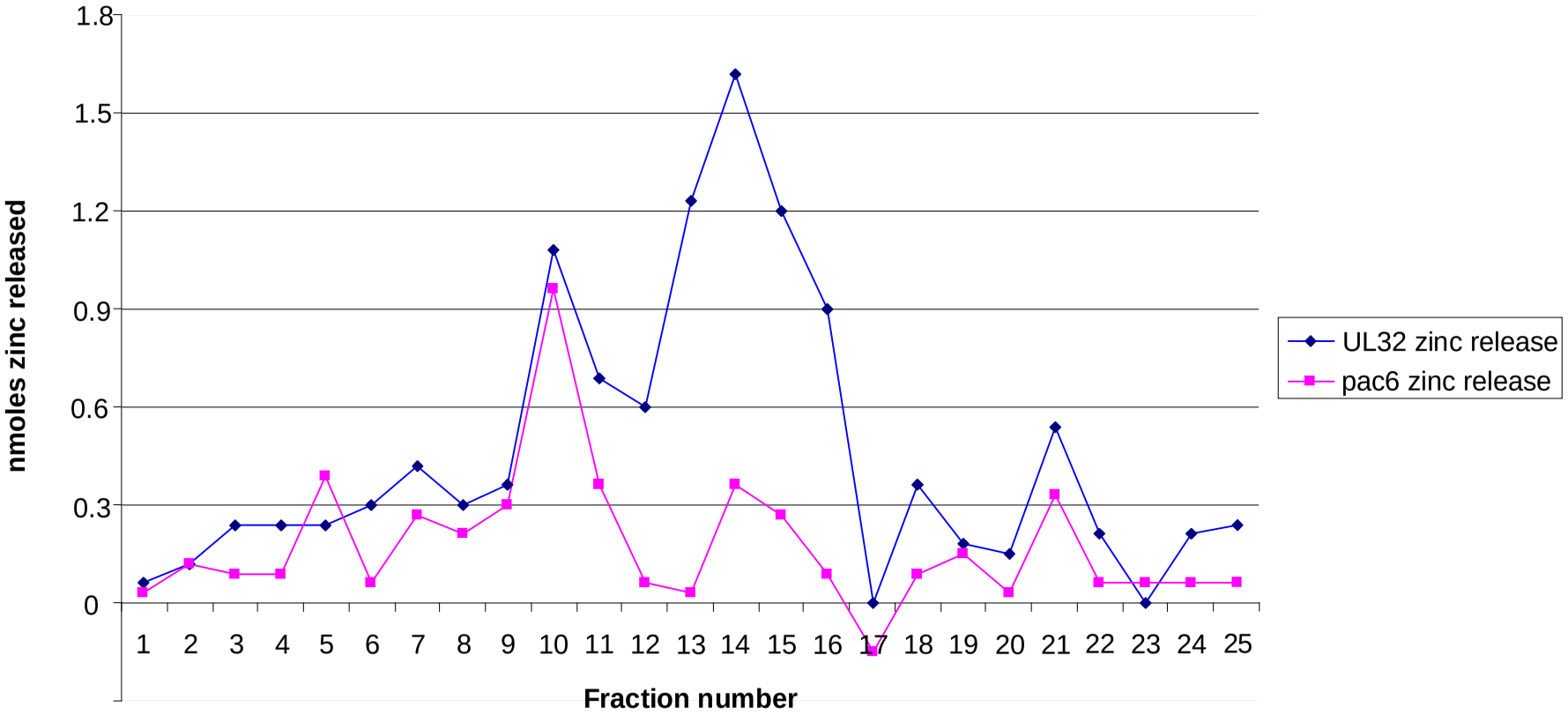

Figure 6.12: Zinc release from UL32-containing fractions eluted from the MonoQ.

Fractions were collected from the MonoQ fractionation of AcUL32 and pac6, as described in the legend to figure 6.10. Duplicate 200 µl protein samples of fractions 1-25 from each fractionation were mixed with 100 µM PAR in the presence and absence of 2 mM PCMB, made up to a total volume of 300 µl. The absorbance was detected at 492 nm and the amount of zinc released upon addition of PCMB calculated by comparison to a standard curve of zinc concentrations. The zinc released from the pac6 fractions is shown in pink and from the AcUL32 fractions is shown in blue.

This zinc release assay was repeated, with similar results. In the second experiment, the peak fraction eluted from the MonoQ contained 0.45 nmoles UL32, and 0.36 nmoles zinc was released specifically from the UL32, giving a ratio of zinc:UL32 of 0.8.

These results from two independent experiments show an approximate 1:1 ratio of zinc release to UL32 protein, suggesting that each molecule of protein binds to one molecule of zinc.

Fraction 16 from the first experiment has a slightly higher zinc:UL32 ratio, but further examination of the Coomassie-stained gel (figure 6.11) showed that the pac6 fraction 16 had an additional band of between 38 and 52 kDa, which is not as prominent in the UL32 fraction 16. It is not known what this band is, but its presence may have led to a small underestimation in UL32 concentration in fraction 16. Using a more highly purified preparation of UL32 in these experiments would be desirable to eliminate such problems, however the attempts to further purify UL32 using a Superose 12 column were unsuccessful (section 6.4).

6.6 Investigation of the DNA binding properties of UL32

For a number of reasons, it was next decided to investigate whether UL32 was able to bind to DNA. Firstly, many zinc-binding proteins have been shown to bind DNA, both sequence specifically and non-specifically. Secondly, data presented in chapter 5 showed that UL32 co-localises with the terminase complex, which is postulated to be directly involved in the recognition, cleavage and packaging of DNA, and therefore UL32 might bind DNA as part of this complex. To analyse the DNA binding properties of UL32, an electrophoresis mobility shift assay (EMSA) was utilised, in which radiolabelled DNA and protein sample are allowed to form protein-DNA complexes that are separated by electrophoresis on non-denaturing gels. This assay relies on the ability of bound protein to reduce the mobility of DNA in the gel, so that protein-DNA complexes will migrate more slowly than the 'free' DNA.

Simultaneous AcUL32 and pac6 infections of *Sf*21 cells were carried out as in section 6.5.2, extracts were fractionated using a MonoQ column and equivalent 0.5 ml fractions collected. 20 µl samples from fractions covering the UL32 peak were analysed by SDS-PAGE and Coomassie staining (as shown in figure 6.13). UL32 was expressed and eluted

A. pac6

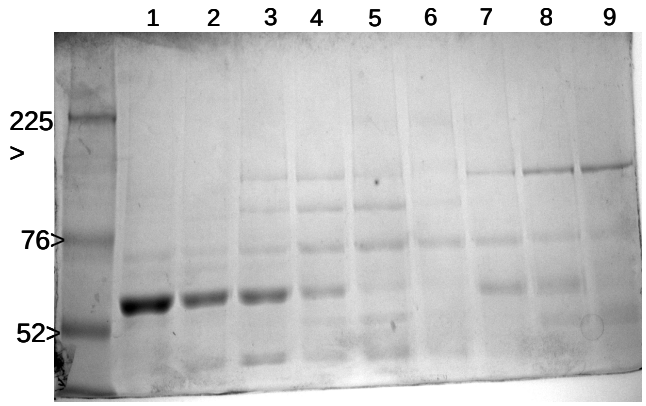

B. AcUL32

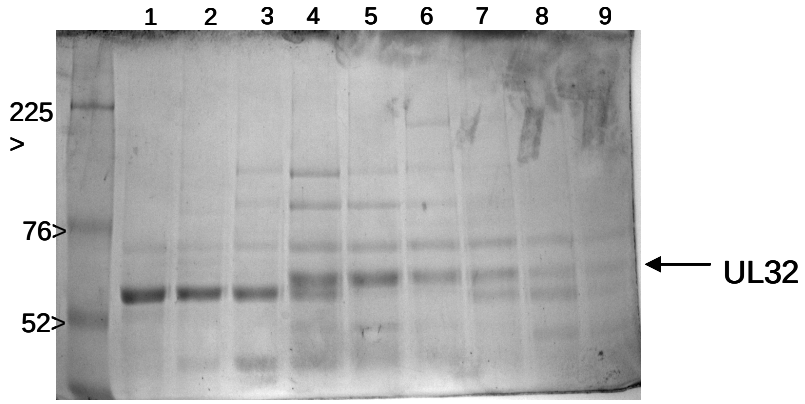

Figure 6.13 : MonoQ fractionation of soluble proteins expressed from AcUL32 and pac6.

*Sf*21 cells were infected with 5 p.f.u./cell pac6 or AcUL32 and soluble proteins harvested after 48 hours. Proteins were applied to a MonoQ column and fractionated as described in the legend to figure 6.10. 20 µl samples of fractions containing UL32 and the equivalent pac6 fractions were separated on 8% polyacrylamide gels and proteins stained using Coomassie Brilliant blue. The position of size makers (kDa) and UL32 are indicated. Note that these fractions are not the same as those in figures 6.10-6.11.

from the MonoQ column in fractions 4-9, with the greatest amount of UL32 in fractions 4-7.

The protein concentration of fractions 1-9 (and the equivalent fractions from the pac6 fractionation) was determined using a Bradford assay. The total protein concentration of the fractions ranged from 200-300 µg/ml, with the peak fractions (4-7) containing approximately 20-30 µg/ml UL32. 10 µl of each protein fraction was used in each experiment, corresponding to approximately 200-300 pg UL32 protein.

6.6.1 Analysis of UL32 binding to the minimal packaging signal

Firstly, the ability of UL32 to specifically bind to the packaging sequences of HSV-1 was analysed, using DNA encoding the minimal packaging signal, Uc-DR1-Ub, excised from pSA1. As previously discussed, the amplicon plasmid pSA1 encodes an HSV-1 origin of replication and also the minimal packaging signal (Abbotts *et al.*, 2000). The 200 bp Uc-DR1-Ub sequence was excised from pSA1 by digestion with *Eco*RI and *Hind*III and purified after separation using agarose gel electrophoresis.

400 ng of the double-stranded Uc-DR1-Ub DNA fragment was 3' end-labelled using 20 µCi α-^{32}P dCTP as described in section 2.2.15.1. This was diluted in H_20 and 3 µl (corresponding to approximately 4 ng DNA) used in each DNA binding reaction. The DNA was incubated with protein fractions to allow binding to occur and protein-DNA complexes were separated by electrophoresis on a non-denaturing polyacrylamide gel (section 2.2.15.2). Gels were fixed and dried and exposed to a phosphorimage screen. A representative gel is shown in figure 6.14.

The free probe migrated predominantly as a sharp fast-migrating band, although some label was detected near the top of the gel, which may have been pSA1 backbone contaminant. The only fractions significantly different to this were 5 and 6 where a complex of intermediate mobility was present. This represents DNA that is present in a protein-DNA complex, showing that proteins within these fractions can bind to the Uc-DR1-Ub DNA fragment. However, no difference was seen between the DNA binding ability of the equivalent UL32 and pac6 fractions, indicating that the DNA binding activity seen was due to baculovirus-expressed or cellular proteins, rather than UL32. Longer exposure of the gel to the phosphor screen did not show any other DNA-protein complexes.

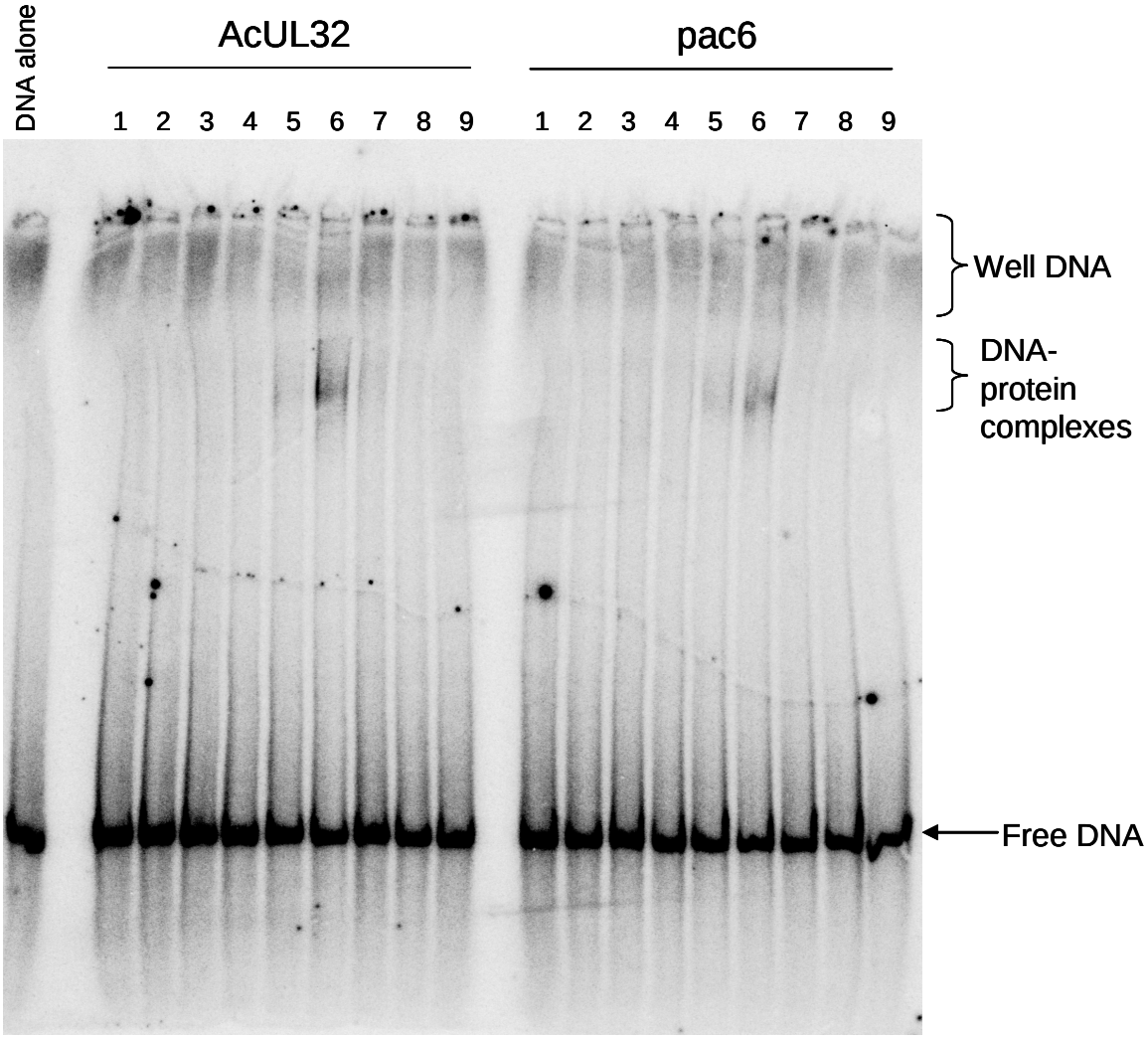

Figure 6.14: UL32 does not bind to the minimal packaging sequence.

Equivalent protein fractions (10 µl each) from the MonoQ fractionation of AcUL32 and pac6 were incubated with 4 ng ^{32}P 3' end-labelled Uc-DR1-Ub for 30 minutes at RT in the presence of buffer M. Samples were separated by electrophoresis on a non-denaturing 8% polyacrylamide gel, fixed and dried. The gel was exposed to a phosphorimage screen.

This experiment was repeated with varied protein and DNA amounts, and varying the concentrations of salt and zinc in the buffer, but no evidence of UL32 binding to the minimal packaging signal Ub-DR1-Uc was seen.

An almost identical result was obtained when the extracts were tested for their ability to bind to a control non-HSV-1 DNA fragment of 200 bp excised from pCMV10 (data not shown). This suggests that at least one protein in fractions 5 and 6 binds non-sequence specifically to dsDNA, but that UL32 itself does not show any DNA binding properties.

6.7 Discussion

This chapter describes further experiments I performed to characterise UL32, in an attempt to better understand its role in the HSV-1 DNA packaging process.

A new UL32 null mutant virus (Δ32EP) was constructed, in which all but 391 bp of the UL32 gene was deleted. This is in contrast to *hr*64, which retains all of the UL32 coding sequence, disrupted by an ICP6:lacZ cassette (Lamberti & Weller, 1998). *hr*64 produces a product of 30 kDa that is recognised by UL32 anti-sera which presumably corresponds to the 273 N-terminal amino acids of UL32, whereas the corresponding product of Δ32EP should contain only 67 N-terminal amino acids. The single step growth curves and amplicon packaging assay showed that Δ32EP is defective for viral growth and DNA packaging, but confirmed the ability of exogenously provided UL32 to complement these defects to levels near to that of wt HSV-1. This indicates that Δ32EP has the same phenotype as *hr*64 and also that the defects seen in Δ32EP were solely due to the deletion of the UL32 gene. These results also confirm that the inserted rpsL-neo-32 cassette had no detrimental effects on the virus. This work has confirmed the packaging-null phenotype for an independently created UL32 mutant HSV-1, indicating that it is unlikely that the N-terminal fragment encoded by *hr*64 performs any function. Finally, the generation of Δ32EP also supports the UL32-null phenotype using a different HSV-1 strain.

The GeneBridges Counter-selection system was a convenient method of generating the UL32 mutant virus. By using homologous recombination between the target gene and a selectable marker, it overcomes many of the limitations associated with conventional methods of cloning. It allows direct introduction of new sequences at any target site within

a cloned full length HSV-1 genome. The mutants can then be easily recovered by transfection of the DNA into mammalian cells. The GeneBridges Counter Selection kit is also designed to allow a second step counter selection, where the selectable marker (rpsL-neo cassette) can be replaced by the original wt gene or a copy carrying a specific mutation. Thus, potentially any of the mutations described in chapter 4 could be recombined into the fΔpac C BAC (section 6.1.4) and viruses generated for further study.

The abilities of UL32 homologues VZV26 and HCMV52 to support the growth and DNA packaging of Δ32EP were analysed, but neither protein was able to substitute for HSV-1 UL32 in these assays. There may be a number of explanations for this which are discussed below.

HCMV is a member of the *Betaherpesvirinae*, and the UL52 protein exhibits relatively poor similarity compared to UL32, with only 17% identical residues, and some large stretches of amino acids that are not present in HSV-1 UL32. UL52 has previously been characterised and was shown to be essential for the cleavage and packaging of HCMV DNA (Borst *et al.*, 2008). However, some differences were reported between HSV-1 UL32 and HCMV UL52. UL52 appears to have a different sub-cellular localisation to HSV-1 UL32, being present in the nucleus but surrounding the replication compartments rather than within them. This might possibly indicate different functions for HCMV UL52 and HSV-1 UL32 and explain the inability of UL52 to substitute for HSV-1 UL32. UL52 also contains a putative nuclear localisation signal not present in HSV-1 UL32 and can enter the nucleus in the absence of other HSV-1 proteins, and so perhaps establishes different protein-protein interactions.

VZV26 has not yet been characterised, but as expected for two viruses belonging to the same sub-family, the VZV and HSV-1 UL32 proteins show a much greater degree of conservation. The two proteins show approximately 45% amino acid identity and this is distributed evenly throughout the protein. Despite being much more similar to HSV-1 UL32 than UL52, VZV26 was still not able to functionally substitute for the HSV-1 protein. A possible explanation is that interactions with other viral proteins are required for UL32 to participate in DNA packaging, and VZV26 may not be able to form these interactions. Although such interactions have not yet been reported in the literature, the possible interaction with the terminase complex described in this thesis may be important.

Previous studies by Mettenleiter's group analysing the functional conservation of some PrV and HSV-1 packaging proteins found that PrV UL32 does not complement the growth of a UL32 mutant HSV-1, but that the HSV-1 UL32 can successfully complement a PrV UL32 mutant virus (Fuchs *et al.*, 2009). PrV and HSV-1 UL32 proteins show approximately 40% amino acid identity (close to the 45% shared by HSV-1 and VZV). It might therefore be interesting to do reciprocals of the experiments I have presented here and examine whether HSV-1 UL32 can similarly support the growth of a UL32 VZV mutant.

I next investigated whether UL32 may have been working in conjunction with the viral alkaline nuclease, UL12, to contribute to the resolution of branched structures in the replicated HSV-1 DNA. However, the two proteins did not interact in an immunoprecipitation assay. Furthermore, the replicated concatemeric DNA produced by Δ32EP showed no evidence of being structurally abnormal when analysed by restriction digest and PFGE. Therefore the CxxC-containing UL32 protein does not appear to contribute towards the alkaline nuclease function of UL12 in an analogous function to the CxxC domain to the phage T4 endonuclease VII protein. This may not be too surprising in view of the different phenotypes of the UL12 and UL32 mutant viruses in non-complementing cells. Whilst *hr*64 and Δ32EP have a completely negative DNA packaging phenotype, the UL12 mutant *amb*UL12 shows only a relatively small reduction in DNA packaging but nevertheless exhibits a 200-1000 fold reduction in virus yield compared to wt HSV-1 (Porter & Stow, 2004b).

Sizing analysis of UL32 using a Superose column suggested that the protein probably forms heterogeneous multimers and aggregates in solution. This also indicates that Superose 12 chromatography is unlikely to be useful for further purification of UL32.

The zinc-binding ability of UL32 was investigated and quantified using a zinc-release colourmetric assay. Chang et al (1996) had previously reported that UL32 was able to bind zinc, as evidenced by the specific binding of radiolabelled zinc to a membrane containing virally-expressed UL32 or a baculovirus-expressed His-tagged UL32 protein. My approach demonstrated the presence of zinc in UL32 more directly, and unlike the zinc blot studies, did not require denaturing and renaturing of the UL32 protein. This was done by measuring the amount of zinc released by protein in solution, and revealed a molar ratio of close to 1:1 zinc:protein.

No zinc finger (ZnF) can be identified within UL32 using prediction programmes, although the region containing the most N-terminal CxxxC motif does show high similarity to the classical Cys_2His_2 (C_2H_2) ZnF motif, as shown below.

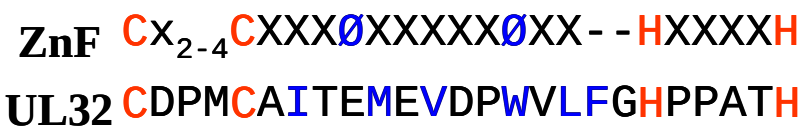

Figure 6.15: Conserved sequence of a C_2H_2 classical Zinc finger motif.
The conserved cysteine and histidines residues are highlighted in red. Ø represents a hydrophobic residue and the hydrophobic residues in UL32 are highlighted in blue.

However, this motif within UL32 contains 14 residues between the second cysteine and first histidines (rather than the consensus 12), and also there is a polar glutamate (E) in the first hydrophobic position. Furthermore, these histidine residues are not well conserved within UL32, with the first His present in only four other herpesvirus sequences, whilst a short stretch including this histidine has been deleted from the *Beta-* and *Gamma-herpesvirina*e. This suggests that these histidines are not essential for the function of UL32 and so are unlikely to be part of a conserved zinc finger.

A number of other viral proteins have been identified containing conserved CxxC motifs that are involved in zinc-binding, including the E6 and E7 proteins of human papilloma virus (HPV). The zinc atoms bound to E7 are co-ordinated by the cysteine residues within the CxxC motifs (Patrick *et al.*, 1992), showing that paired CxxC motifs alone can be used to coordinate zinc atoms, as may be the case in UL32. It is interesting to compare the zinc binding results with my mutational analysis of UL32 showing that the first and third CxxC/CxxxC motifs are absolutely essential for function, whereas when the central CxxC is mutated the UL32 protein retains a degree of function. This might suggest that the zinc atoms in UL32 are chelated by the outer CxxC/CxxxC motifs, and this will be discussed further in chapter 7. It would have been extremely interesting to have examined the zinc-binding ability of the CxxC/CxxxC mutants, but unfortunately time constraints prevented this. 4 moles of PCMB are required to release zinc chelated by 4 cysteine residues and my results could be furthered by performing a titration of PCMB to determine how many cysteines are involved in chelating the zinc.

A common feature of zinc binding proteins is their ability to bind DNA. Since the work presented in chapter 5 suggested that UL32 may form a complex with the terminase, and this enzyme is known to be directly involved in the cleavage and packaging of DNA, the ability of UL32 to bind to DNA was investigated. However an electrophoresis mobility shift assay found no evidence that UL32 bound to either the 200 bp HSV-1 minimal packaging sequence (Uc-DR1-Ub) or a non-HSV-1 control fragment.

EMSAs provide a useful initial study of the DNA binding properties of a protein. However, the fact that these results were negative does not completely eliminate the possibility of UL32 being involved in DNA binding. The UL28 subunit of the terminase was previously reported to bind to a novel DNA confirmation formed by the heat treatment of pac1, whereas it did not bind to the dsDNA sequence (Adelman *et al.*, 2001). Although these results have not been repeated, this raises the possibility that the Uc-DR1-Ub sequence may adopt a different structure within cells which is required for protein binding. In addition, the UL28 homologue in HCMV, UL56, has been shown to interact with single stranded DNA sequences bearing the pac1 and pac2 motifs (Bogner *et al.*, 1998). It might therefore be interesting to determine whether UL32 exhibits DNA binding activity in the presence of the terminase, or when alternative DNA fragments are examined. Another method of detecting DNA binding that could be employed is using chromatin immunoprecipitation (ChIP) which has the advantage of allowing an *in vivo* determination of DNA binding activity. The epitope-tagged recombinant HSV-1 HA32EP might prove useful for testing whether UL32 interacts with DNA *in vivo* and, if so, to which sequences it binds.

Several of the experiments described in this chapter would have benefitted if the UL32 protein was of a higher purity than that achieved by MonoQ column fractionation. This might be possible to achieve by employing additional columns for example hydrophobic interaction chromatography. Alternatively, protein from a different source could be used, for example a bacterially-expressed protein that could be purified by virtue of a suitable cleavable affinity tag (e.g. GST or 6xHis tag). The availability of more highly purified UL32 would also allow alternative zinc-binding assays to be employed, for example atomic absorption spectroscopy or Extended X-ray Absorption Fine Structure spectroscopy (EXAFS). EXAFS has been used along with biochemical approaches for examining the zinc binding properties of HPV E7 (Patrick *et al.*, 1992) and a number of other proteins. These techniques, along with examination of the CxxC/CxxxC mutant proteins, could give a more accurate determination of how the zinc is chelated within the UL32 protein.

7 Discussion

Previous work had identified UL32 as a predominantly cytoplasmic HSV-1 protein essential for the growth of HSV-1 and DNA packaging, although dispensable for viral DNA replication (Chang *et al.*, 1996; Lamberti & Weller, 1998; Sherman & Bachenheimer, 1987; 1988). The work presented in this thesis has in some parts supported this previous characterisation, providing clues as to the function of UL32 within HSV-1 DNA packaging, and also characterising other properties of UL32.

Chapter 4 described the isolation of a panel of 37 insertional mutants and four site-specific mutants of the UL32 protein, in an attempt to characterise the structure-function relationship of UL32 and provide some insight into its role in HSV-1 DNA packaging. The ability of each mutant to support DNA packaging correlated precisely with their capacity to complement the growth of a UL32 mutant virus, *hr*64. This suggests that the only essential function of UL32 involves the DNA packaging pathway. Perhaps unsurprisingly, the functionality of mutants in these two assays also correlated with the degree of conservation within the UL32 protein, with those mutants in the most conserved regions being non-functional and those in areas of low conservation being more tolerant of insertions. The site-specific substitution of the cysteine residues within the conserved CxxC/CxxxC motifs showed that whilst the outer motifs were absolutely essential for the function of UL32, mutation of the central CxxC does not completely abrogate DNA packaging. This is discussed later in greater detail in the context of the zinc-binding properties of UL32. The deletion of the extreme C-terminus (four amino acids) also generated a non-functional protein.

The generation of a recombinant HSV-1 expressing an HA-tagged UL32 protein allowed analysis of the localisation of UL32 within virus infected cells and it was found that UL32 localised entirely to the replication compartments (RCs) at 6 hours post infection. As discussed in section 5.7, this is in contrast to previous reports in which UL32 was found to be either entirely cytoplasmic or predominantly cytoplasmic with a small portion within the RCs. My results indicate that UL32 shows a similar localisation to the other packaging proteins and capsids during infection, as would be expected for a protein involved in DNA packaging. As UL32 is cytoplasmic when expressed alone, there must be a mechanism by which it is directed to the RCs during HSV-1 infection. One possibility was identified by examination of the interactions between UL32 and other HSV-1 proteins.

Immunofluorescence data presented in chapter 5 suggested that UL32 may interact with the terminase complex, as UL32 was relocalised to the nucleus in the presence of the three putative terminase subunits, UL15, UL28 and UL33. Co-transfection with UL15 alone also caused the partial relocalisation of UL32 to the nucleus, indicating that these two proteins might interact with each other perhaps weakly or transiently. It was found that UL15 and UL28 together are sufficient for the complete relocalisation of UL32 to the nucleus, with UL33 appearing to play a minor or no role. The requirement for UL28 suggests that UL32 may also bind to UL28 (possibly using different regions of the protein for interacting with UL15 and UL28), or that the addition of UL28 alters the conformation of UL15, allowing it to interact more strongly with UL32. Co-immunoprecipitation analysis from baculovirus-infected insect cells demonstrated no interaction between UL32 and any of the terminase components proteins alone, supporting the idea that more than one of these subunits are required for stable interaction with UL32.

A recent paper from Yang (2007) showed that the terminase complex forms in the cytoplasm of cells and then is directed into the nucleus by virtue of the NLS within UL15. This might provide the mechanism for the localisation of UL32 to RCs as well, if UL32 can bind to the cytoplasmic terminase complex and be transported into the nucleus. This could be tested by the introduction of a UL15 deletion into HA32EP, to visualise the localisation of UL32 in the absence of UL15.

The localisation of each of the mutants generated in chapter 4 was then examined in this assay and the colocalisation of the mutant UL32 proteins with the terminase proteins correlated almost exactly with their functionality, with 13 of the 15 functional mutants showing complete relocalisation to the nucleus, and the remaining two (in328 and in376) showing partial relocalisation. These data suggest that the interaction with the terminase is essential for UL32 function. Interestingly, however, mutants in328 and in376 were not impaired at all in the complementation and packaging assays. It may be that in these transfection/superinfection assays, enough of these mutant UL32 proteins is localised to the nucleus to allow full functionality. The presence of UL32 in the nucleus is nevertheless not sufficient for packaging to occur, as two mutants (in338 and in398) were both able to completely co-localise with the terminase, but did not support viral growth or DNA packaging. It would be interesting to examine all four of these mutants in the context of a full viral infection to compare their phenotype to wt UL32.

If UL32 does indeed form part of the terminase complex, a number of possibilities can be envisaged for what role it might play. These include: (i) it may ensure that the terminase complex is correctly folded and assembled; (ii) it may mediate the interaction of the terminase with the DNA (iii) it may mediate the interaction of the terminase/DNA complex with the capsid; (iv) it may have an enzymatic role *per se*; (v) it may regulate the enzymatic activities of the terminase. I consider that my results are more consistent with possibilities (iv) or (v), as discussed below.

The three terminase components UL28, UL15 and UL33 have been shown to interact using immunoprecipitation of proteins expressed by recombinant baculoviruses (Beard *et al.*, 2002). This shows that they can form a stable complex in the absence of other HSV-1 proteins and that UL32 is not required to allow the terminase proteins to associate. It may of course be that the situation in infected cells is different, but it seems unlikely that UL32 is required for association of the terminase components. Furthermore, my immunofluorescence data showed that UL33, UL28 and UL15 all localised to the RCs during *hr*64 infection. The terminase proteins UL15 and UL28 have been shown to interact with the portal protein, UL6 and it was proposed that this is the mechanism by which the terminase interacts with the pre-formed capsid (White *et al.*, 2003). I found no interaction between UL32 and UL6, suggesting that UL32 has no involvement in mediating the terminase-capsid interaction.

Possibilities (iv) and (v) appear more likely, in which UL32 either performs an enzymatic activity itself, or in some way activates or regulates the enzymatic activity of the terminase. Bioinformatic analysis failed to reveal any sequence similarity between UL32 and the DNA packaging proteins of either bacteriophage or other DNA viruses excluding herpesviruses. Indeed, BLAST analysis of the UL32 protein sequence retrieved only herpesvirus UL32 gene homologues from the RefSeq protein database. These analyses therefore provided no further clues regarding the function of UL32 and any possible enzymatic activities it might possess. The EMSA presented in section 6.6 did not identify any dsDNA binding activity of UL32, possibly indicating that UL32 does not play a DNA binding role within the terminase. However, as previously discussed, the only DNA binding reported for UL28 required a novel conformation of the DNA (Adelman *et al.*, 2001). Therefore, more work needs to be carried out with varying DNA substrates and possibly investigating the DNA binding of UL32 in the context of the terminase before this possibility can be completely rejected.

A number of accessory proteins have been identified in bacteriophage (especially phage λ) which are directly involved in regulating the packaging process and act in concert with the terminase, for which analogous proteins have not been identified in herpesviruses. One of these is gpFI in phage λ, which is not required for DNA replication but is essential for cleavage at the *cos* sequence and DNA packaging. The exact role of gpFI is unknown but it is thought to be required for the transition of the terminase from a stable but inactive complex to a packaging machine that is capable of translocation of the DNA into the capsid (Catalano & Tomka, 1995). This involves activation of the ATPase subunit (gpA in phage λ) and switching the terminase complex from a form that is specifically bound to *cos* to one which can bind tightly but non-specifically to DNA to allow packaging. An additional protein required in bacteriophage λ packaging is the host protein IHF, which binds to a specific sequence of viral dsDNA and introduces a 180° bend into the DNA, to bring the terminase binding sites into the correct orientation (Ortega & Catalano, 2006). It is possible that UL32 might play a role analogous to one of these proteins in HSV-1 DNA packaging, as an accessory protein for the cleavage and packaging reaction.

Other possibilities do exist, for example UL32 might be required to make capsids competent for DNA packaging to occur. Procapsids and B capsids are produced in the absence of UL32, but these may be unsuitable for packaging. It might be that a transitory association of UL32 with the procapsid is required, for example to "activate" the portal. An interaction between UL32 and the capsid has not been demonstrated making this seem unlikely, but it could be investigated by determining the structure of the capsids produced during wt HSV-1 and *hr*64 or Δ32EP infections by cryo-electron microscopy, to see if they have an altered structure.

It has also previously been suggested that UL32 may act as a chaperone protein involved in the correct localisation of capsids or the capsid proteins VP19C and VP23 to replication compartments (Lamberti & Weller, 1998). CxxC motifs are common in redox chaperone proteins, where they are used for the formation and reduction of disulphide bonds in target proteins, and disulphide bonds have been reported in HSV-2 capsids (Zweig *et al.*, 1979). As previously mentioned, a number of proteins have been identified in viruses such as Sindbis virus and African swine fever virus (ASFV), which act as redox chaperones, using conserved cysteine residues to aid the correct folding of virion components (Cobbold *et al.*, 2001; Parrott *et al.*, 2009). However, unlike UL32, these proteins have well-documented interactions with their target proteins. Furthermore, both of these viruses assemble their capsids in the cytoplasm of cells, which is a much more reducing environment than the

nucleus, and so the requirement for redox chaperones may be different. Sequence analysis of UL32 using the BLAST programmes did not yield any further similarities to proteins involved in redox reactions. This is in contrast to one of the chaperones from ASFV, pB119L, which shows similarity to the Erv1p/Alrp family of sulfhydryl oxidases and so could clearly be identified as a redox-chaperone (Rodriguez *et al.*, 2006). In the work presented here, I found no evidence of mis-localisation of capsids or capsid proteins in *hr*64-infected cells. Furthermore, no disulphide bonds have been found within HSV-1 capsids, and capsid proteins VP19C and VP23 or VP19C and VP5 do not appear to be disulphide-linked (Dr F. Rixon, personal communication). Taking all this data together, it seems unlikely that UL32 acts as a chaperone for the folding or localisation of capsid components.

As discussed in section 5.7, there may be a number of ways in which one protein might influence the localisation of another without a direct interaction, and so it is essential to verify the UL32-terminase interaction using an independent assay. Recent work in our laboratory using insect cells multiply-infected with recombinant baculoviruses encoding UL32, UL28, UL15 and UL33 has demonstrated that UL32 and UL28 can be co-precipitated, although other possible interactions have not yet been studied (Dr N. Stow, personal communication). This supports the theory that UL32 can stably interact with the terminase but not its individual subunits. This work will be furthered to identify the direct interactions between the four proteins.

Work presented in chapter 6 confirmed and quantified the zinc-binding properties of UL32. It was calculated that UL32 bound zinc at an approximate molar ratio of 1:1 zinc: UL32. This work did not identify the residues involved in the zinc chelation, but the cysteine residues are likely to be involved. As previously discussed, many zinc binding proteins chelate the zinc atom using a combination of cysteines and histidines, with four residues (Cys or His) often involved in the chelation of one atom of zinc. As discussed in section 6.7, UL32 does not correspond to a classical C_2H_2 zinc finger (ZnF) protein, but it does show similarity to some C_4-containing ZnFs. These encompass a wide range of proteins that chelate the zinc atoms using 4 cysteines distributed within two CxxC motifs, as reviewd by Grant (2007). However, a number of factors appear to separate UL32 from these identified ZnF proteins. These proteins commonly contain the cysteines residues within close proximity, whereas the CxxC/CxxxC motifs in UL32 are much more widely separated. Many of these proteins also contain multiple ZnF motifs chelating multiple zinc atoms, whereas UL32 encodes only three conserved CxxC/CxxxC motifs. A fourth motif

(CAKC in HSV-1 UL32) is separated from the N-terminal CxxC by only 23 aa, but this fourth motif is not conserved within the herpesviruses, possibly indicating that it is not essential for the function of UL32. However, caution must be applied when using relative conservation in interpreting the zinc-binding properties of UL32, as none of the other herpesvirus UL32 homologues have yet been shown to bind zinc.

The mutational analysis of the CxxC/CxxxC motifs presented in chapter 4 provided information on which residues might be important for zinc binding. Although the second and third CxxC/CxxxC motifs are reminiscent of those found in ZnFs, the functional analysis indicates that the central CxxC is not absolutely essential for a functional protein. Instead, knock-out of either of the outer motifs was sufficient to abrogate function, suggesting that these are the more important residues. If the zinc-binding ability of UL32 is essential for its function, it may be that this central CxxC motif is not involved. A situation can be envisaged in which the native structure of the protein is such that the two terminal regions loop round in close proximity to each other. In this case, the cysteines within the two outer motifs might be involved in zinc chelation, explaining why these are absolutely essential for function of the protein. It would be interesting to introduce the panel of CxxC mutations into baculovirus so that the zinc-binding abilities of these mutated proteins could be examined, in order to determine whether this is the case. Mutational analysis of T4 endonuclease VII revealed that the outer cysteines within the paired CxxC/CxxxC motifs were essential for the zinc-binding(Giraud-Panis *et al.*, 1995), and a similar more detailed mutational analysis could be carried out with UL32 to determine which individual cysteine residues are essential for the function of UL32.

7.1 Future perspectives

While the work presented in this thesis has provided a number of interesting insights into the function of UL32, it also raises many future possibilities to further this work.

A number of other experiments can be designed in order to verify whether there is a direct interaction between UL32 and the terminase complex, and if this is required during normal HSV-1 infection, many of which can be performed using reagents generated in this thesis. The generation of a functional HA-tagged UL32 protein, and its introduction into virus provided a sensitive way to examine the localisation of UL32 during infection. Deletion of

UL15 and/or UL28 from this virus would allow the study of whether the terminase proteins are essential for the correct localisation of UL32. The HA-tag could also be used for immunoprecipitation from HSV-1 infected cells, to examine whether UL32 can interact with the terminase. Some of the non-functional mutants that did not co-localise to the nucleus of transfected cells with the terminase proteins could also be introduced into virus using the Red/Et counter selection method, to analyse their localisation during normal virus infection.

It would be extremely useful to generate a more highly purified preparation of UL32 protein than that which was achieved by MonoQ fractionation. The size exclusion chromatography did not allow for further purification due to the aggregation of UL32, but as mentioned in section 6.7, other chromatography approaches could be used, or affinity purification by use of a tagged-UL32 protein. The generation of the rabbit antisera described in chapter 4 show that by nature, the UL32 protein is immunogenic. A panel of mouse monoclonal antibodies could therefore be isolated (using the immunogen from MonoQ fractionation) which might be useful sensitive reagents. These might possibly provide further information on structurally important regions, for example by testing whether they can block the UL32/terminase interaction.

If a large enough amount of purified UL32 could be obtained, it might be possible to determine the crystallographic structure, which would provide useful insights into the analysis of my mutagenesis experiments by indicating which residues lie near to each other in the native protein. This would allow functional regions of the proteins to be more easily identified, and further site-specific mutagenesis could be carried out. The crystallographic structure would also provide important information as to where the cysteines lie and how the zinc is chelated.

A major step forward would be the development of a cell-free system for HSV-1 DNA packaging similar to those reported for several dsDNA bacteriophage, although this will not be easy because of the poor solubility of several of the HSV-1 proteins. Development of such a system might allow the role of each terminase protein to be confirmed and could also provide a useful assay to investigate whether UL32 is directly required for the cleavage of DNA, or has an alternative role in packaging.

References

Abbotts, A. P., Preston, V. G., Hughes, M., Patel, A. H. & Stow, N. D. (2000). Interaction of the herpes simplex virus type 1 packaging protein UL15 with full-length and deleted forms of the UL28 protein. *J Gen Virol* **81**, 2999-3009.

Adamson, W. E., McNab, D., Preston, V. G. & Rixon, F. J. (2006). Mutational analysis of the herpes simplex virus triplex protein VP19C. *J Virol* **80**, 1537-1548.

Adelman, K., Salmon, B. & Baines, J. D. (2001). Herpes simplex virus DNA packaging sequences adopt novel structures that are specifically recognised by a component of the cleavage and packaging machinery. *PNAS* **98**, 3086-3091.

Ahmed, M., Lock, M., Miller, C. G. & Fraser, N. W. (2002). Regions of the herpes simplex virus type 1 latency-associated transcript that protect cells from apoptosis in vitro and protect neuronal cells in vivo. *J Virol* **76**, 717-729.

André, W., Claus-Henning, N., Kerstin, R., Katinka, D., Victoria, J. A. & Beate, S. (2006). The inner tegument promotes herpes simplex virus capsid motility along microtubules in vitro. *Traffic* **7**, 227-237.

Arbuckle, M. I. & Stow, N. D. (1993). A mutational analysis of the DNA-binding domain of the herpes simplex virus type 1 UL9 protein. *J Gen Virol* **74**, 1349-1355.

Arzul, I., Nicolas, J.-L., Davison, A. J. & Renault, T. (2001). French scallops: A new host for ostreid herpesvirus-1. *Virology* **290**, 342-349.

Baines, J. D., Cunningham, C., Nalwanga, D. & Davison, A. (1997). The U(L)15 gene of herpes simplex virus type 1 contains within its second exon a novel open reading frame that is translated in frame with the U(L)15 gene product. *J Virol* **71**, 2666-2673.

Baines, J. D., Hsieh, C.-E., Wills, E., Mannella, C. & Marko, M. (2007). Electron tomography of nascent herpes simplex virus virions. *J Virol* **81**, 2726-2735.

Baker, M. L., Jiang, W., Rixon, F. J. & Chiu, W. (2005). Common ancestry of herpesviruses and tailed DNA bacteriophages. *J Virol* **79**, 14967-14970.

Banks, L., Purifoy, D. J., Hurst, P. F., Killington, R. A. & Powell, K. L. (1983). Herpes simplex virus non-structural proteins IV. Purification of the virus-induced deoxyribonuclease and characterisation of the enzyme using monoclonal antibodies. *J Gen Virol* **64**, 2249-2260.

Barnard, E. C., Brown, G. & Stow, N. D. (1997). Deletion mutants of the herpes simplex virus type 1 UL8 protein: Effect on DNA synthesis and ability to interact with and influence the intracellular localization of the UL5 and UL52 proteins. *Virology* **237**, 97-106.

Beard, P. M. & Baines, J. D. (2004). The DNA cleavage and packaging protein encoded by the UL33 gene of herpes simplex virus 1 associates with capsids. *Virology* **324**, 475-482.

Beard, P. M., Duffy, C. & Baines, J. D. (2004). Quantification of the DNA cleavage and packaging proteins UL15 and UL28 in A and B capsids of herpes simplex virus type 1. *J Virol* **78**, 1367-1374.

Beard, P. M., Taus, N. S. & Baines, J. D. (2002). DNA cleavage and packaging proteins encoded by genes UL28, UL15, and UL33 of herpes simplex virus type 1 form a complex in infected cells. *J Virol* **76**, 4785-4791.

Beilstein, F., Higgs, M. R. & Stow, N. D. (2009). Mutational analysis of the herpes simplex virus type 1 DNA packaging protein UL33. *J Virol* **83**, 8938-8945.

Bender, F. C., Whitbeck, J. C., Lou, H., Cohen, G. H. & Eisenberg, R. J. (2005). Herpes simplex virus glycoprotein B binds to cell surfaces independently of heparan sulfate and blocks virus entry. *J Virol* **79**, 11588-11597.

Berndt, C., Lillig, C. H. & Holmgren, A. (2008). Thioredoxins and glutaredoxins as facilitators of protein folding. *Biochimica et Biophysica Acta (BBA) - Molecular Cell Research* **1783**, 641-650.

Bhella, D., Rixon, F. J. & Dargan, D. J. (2000). Cryomicroscopy of human cytomegalovirus virions reveals more densely packed genomic DNA than in herpes simplex virus type 1. *Journal of Molecular Biology* **295**, 155-161.

Bishop, D. H. L. (1992). Baculovirus expression vectors. *Seminars in Virology* **3**, 253-264.

Bjornsti, M. A., Reilly, B. E. & Anderson, D. L. (1982). Morphogenesis of bacteriophage phi 29 of Bacillus subtilis: DNA-gp3 intermediate in in vivo and in vitro assembly. *J Virol* **41**, 508-517.

Blanco, L., Bernad, A., Blasco, M. A. & Salas, M. (1991). A general structure for DNA-dependent DNA polymerases. *Gene* **100**.

Blumel, J. & Matz, B. (1995). Thermosensitive UL9 gene function is required for early stages of herpes simplex virus type 1 DNA synthesis. *J Gen Virol* **76**, 3119-3124.

Boehmer, P. E., Dodson, M. S. & Lehman, I. R. (1993). The herpes simplex virus type-1 origin binding protein. DNA helicase activity. *J Biol Chem* **268**, 1220-1225.

Bogner, E., Radsak, K. & Stinski, M. F. (1998). The gene product of human cytomegalovirus open reading frame UL56 binds the pac motif and has specific nuclease activity. *J Virol* **72**, 2259-2264.

Booy, F. P., Newcomb, W. W., Trus, B. L., Brown, J. C., Baker, T. S. & Steven, A. C. (1991). Liquid-crystalline, phage-like packing of encapsidated DNA in herpes simplex virus. *Cell* **64**, 1007-1015.

Booy, F. P., Trus, B. L., Davison, A. J. & Steven, A. C. (1996). The capsid architecture of channel catfish virus, an evolutionarily distant herpesvirus, is largely conserved in the absence of discernible sequence homology with herpes simplex virus. *Virology* **215**, 134-141.

Borst, E. M., Wagner, K., Binz, A., Sodeik, B. & Messerle, M. (2008). The essential human cytomegalovirus gene UL52 is required for cleavage-packaging of the viral genome. *J Virol* **82**, 2065-2078.

Bowman, B. R., Welschhans, R. L., Jayaram, H., Stow, N. D., Preston, V. G. & Quiocho, F. A. (2006). Structural characterization of the UL25 DNA-packaging protein from herpes simplex virus type 1. *J Virol* **80**, 2309-2317.

Bradford, M. (1976). A rapid and sensitive method for the quantitation of microgram quantities of protein utilizing the principle of protein-dye binding. *Anal Biochem* **72**, 248-254.

Brady, R. C. & Bernstein, D. I. (2004). Treatment of herpes simplex virus infections. *Antiviral Research* **61**, 73-81.

Brideau, A. D., Enquist, L. W. & Tirabassi, R. S. (2000). The role of virion membrane protein endocytosis in the herpesvirus life cycle. *Journal of Clinical Virology* **17**, 69-82.

Burch, A. D. & Weller, S. K. (2004). Nuclear sequestration of cellular chaperone and proteasomal machinery during herpes simplex virus type 1 infection. *J Virol* **78**, 7175-7185.

Butcher, S. J., Aitken, J., Mitchell, J., Gowen, B. & Dargan, D. J. (1998). Structure of the human cytomegalovirus B capsid by electron cryomicroscopy and image reconstruction. *Journal of Structural Biology* **124**, 70-76.

Calder, J. M. & Stow, N. (1990). Herpes simplex virus helicase-primase: the UL8 protein is not required for DNA-dependent ATPas and DNA helicase activities. *Nuc Acid Res* **18**, 3573-3578.

Cardone, G., Winkler, D. C., Trus, B. L., Cheng, N., Heuser, J. E., Newcomb, W. W., Brown, J. C. & Steven, A. C. (2007). Visualization of the herpes simplex virus portal in situ by cryo-electron tomography. *Virology* **361**, 426-434.

Catalano, C. E., Cue, D. & Feiss, M. (1995). Virus DNA packaging: the strategy used by phage lambda. *Mol Microbiol* **16**, 1075-1086.

Catalano, C. E. & Tomka, M. A. (1995). Role of gpFI protein in DNA packaging by bacteriophage lambda. *Biochemistry* **34**, 10036-10042.

Cerritelli, M. E., Cheng, N., Rosenberg, A. H., McPherson, C. E., Booy, F. P. & Steven, A. C. (1997). Encapsidated conformation of bacteriophage T7 DNA. *Cell* **91**, 271-280.

Chang, J. T., Schmid, M. F., Rixon, F. J. & Chiu, W. (2007). Electron cryotomography reveals the portal in the herpesvirus capsid. *J Virol* **81**, 2065-2068.

Chang, Y., Poon, A. & Roizman, B. (1996). Properties of the protein encoded by the UL32 open reading frame of herpes simplex virus 1. *J Virol* **70**, 3938-3946.

Chen, Y.-M. & Knipe, D. M. (1996). A dominant mutant form of the herpes simplex virus ICP8 protein decreases viral late gene transcription. *Virology* **221**, 281-290.

Cobbold, C., Windsor, M. & Wileman, T. (2001). A virally encoded chaperone specialised for the folding of the major capsid protein of African swine fever virus. *J Virol* **75**, 7221-7229.

Cockrell, S. K., Sanchez, M. E., Erazo, A. & Homa, F. L. (2009). Role of the UL25 protein in herpes simplex virus DNA encapsidation. *J Virol* **83**, 47-57.

Coller, K. E., Lee, J. I. H., Ueda, A. & Smith, G. A. (2007). The capsid and tegument of the alphaherpesviruses are linked by an interaction between the UL25 and VP1/2 proteins. *J Virol* **81**, 11790-11797.

Conway, J. F., Cockrell, S. K., Copeland, A. M., Newcomb, W. W., Brown, J. C. & Homa, F. L. (2010). Labeling and localization of the herpes simplex virus capsid protein UL25 and its interaction with the two triplexes closest to the penton. *Journal of Molecular Biology* **397**, 575-586.

Crump, C. M., Bruun, B., Bell, S., Pomeranz, L. E., Minson, T. & Browne, H. M. (2004). Alphaherpesvirus glycoprotein M causes the relocalization of plasma membrane proteins. *J Gen Virol* **85**, 3517-3527.

Crumpacker, C. S. & Schaffer, P. A. (2002). New anti-HSV therapeutics target the helicase-primase complex. *Nat Med* **8**, 327-328.

Dasgupta, A. & Wilson, D. (1999). ATP depletion blocks herpes simplex virus DNA packaging and capsid maturation. *J Virol* **73**, 2006-2015.

Davison, A. (1992). Channel catfish virus: a new type of herpesvirus. *Virology* **186**, 9-14.

Davison, A. & Clements, J. B. (1997). Herpesviruses: general properties. In *Topley and Wilson's principles of bacteriology, virology and immunology*, 9 edn. Edited by B. W. J. Maly & L. H. Collier. London: Edward Arnold.

Davison, A., Eberle, R., Ehlers, B., Hayward, G., McGeoch, D., Minson, A., Pellett, P., Roizman, B., Studdert, M. & Thiry, E. (2009). The order Herpesvirales. *Archives of Virology* **154**, 171-177.

Davison, A. J. (2002). Evolution of the herpesviruses. *Veterinary Microbiology* **86**, 69-88.

Davison, A. J. & Davison, M. D. (1995). Identification of structural proteins of channel catfish virus by mass spectrometry. *Virology* **206**, 1035-1043.

Davison, A. J. & Scott, J. E. (1983). Molecular cloning of the varicella-zoster virus genome and derivation of six restriction endonuclease maps. *J Gen Virol* **64**, 1811-1814.

Davison, A. J. & Scott, J. E. (1986). The complete DNA sequence of varicella-zoster virus. *J Gen Virol* **67**, 1759-1816.

Davison, A. J., Trus, B. L., Cheng, N., Steven, A. C., Watson, M. S., Cunningham, C., Deuff, R.-M. L. & Renault, T. (2005). A novel class of herpesvirus with bivalve hosts. *J Gen Virol* **86**, 41-53.

Davison, A. J. & Wilkie, N. M. (1981). Nucleotide sequences of the joint between the L and S segments of herpes simplex virus types 1 and 2. *J Gen Virol* **55**, 315-331.

de Bruyn Kops, A., Uprichard, S. L., Chen, M. & Knipe, D. M. (1998). Comparison of the intranuclear distributions of herpes simplex virus proteins involved in various viral functions. *Virology* **252**, 162-178.

de Massy, B., Weisberg, R. A. & Studier, F. W. (1987). Gene 3 endonuclease of bacteriophage T7 resolves conformationally branched structures in double-stranded DNA. *Journal of Molecular Biology* **193**, 359-376.

Deiss, L., Chou, J. & Frenkel, N. (1986). Functional domains within the a sequence involved in the cleavage-packaging of herpes simplex virus DNA. *J Virol* **59**, 605-618.

Deng, B., O'Connor, C. M., Kedes, D. H. & Zhou, Z. H. (2007). Direct visualization of the putative portal in the Kaposi's sarcoma-associated herpesvirus capsid by cryoelectron tomography. *J Virol* **81**, 3640-3644.

Desai, P., Sexton, G. L., McCaffery, J. M. & Person, S. (2001). A null mutation in the gene encoding the herpes simplex virus type 1 UL37 polypeptide abrogates virus maturation. *J Virol* **75**, 10259-10271.

Desai, P. J. (2000). A null mutation in the UL36 gene of herpes simplex virus type 1 results in accumulation of unenveloped DNA-filled capsids in the cytoplasm of infected cells. *J Virol* **74**, 11608-11618.

Digard, P., Bebrin, W. R., Weisshart, K. & Coen, D. M. (1993). The extreme C terminus of herpes simplex virus DNA polymerase is crucial for functional interaction with processivity factor UL42 and for viral replication. *J Virol* **67**, 398-406.

Dittmer, A. & Bogner, E. (2006). Specific short hairpin RNA-mediated inhibition of viral DNA packaging of human cytomegalovirus. *FEBS Letters* **580**, 6132-6138.

Dodson, M. S. & Lehman, I. R. (1991). Association of DNA helicase and primase activities with a subassembly of the herpes simplex virus 1 helicase-primase composed of the UL5 and UL52 gene products. *PNAS* **88**, 1105-1109.

Dohner, K., Wolfstein, A., Prank, U., Echeverri, C., Dujardin, D., Vallee, R. & Sodeik, B. (2002). Function of dynein and dynactin in herpes simplex virus capsid transport. *Mol Biol Cell* **13**, 2795-2809.

Dwyer, D. & Cunningham, A. (2002). Herpes simplex and varicella-zoster virus infections. *Med J Aust* **177**, 267-273.

Elias, P. & Lehman, I. R. (1998). Interaction of origin binding protein with an origin of replication of herpes simplex virus 1. *PNAS* **85**, 2959-2963.

Everett, R., Sourvinos, G., Leiper, C., Clements, J. & Orr, A. (2004). Formation of nuclear foci of the herpes simplex type 1 regulatory protein ICP4 at early times of infection: localization, dynamics, recruitment of ICP27, an evidence for the de novo induction of ND10-like complexes. *J Virol* **78**, 1903-1917.

Everett, R. D., Freemont, P., Saitoh, H., Dasso, M., Orr, A., Kathoria, M. & Parkinson, J. (1998). The disruption of ND10 during herpes simplex virus

infection correlates with the Vmw110- and proteasome-dependent loss of several PML isoforms. *J Virol* **72**, 6581-6591.

Everett, R. D. & Murray, J. (2005). ND10 components relocate to sites associated with herpes simplex virus type 1 nucleoprotein complexes during virus infection. *J Virol* **79**, 5078-5089.

Farley, C. A., Banfield, W. G., Kasnic, J. R. G. & Foster, W. S. (1972). Oyster herpes-type virus. *Science* **178**, 759-760.

Farnsworth, A., Wisner, T., Webb, M., Roller, R., Cohen, G. H., Eisenberg, R. J. & Johnson, D. C. (2007). Herpes siplex virus glycoproteins gB and gH function in fusion between the virion envelope and the outer nuclear membrane. *PNAS* **104**, 10187-10192.

Feierbach, B., Piccinotti, S., Bisher, M., Denk, W. & Enquist, L. W. (2006). Alpha-herpesvirus infection induces the formation of nuclear actin filaments. *PLoS Pathog* **2**, eg85.

Feiss, M. & Catalano, C. E. (2005). Bacteriophage lambda terminase and the mechanisms of viral DNA packaging. In *Viral Genome Packaging Machines: Genetics, Structure and Mechanism*, pp. 5-39. Edited by C. E. Catalano. New York: Kluwer Academic/ Plenum Publishers.

Fomenko, D. E. & Gladyshev, V. N. (2003). Identity and functions of CxxC-derived motifs. *Biochemistry* **42**, 11214-11225.

Fruh, K., Ahn, K., Djaballah, H., Sempe, P., van Endert, P. M., Tampe, R., Peterson, P. A. & Yang, Y. (1995). A viral inhibitor of peptide transporters for antigen presentation. *Nature* **375**, 415-418.

Fuchs, W., Klupp, B. G., Granzow, H., Leege, T. & Mettenleiter, T. C. (2009). Characterisation of pseudorabies virus (PrV) cleavage-encapsidation proteins and functional complementation of PrV pUL32 by the homologous protein of herpes simplex virus type 1. *J Virol* **83**, 3930-3943.

Fuchs, W., Klupp, B. G., Granzow, H., Osterrieder, N. & Mettenleiter, T. C. (2002). The interacting UL31 and UL34 gene products of pseudorabies virus are involved in egress from the host-cell and represent components of primary enveloped but not mature virions. *J Virol* **76**, 364-378.

Fujisawa, H. & Morita, M. (1997). Phage DNA packaging. *Genes Cells* **2**, 537-545.

Garber, D. A., Beverley, S. M. & Coen, D. M. (1993). Demonstration of circularization of herpes simplex virus DNA following infection using pulsed field gel electrophoresis. *Virology* **197**, 459-462.

Garner, J. A. (2003). Herpes simplex virion entry into and intracellular transport within mammalian cells. *Advanced Drug Delivery Reviews* **55**, 1497-1513.

Gasteiger, E., Gattiker, A., Hoogland, C., Ivanyi, I., Appel, R. D. & Bairoch, A. (2003). ExPASy: the proteomics server for in-depth protein knowledge and analysis. *Nucl Acids Res* **31**, 3784-3788.

Geraghty, R. J., Krummenacher, C., Cohen, G. H., Eisenberg, R. J. & Spear, P. G. (1998). Entry of alphaherpesviruses mediated by poliovirus receptor-related protein 1 and poliovirus receptor. *Science* **280**, 1618-1620.

Gibson, W. & Roizman, B. (1971). Compartmentalization of spermine and apermidine in the herpes simplex virion. *PNAS* **68**, 2818-2821.

Gibson, W. & Roizman, B. (1972). Proteins specified by herpes simplex virus VIII. Characterization and composition of multiple capsid forms of subtypes 1 and 2. *J Virol* **10**, 1044-1052.

Giraud-Panis, M.-J. E., Duckett, D. R. & Lilley, D. M. J. (1995). The modular character of a DNA junction-resolving enzyme: A zinc-binding motif in bacteriophage T4 endonuclease VII. *Journal of Molecular Biology* **252**, 596-610.

Grant, R., Crossley, M. & Mackay, J. (2007). Zinc-finger genes. In *ENCYCLOPEDIA OF LIFE SCIENCES*. http://www.els.net [doi:10.1002/9780470015902.a0005047.pub2].

Granzow, H., Klupp, B. G., Fuchs, W., Veits, J., Osterrieder, N. & Mettenleiter, T. C. (2001). Egress of alphaherpesviruses: Comparative ultrastructural study. *J Virol* **75**, 3675-3684.

Grondin, B. & DeLuca, N. (2000). Herpes simplex virus type 1 ICP4 promotes transcription preinitiation complex formation by enhancing the binding of TFIID to DNA. *J Virol* **74**, 11504-11510.

Grunewald, K., Desai, P., Winkler, D. C., Heymann, J. B., Belnap, D. M., Baumeister, W. & Steven, A. C. (2003). Three-dimensional structure of herpes simplex virus from cryo-electron tomography. *Science* **302**, 1396-1398.

Guo, P. X., Erickson, S. & Anderson, D. (1987). A small viral RNA is required for in vitro packaging of bacteriophage phi 29 DNA. *Science* **236**, 690-694.

Hagglund, R. & Roizman, B. (2004). Role of ICP0 in the strategy of conquest of the host cell by herpes simplex virus 1. *J Virol* **78**, 2169-2178.

Halford, W. P. & Schaffer, P. A. (2001). ICP0 is required for efficient reactivation of herpes simplex virus type 1 from neuronal latency. *J Virol* **75**, 3240-3249.

Hamatake, R. K., Bifano, M., Hurlburt, W. W. & Tenney, D. J. (1997). A functional interaction of ICP8, the herpes simplex virus single- stranded DNA-binding protein, and the helicase-primase complex that is dependent on the presence of the UL8 subunit. *J Gen Virol* **78**, 857-865.

Hammarsten, O., Yao, X. & Elias, P. (1996). Inhibition of topoisomerase II by ICRF-193 prevents efficient replication of herpes simplex virus type 1. *J Virol* **70**, 4523-4529.

Hardwicke, M. A. & Sandri-Goldin, R. M. (1994). The herpes simplex virus regulatory protein ICP27 contributes to the decrease in cellular mRNA levels during infection. *J Virol* **68**, 4797-4810.

Hayward, G., Jacob, R., Wadsworth, S. & Roizman, B. (1975). Anatomy of herpes simplex virus DNA: Evidence for four populations that differ in the relative orientations of their long and short components. *Proc Nat Acad Sci USA* **72**, 4243-4247.

Herold, B. C., Visalli, R. J., Susmarski, N., Brandt, C. R. & Spear, P. G. (1994). Glycoprotein C-independent binding of herpes simplex virus to cells requires cell surface heparan sulphate and glycoprotein B. *J Gen Virol* **75**, 1211-1222.

Higgs, M. R., Preston, V. G. & Stow, N. D. (2008). The UL15 protein of herpes simplex virus type 1 is necessary for the localization of the UL28 and UL33 proteins to viral DNA replication centres. *J Gen Virol* **89**, 1709-1715.

Hodge, P. D. & Stow, N. D. (2001). Effects of mutations within the herpes simplex virus type 1 DNA encapsidation signal on packaging efficiency. *J Virol* **75**, 8977-8986.

Holmes, D. S. & Quigley, M. (1981). A rapid boiling method for the preparation of bacterial plasmids. *Analytical Biochemistry* **114**, 193-197.

Homa, F. & Brown, J. (1997). Capsid assembly and DNA packaging in herpes simplex virus. *Reviews in Medical Virology* **7**, 107-122.

Honess, R. & Roizman, B. (1974). Regulation of herpes virus macromolecular synthesis I: Cascade regulation of the synthesis of the three groups of proteins. *J Virol* **14**, 8-19.

Hong, Z., Beaudet-Miller, M., Durkin, J., Zhang, R. & Kwong, A. D. (1996). Identification of a minimal hydrophobic domain in the herpes simplex virus type 1 scaffolding protein which is required for interaction with the major capsid protein. *J Virol* **70**, 533-540.

Huff, J. L. & Barry, P. A. (2003). B virus (Cercopithecine herpesvirus 1) infection in humans and macaques: potential for zoonotic disease. *Emerging Infectious Diseases* **9**, 246-250.

Hunt, J. B., Neece, S. H. & Ginsburg, A. (1985). The use of 4-(2-pyridylazo)resorcinol in studies of zinc release from Escherichia coli aspartate transcarbamoylase. *Analytical Biochemistry* **146**, 150-157.

Hunt, J. B., Neece, S. H., Schachman, H. K. & Ginsburg, A. (1984). Mercurial-promoted Zn2+ release from Escherichia coli aspartate transcarbamoylase. *Journal of Biological Chemistry* **259**, 14793-14803.

Hutchinson, L., Browne, H., Wargent, V., Davis-Poynter, N., Primorac, S., Goldsmith, K., Minson, A. C. & Johnson, D. C. (1992). A novel herpes simplex virus glycoprotein, gL, forms a complex with glycoprotein H (gH) and affects normal folding and surface expression of gH. *J Virol* **66**, 2240-2250.

Hwang, J.-S. & Bogner, E. (2002). ATPase activity of the terminase subunit pUL56 of human cytomegalovirus. *J Biol Chem* **277**, 6943-6948.

Hwang, Y. & Feiss, M. (1996). Mutations affecting the high affinity ATPase center of gpA, the large subunit of bacteriophage lambda terminase, inactivate the endonuclease activity of terminase. *Journal of Molecular Biology* **261**, 524-535.

Igarashi, K., Fawl, R., Roller, R. J. & Roizman, B. (1993). Construction and properties of a recombinant herpes simplex virus 1 lacking both S-component origins of DNA synthesis. *J Virol* **67**, 2123-2132.

Itzhaki, R. (2004). Herpes simplex virus type 1, apolipoprotein E and Alzheimer's disease. *Herpes* **11**, 77A-82A.

Johnson, D. C. & Huber, M. T. (2002). Directed egress of animal viruses promotes cell-to-cell spread. *J Virol* **76**, 1-8.

Jones, C. (2003). Herpes simplex virus type 1 and bovine herpesvirus 1 latency. *Clin Microbiol Rev* **16**, 79-95.

Jones, D. T. (1999). Protein secondary structure prediction based on position-specific scoring matrices. *Journal of Molecular Biology* **292**, 195-202.

Joseph, S. P. (1999). Epstein-Barr virus: The first human tumor virus and its role in cancer. *Proceedings of The Association of American Physicians* **111**, 573-580.

Kelly, B. J., Fraefel, C., Cunningham, A. L. & Diefenbach, R. J. (2009). Functional roles of the tegument proteins of herpes simplex virus type 1. *Virus Research* **145**, 173-186.

Kemper, B. & Garabett, M. (1981). Studies on T4-head maturation. 1. Purification and characterization of gene-49-controlled endonuclease. *European Journal of Biochemistry* **115**, 123-131.

Kemper, B. & Janz, E. (1976). Function of gene 49 of bacteriophage T4. I. Isolation and biochemical characterization of very fast-sedimenting DNA. *J Virol* **18**, 992-999.

Klupp, B. G., Granzow, H. & Mettenleiter, T. C. (2000). Primary envelopment of pseudorabies virus at the nuclear membrane requires the UL34 gene product. *J Virol* **74**, 10063-10073.

Knopf, K. W. (1979). Properties of herpes simplex virus DNA polymerase and characterization of its associated exonuclease activity. *European Journal of Biochemistry* **98**, 231-244.

Kondabagil, K. R., Zhang, Z. & Rao, V. B. (2006). The DNA translocating ATPase of bacteriophage T4 packaging motor. *J Mol Biol* **363**, 786-799.

Koslowski, K. M., Shaver, P. R., Casey, J. T., II, Wilson, T., Yamanaka, G., Sheaffer, A. K., Tenney, D. J. & Pederson, N. E. (1999). Physical and functional interactions between the herpes simplex virus UL15 and UL28 DNA cleavage and packaging proteins. *J Virol* **73**, 1704-1707.

Kristie, T. M. & Roizman, B. (1986). DNA-binding site of major regulatory protein alpha 4 specifically associated with promoter-regulatory domains of alpha genes of herpes simplex virus 1. *PNAS* **83**, 4700-4704.

Kristie, T. M., Vogel, J. L. & Sears, A. E. (1999). Nuclear localization of the C1 factor (host cell factor) in sensory neurons correlates with reactivation of herpes simplex virus from latency. *PNAS* **96**, 1229-1233.

Kubat, N. J., Amelio, A. L., Giordani, N. V. & Bloom, D. C. (2004). The herpes simplex virus type 1 latency-associated transcript (LAT) enhancer/rcr is hyperacetylated during latency independently of LAT transcription. *J Virol* **78**, 12508-12518.

La Boissiere, S., Hughes, T. & O'Hare, P. (1999). HCF-dependent nuclear import of VP16. *EMBO J* **18**, 480-489.

Lamberti, C. & Weller, S. K. (1998). The herpes simplex virus type 1 cleavage/packaging protein, UL32, is involved in efficient localization of capsids to replication compartments. *J Virol* **72**, 2463-2473.

Laquerre, S., Argnani, R., Anderson, D. B., Zucchini, S., Manservigi, R. & Glorioso, J. C. (1998). Heparan sulfate proteoglycan binding by herpes simplex virus type 1 glycoproteins B and C, which differ in their contributions to virus attachment, penetration, and cell-to-cell spread. *J Virol* **72**, 6119-6130.

Lehman, I. R. & Boehmer, P. E. (1999). Replication of herpes simplex virus DNA. *J Biol Chem* **274**, 28059-28062.

Leuzinger, H., Ziegler, U., Schraner, E. M., Fraefel, C., Glauser, D. L., Heid, I., Ackermann, M., Mueller, M. & Wild, P. (2005). Herpes simplex virus 1 envelopment follows two diverse pathways. *J Virol* **79**, 13047-13059.

Loret, S., Guay, G. & Lippe, R. (2008). Comprehensive characterization of extracellular herpes simplex virus type 1 virions. *J Virol* **82**, 8605-8618.

Lyman, M. G. & Enquist, L. W. (2009). Herpesvirus interactions with the host cytoskeleton. *J Virol* **83**, 2058-2066.

MacPherson, I. & Stoker, M. (1962). Polyoma transformation of hamster cell clones - an investigation of genetic factors affecting cell competence. *Virology* **16**, 147-151.

Maluf, N. K., Yang, Q. & Catalano, C. E. (2005). Self-association properties of the bacteriophage lambda terminase holoenzyme: Implications for the DNA packaging motor. *Journal of Molecular Biology* **347**, 523-542.

Martinez, R., Sarisky, R., Weber, P. & Weller, S. (1996a). Herpes simplex virus type 1 alkaline nuclease is required for efficient processing of viral DNA replication intermediates. *J Virol* **70**, 2075-2085.

Martinez, R., Shao, L., Bronstein, J., Weber, P. & Weller, S. (1996b). The product of a 1.9-kb mRNA which overlaps the HSV-1 alkaline nuclease gene (UL12) cannot relieve the growth defects of a null mutant. *Virology* **215**, 152-164.

Maul, G. G., Guldner, H. H. & Spivack, J. G. (1993). Modification of discrete nuclear domains induced by herpes simplex virus type 1 immediate early gene 1 product (ICP0). *J Gen Virol* **74**, 2679-2690.

McClelland, D. A., Aitken, J. D., Bhella, D., McNab, D., Mitchell, J., Kelly, S. M., Price, N. C. & Rixon, F. J. (2002). pH reduction as a trigger for dissociation of herpes simplex virus type 1 scaffolds. *J Virol* **76**, 7407-7417.

McGeoch, D. & Davison, A. (1999). The molecular evolutionary history of the herpesviruses. In *Origin and Evolution of Viruses*, pp. 441-465. Edited by E. Domingo, R. Webster & J. Holland. London: Academic Press.

McGeoch, D. J., Cook, S., Dolan, A., Jamieson, F. E. & Telford, E. A. R. (1995). Molecular phylogeny and evolutionary timescale for the family of mammalian herpesviruses. *Journal of Molecular Biology* **247**, 443-458.

McGeoch, D. J., Dalrymple, M. A., Davison, A., Dolan, A., Frame, M. C., McNab, D., Perry, L. J., Scott, J. E. & Taylor, P. (1988). The complete DNA sequence of the long unique region int he genome of herpes simplex virus type 1. *J Gen Virol* **69**, 1531-1574.

McGuffin, L., Bryson, K. & Jones, D. (2000). The PSIPRED protein structure prediction server. *Bioinformatics* **16**, 404-405.

McNab, A. R., Desai, P., Person, S., Roof, L. L., Thomsen, D. R., Newcomb, W. W., Brown, J. C. & Homa, F. L. (1998). The product of the herpes simplex virus type 1 UL25 gene is required for encapsidation but not for cleavage of replicated viral DNA. *J Virol* **72**, 1060-1070.

McVoy, M. A., Nixon, D. E., Adler, S. P. & Mocarski, E. S. (1998). Sequences within the Herpesvirus-Conserved pac1 and pac2 Motifs Are Required for Cleavage and Packaging of the Murine Cytomegalovirus Genome. *J Virol* **72**, 48-56.

McVoy, M. A., Nixon, D. E., Hur, J. K. & Adler, S. P. (2000). The Ends on Herpesvirus DNA Replicative Concatemers Contain pac2 cis Cleavage/Packaging Elements and Their Formation Is Controlled by Terminal cis Sequences. *J Virol* **74**, 1587-1592.

Mettenleiter, T. C. (2002). Herpesvirus assembly and egress. *J Virol* **76**, 1537-1547.

Mettenleiter, T. C. (2006). Intriguing interplay between viral proteins during herpesvirus assembly or: The herpesvirus assembly puzzle. *Veterinary Microbiology* **113**, 163-169.

Mettenleiter, T. C., Klupp, B. G. & Granzow, H. (2009). Herpesvirus assembly: An update. *Virus Research* **143**, 222-234.

Michael, N., Spector, D., P, M.-N., Kristie, T. M. & Roizman, B. (1988). The DNA-binding properties of the major regulatory protein alpha 4 of herpes simplex viruses. *Science* **239**, 1531-1534.

Mocarski, E. S. & Roizman, B. (1982). Structure and role of the herpes simplex virus DNA termini in inversion, circularization and generation of virion DNA. *Cell* **31**, 89-97.

Montgomery, R. I., Warner, M. S., Lum, B. J. & Spear, P. G. (1996). Herpes simplex virus-1 entry into cells mediated by a novel member of the TNF/NGF receptor family. *Cell* **87**, 427-436.

Mossman, K. L., Sherburne, R., Lavery, C., Duncan, J. & Smiley, J. R. (2000). Evidence that herpes simplex virus VP16 is required for viral egress downstream of the initial envelopment event. *J Virol* **74**, 6287-6299.

Mou, F., Wills, E. G., Park, R. & Baines, J. D. (2008). Effects of lamin A/C, lamin B1, and viral US3 kinase activity on viral infectivity, virion egress, and the targeting of herpes simplex virus UL34-encoded protein to the inner nuclear membrane. *J Virol* **82**, 8094-8104.

Muylaert, I. & Elias, P. (2007). Knock-down of DNA ligase IV/XRCC4 by RNAi inhibits herpes simplex virus type I DNA replication. *Journal of Biological Chemistry* **282**, 10865-10872.

Nakai, K. & Horton, P. (1999). PSORT: a program for detecting sorting signals in proteins and predicting their subcellular localization. *Trends in Biochemical Sciences* **24**, 34-35.

Nasseri, M. & Mocarski, E. S. (1988). The cleavage recognition signal is contained within sequences surrounding an a-a junction in herpes simplex virus DNA. *Virology* **167**, 25-30.

Negorev, D. & Maul, G. (2001). Ceullular proteins localized at and interacting within ND10/PML nuclar bodies/PODs suggest functions of a nuclear depot. *Oncogene* **20**, 7234-7242.

Nellissery, J. K., Szczepaniak, R., Lamberti, C. & Weller, S. K. (2007). A putative leucine zipper within the herpes simplex virus type 1 UL6 protein is required for portal ring formation. *J Virol* **81**, 8868-8877.

Newcomb, W. W., Booy, F. P. & Brown, J. C. (2007). Uncoating the herpes simplex virus genome. *Journal of Molecular Biology* **370**, 633-642.

Newcomb, W. W., Homa, F. L. & Brown, J. C. (2005). Involvement of the portal at an early step in herpes simplex virus capsid assembly. *J Virol* **79**, 10540-10546.

Newcomb, W. W., Homa, F. L. & Brown, J. C. (2006). Herpes simplex virus capsid structure: DNA packaging protein UL25 is located on the external surface of the capsid near the vertices. *J Virol* **80**, 6286-6294.

Newcomb, W. W., Homa, F. L., Thomsen, D. R., Booy, F. P., Trus, B. L., Steven, A. C., Spencer, J. V. & Brown, J. C. (1996). Assembly of the herpes simplex virus capsid: Characterization of intermediates observed during cell-free capsid formation. *Journal of Molecular Biology* **263**, 432-446.

Newcomb, W. W., Homa, F. L., Thomsen, D. R., Trus, B. L., Cheng, N., Steven, A., Booy, F. & Brown, J. C. (1999). Assembly of the herpes simplex virus procapsid from purified components and identification of small complexes containing the major capsid and scaffolding proteins. *J Virol* **73**, 4239-4250.

Newcomb, W. W., Juhas, R. M., Thomsen, D. R., Homa, F. L., Burch, A. D., Weller, S. K. & Brown, J. C. (2001). The UL6 gene product forms the portal for entry of DNA into the herpes simplex virus capsid. *J Virol* **75**, 10923-10932.

Nicola, A. V., McEvoy, A. M. & Straus, S. E. (2003). Roles for endocytosis and low pH in herpes simplex virus entry into HeLa and chinese hamster ovary cells. *J Virol* **77**, 5324-5332.

O'Hara, M., Rixon, F. J., Stow, N. D., Murray, J., Murphy, M. & Preston, V. G. (2010). Mutational analysis of the herpes simplex virus type 1 UL25 DNA packaging protein reveals regions that are important after the viral DNA has been packaged. *J Virol* **84**, 4252-4263.

Ogasawara, M., Suzutani, T., Yoshida, I. & Azuma, M. (2001). Role of the UL25 gene product in packaging DNA into the herpes simplex virus capsid: Location of UL25 product in the capsid and demonstration that it binds DNA. *J Virol* **75**, 1427-1436.

Ojala, P. M., Sodeik, B., Ebersold, M. W., Kutay, U. & Helenius, A. (2000). Herpes simplex virus type 1 entry into host cells: Reconstitution of capsid binding and uncoating at the nuclear pore complex in vitro. *Mol Cell Biol* **20**, 4922-4931.

Ortega, M. E. & Catalano, C. E. (2006). Bacteriophage lambda gpNu1 and Escherichia coli IHF proteins cooperatively bind and bend viral DNA:Implications for the assembly of a genome-packaging motor *Biochemistry* **45**, 5180-5189.

Park, R. & Baines, J. D. (2006). Herpes simplex virus type 1 infection induces activation and recruitment of protein kinase C to the nuclear membrane and increased phosphorylation of lamin B. *J Virol* **80**, 494-504.

Parrott, M. M., Sitarski, S. A., Arnold, R. J., Picton, L. K., Hill, R. B. & Mukhopadhyay, S. (2009). Role of conserved cysteines in the alphavirus E3 protein. *J Virol* **83**, 2584-2591.

Pasdeloup, D., Blondel, D., Isidro, A. L. & Rixon, F. J. (2009). Herpesvirus capsid association with the nuclear pore complex and viral DNA release involve the nucleoporin CAN/Nup214 and the capsid protein pUL25. *J Virol* **83**, 6610-6623.

Patel, A. & Maclean, J. B. (1995). The product of the UL6 gene of herpes simplex virus type 1 is associated with virus capsids. *Virology* **206**, 465-478.

Patel, A., Rixon, F., Cunningham, C. & Davison, A. (1996a). Isolation and characterization of herpes simplex virus type 1 mutants defective in the UL6 gene. *Virology* **217**, 111-123.

Patel, A. H., Subak-Sharpe, J. H., Stow, N. D., Marsden, H. S., Maclean, J. B. & Dargan, D. J. (1996b). Suppression of amber nonsense mutations of herpes simplex virus type 1 in a tissue culture system. *J Gen Virol* **77**, 199-209.

Patrick, D. R., Zhang, K., Defeo-Jones, D., Vuocolo, G. R., Maigetter, R. Z., Sardana, M. K., Oliff, A. & Heimbrook, D. C. (1992). Characterization of functional HPV-16 E7 protein produced in Escherichia coli. *Journal of Biological Chemistry* **267**, 6910-6915.

Phelan, A., Dunlop, J., Patel, A. H., Stow, N. D. & Clements, J. B. (1997). Nuclear sites of herpes simplex virus type 1 DNA replication and transcription colocalize at early times postinfection and are largely distinct from RNA processing factors. *J Virol* **71**, 1124-1132.

Poffenberger, K. L. & Roizman, B. (1985). A noninverting genome of a viable herpes simplex virus 1: presence of head-to-tail linkages in packaged genomes and requirements for circularization after infection. *J Virol* **53**, 587-595.

Polvino-Bodnar, M., Orberg, P. K. & Schaffer, P. A. (1987). Herpes simplex virus type 1 oriL is not required for virus replication or for the establishment and reactivation of latent infection in mice. *J Virol* **61**.

Porter, I. M. & Stow, N. D. (2004a). Replication, recombination and packaging of amplicon DNA in cells infected with the herpes simplex virus type 1 alkaline nuclease null mutant ambUL12. *J Gen Virol* **85**, 3501-3510.

Porter, I. M. & Stow, N. D. (2004b). Virus particles produced by the herpes simplex virus type 1 alkaline nuclease null mutant ambUL12 contain abnormal genomes. *J Gen Virol* **85**, 583-591.

Preston, C. & Nicholl, M. (1997). Repression of gene expression upon infection of cells with herpes simplex virus type 1 mutants impaired for immediate-early protein synthesis. *J Virol* **71**, 7807-7813.

Preston, V. G., Coates, J. A. V. & Rixon, F. J. (1983). Identification and characterization of a herpes simplex virus gene product required for encapsidation of virus DNA. *J Virol* **45**, 1056-1064.

Preston, V. G., Murray, J., Preston, C. M., McDougall, I. M. & Stow, N. D. (2008). The UL25 gene product of herpes simplex virus type 1 is involved in uncoating of the viral genome. *J Virol* **82**, 6654-6666.

Przech, A. J., Yu, D. & Weller, S. K. (2003). Point mutations in exon I of the herpes simplex virus putative terminase subunit, UL15, indicate that the most conserved residues are essential for cleavage and packaging. *J Virol* **77**, 9613-9621.

Qin, L., Fokine, A., O'Donnell, E., Rao, V. B. & Rossmann, M. G. (2010). Structure of the small outer capsid protein, soc: A clamp for stabilizing capsids of T4-like phages. *Journal of Molecular Biology* **395**, 728-741.

Quinlan, M. P., Chen, L. B. & Knipe, D. M. (1984). The intranuclear location of a herpes simplex virus DNA-binding protein is determined by the status of viral DNA replication. *Cell* **36**, 857-868.

Rao, V. B. & Black, L. W. (1988). Cloning, overexpression and purification of the terminase proteins gp16 and gp17 of bacteriophage T4 : Construction of a defined in-vitro DNA packaging system using purified terminase proteins. *Journal of Molecular Biology* **200**, 475-488.

Rao, V. B. & Feiss, M. (2008). The bacteriophage DNA packaging motor. *Annual Review of Genetics* **42**, 647-681.

Remillard-Labrosse, G., Guay, G. & Lippe, R. (2006). Reconstitution of herpes simplex virus type 1 nuclear capsid egress in vitro. *J Virol* **80**, 9741-9753.

Reuven, N. B., Staire, A. E., Myers, R. S. & Weller, S. K. (2003). The herpes simplex virus type 1 alkaline nuclease and single-stranded DNA binding protein mediate strand exchange in vitro. *J Virol* **77**, 7425-7433.

Reuven, N. B. & Weller, S. K. (2005). Herpes simplex virus type 1 single-strand DNA binding protein ICP8 enhances the nuclease activity of the UL12 alkaline nuclease by increasing its processivity. *J Virol* **79**, 9356-9358.

Richman, L. K., Montali, R. J., Garber, R. L., Kennedy, M. A., Lehnhardt, J., Hildebrandt, T., Schmitt, D., Hardy, D., Alcendor, D. J. & Hayward, G. S. (1999). Novel endotheliotropic herpesviruses fatal for Asian and African elephants. *Science* **283**, 1171-1176.

Rigby, P. W. J., Dieckmann, M., Rhodes, C. & Berg, P. (1977). Labeling deoxyribonucleic acid to high specific activity in vitro by nick translation with DNA polymerase I. *J Mol Biol* **113**, 237-251.

Rixon, F., Addison, C., McGregor, A., Macnab, S. J., Nicholson, P., Preston, V. G. & Tatman, J. D. (1996). Multiple interactions control the intracelular localization of the herpes simplex virus type 1 capsid proteins. *J Gen Virol* **77**, 2251-2260.

Roberts, A. P. E., Abaitua, F., O'Hare, P., McNab, D., Rixon, F. J. & Pasdeloup, D. (2009). Differing roles of inner tegument proteins pUL36 and pUL37 during entry of herpes simplex virus type 1. *J Virol* **83**, 105-116.

Rock, D. & Fraser, N. W. (1983). Detection of HSV-1 genome in central nervous system of latently infected mice. *Nature* **302**, 523-525.

Rodriguez, I., Redrejo-Rodriguez, M., Rodriguez, J. M., Alejo, A., Salas, J. & Sala, M. (2006). African swine fever virus pB119L protein is a flavin adenine dinucleotide-linked sulfhydryl oxidase. *J Virol* **80**, 3157-3166.

Roizman, B. & Knipe, D. (2001). Herpes Simple Viruses and Their Replication. In *Fields Virology*. Edited by B. Fields, Knipe, D, Howley, P.

Roller, R. J., Zhou, Y., Schnetzer, R., Ferguson, J. & DeSalvo, D. (2000). Herpes simplex virus type 1 UL34 gene product is required for viral envelopment. *J Virol* **74**, 117-129.

Roos, W. H., Radtke, K., Kniesmeijer, E., Geertsema, H., Sodeik, B. & Wuite, G. J. (2009). Scoffold expulsion and genome packaging trigger stabilization of herpes simple virus capsids. *PNAS* **106**, 9673-9678.

Rosenthal, K., Leuther, M. D. & Barisas, B. G. (1984). Herpes simplex virus binding and entry modulate cell surface protein mobility. *J Virol* **49**, 980-983.

Ruyechan, W. T. & Weir, A. C. (1984). Interaction with nucleic acids and stimulation of the viral DNA polymerase by the herpes simplex virus type 1 major DNA-binding protein. *J Virol* **52**, 727-733.

Saeki, Y., Ichikawa, T., Saeki, A., Chiocca, E. A., Tobler, K., Ackermann, M., Breakefield, X. O. & Fraefel, C. (1998). Herpes simplex virus type 1 DNA amplified as bacterial artificial chromosome in Escherichia coli: Rescue of replication-competent virus progeny and packaging of amplicon vectors. *Human Gene Therapy* **9**, 2787-2794.

Salmon, B. & Baines, J. D. (1998). Herpes simplex virus DNA cleavage and packaging: Association of multiple forms of UL15-encoded proteins with B capsids requires at least the UL6, UL17, and UL28 genes. *J Virol* **72**, 3045-3050.

Salmon, B., Cunningham, C., Davison, A. J., Harris, W. J. & Baines, J. D. (1998). The herpes simplex virus type 1 UL17 gene encodes virion tegument proteins that are required for cleavage and packaging of viral DNA. *J Virol* **72**, 3779-3788.

Sambrook, J., Fritsch, E. & Maniatis, T. (1989). Preparation of radiolabeled DNA and RNA probes. In *Molecular Cloning, A Laboratory Manual*, 2 edn, pp. 10.16-10.12: Cold Spring Harbour Laboratory Press.

Sambrook, J. & Russell, D. (2001a). Isolation of BAC DNA from small scale cultures (4.53). In *Molecular Cloning, A Laboratory Manual*, 3 edn: Coldspring Harbour Laboratory Press.

Sambrook, J. & Russell, D. (2001b). Southern blotting: Capillary transfer of DNA to membranes. In *Molecular Cloning, A Laboratory Manual*, 3 edn: Coldspring Harbour Laboratory Press.

Sawtell, N. M. (1997). Comprehensive quantification of herpes simplex virus latency at the single-cell level. *J Virol* **71**, 5423-5431.

Schaeffer, P. A., Aron, G. M., Biswal, N. & Benyesh-Melnick, M. (1973). Temperature-sensitive mutants of herpes simplex virus type 1: isolation, complementation and partial characterization. *Virology* **52**, 57-71.

Schaeffer, P. A., Brunschwig, J. P., McCombs, R. M. & Benyesh-Melnick, M. (1974). Electron microscopic studies of temperature-sensitive mutants of herpes simplex virus type 1. *Virology* **92**, 444-457.

Scheffczik, H., Savva, C. G. W., Holzenburg, A., Kolesnikova, L. & Bogner, E. (2002). The terminase subunits pUL56 and pUL89 of human cytomegalovirus are DNA-metabolizing proteins with toroidal structure. *Nuc Acid Res* **30**, 1695-1703.

Scholtes, L. & Baines, J. D. (2009). Effects of major capsid proteins, capsid assembly, and DNA cleavage/packaging on the pUL17/pUL25 complex of herpes simplex virus 1. *J Virol* **83**, 12725-12737.

Shao, L., Rapp, L. M. & Weller, S. K. (1993). Herpes simplex virus 1 alkaline nuclease is required for efficient egress of capsids from the nucleus. *Virology* **196**, 146-162.

Sheaffer, A. K., Newcomb, W. W., Gao, M., Yu, D., Weller, S. K., Brown, J. C. & Tenney, D. J. (2001). Herpes simplex virus DNA cleavage and packaging proteins associate with the procapsid prior to its maturation. *J Virol* **75**, 687-698.

Sherman, G. & Bachenheimer, S. (1987). DNA processing in termperature-sensitive morphogenic mutants of HSV-1. *Virology* **158**, 427-430.

Sherman, G. & Bachenheimer, S. (1988). Characterisation of intranuclear capsids made by ts morphogenic mutants of HSV-1. *Virology* **163**, 471-480.

Shukla, D., Liu, J., Blaiklock, P., Shworak, N. W., Bai, X., Esko, J. D., Cohen, G. H., Eisenberg, R. J., Rosenberg, R. D. & Spear, P. G. (1999). A novel role for 3-O-sulfated heparan sulfate in herpes simplex virus 1 entry. *Cell* **99**, 13-22.

Simpson-Holley, M., Baines, J. D., Roller, R. & Knipe, D. (2004). Herpes simplex virus 1 UL31 and UL34 gene products promote the late maturation of viral replication compartments to the nuclear periphery. *J Virol* **78**, 5591-5600.

Sinclair, J. & Sissons, P. (2006). Latency and reactivation of human cytomegalovirus. *J Gen Virol* **87**, 1763-1779.

Singer, G. P., Newcomb, W. W., Thomsen, D. R., F, H. & J, B. (2005). Identification of a region in the herpes simplex virus scaffolding protein required for interaction with the portal. *J Virol* **79**, 132-139.

Skaliter, R. & Lehman, I. R. (1994). Rolling circle DNA replication in vitro by a complex of herpes simplex virus type 1-encoded enzymes. *PNAS* **91**, 10665-10669.

Smiley, J., Duncan, J. & Howes, M. (1990). Sequence requirements for DNA rearrangements induced byt he terminal repeat of herpes simplex virus type 1 KOS DNA. *J Virol* **64**, 5036-5050.

Smith, R. W. P., Mailk, P. & Clements, J. B. (2005). The herpes simplex virus ICP27 protein: a multifunctional post-transcriptional regulator of gene expression. *Biochemical Society Transactions* **33**.

Spaete, R. R. & Frenkel, N. (1985). The herpes simplex virus amplicon: analyses of cis-acting replication functions. *PNAS* **82**, 694-698.

Spaete, R. R. & Mocarski, E. S. (1985). The alpha sequence of the cytomegalovirus genome functions as a cleavage/packaging signal for herpes simplex virus defective genomes. *J Virol* **54**, 817-824.

Stevens, J. G. & Cook, M. L. (1971). Latent herpes simplex virus in spinal ganglia of mice. *Science* **173**, 843-845.

Stow, N. (1982). Localization of an origin of DNA replication within the TRS/IRS repeated region of the herpes simplex virus type 1 genome. *EMBO J* **1**, 863-867.

Stow, N., McMonagle, E. & Davison, A. (1983). Fragments from both termini of the herpes simplex virus type 1 genome contain signals required for the encapsidation of viral DNA. *Nuc Acid Res* **11**, 8205-8220.

Stow, N. D. (1993). Sequences at the C-terminus of the herpes simplex virus type 1 UL30 protein are dispensable for DNA polymerase activity but not for viral origin-dependent DNA replication. *Nucl Acids Res* **21**, 87-92.

Stow, N. D. (2001). Packaging of genomic and amplicon DNA by the herpes simplex virus type 1 UL25-null mutant KUL25NS. *J Virol* **75**, 10755-10765.

Stow, N. D., Hammarsten, O., Arbuckle, M. I. & Elias, P. (1993). Inhibition of herpes simplex virus type 1 DNA replication by mutant forms of the origin-binding protein. *Virology* **196**, 413-418.

Stow, N. D. & Wilkie, N. M. (1976). An improved technique for obtaining enhanced infectivity with herpes simplex virus type 1 DNA. *J Gen Virol* **33**, 447-458.

Strang, B. & Stow, N. (2005). Circularization of the herpes simplex virus type 1 genome upon lytic infection. *J Virol* **79**, 12478-12494.

Strang, B. & Stow, N. (2007). Blocks to herpes simplex virus type 1 replication in a cell line, tsBN2, encoding a temperature-sensitive RCC1 protein. *J Gen Virol* **88**, 376-383.

Su, Y.-H., Zhang, X., Wang, X., Fraser, N. W. & Block, T. M. (2006). Evidence that the immediate-early gene product ICP4 is necessary for the genome of the herpes simplex virus type 1 ICP4 deletion mutant strain d120 to circularize in infected cells. *J Virol* **80**, 11589-11597.

Tatman, J. D., Preston, V. G., Nicholson, P., Elliott, R. M. & Rixon, F. J. (1994). Assembly of herpes simplex virus type 1 capsids using a panel of recombinant baculoviruses. *J Gen Virol* **75**, 1101-1113.

Taus, N., Salmon, B. & Baines, J. D. (1998). The herpes simplex virus 1 UL17 gene is required for localisation of capsids and major and minor capsid proteins to intranuclear sites where viral DNA ia cleaved and packaged. *Virology* **252**, 115-125.

Taus, N. S. & Baines, J. D. (1998). Herpes simplex virus 1 DNA cleavage/packaging: The UL28 gene encodes a minor component of B capsids. *Virology* **252**, 443-449.

Tavares, P., Dröge, A., Lurz, R., Graeber, I., Orlova, E., Dube, P. & van Heel, M. (1995). The SPP1 connection. *FEMS Microbiology Reviews* **17**, 47-56.

Taylor, T. J. & Knipe, D. M. (2004). Proteomics of Herpes Simplex Virus Replication Compartments: Association of Cellular DNA Replication, Repair, Recombination, and Chromatin Remodeling Proteins with ICP8. *J Virol* **78**, 5856-5866.

Tengelsen, L. A., Pederson, N. E., Shaver, P. R., Wathen, M. W. & Homa, F. L. (1993). Herpes simplex virus type 1 DNA cleavage and encapsidation require the product of the UL28 gene: isolation and characterization of two UL28 deletion mutants. *J Virol* **67**, 3470-3480.

Thompson, R. L., Preston, C. M. & Sawtell, N. M. (2009). De novo synthesis of VP16 coordinates the exit from HSV latency in vivo. *PLoS Pathog* **5**.

Thurlow, J. K., Murphy, M., Stow, N. D. & Preston, V. G. (2006). Herpes simplex virus type 1 DNA-packaging protein UL17 is required for efficient binding of UL25 to capsids. *J Virol* **80**, 2118-2126.

Thurlow, J. K., Rixon, F. J., Murphy, M., Targett-Adams, P., Hughes, M. & Preston, V. G. (2005). The herpes simplex virus type 1 DNA packaging protein UL17 is a virion protein that is present in both the capsid and the tegument compartments. *J Virol* **79**, 150-158.

Tilly, K., Murialdo, H. & Georgopoulos, C. (1981). Identification of a second Escherichia coli groE gene whose product is necessary for bacteriophage morphogenesis. *PNAS* **78**, 1629-1633.

Tong, L. & Stow, N. D. (2010). Analysis of herpes simplex virus type 1 DNA packaging signal mutations in the context of the viral genome. *J Virol* **84**, 321-329.

Topp, K. S., Bisla, K., Saks, N. D. & Lavail, J. H. (1996). Centripetal transport of herpes simplex virus in human retinal pigment epithelial cells in vitro. *Neuroscience* **71**, 1133-1144.

Topp, K. S., Meade, L. B. & Lavail, J. H. (1994). Retrograde transport of herpes simplex virus in trigeminal neurons is dependent on intact microtubules. *J Neuroscience* **17**, 318-325.

Trus, B. L., Cheng, N., Newcomb, W. W., Homa, F. L., Brown, J. C. & Steven, A. C. (2004). Structure and polymorphism of the UL6 portal protein of herpes simplex virus type 1. *J Virol* **78**, 12668-12671.

Trus, B. L., Newcomb, W. W., Cheng, N., Cardone, G., Marekov, L., Homa, F. L., Brown, J. C. & Steven, A. C. (2007). Allosteric signaling and a nuclear exit strategy: Binding of UL25/UL17 heterodimers to DNA-filled HSV-1 capsids. *Molecular Cell* **26**, 479-489.

Twigg, A. J. & Sherratt, D. (1980). Trans-complementable copy-number mutants of plasmid ColE1. *Nature* **282**, 216-218.

Umene, K. & Nishimoto, T. (1996). Replication of herpes simplex virus type 1 DNA is inhibited in a temperature-sensitive mutant of BHK-21 cells lacking RCC1 (regulator of chromosome condensation) and virus DNA remains linear. *J Gen Virol* **77**, 2261-2270.

van der Vies, S. M., Gatenby, A. A. & Georgopoulos, C. (1994). Bacteriphage T4 encodes a co-chaperonin that can substitute for Escherichia coli GroES in protein folding. *Nature* **368**, 654-656.

van Ham, M. & Hendriks, W. (2003). PDZ domains – glue and guide. *Molecular Biology Reports* **30**, 69-82.

Varmuza, S. & Smiley, J. (1985). Signals for site specific cleavage of HSV DNA: maturation involves two separate cleavage events at sites distal to the recognition sequences. *Cell* **41**, 793-802.

Vittone, V., Diefenbach, E., Triffett, D., Douglas, M. W., Cunningham, A. L. & Diefenbach, R. J. (2005). Determination of interactions between tegument proteins of herpes simplex virus type 1. *J Virol* **79**, 9566-9571.

Walker, J. E., Saraste, M., Runswick, M. J. & Gay, N. J. (1982). Distantly related sequences in the alpha- and beta-subunits of ATP synthase, myosin, kinases and other ATP-requireing enzymes and a common nucleotide binding fold. *EMBO J* **1**, 945-951.

Watson, R. J. & Clements, J. B. (1980). A herpes simplex virus type 1 function continuously required for early and late virus RNA synthesis. *Nature* **285**.

Weller, S., Seghatoleslami, M. R., Shao, L., Rowse, D. & Carmichael, E. P. (1990). The herpes simplex virus type 1 alkaline nucleus is not essential for viral DNA synthesis: isolation and characterization of a lacZ insertion mutant. *J Gen Virol* **71**, 2941-2952.

White, C. A., Stow, N. D., Patel, A. H., Hughes, M. & Preston, V. G. (2003). Herpes simplex virus type 1 portal protein UL6 interacts with the putative terminase subunits UL15 and UL28. *J Virol* **77**, 6351-6358.

Whitlow, Z. W. & Kristie, T. M. (2009). Recruitment of the transcriptional coactivator HCF-1 to viral immediate-early promoters during initiation of reactivation from latency of herpes simplex virus type 1. *J Virol* **83**, 9591-9595.

Wittels, M. & Spear, P. G. (1991). Penetration of cells by herpes simplex virus does not require a low pH-dependent endocytic pathway. *Virus Research* **18**, 271-290.

Wojtyra, U. A., Thibault, G., Tuite, A. & Houry, W. A. (2003). The N-terminal zinc binding domain of ClpX is a dimerization domain that modulates the chaperone function. *Journal of Biological Chemistry* **278**, 48981-48990.

Wu, C. A., Nelson, N. J., McGeoch, D. J. & Challberg, M. D. (1988). Identification of herpes simplex virus type 1 genes required for origin-dependent DNA synthesis. *J Virol* **62**, 435-443.

Yang, K. & Baines, J. D. (2006). The putative terminase subunit of herpes simplex virus 1 encoded by UL28 is necessary and sufficient to mediate interaction between pUL15 and pUL33. *J Virol* **80**, 5733-5739.

Yang, K., Homa, F. & Baines, J. D. (2007). Putative terminase subunits of herpes simplex virus 1 form a complex in the cytoplasm and interact with portal protein in the nucleus. *J Virol* **81**, 6419-6433.

Yu, D., Sheaffer, A. K., Tenney, D. J. & Weller, S. K. (1997). Characterization of ICP6::lacZ insertion mutants of the UL15 gene of herpes simplex virus type 1 reveals the translation of two proteins. *J Virol* **71**, 2656-2665.

Yu, D. & Weller, S. K. (1998a). Genetic analysis of the UL15 gene locus for the putative terminase of herpes simplex virus type 1. *Virology* **243**, 32-44.

Yu, D. & Weller, S. K. (1998b). Herpes simplex virus type 1 cleavage and packaging proteins UL15 and UL28 are associated with B but not C capsids during packaging. *J Virol* **72**, 7428-7439.

Zeilstra-Ryalls, J., Fayet, O. & Georgopoulos, C. (1991). The universally conserved GroE (Hsp60) chaperonins. *Annual Review of Microbiology* **45**, 301-325.

Zhao, H., Finch, C. J., Sequeira, R. D., Johnson, B. A., Johnson, J. E., Casjens, S. R. & Tang, L. (2010). Crystal structure of the DNA-recognition component of the bacterial virus Sf6 genome-packaging machine. *Proceedings of the National Academy of Sciences* **107**, 1971-1976.

Zhou, Z. H., Chen, D. H., Jakana, J., Rixon, F. J. & Chiu, W. (1999). Visualization of tegument-capsid interactions and DNA in intact herpes simplex virus type 1 virions. *J Virol* **73**, 3210-3218.

Zweig, M., Heilman, C. & Hampar, B. (1979). Identification of disulphide-linked protein complexes in the nucleocapsids of herpes simplex virus type 2. *Virology* **94**, 442-450.